

The influence the oceanographic variability has on the top predators of the sub-Antarctic domain

by

Sean Evans (EVNSEA001)



Supervisors:

Dr M. du Plessis^{1,2}, Dr M. Wege³, Prof. I. Ansorge¹, Dr A. Lowther⁴, Ass. Prof. N. de Bruyn³.

¹Department of Oceanography, University of Cape Town, ²Department of Marine Sciences, University of Gothenburg, Sweden; ³Department of Zoology & Entomology, University of Pretoria, South Africa; ⁴Norwegian Polar Institute, Norway.

Dissertation presented in full fulfilment of the requirements for the Degree of

Master of Science

in the Department of Oceanography

University of Cape Town

May 2021

I know the meaning of plagiarism and declare that all the work in the dissertation, save for that which is properly acknowledged, is my own.

The copyright of this thesis vests in the author. No quotation from it or information derived from it is to be published without full acknowledgement of the source. The thesis is to be used for private study or non-commercial research purposes only.

Published by the University of Cape Town (UCT) in terms of the non-exclusive license granted to UCT by the author.

Declaration of originality

I, Sean Evans, declare that this dissertation, which I hereby submit for the degree MSc (Ocean and Atmospheric Science) at the University of Cape Town, is my own work and has not previously been submitted by me for a degree at this or any other tertiary institution.

Signature:

Signed by candidate

Date: **07/05/2021**

This dissertation should be cited as: Evans, S. (2021) 'The influence the oceanographic variability has on the top predators of the sub-Antarctic domain', *MSc dissertation, University of Cape Town.*

Acknowledgements

My family and friends for supporting me. A special mention to the David, Brenda, and Robyn Evans. Thank you to Melissa Schulze for all her help and patience.

Thank you to all the past sealers who have made the incredible effort to deploy and retrieve the devices used to collect data for this thesis. The South African Department of Environmental Affairs for providing logistical support within the South African National Antarctic Programme (SANAP) and the Department of Science and Technology (administered through the National Research Foundation) for funding my studies.

I would like to thank my supervisors for their tireless efforts in keeping me on track and guiding me through the process of formulating this thesis. I have learned so much from you and look forward to working by your side in any future endeavours that may arise. Dr Marcel du Plessis, thank you for being so approachable, for pushing me and providing feedback even at the busiest of times. Moreover, thank you for being so accommodating in Sweden. You have gone over and above for me so thank you. Dr Mia Wege, a fellow sealer, and dedicated supervisor. You have gained all my respect and gratitude and I look up to you not only as a scientist, but also as a role model. Thank you for all the constructive advice. Finally, thank you for your time in Pretoria.

Dr Andrew Lowther for sparking my interest in Southern Ocean work and welcoming me to Norway for a short, yet productive visit. Assoc. Prof. Sebastiaan Swart and his team in Sweden, Gothenburg for providing constructive feedback for being incredibly accommodating. Fabien Roquet for taking some time to discuss ideas for my thesis and supplying helpful code for exploratory analysis.

Assoc. Prof. Nico de Bruyn for supporting my year on Marion Island and believing in my abilities as a MIMMP member, including the support shown for my trip to Sweden. You have also been extremely accommodating, especially during my trips to Pretoria. Finally, a special thank you to Prof. Isabelle Ansorge for always supporting my academics and supplying endless opportunities for me to further my career.

Abstract

Historically, a lack of small-scale physical oceanographic (hours to days, 1-10 km) and behavioural (<10 sec, ~1 m) observations in the relatively inaccessible Southern Ocean has led to poor quantification of marine mammal foraging behaviour and the physical upper ocean processes that may influence them. *In situ* temperature and depth profiles from 2009-2015 were obtained from devices fitted to 39 adult Subantarctic fur seal (SAFS) (*Arctocephalus tropicalis*) females inhabiting the Prince Edward Islands (PEI). This provided a unique opportunity to study the fine-scale effects of thermal water column structure and upper ocean submesoscale processes on the diving behaviour and vertical foraging effort of SAFS. Seasonal and diel trends of foraging effort were investigated and compared to upper ocean thermal structure. Dives were distinguished using the Clustering for Large Applications algorithm according to vertical movements made by the seals. Shallow, high effort dives differentiated from deep, low effort dives, primarily based on bottom effort. High effort dives, associated with high vertical foraging effort, bottom effort, and dive efficiency, were more numerous when the seals were in well-mixed water columns. Generalised additive mixed-effects models showed that thermal water column structure plays a significant role in modulating dive types made by seals. The probability of high effort dives decreased with increasing stratification, while the relationship with the stability and mean temperature of the water column was complex, yet significant. Overall, seals are predicted to enhance vertical foraging effort and dive shallower in well-mixed, warmer water columns, with a strong association to diel and seasonal trends in mixing found. However, seals do not appear to align their distribution of foraging depth with the MLD in either season. Investigation into what upper ocean processes may be driving variation in thermal water column structure surrounding the islands led to investigations into the downstream effects of the small-scale topography of the islands on ocean variability. Results show that the PEI act as a solid obstruction to the relatively laminar flow of the Antarctic Circumpolar Current and coherent eddy structures moving through the Archipelago region. The topographic influence of the PEI on multiple scales of local ocean variability in the region, from mesoscale (10-100 km, days to weeks) to submesoscale (1-10 km, hours to days) and vertical mixing (<1 m, <10 sec), is illustrated. Downstream enhanced squeezing and stretching of mesoscale and submesoscale gradients intensify restratification and stability in the lee of the Islands with the potential to enhance biological productivity. Seals do not appear to adjust their fine-scale foraging

behaviour to these downstream processes. By improving our understanding of SAFS habitat use, we can more accurately predict how regional and global change may affect populations in the future, linking to more effective conservation management and policy. Furthermore, this study emphasizes how concurrent measurements of oceanographic and behavioural data collected from diving samplers can be used to study the downstream effects on both physical oceanography and foraging ecology surrounding small islands.

Disclaimer

Chapters 2 and 3 of this dissertation were prepared for publication as separate manuscripts. Therefore, each of these chapters are in publication format. Consequently, I apologise to the reader for any repetition that they may be subjected to, especially in the introduction and methods sections. The journal proposed for both Chapter 2 and 3 is the Marine Ecology Progress Series.

Chapter 2:

Evans, S. (2021) 'Influence of upper ocean thermal structure on diving and foraging behaviour of subantarctic fur seals at Marion Island: A fine-scale study using on-board data loggers', *In Prep. Mar Ecol Prog Ser.*

Chapter 3:

Evans, S. (2021) 'Small-scale topographic influences on seasonal submesoscale processes and restratification at the Prince Edward Islands and links to fur seal foraging effort: An upstream versus downstream comparison', *In Prep. Mar Ecol Prog Ser.*



A female subantarctic fur seal.



Table of contents

Declaration of originality	ii
Acknowledgements	iii
Abstract	iv
Disclaimer	vi
Table of contents	vii
List of Figures	x
List of tables	xv
List of supplementary materials	xvi
Chapter 1: General Introduction	1
Biologging in the Southern Ocean	1
Southern Ocean variability and impacts on biological productivity	3
The Prince Edward Islands: Importance, physical oceanography and ecology	6
Upper ocean dynamics and impacts on biology: Turbulent mixing and the MLD	9
Topographic influences on upper ocean dynamics and marine top predator behaviour	11
Subantarctic fur seal foraging ecology at Marion Island	13
Dissertation structure, aims and objectives	15
Chapter 2: Influence of upper ocean thermal structure on diving and foraging behaviour of subantarctic fur seals at Marion Island: A fine-scale study using on-board data loggers.	18
Abstract	19
Aims and objectives	22
Materials and methods	23
Ethics statement	23
Study site, animal handling and instrumentation	23
Tracking data and horizontal area-restricted search (hARS)	25

Vertical movements	27
Classifying dive types (Response variable)	29
Upper ocean thermal structure and vertical mixing (Explanatory variables)	31
Generalized Additive Mixed-Effects Model (GAMM) framework	35
Diurnal trends in stratification and foraging and seasonal differences between MLD and foraging depth	37
Results	38
Seasonal summary statistics of seal foraging behaviour and upper ocean thermal structure	38
What kind of dives do subantarctic fur seals make?	39
Associations between foraging behaviour and upper ocean thermal structure: Seasonal and diel trends	42
Response of diving and foraging behaviour to immediate oceanography	46
Discussion	50
Types of dives made by SAFS	51
Seasonal foraging trends in relation to seasonality of the upper ocean thermal structure	53
Diel foraging trends in relation to patterns of the upper ocean thermal structure	55
Effect of upper ocean thermal structure on fine-scale diving and foraging behaviour	56
Conclusions	58
Chapter 3: Small-scale topographic influences on seasonal submesoscale processes and restratification at the Prince Edward Islands and links to fur seal foraging effort: An upstream versus downstream comparison	60
Abstract	61
Introduction	62
Study area: Prince Edward Islands (PEI) within the Southern Ocean	62
Mesoscale activity and biological impact	63

The role of submesoscales in marine ecology	64
Topographic influences on downstream ocean variability and impacts on marine ecology	65
Subantarctic fur seals (SAFS) and using seals as ocean samplers	69
Aims and objectives	70
Methods	71
Study site, animal handling, instrumentation, and behavioural indexes	71
In situ upper ocean thermal structure: mixed layer depth (MLD), stratification, stability and horizontal buoyancy gradients (b_x)	72
Satellite remote sensing of flow variability	74
Results	76
Contribution of temperature and salinity to density gradients	76
Time-mean and time-varying local ocean circulation, stirring and mixing	77
Submesoscale variability determined from seal-track data	82
Case study (summer 2012): Topographic influences on downstream upper ocean physics	84
Comparisons between seasonal upstream and downstream vertical structure and seal behaviour	88
Discussion	92
Geostrophic and inertial ocean circulation surrounding the Prince Edward Islands	92
Seasonality of (sub-)mesoscale flows and mixing within the upper ocean	94
Topographic influences on downstream local variability in the upper ocean	99
Does seasonally- and topographically influenced oceanography surrounding the PEI impact seasonal seal foraging effort?	105
Limitations of the study	106
Conclusions	108
Chapter 4: General conclusion	109

Synthesis	109
Foraging and dive strategies	109
What can animal-borne data loggers inform about the Prince Edward Islands surrounding physical oceanographic landscape?	110
Importance and future work	111
Oceanography and climate models	111
Climate change, conservation and management	112
Supplementary Material	115
REFERENCES	120

List of Figures

Figure 1.1: A depiction of the climate model CM2.6. surface speed throughout the Southern Ocean, emphasising the heterogeneity of ocean flows. This image is courtesy of Adele Morrison and is available at https://stephengriffies.github.io	2
Figure 1.2: Illustration of physical and biological oceanographic features of an idealized Antarctic Circumpolar Current (ACC) front. At the front, a strong jet associated with the ACC flows from West to East and isopycnals slope towards the surface. The front is associated with horizontal mesoscale and submesoscale structures such as eddies and filaments. Adapted from Chapman et al., 2020 with credit to Christopher Chapman and Louise Bell.	3
Figure 1.3: A snapshot (1st June 2012) of a mesoscale stirring field (represented by Finite-Size Lyapunov Exponents [days ⁻¹]) surrounding the Prince Edward Islands (white triangle). This depicts the variability in ocean flows surrounding the Prince Edward Islands.	5
Figure 1.4: The root mean square values of sea level anomaly [cm] derived from 13 years of altimetry shows eddy variability associated with the Agulhas Retroflection and the Southwest Indian Ridge (SWIR). This image is sourced from Durgadoo et al. (2010). The location of the Prince Edward Islands is shown in relation to South Africa and large topographic features, indicated in white (-3000 m, -2000 m, -1000 m) and labelled in black. The average positions of the Antarctic Circumpolar Current fronts, the Subtropical Convergence (STC), sub-Antarctic Front (SAF), and the Antarctic Polar Front (APF), are indicated (black line). The Andrew Bain Fracture Zone is the core of the variability along the SWIR (indicated by the orange line). The position of the Abyssal Plane (AP), Del Cano Rise (DCR), Conrad Rise (CR), and three major basins are also shown.	7
Figure 1.5: Observations at Marion Island (black shaded region in (a) and grey shaded region in (b)) of a) density (kg.m ⁻³) at 200 metres depth and b) dynamic height (at 0 db referenced to 1500 db) with overlaid surface geostrophic velocities. These figures were adapted from Ansorge and Lutjeharms (2002) and the data were collected by ship measurements (black dots) during the a) Marion Offshore Ecological Study 2 in 1989 and the b) Marion Island Oceanographic Survey 2 in 1997. These figures illustrate the upstream and downstream variability of the region.	12

Figure 2.1: Bathymetry map (elevation in metres) obtained from the 'GEBCO_2020' global bathymetric gridded product released by the General Bathymetric Chart of the Oceans (GEBCO Compilation Group 2020) with a 1/240° resolution. The location of the Prince Edward Archipelago's is shown in relation to South Africa and large topographic features (Fisher & Goodwillie, 1997). A zoomed-in map shows the two deployment colonies on Marion Island, with Prince Edward Island approximately 20 km from Marion. The Van den Boogaard SAFS rookery is situated on the east side of the island, while the Mixed Pickle rookery is on the west. **Error! Bookmark not defined.**

Figure 2.2: A schematic of Wildlife Computers' SPLASH 10-351 tag (a) (Adapted from Wildlife Computers' product feature sheets) attached to a subantarctic fur seal (b) at Marion Island and a Wildlife Computers' TDR-MK9 (c) alongside a PTT tag (d). Pictures (b) and (c) were taken by Sean Evans, while (d) was taken by Chris Oosthuizen. A modified hoop net (± 1 m diameter, ± 8 kg) was used to catch seals for deployment. The devices were attached, using a double-component, quick-setting epoxy resin (Araldite AW2101, CIBA-GEIGY Ltd), through an opening of the net created by opening a dorsal aperture in the cone of the net while the seal was physically restrained. 24

Figure 2.3: a) Schematic of a typical seal dive profile (black). The green segments within a dive are declared as 'foraging' segments according to the broken stick method (Heerah et al., 2014), while the rest of the time the seal is predicted to be in 'transit' mode. Blue bars indicate the amount of time spent hunting within a foraging segment. The foraging depth is calculated as the vARS depth using the mean depth of the longest foraging segment within a given dive. The post dive surface interval (grey bar) is the amount of time it takes for the seal to transit from when it surfaces above four metres after a dive until it dives again below four metres. The bottom phase of the dive is defined as that below 80% of the maximum depth. b) An example of an interpolated (solid red), a one second sampling rate (dotted red) and a five second sampling rate (dotted blue) downcast temperature profile. 27

Figure 2.4: Seasonal differences (summer - red, winter - blue) in maternal fur seal movements from two subantarctic fur seal colonies at Marion Island (black triangle). Data are overlaid on a bathymetry map with contours at 1000, 2000, 3500 and 5000 m depth. Summer is defined as between 15 October and 15 April and winter as between 15 April and 15 October. 38

Figure 2.5: Principal component analyses showing the contribution (contrib) [%] of diving and foraging effort variables to the first two dimensions in summer (a,c) and winter (b,d). The red line in c) and d) indicates the expected average contribution to variance per season according to the methods in Husson et al. (2017). The bottom effort (X.bt.dt), dive efficiency, dive residual (dive_res), vertical area-restricted search (vARS interchangeable with ht_rat and vertical foraging effort), dive duration (all.dur), maximum depth (max.d), post dive surface interval (pdsi) and horizontal area-restricted search (hARS) are all analysed within the PCAs. 40

Figure 2.6: Silhouette plots for summer (grey) and winter (black), illustrating the decreasing trend in average silhouette width [unitless] with increasing number of clusters (k). 41

Figure 2.7: Cluster plots of a) summer (grey) and b) winter (black), where the number of clusters (k) were given as two. 'Dim1' and 'Dim2' are dimensions 1 and 2 that explain the magnitude of variance represented in round brackets. The two clusters are named 'Divetype 1' and 'Divetype 2' and represent 'low effort' and 'high effort' dives. 42

Figure 2.8: Percentage of stratified profiles per hour of the day from 14:00 to 07:00 in a) summer and b) winter, along with boxplots of maximum depth per hour of the day [m] in c) summer and d) winter. The corresponding sample number of dives used for each hour

- based on local time of dives is indicated above points in (a) and (b). In summer, seals follow diel vertical migration to optimize energy-efficiency in prey capture. 44
- Figure 2.9: Diel patterns of vARS (vertical foraging effort) [%] (a,b) and maximum depth [m] (c,d) between stratified and mixed water masses in summer (a,c) and winter (b,d). 45
- Figure 2.10: Summer model smooth estimates for the partial effects of stability in mixed (a) and stratified (b) water and mean temperature (c) on behavioural response. The y-axis is scaled by the smooth function of explanatory variables and the model intercept is indicated by a horizontal dotted line. All plots are converted to the probability scale for interpretation from the log scale of model outputs. The vertical dotted line represents the mean for each scaled variable. The difference between mixed and stratified effects of stability are shown in (d). The horizontal dotted line signifies zero difference, while the vertical line indicates the centre of log-transformed and scaled stability. The grey bands represent 95% confidence intervals in all plots. The effective degrees of freedom are shown in brackets for each smooth function estimate. 48
- Figure 2.11: Winter model smooth estimates for the partial effects of stability [sec^{-2}] in a) mixed and b) stratified water and c) mean temperature [$^{\circ}\text{C}$] on dive type response. The y-axis is scaled by the smooth function of explanatory variables and the model intercept is indicated by a horizontal dotted line. All plots are converted to the probability scale for interpretation from the log scale of model outputs. The vertical dotted line represents the mean for each scaled variable. The difference between mixed and stratified effects of stability are shown in (d). The horizontal dotted line signifies zero difference, while the vertical line indicates the centre of log-transformed and scaled stability. The grey bands represent 95% confidence intervals in all plots. The effective degrees of freedom are shown in brackets for each smooth function estimate. 50
- Figure 2.12: Density plots of mean foraging depth minus mixed layer depth (MLD) [m] for summer (a) and winter (b) dives. Positive values illustrate dives with deeper foraging depth than MLD. Only dives where the maximum depth extends beyond the mixed layer (i.e. stratified water column) are represented. Blue lines associated with annotated numbers indicate 1 standard deviation from the mean difference (green). The mean differences were 10.1 and 7.6 m for summer and winter, respectively. The grey dotted line is a reference to zero difference between mean foraging depth and MLD. 53
- Figure 3.1: Bathymetry map (elevation in metres) obtained from the 'GEBCO_2020' global bathymetric gridded product released by the General Bathymetric Chart of the Oceans (GEBCO Compilation Group 2020) with a $1/240^{\circ}$ resolution. The location of the Prince Edward Islands is shown in relation to South Africa and large topographic features. 62
- Figure 3.3: A snapshot (1st June 2012) of a mesoscale stirring field (represented by Finite-Size Lyapunov Exponents [days $^{-1}$]) surrounding the Prince Edward Islands (white triangle). This depicts the variability in ocean flows surrounding the Prince Edward Islands..... 64
- Figure 3.4: Observations at Marion Island (black) of a) the mixed layer depth [m] and b) zooplankton biomass [ml DV m^{-3}] in the upper 100-300 m layer. These figures were adapted from Perissinotto et al. (2000) and the data were collected by ship measurements (black dots) between 7 and 19 April 1989. These figures illustrate the upstream and downstream variability of the region, and downstream effects on biological productivity... 67
- Figure 3.5: b) Distribution of 39 lactating subantarctic fur seals from Marion Island from 2009-2015 during summer and winter. Seal distributions (in black) are overlaid on a bathymetry map (elevation in metres) (GEBCO $1/240^{\circ}$ resolution grid). The mean (from 1993-2012) position of the sub-Antarctic Front (SAF) and the Polar Front (PF) are shown as white dotted lines, obtained from Park and Durand (2019), as well as the position of the Southwest Indian Ridge (SWIR) and Prince Edward Islands (PEI) region. c) A zoomed-in

map of the Prince Edward Archipelago. The two deployment colonies are Van den Boogaard beach and Mixed Pickle Cove. Seasonal a) latitudinal and d) longitudinal distributions of seal foraging trips, with blue dotted lines indicating the coordinates of the Prince Edward Archipelago. The area to the west of the islands is characterised in this chapter as ‘upstream’ and the area to the east as ‘downstream’.....	71
Figure 3.6: Seasonal distribution of temperature profiles collected by the 39 animal-borne loggers on 39 different diving seals from winter 2009 to the first summer months of 2015. The blue vertical line represents the first Julian day (‘JDay’) of the ‘winter’ period (15th April), while the red vertical line represents the first day of the ‘summer’ period (15th October), as defined in this dissertation.	72
Figure 3.7: Mean contribution of variations in heat (Temperature contribution [%]) to stratification over a constant depth range of 15 m, directly below the mixed layer base for summer (a) and winter (b). Mean stability ratio (R) is also plotted for summer (c) and winter (d) where values of $ R_p > 1$ indicate that heat contributes to stratification and values where $ R_p < 1$ indicates that salt contributes to stratification. Horizontal white lines represent the meridional extent of subantarctic fur seals (and thus available profiles) during this study, while the green triangles indicate the position of the Prince Edward Islands.	77
Figure 3.8: Time-mean winter (a,b) and summer (c,d) daily absolute surface geostrophic velocities from 2009-2015 at a 0.25° resolution. The zonal (a,c) and meridional (b,d) components are depicted with seasonal anomalies (winter-summer values) (e,f), with negative values representing higher mean summer velocities than winter. Positive zonal and meridional values indicate west to east and south to north flow, respectively. The position of the Prince Edward Islands is indicated by a small white triangle.	78
Figure 3.9: Seasonal climatology of winter (a) and summer (b) surface eddy kinetic energy (EKE) (m^2/s^2) from 2009-2015 at a 0.25° resolution, calculated using geostrophic velocity anomalies within the spatial extent of seal foraging trips. c) The seasonal anomaly (winter-summer values) of EKE is also presented. Negative values represent higher mean summer EKE than mean winter EKE. The Southwest Indian Ridge region (SWIR) (48.6–52.6 °S; 27–33 °E) and Prince Edward Islands (PEI) (white triangle - 44.6–48.6 °S; 35–41 °E) are indicated.	79
Figure 3.10: Hovmöller plots of daily surface eddy kinetic energy (EKE)[m/s] from 2009-2015 calculated as the a) mean EKE within the maximum extent of seal foraging trips, i.e. available profiles (42-52 °S; 20-50 °E), which overlap with the Southwest Indian Ridge region (48.6–52.6 °S; 27–33 °E) and PEI region (44.6–48.6 °S; 35–41 °E) defined by Lamont et al. (2020), and the b) mean EKE within the maximum extent of seal foraging trips in summer (45-49 °S; 32-45 °E), which overlaps only with the PEI region only. The longitudinal position of Marion Island is indicated by the blue vertical line in each plot, while vertical grey lines in (a) represent the longitudinal range in (b).	80
Figure 3.11: Time-mean (a,c) and standard deviation (b,d) of winter (a,b) and summer (c,d) Finite-Size Lyapunov Exponents (FSLE)[days ⁻¹]. The seasonal anomaly (winter-summer values) of time-mean (e) and standard deviation (f) of FSLE, where negative values indicate higher values in summer than in winter, are shown. Triangles represent the position of the Prince Edward Islands (PEI). Boxes represent the Prince Edward Island and Southwest Indian Ridge (SWIR) regions. Geographical areas of different levels of mixing activity and variation in mixing activity can be observed.	81
Figure 3.12: a) Seasonal distribution of absolute horizontal buoyancy gradients ($ b_x $) are presented along with b) winter and c) summer comparisons between upstream (orange) and downstream (green) $ b_x $ distributions averaged from 10-20 metres depth.....	83
Figure 3.13: Spatial distribution of summer mixed layer depth (MLD) (here labelled as ‘T dep’) for summers of 2011 (a), 2013 (b), 2014 (c) and 2015 (d). Data are gridded at a 0.1° spatial resolution. Grey cells indicate profiles that are insufficiently deep for MLD presence; here	

the mixed layer is deeper than the maximum depth of the gridded mean profile. The mean (from 1993-2012) position of the sub-Antarctic Front (SAF) and the Polar Front (PF) are shown as black dotted lines, obtained from Park and Durand (2019). Zero (grey cells) 'T dep' represents dives within well-mixed water masses where profiles are insufficiently deep for MLD presence. 84

Figure 3.14: Mean gridded (0.1°) mixed layer depth (MLD) for summer of 2012 are presented in (a). Grey cells indicate profiles that are insufficiently deep for MLD presence i.e. well-mixed. Mean temperature [°C] (red line) profiles with standard deviation (red shading) from upstream (n= 14170 dives) (b) and downstream (n=21396 dives) (c) dives are shown with mean (blue line) and standard deviation (blue shading) of the MLD. The mean maximum seal-derived profile depth upstream and downstream is shown by a green line. Vertical stability (Nt^2 [$1e^{-5}/s^2$]) changes with depth (mean \pm SD) upstream (d) and downstream (e) of the Prince Edward Islands are shown in red. Correspondingly, (f) and (g) illustrate the percentage of seal occurrence per depth bin (1 m). The mean (from 1993-2012) position of the sub-Antarctic Front (SAF) and the Polar Front (PF) are shown as black dotted lines, obtained from Park and Durand (2019). 86

Figure 3.15: Distributions of absolute horizontal buoyancy gradients ($|b_x|$) were compared between upstream (orange) and downstream (green), averaged from 10-20 metres depth. 87

Figure 3.16: Time evolution of mesoscale activity and stirring, upstream (west of 37° 45' E) and downstream (east of 37° 45' E) of the Prince Edward Islands. Hovmöller plot of daily surface mesoscale Eddy Kinetic Energy (EKE) [m^2/s^2] (a) and daily Finite-Size Lyapunov Exponents (FSLE) [day^{-1}] (b) averaged over the latitudinal extent of summer seal foraging trips (-49° to -45° latitude). The blue line represents the longitude of Marion Island (37° 45' E). 88

Figure 3.17: Graphs of summer gridded (0.1°) mean estimates presented for the period 2009-2015. Stratification [%] (a), stability [$1e^{-5}/s^2$] (c), and mean temperature (e) are the environmental variables used for comparison with spatial distribution of foraging effort in summer. Foraging effort is represented by mean (of maximums) depth [m] (b), vertical area-restricted search (vARS) [%] (d), and horizontal area-restricted search (hARS) [%] (f). Zero (grey cells) stratification and stability represents dives within well-mixed water masses where temperature ceases to change with depth within a given profile and does not necessarily indicate low stratification and stability, respectively. The position of Marion Island is represented by the black triangle, while the mean (from 1993-2012) position of the sub-Antarctic Front (SAF) and the Polar Front (PF) are shown as black dotted lines, obtained from Park and Durand (2019). The top text in each graph illustrates the mean (\pm SD) for each variable to the 'East' (i.e. Upstream) and the 'West' (i.e. Downstream) of the islands. 89

Figure 3.18: Graphs of winter gridded (0.1°) mean estimates presented for the period 2009-2015. Stratification [%] (a), stability [$1e^{-5}/s^2$] (c), and mean temperature (e) are the environmental variables used for comparison with spatial distribution of foraging effort in winter. Foraging effort is represented by mean (of maximums) depth [m] (b), vertical area-restricted search (vARS) [%] (d), and horizontal area-restricted search (hARS) [%] (f). The position of Marion Island is represented by the black triangle, while the mean (from 1993-2012) position of the Subtropical Front (STF), sub-Antarctic Front (SAF) and the Polar Front (PF) are shown as white dotted lines, obtained from Park and Durand (2019). The bottom text in each graph illustrates the mean (\pm SD) for each variable to the 'East' (i.e. Upstream) and the 'West' (i.e. Downstream) of the islands. 91

Figure 3.19: Geostrophic current velocities [$m \cdot s^{-1}$] from 1993 to 2016, and branches of the Antarctic Circumpolar Current fronts in relation to the Prince Edward Islands (PEI), with overlaid bathymetry, indicated in white (-3000 m, -2000 m, -1000 m). The Prince Edward Island region is indicated by a black square. This image is sourced from Toolsee et al.

(2021), who states 'The northern (N-SAF), middle (M-SAF), and southern (S-SAF) branches of the sub-Antarctic Front are represented by the dotted/solid/dashed black lines, respectively. The northern (N-APF), middle (M-APF), and southern (S-APF) branches of the Antarctic Polar Front are represented by the solid/dotted/dashed red lines, respectively.' ABFZ=Andrew Bain Fracture Zone, SWIR = Southwest Indian Ridge. 94

Figure 3.20: Winter (a) and summer (b) stratification. Grid cells represent the proportion of presence vs absence of a mixed layer depths in the profiles for that location. A total of 264670 and 82090 profiles were sampled in winter and summer, respectively. Total number of west (upstream) and east (downstream) profiles representing stratified water masses (proportion of stratified profiles relative to the number of profiles available to the west and east separately) indicated by text. Zero stratification indicates profiles that are insufficiently deep for MLD presence. The mean (from 1993-2012) position of the sub-Antarctic Front (SAF) and the Polar Front (PF) are shown as white dotted lines, obtained from Park and Durand (2019). 97

Figure 3.21: Case study showing a single subantarctic fur seal's (seal ID = 21) foraging track data in the summer of 2012. Mean along-track absolute horizontal buoyancy gradients ($|b_x|$) [$1-7/s^{-2}$], calculated between 10 and 15 m depth from seal-derived profiles, and corresponding (in space and time) surface Finite-Size Lyapunov Exponents (FSLE) [$days^{-1}$] are depicted in (a). Plots are zoomed into the 3rd (b,d) and 7th (c,e) foraging trips. Maps of cross-frontal (d) and along-frontal (e) trajectories of seal tracks are overlaid on FSLE averaged over the time extent of each respective foraging trip (typically ~8 days in summer). 102

List of tables

Table 2.1: Seasonal foraging trip- and dive-scale statistics of female subantarctic fur seal behaviour and upper ocean thermal structure from 2009-2015 deployments. Values are given as mean \pm SD. 'vARS' refers to vertical area-restricted Search - interchangeable with vertical foraging effort in this study. 39

Table 2.2: Seasonal mean (\pm SD) foraging and associated mixed layer properties between stratified and mixed water columns collected by seal-borne devices attached to subantarctic fur seals at Marion Island. Note, foraging (given by vertical area-restricted search) does not occur in all dives. Positive values of 'Difference between mean foraging depth and MLD' indicate deeper mean foraging depth than mixed layer depth (MLD). Maximum depth is always deeper than MLD and foraging depth. 43

Table 2.3: Summary of generalised additive mixed-effects model (GAMM) comparisons: GAMMs of a) summer and b) winter dive types proportions. The chosen model is in bold. "mean_Temperature" = mean temperature of the water column per dive; "Stratification" = categorical variable representing a mixed or stratified water column; "Stability" = vertical stability averaged throughout a dive; "AICc" = Akaike's Information Criterion corrected for finite sample sizes; " Δ AICc" = difference in AICc from that of the best fitting model; "R-sq (adj)" = Adjusted R^2 value; "REML" = Restricted maximum likelihood; "k" = Number of base functions used in the model. 46

Table 2.4: Parametric coefficients and approximate significance of smooth terms from generalised additive mixed-effects models (GAMMs). Summer and winter results are presented for comparison. "edf" = Expected degrees of freedom; "Ref.df" = Reference degrees of freedom. Test statistics are given as 'Z value' and 'Chi.sq'. 'log_Nt' = Vertical stability (Nt^2) on the log scale. 47

Table 2.5: Seasonal diving parameters associated with each dive type of female subantarctic fur seals from 2009-2015 deployments. 'vARS' refers to vertical area-restricted Search/vertical

foraging effort. Values are given as mean \pm SD. Scaled and centred differences are illustrated by the confidence interval (CI) of a Welch Two Sample t-test. CI values are therefore unitless. All differences were significant at $p < 0.001$. Parameters are sorted from largest to smallest differences between dive types. 51

Table 3. 1: Seasonal upstream and downstream differences in diving behaviour relative to thermal water column structure. Positive values of 'distance to MLD [m]' indicate deeper foraging depth than mixed layer depth (MLD), while negative values indicate the opposite. Values are given as mean \pm SD. 92

List of supplementary materials

- Supp.Figure 1: Broken stick model example dive by a seal at night. a) Gompertz model curve (red line) for the determination of the inflection point (red dot), describing the optimal number of broken stick points to adequately describe segments of 'wiggleness' (Heerah et al., 2014). b) Original (black line) and reconstructed dive profiles with red ('hunting') and blue ('transit') segments. 116
- Supp.Figure 2: Determining the sinuosity threshold (0.9) for the broken stick model. 116
- Supp.Figure 3: Quantile-quantile plots of deviance residuals against theoretical quantiles for a) summer and b) winter generalised additive mixed-effects models (GAMMs). Both models show a straight-line trend. 117
- Supp.Figure 4: Climatology of mixed layer depths (MLD) for summer (a,c) and winter (b,d) observations within the first 500 metres of the upper water column derived from objective analysis data. Means are presented for the spatial extent of seal foraging trips in summer (a,b) and winter (c,d), where foraging trips are further from the island in winter than summer. 117
- Supp.Figure 5: Histograms showing distributions of distances (Δx) [km] between mean temperature profiles per foraging trip in winter (a,b) and summer (c,d) downstream (green) and upstream (orange) of Marion Island for the calculation of horizontal buoyancy fluxes. The estimated time difference between profiles is shown in e). The dashed lines represent the 50th percentile of the data. 118
- Supp.Figure 6: The percentage of dives beyond the mixed layer in summer (a) and winter (b) grouped by sampling rate [sec]. The number of dives extending below the mixed layer are annotated beside each point on the graph (a,b). Vertical stability (Nt^2) [$1e^{-5}/\text{sec}^2$] was calculated from records deployed at various sampling rates for summer (c) and winter (d). Note that summer devices were set at 1, 5 and 10 seconds, while winter devices were set at 1, 2 and 5 seconds. 119
- Supp.Figure 7: Vertical stability (Nt^2) ($1e^{-4}/\text{s}^2$) downstream vs upstream of Marion Island calculated from 2012 summer and winter devices that were set up to sample temperature at 5 sec intervals only. The number of summer dives to the upstream. 119
- Supp.Table 1: Deployments on Subantarctic fur seals at Marion Island from 2009-2015. Deployments were 89 days long on average (min = 22 days, max = 276 days). 'ID' is the unique number given to each seal in the study. Seal 5 was deployed on twice. Major seal colonies on Marion Island have an associated site code (MM067 =Van den Boogaard, MM042=Mixed Pickle). In summer, individual seals either travelled west (upstream) or east (downstream) ('WE') of Marion Island. N/A values indicate foraging trips that cover both

upstream and downstream regions. Sampling rates for depth (Dive interval) and external temperature (Ext Temp) are given in units of seconds. 115

Chapter 1: General Introduction



A subantarctic fur seal pup warms up in the sun.

Biologging in the Southern Ocean

The Indian sector of the Southern Ocean (south of 40 °S), a remote and heterogeneous environment (Figure 1.1), spans approximately 10% of the world's ocean surface and plays an important role in supporting the global marine ecosystem (Grant *et al.*, 2006). In particular, the Southern Ocean is home to mobile marine mammals that roam the high seas for food. Since the start of biologging, the deployment of animal-borne loggers has revolutionized the study of marine diving mammals and the environments in which they forage (Fedak, 2004; Kooyman, 2004; Hussey *et al.*, 2015), by allowing for the collection of valuable data obtained from remote areas frequented by these animals (Treasure *et al.*, 2017). Collecting direct observations of prey consumption by marine top predators remains difficult due to the human limitations in assessing the isolated regions which these animals inhabit (Harcourt *et al.*, 2019). Similarly, the Southern Ocean is poorly monitored (Treasure *et al.*, 2017) and data-sparse (Chapman *et al.*, 2020) due to the costs involved with assessing this harsh environment. For example, ship measurements in the Southern Ocean are chiefly limited by hostile weather, ocean and sea-ice conditions that make ship operations slow, labour intensive, logistically challenging and expensive

(de Boyer Montégut *et al.*, 2004). Biologging therefore provides an opportunity for cost-effective Southern Ocean sampling (Fedak, 2004).

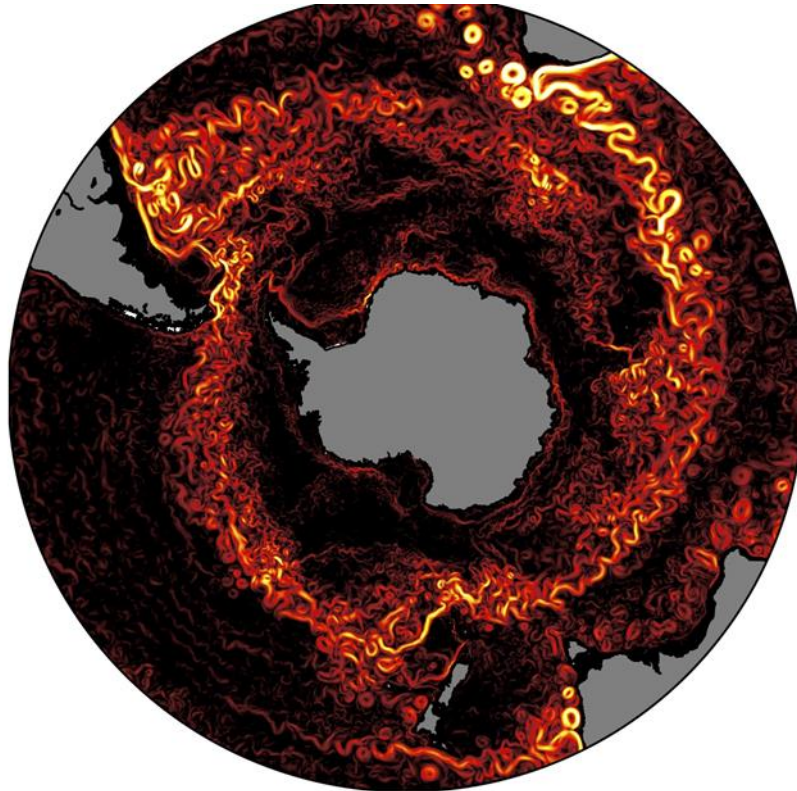


Figure 1.1: A depiction of the climate model CM2.6. surface speed throughout the Southern Ocean, emphasising the heterogeneity of ocean flows. This image is courtesy of Adele Morrison and is available at <https://stephengriffies.github.io>

Animal-borne loggers can record high spatial resolution (vertical ~ 1 m; horizontal < 5 km), *in situ*, simultaneous behavioural and physical oceanographic data (Harcourt *et al.*, 2019), contributing dramatically to the ocean observing system (Hindell *et al.*, 2008). This is advantageous for both biological and physical oceanographic studies (Ansorge, Durgadoo and Treasure, 2014; Treasure *et al.*, 2017), as well as studies relating physical oceanography to marine mammal movements (Carter *et al.*, 2016). Fine-resolution data has been recognized by the scientific community as a key missing link towards improving our understanding of the sensitivity of the Southern Ocean and its species to climate change. It has, therefore, been suggested that more studies are required to better understand the importance of physical oceanography on seal diving and foraging behaviours (Carter *et al.*, 2016).

Despite the lack of quantitative information of foraging success, foraging effort can be inferred from movement data (biotelemetry and biologging) and provides a temporal-spatial distribution of energy expenditure (Arnould, Boyd and Speakman, 1996; Arce *et*

al., 2019) without having to directly observe prey capture and consumption (Pirodda *et al.*, 2014).

Southern Ocean variability and impacts on biological productivity

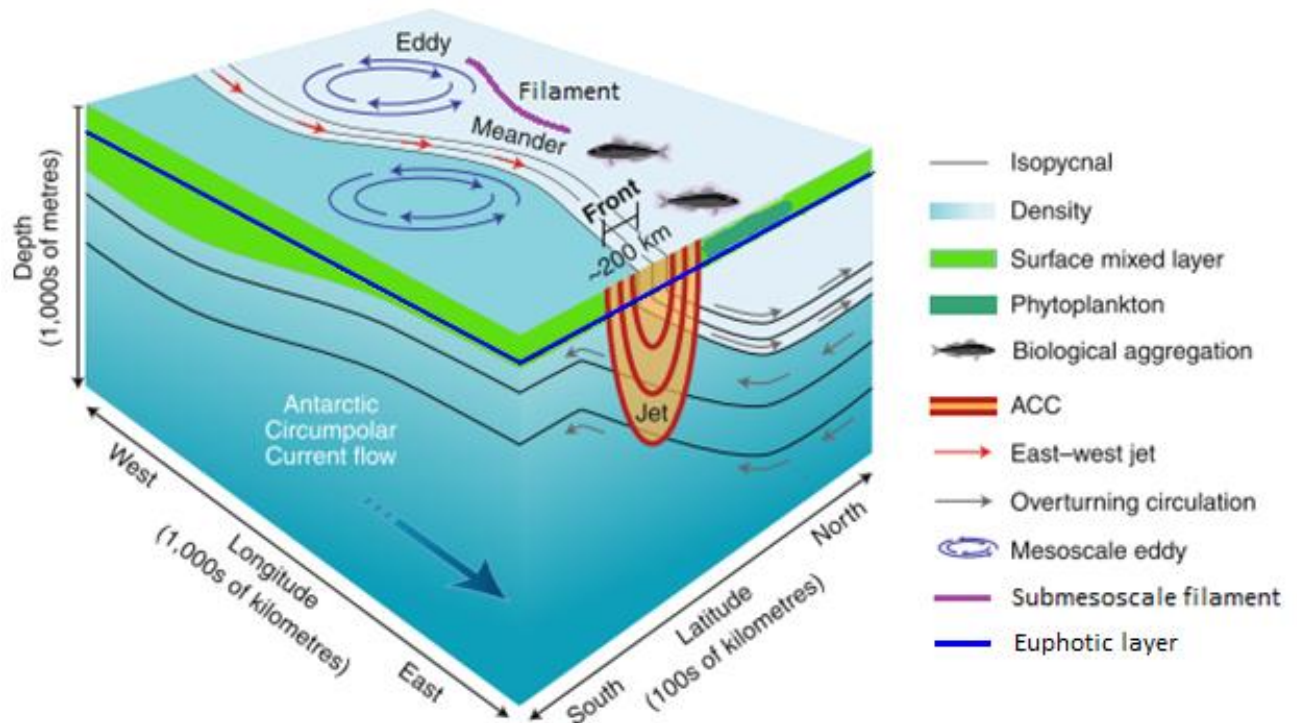


Figure 1.2: Illustration of physical and biological oceanographic features of an idealized Antarctic Circumpolar Current (ACC) front. At the front, a strong jet associated with the ACC flows from West to East and isopycnals slope towards the surface. The front is associated with horizontal mesoscale and submesoscale structures such as eddies and filaments. Adapted from Chapman *et al.*, 2020 with credit to Christopher Chapman and Louise Bell.

Marine environmental resources are generally patchy, and dynamic in nature (Stevick, McConnell and Hammond, 2002, Pinaud and Weimerskirch, 2005). The Southern Ocean is mostly low in nutrients with ephemeral spring phytoplankton blooms contributing substantially to Southern Ocean productivity (Smetacek and Nicol, 2005). The world's largest ocean current (Rintoul, Hughes and Olbers, 2001), the Antarctic Circumpolar Current (ACC), spans the Southern Ocean (Sokolov and Rintoul, 2007). Blooms predictably tend to occur within the ACC on island shelves, along surface geostrophic fronts, and edges of mesoscale eddies, when nutrients become available through interactions between the sea floor, water mass properties and the currents of the ACC (Moore and Abbott, 2000) (Figure 1.2). However, in the open ocean high biomass can be associated with relatively unpredictable physical ocean variability at a multitude of scales

(Stevick *et al.*, 2002). Understanding how abiotic factors drive the foraging ecology of marine top predators through bottom-up control could unravel clues for future foraging ecology of marine top predators and therefore the robustness and effectiveness of conservation management in the Southern Ocean (Leathwick, Elith and Hastie, 2006; Biuw *et al.*, 2007; Pirodda *et al.*, 2014), especially in the context of climate change and the consequent changes in ocean circulation and biogeochemistry.

Broad principal foraging strategies (e.g. seasonal, annual, within a lifetime) may include short-term decision-making components (e.g. dive, bout, foraging trip) (Bailleul *et al.*, 2008; Arthur *et al.*, 2016). Because marine environmental variability and associated ocean productivity is a function of scale (Stevick *et al.*, 2002), caution needs to be taken when assuming confined scales, both spatial and temporal, of mobile marine top predator foraging movements in telemetry studies (Pirodda *et al.*, 2014). Furthermore, Bailleul *et al.* (2008) illustrated that it is essential to include the vertical dimension when identifying the spatial scale of foraging areas of diving animals.

Marine diving predators have been shown to target predictable ocean features (Scales *et al.*, 2014) over various scales (Lévy *et al.*, 2012; Stevick *et al.*, 2002). These features hold favourable resources and attract prey (Bost *et al.*, 2009). Foraging seals from sub-Antarctic islands appear to target exceptionally productive mesoscale fronts and eddies (Biuw *et al.*, 2007; Bost *et al.*, 2009; Tosh *et al.*, 2012, 2015; Cotté *et al.*, 2015; Arthur *et al.*, 2016). Furthermore large-scale (>100 km) bathymetry and sea surface temperature fronts are predicted to have the largest impact on horizontal foraging movements of SAFS in the Southern Ocean (Beauplet *et al.*, 2004; De Bruyn *et al.*, 2009; Kirkman *et al.*, 2016; Georges *et al.*, 2018).

The Richardson number (Ri) indicates the preconditioning of water parcels to mix through turbulence and dictates stratification, while the Rossby number (Ro) indicates the relative importance of the rotation of the earth (Coriolis force) versus inertial forces in ocean flows (Boccaletti, Ferrari and Fox-Kemper, 2007). Flows are distinguished as mesoscale by low ($\ll 1$) Richardson and Rossby numbers. These strong surface currents (Klein and Lapeyre, 2009) typically occur at lateral length scales of 100-200 kilometres (mesoscales), timescales of a few weeks, and are steered by the balance between Coriolis and pressure gradient forces. More than half of the ocean variability in flows is contained in eddies which are mesoscale (100-200 km across), deep reaching (>800 m)

(Orsi, Whitworth and Nowlin, 1995; Asdar, 2018), and most of which are non-linear (Chelton *et al.*, 2007). These eddies can be generated by baroclinic instabilities along topographic ridges and barotropic instabilities as flows interact with ridge topography (Asdar, 2018). Eddies in the surrounding waters of the PEI are mostly shed (pinch off) from frontal meanders (Chown and Froneman, 2008; Lamont and van den Berg, 2020).

These intense eddy structures are associated with high mesoscale and submesoscale turbulence and are dissipated irregularly throughout the ACC region (Asdar, 2018). Furthermore, high mesoscale activity in the form of eddy kinetic energy (EKE) is higher in summer than in winter in simulations throughout the global ocean (Uchida *et al.*, 2017) and observed within the PEI region (Asdar, 2018). Although mesoscale activity has large intra- and inter-annual variability within the PEI region, EKE has decreased over the last few decades, associated with the southward shift of the sub-Antarctic Front and the Polar Front (Asdar, 2018; Billany *et al.*, 2010).

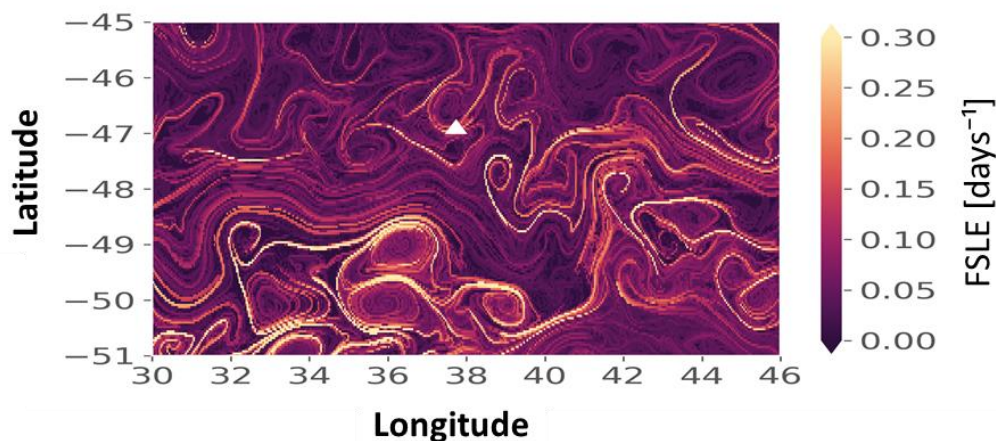


Figure 1.3: A snapshot (1st June 2012) of a mesoscale stirring field (represented by Finite-Size Lyapunov Exponents [days⁻¹]) surrounding the Prince Edward Islands (white triangle). This depicts the variability in ocean flows surrounding the Prince Edward Islands.

In the upper ocean, mesoscale stirring (see example in Figure 1.3) generates a field of submesoscale ocean filaments associated with gradients of all ocean tracers, including temperature. These filaments evolve into horizontal buoyancy/density gradients in a process called frontogenesis (Lévy *et al.*, 2012). Upper ocean baroclinic instabilities grow as baroclinic waves along submesoscale fronts (Boccaletti *et al.*, 2007) and can rearrange horizontal buoyancy gradients associated with fronts to vertical stratification (Fox-Kemper, Ferrari and Hallberg, 2008). This is done through an ageostrophic secondary

circulation, where the more-buoyant side of the front is upwelled over the denser side (Fox-Kemper *et al.*, 2008).

Submesoscale flows deviate from the balance between Coriolis and pressure gradient forces through inertial and centrifugal force dominance and are confined to horizontal length scales of 1-10 kilometres and time scales of hours to days (Fox-Kemper *et al.*, 2008). Moreover sharp submesoscale fronts are represented by Richardson and Rossby numbers approaching $O(1)$ (Boccaletti *et al.*, 2007; Thomas, Tandon and Mahadevan, 2008; Siegelman *et al.*, 2020). Submesoscale dynamics generate vertical velocities as large as hundreds of metres per day (Lodise *et al.*, 2020). They arise in the upper ocean through the intensification of fronts and other instabilities, but are impacted by buoyancy fluxes (e.g., cooling) and frictional effects (e.g., wind stress) at the ocean's surface or bottom boundary (Lévy *et al.*, 2012). Such processes are particularly prevalent in the upper ocean and have changed our understanding of how the upper ocean communicates with the interior and evolves its density structure and stratification.

In the upper ocean, submesoscale turbulence is stronger in winter than in summer (Callies *et al.*, 2015; Buckingham *et al.*, 2016). Enhanced submesoscale features in winter, which are set by buoyancy losses and wind stresses, have been found to sustain winter mesoscale eddy structures and EKE (Sasaki *et al.*, 2014). (Sub-)mesoscale stirring processes are related to the strain rate of flows and can therefore be measured in the ocean using satellite remote-sensed Finite Size Lyapunov Exponents (d'Ovidio *et al.*, 2009), representing submesoscale filaments. Primary productivity is enhanced at these submesoscale filaments (D'Ovidio *et al.*, 2010; Lévy *et al.*, 2012; Mahadevan, 2016), supporting predictable prey patches for diving marine predators throughout the Southern Ocean (Nordstrom *et al.*, 2012; Benoit-Bird *et al.*, 2013; Lowther *et al.*, 2014; Cotté *et al.*, 2015; Whitehead *et al.*, 2016; Siegelman *et al.*, 2019).

The Prince Edward Islands: Importance, physical oceanography and ecology

The Prince Edward Islands (46° 54' S, 37° 45' E) (PEI) (Marion Island and Prince Edward Island) are of particular importance to the Southern Ocean system due to their pristine state (Ansorge and Lutjeharms, 2007), sensitivity to climate-scale perturbations (Ansorge *et al.*, 2014) and profitable surrounding ocean dynamics (Durgadoo *et al.*, 2008).

Moreover, the declaration of a special Marine Protected Area (MPA) in 2013 in the Exclusive Economic Zone of the islands has served to protect and conserve the flora and fauna of the islands and surrounding waters (Lombard *et al.*, 2007), including the marine top predators who forage within these waters (Reisinger *et al.*, 2018). The MPA aims to contribute to the ongoing global initiatives towards marine protection (Lombard *et al.*, 2007).

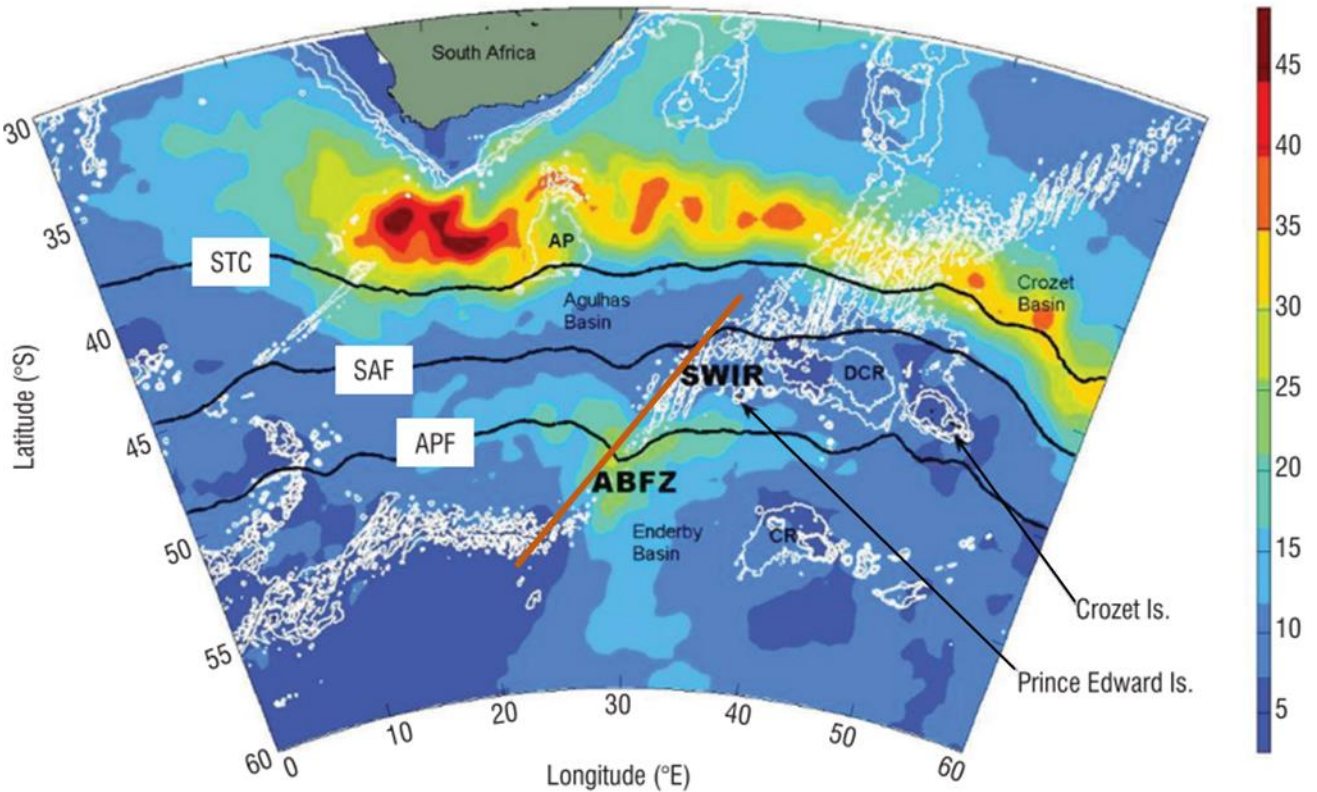


Figure 1.4: The root mean square values of sea level anomaly [cm] derived from 13 years of altimetry shows eddy variability associated with the Agulhas Retroflection and the Southwest Indian Ridge (SWIR). This image is sourced from Durgadoo *et al.* (2010). The location of the Prince Edward Islands is shown in relation to South Africa and large topographic features, indicated in white (-3000 m, -2000 m, -1000 m) and labelled in black. The average positions of the Antarctic Circumpolar Current fronts, the Subtropical Convergence (STC), sub-Antarctic Front (SAF), and the Antarctic Polar Front (APF), are indicated (black line). The Andrew Bain Fracture Zone is the core of the variability along the SWIR (indicated by the orange line). The position of the Abyssal Plane (AP), Del Cano Rise (DCR), Conrad Rise (CR), and three major basins are also shown.

These islands are located in the roaring forties and north of the furious fifties (Froneman *et al.*, 1999) and are located in the path of the ACC within the Polar Frontal Zone (Lutjeharms and Valentine 1984; Lutjeharms, Walters and Allanson, 1985). The ACC, often referred to as the 'West Wind Belt' (Ansorge and Lutjeharms, 2007), is driven by the strong and persistent westerly wind belt, and is responsible for most of the Southern

Ocean zonal transport (Hofmann, 1985; Ansorge and Lutjeharms, 2007). The sub-Antarctic Front and Polar Front form two major fronts of this intense eastward-flowing current (Chapman *et al.*, 2020), with the sub-Antarctic Front situated to the north of the islands and the Polar Front to the south (Orsi *et al.*, 1995; Rintoul *et al.*, 2001) (Figure 1.4). These fronts are responsible for most of the Southern Ocean zonal transport (Hofmann, 1985; Ansorge and Lutjeharms, 2007) and weak and deep stratification (Rintoul and Garabato, 2013). These fronts are not zonally coherent, but rather consist of a braided pattern of multiple eddies, filaments, and jets (Sokolov and Rintoul, 2007; Chapman *et al.*, 2020), which are characterised by strong lateral temperature, salinity, and density gradients (Bost *et al.*, 2009; Chapman *et al.*, 2020). In the location of the PEI, the mean current flow of the ACC and its eddies are steered by bottom topography (Ansorge and Lutjeharms, 2007; Asdar, 2018; Lamont and van den Berg, 2020).

When the ACC passes over a topographic feature known as the Andrew Bain Fracture Zone of Southwest Indian Ridge, to conserve potential vorticity, relative vorticity changes (Hogg, 1973; Moore, Abbott and Richman, 1999), resulting in the generation of mesoscale eddies (Figure 1.4). These eddies are known to be transported towards the islands by the advective forces of the ACC (Ansorge and Lutjeharms, 2002, 2005). However, very few eddies produced here have been observed to reach the PEI region and are instead trapped within the polar frontal zone (Ansorge *et al.*, 1999; 2000; Lamont and van den Berg, 2020) with relatively small (<150 km) eddy propagation distances from their source. Nevertheless, the Prince Edward Island's ecosystem benefits from their position downstream of the eddy corridor (Durgadoo, Ansorge and Lutjeharms, 2010; Ansorge *et al.*, 2014). Enhanced mesoscale variability associated with the corridor could be increasing local primary productivity within the Polar Frontal Zone (Ansorge *et al.*, 1999), affecting the community composition of zooplankton and the distribution of food to Marion's top pelagic predators (Pakhomov and Froneman, 1999; Pakhomov and Chown, 2003). Thus, the dynamics of ocean surface fronts and mesoscale eddies in this part of the Southern Ocean are a key component in understanding the ecosystems of the islands (McQuaid and Froneman, 2004).

The PEIs have been considered as sentinels to climate change (Ansorge *et al.*, 2014). There is considerable temporal variability associated with the meridional extent of the ACC fronts over intra- (monthly) and inter-annual (yearly) time scales in their position in the PEIs region (Chown and Froneman, 2008; Hunt, Pakhomov and McQuaid, 2001),

related to atmospheric oscillations such as the Southern Annular Mode (SAM), sub-Antarctic Oscillation (SAO) and ENSO (El Niño Southern Oscillation) (Tosh *et al.*, 2015; Asdar, 2018). However, an *in situ* climatological rise in sea surface temperatures in the Southern Ocean of >1 °C since the 1950s (Mélise *et al.*, 2003; Ansorge *et al.*, 2014) and the historical (backward >50 years) and expected (forward >100 years) long-term southward shift of the ACC fronts (Turner *et al.*, 2014; Asdar, 2018), along with the possibility of enhancing eddy kinetic energy (EKE) within the PEI region (Lamont *et al.*, 2019), is predicted to have implications for marine species distributions (Turner *et al.*, 2014), foraging ecology (Bost *et al.*, 2015; Carpenter-Kling *et al.*, 2019) and demography (Tosh *et al.*, 2015; Massardier-Galatà *et al.*, 2017) of central place foragers, as well as Southern Ocean productivity as a whole (Ansorge *et al.*, 2014). These factors are all thought to be modulated by climate model predictions of an underlying long-term increase in zonal wind stress which drives the ACC (Fyfe and Saenko, 2006). The PEI ecosystem is therefore ideally positioned to enable the identification and monitoring of the impacts of climate change (Ansorge *et al.*, 2014; Constable *et al.*, 2014).

Top predators play a critical role in marine ecosystem function, structure and dynamics through trophic interactions and the abiotic factors that may be influencing them (Phillips and Harvey, 2009; Kirkman *et al.*, 2019). The complex interactions between the seals at-sea behaviour and the physics of the surrounding environment therefore has an influence on the ocean ecosystem surrounding the PEI (Ansorge and Lutjeharms, 2000). With a changing climate affecting the PEI and surrounding environment (Smith, 2002; Ansorge *et al.*, 2014; Turner *et al.*, 2014; Asdar, 2018) greater understanding of seal foraging ecology may aid in the development of improved conservation management and policy (Lombard *et al.*, 2007; Kirkman *et al.*, 2016; Taylor *et al.*, 2011).

Upper ocean dynamics and impacts on biology: Turbulent mixing and the MLD

The upper ocean layer is associated with turbulence and is largely characterised by vertical gradients in physical ocean properties that are set by active mixing through atmospheric forcing (wind stress) and the stabilizing effect (slumping) of energy dissipation through buoyancy fluxes (Rudnick and Martin, 2002; Maes and Kane, 2014).

Temperature and salinity changes in the vertical each contribute to vertical density changes and therefore the vertical positioning of the seasonal and permanent pycnocline, the depth of maximum vertical density change. The magnitude of each contribution varies throughout the global ocean (Stewart and Haine, 2016). The pycnocline lies below the mixed layer, a layer defined by homogenous temperature and salinity, and thus density, in the vertical plane. In an ocean where vertical temperature and salinity changes contribute equally to vertical density changes, temperature and salinity compensate each other in their effects on density, i.e. as temperature decreases with depth, salinity would increase to keep density constant. However, the upper ocean surrounding the PEIs can be characterised as an alpha ocean, where waters are predominantly stratified by temperature, instead of salinity (Stewart and Haine, 2016), i.e. salinity effects are too small relative to temperature effects to be the primary influence on density change.

The mixed layer depth (MLD) is an important oceanographic and biological parameter (Kara, Rochford and Hurlburt, 2000; Thompson, Moss and Lovell, 2003; Dong *et al.*, 2008; Roquet *et al.*, 2013; Lowther, Lydersen and Kovacs, 2015; Pellichero *et al.*, 2017). It controls vertical fluxes of nutrients, heat, carbon and momentum between the atmosphere and the ocean interior (Thomas *et al.*, 2008; Sallée *et al.*, 2021). Ocean stratification, the layering of the ocean, can therefore modulate the vertical distribution of tracer properties which are required for marine biological productivity, directly impacting phytoplankton blooms when phytoplankton growth is limited by light (Swart, Thomalla and Monteiro, 2015). Diving marine top predators are known to target different layers in the water column, following dynamic, but predictable prey patches. At Southern Ocean fronts and eddy edges predators, such as southern elephant seals, tend to dive in and below the thermocline where foraging success (i.e. catches per unit effort) is high (Bost *et al.*, 2009). Although the strength of the thermocline does not appear to influence diving behaviour of Northern fur seals, they are thought to forage at depths which are in close association with the thermocline depth (Kuhn, 2011; Benoit-Bird *et al.*, 2013) 2013) and the MLD (Pelland *et al.*, 2014). Harbour seals and southern elephant seals have also been shown to target the MLD (Boyd and Arnborn, 1991; Blanchet *et al.*, 2015).

Topographic influences on upper ocean dynamics and marine top predator behaviour

Phytoplankton production decreases longitudinally from the Antarctic Peninsula to islands in the Indian Ocean sector of the Southern Ocean (Perissinotto, Laubscher and McQuaid, 1992). Localized regions of downstream blooms may act as biological hotspots in this vast desert ocean environment (Perissinotto *et al.*, 1992; Venables, Pollard and Popova, 2007). The interaction of the ACC with the PEI bathymetry produces an island mass effect (Boden, 1988; Treasure *et al.*, 2015), a downstream periodic enhancement of phytoplankton biomass, that is found throughout the Southern Ocean where the ACC interacts with small islands (Sergi *et al.*, 2020). Topographic disturbance of geostrophic currents increases submesoscale activity at the PEI (Perissinotto, Lutjeharms and Van Ballegooyen, 2000) (Figure 1.5), enhancing downstream turbulence and shoaling of the MLD. A downstream zone of enhanced productivity and prey (Koubbi *et al.*, 2011) has had cascading effects on higher trophic levels. Southern elephant seals, for example, have been found to use downstream phytoplankton plumes (O'Toole *et al.*, 2017) as foraging 'hotspots'.

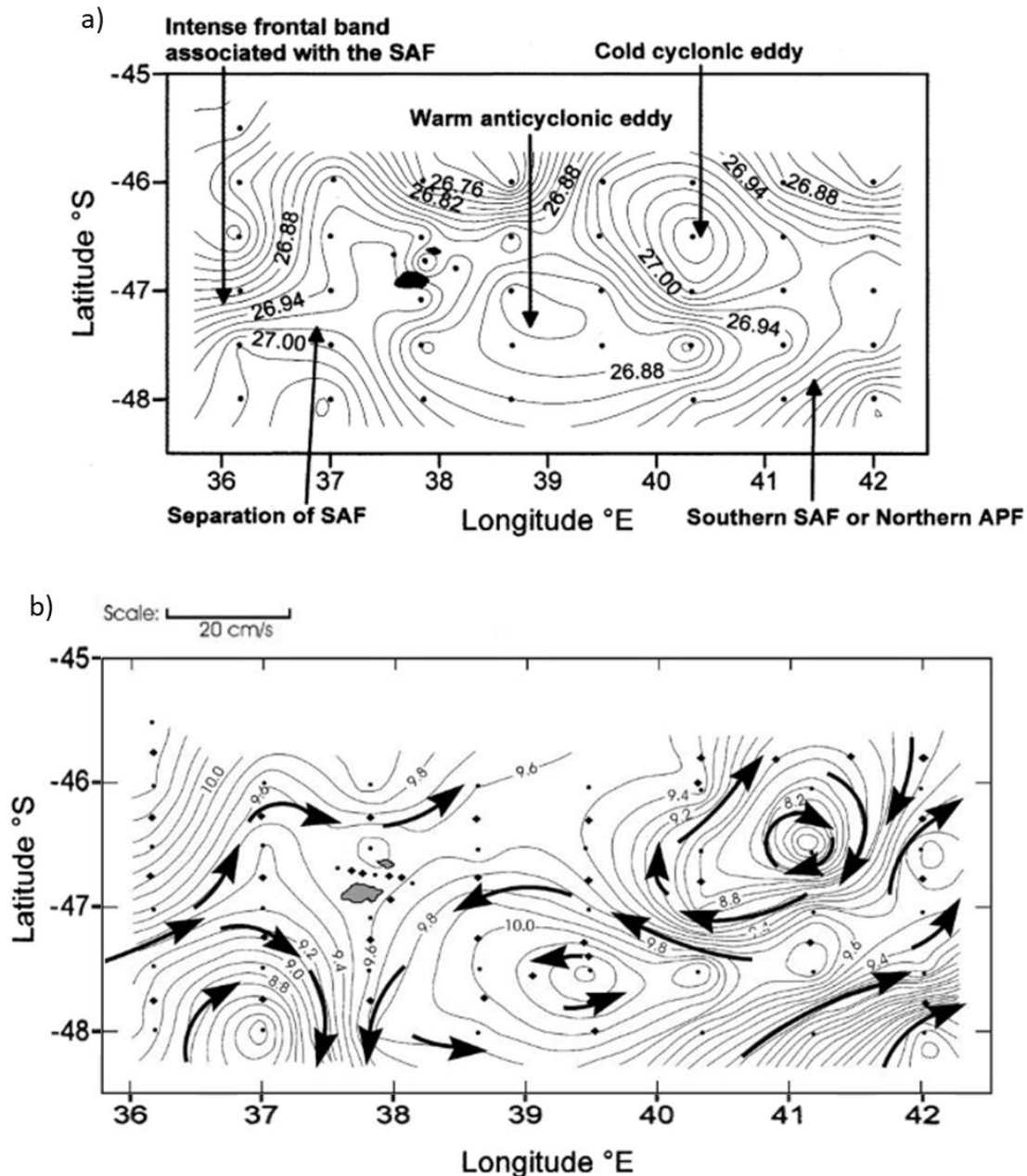


Figure 1.5: Observations at Marion Island (black shaded region in (a) and grey shaded region in (b)) of a) density ($\text{kg}\cdot\text{m}^{-3}$) at 200 metres depth and b) dynamic height (at 0 db referenced to 1500 db) with overlaid surface geostrophic velocities. These figures were adapted from Ansorge and Lutjeharms (2002) and the data were collected by ship measurements (black dots) during the a) Marion Offshore Ecological Study 2 in 1989 and the b) Marion Island Oceanographic Survey 2 in 1997. These figures illustrate the upstream and downstream variability of the region.

The flow regime downstream of the PEI is complex and dynamic (Ansorge and Lutjeharms, 2002). The PEIs may form important local restrictions to the flow of the dominant ACC (Chown and Froneman, 2008). Based on phytoplankton community structure, Pakhomov *et al.* (2000) showed that the disturbance of the ACC flow around the PEIs may induce meridional mesoscale mixing in the downstream region of the islands. Asdar (2018) has shown evidence for long-term (8-year means) downstream

eddy dissipation over a large-scale (35-47 °E) using idealised regional simulations. No studies have further investigated the topographic effects of the PEI on downstream submesoscale processes and its impacts on marine top predator ecology.

Subantarctic fur seal foraging ecology at Marion Island

Marion Island is inhabited by three species of seals (Pinnipeds). Two species of fur seals, Antarctic fur-seals (*Arctocephalus gazella*) and Subantarctic fur seals (hereafter referred to as SAFS) (*Arctocephalus tropicalis*), share the beaches with southern elephant seals (*Mirounga leonina*) (Chown and Froneman, 2008). This is the largest sympatric population of Antarctic and subantarctic fur seals in the world (Hofmeyr *et al.*, 2006; Reisinger *et al.*, 2018). Fur seals are members of the family Otariidae, who are distinguished by their external ear spinae (Hofmeyr and Bester, 2018). They are well adapted to cold environments with a thick, insulating underfur layer and are mobile on land, with the ability to turn their hind limbs forward, and at sea, using their flippers to propel themselves through the water (Hofmeyr, 2015).

Fur seals were historically (from the 1800's) exploited for their pelts (skin and fur), but populations recovered worldwide to about 400 000 individuals in the early 2000s (Chown and Froneman, 2008; Hofmeyr, 2015). The population at Marion Island increased steadily from 1981 to the early 2000s (Hofmeyr *et al.*, 2006). Although, the pup population declined by 46% from 2004 to 2013 (Wege *et al.*, 2016), it remained at an estimated ~8500 pups from 1989 to 2015 (Hofmeyr *et al.*, 2016). Currently, the cause for the decline between 2004 and 2013 is unknown, and further research is ongoing with focus on possible future trends (Hofmeyr *et al.*, 2016). The Prince Edward Islands cumulatively support approximately 30% of all SAFS and about 25% of global pup production (Hofmeyr *et al.*, 2006; Wege, 2013). With the introduction of animal-borne sensors, a continuous data record has been established by the Marion Island Marine Mammal Programme for purposes of foraging ecology studies, thus improving our understanding of observed population trends (Bester *et al.*, 2011).

SAFS exhibit sexual dimorphism, with larger males (~70-165 kg) than females (~25-67 kg) (Hofmeyr, 2015). Pups weigh about 4 kg at birth on average and grow rapidly within the first 200 days (Kerley, 1985). Adults breed on land and are polygynous, i.e. males mate with more than one female. Females reach sexual maturity at the age of five (Bester,

1995). The males are territorial and fight for their beach territory and subsequent females (Bester, 1981). The median pupping date is the 18th December (Hofmeyr *et al.*, 2007). SAFS females lactate and nurse their pups from December to October (~300 days) (Wege *et al.*, 2019). They are carnivorous and those at Marion Island feed mainly on myctophid fish, followed by small amounts of cephalopods (squid) (Klages and Bester, 1998; Makhado *et al.*, 2013). Mesopelagic myctophid fish dominate the oceanic zone in the Southern Ocean (Koubbi *et al.*, 2011).

Females must feed during the lactation interval to provision for both themselves and their pups. A major downfall to this evolutionary strategy is the need for favourable foraging conditions over the lactation interval when feeding ranges become limited by pup fasting ability (Wege, 2013). As central place foragers, SAFS females make short foraging trips (six to 12 days) in early summer soon after giving birth, during which pups fast until the female returns with milk to suckle (Kirkman *et al.*, 2002; Wege *et al.*, 2014). These short trips increase nutrient and energy investment in the pup (Georges and Guinet, 2000). The foraging trips slowly become longer as the pups grow and their ability to store more energy, thus fasting for longer, increases. By the end of the lactation period, foraging trips are 20-40 days in length (Kirkman *et al.*, 2002; Wege *et al.*, 2014). At high density colonies at Marion Island, SAFS also make intermittent overnight foraging trips. Although it remains unclear as to the purpose of overnight foraging trips (Luque *et al.*, 2007), it is thought that these trips act as an extra supplement for the lactating females themselves, instead of for the benefit of their pups (Wege, 2017). After 10 months (mid-October) the pups are weaned and no longer depend on their mother for milk (Kerley, 1985). Breeding females are, thereafter, free to forage away from the island until mid-December when they may give birth again.

With the introduction of animal-borne sensors, a continuous data record of environmental and biological metrics has been established by the Marion Island Marine Mammal Programme for purposes of foraging ecology studies (Bester *et al.*, 2011), and for the purpose of ocean observation (Treasure *et al.*, 2017). Marion SAFS mostly dive at night (Wege, 2013). Seasons influence the diving behaviour of these SAFS (Wege, 2017), with deeper and longer dives in winter relative to summer (Wege, 2013), like SAFS at Amsterdam Island (Georges, Tremblay and Guinet, 2000). Longer night durations in winter allows for increased opportunities for feeding (Arthur *et al.*, 2016). At smaller temporal scales, the diel cycle has had a strong influence on maximum dive depth, dive

duration and dive effort of SAFS at Marion Island (Wege, 2017). In summer, Marion SAFS are thought to follow the diel vertical migration of their prey (myctophid fish). However, drivers of winter diel patterns in diving behaviour have remained unclear (Wege, 2013, 2017).

Kirkman *et al.* (2016) used horizontal area-restricted search methods to investigate suitable foraging areas for SAFS on neighbouring Prince Edward Island and found that the most important factors for predicting suitable foraging habitat were maximum distance from the colony, longitude, and distance from the sub-Antarctic Front. Large lateral-scale (>100 km) bathymetric features and sea-surface height anomalies appear to be important foraging areas for Marion SAFS (De Bruyn *et al.*, 2009). Although sea surface temperature fronts, such as the sub-Antarctic Front, have been shown to be areas of enhanced primary productivity (Lutjeharms, Walters and Allanson, 1985; Hunt *et al.*, 2001), greater abundance of zooplankton (Pakhomov, Perissinotto and McQuaid, 1994; Hunt and Hosie, 2005), fish, squid and other top marine predators (Beauplet *et al.*, 2004), they do not appear to be of great importance to SAFS foraging movements (de Bruyn *et al.*, 2009; Wege *et al.*, 2019). However, habitat modelling showed that the relative contributions of bathymetry and sea surface temperature gradient were the largest to subantarctic fur seal distributions (Taylor *et al.*, 2011). Furthermore, sharp SST gradients (fronts) are associated with bathymetric features along SAFS seal tracks (Taylor *et al.*, 2011). The upwelling of nutrients is localized where ocean fronts and bathymetry interact throughout the Southern Ocean (Chapman *et al.*, 2020). In contrast to these findings, Wege *et al.* (2019) used Boosted Regression Tree species distribution models to suggest that, at the >100 km horizontal scale, latitude, longitude, and current speeds influence horizontal area-restricted search of Marion SAFS, while other environmental variables, such as bathymetry, sea surface temperature and sea surface height are not as important in predicting their lateral movements. No studies at Marion Island have focussed on both vertical (diving) and horizontal foraging behaviour at fine vertical (~1 m, <10 sec) and horizontal (<10 km, <24 hr) scales.

Dissertation structure, aims and objectives

Interpreting foraging strategies of central-place foraging marine mammals in relation to the marine habitat relies on the time and space scale considered (Pinaud and

Weimerskirch, 2005, 2007; Pirotta *et al.*, 2014). In this study, I aimed to identify horizontal and vertical (three dimensional) patterns of habitat use across multiple spatial and temporal scales of foraging behaviour of SAFS at Marion Island. The overarching objective of this dissertation was to investigate the influence of upper ocean thermal structure on fine-scale (~1 m, <10 sec) diving and foraging behaviour of female lactating SAFS, and seasonal links to impacts of small-scale topography on the meso- to submesoscale ocean variability both up- and downstream of the Prince Edward Island. This work was done at two Marion Island SAFS colonies: Van den Boogaard beach on the east and Mixed Pickle Cove on the west. The main objectives were achieved through the acquisition of seal-borne and satellite data.

The dissertation is organised into four research chapters, with chapters 2 and 3 addressing key objectives. I wrote chapters 2 & 3 as independent manuscripts for publication. As such, some repetition was unavoidable, especially within the methods sections. A brief outline for each chapter and their associated aims and objectives is presented below.

Chapter 2

Chapter 2 aims to investigate the influences of upper ocean thermal structure on fine-scale (<1 m, <10 sec) foraging and diving behaviour of SAFS per dive.

Main objectives:

- (1) Identify and describe the distinct types of dives made by SAFS representative of diving and foraging behaviour in three-dimensional space.
- (2) Assess the influence of vertical water column mixing in the upper ocean on Marion SAFS diving behaviour over seasonal and diel time scales.
- (3) Determine whether fine-scale diving and foraging behaviour is modulated by the upper ocean thermal structure.

Findings from chapter 2 sets up the knowledge base for the foraging ecology section of chapter 3.

Chapter 3

Chapter 3 aims to provide comprehensive evidence for topographically enhanced downstream submesoscale variability and associated restratification. Additionally, if evidence is found, I investigated the impact, whether direct or indirect, of this

phenomenon on SAFS fine-scale foraging behaviour over large temporal (seasonal) and spatial (>500 km) scales.

Main objectives:

(1) describe the topographic influence of the Prince Edward Islands on meso- (100-200 km, days to weeks) and submesoscale (1-10 km, hours to days) ocean variability, and upper ocean thermal structure (<1 m, <10 sec), and (2) assess differences between seasonal climatologies of upstream versus downstream foraging and diving behaviour of SAFS.

Chapter 4

I summarise Chapter 2 and 3 and suggest a way forward for better understanding marine top predator foraging ecology and Southern Ocean submesoscale variability.

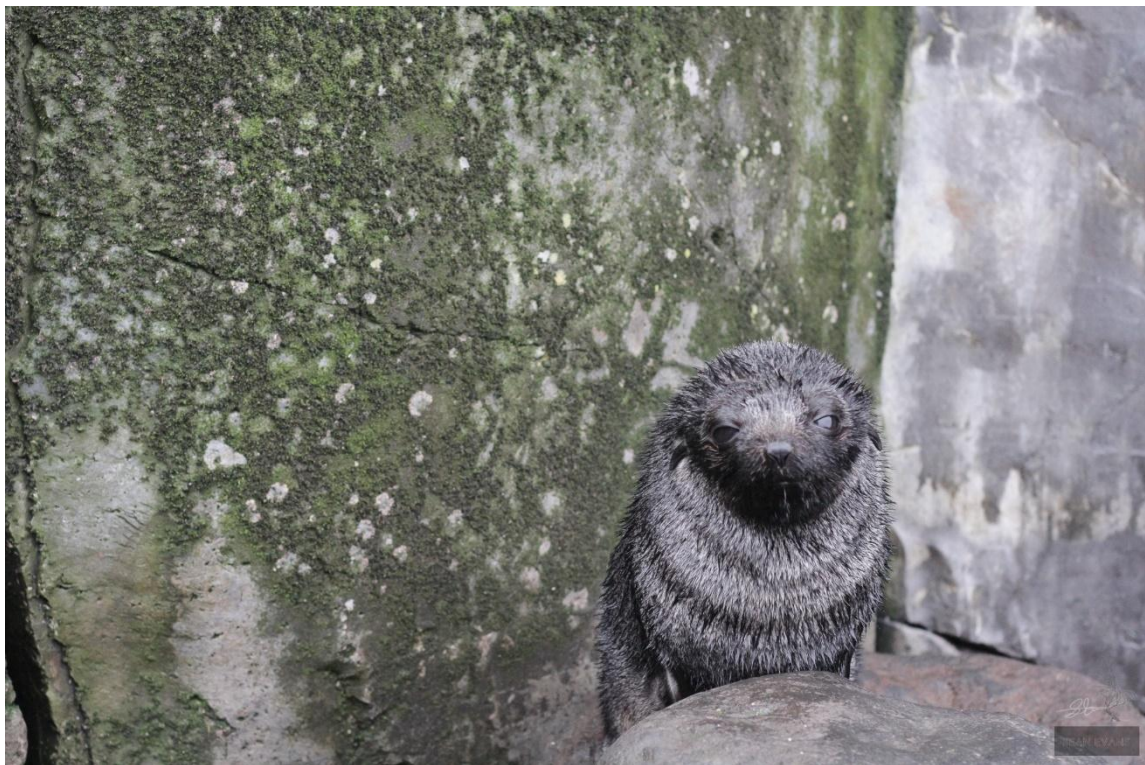
All references are included in a single list at the end of the dissertation.

Chapter 2: Influence of upper ocean thermal structure on diving and foraging behaviour of subantarctic fur seals at Marion Island: A fine-scale study using on-board data loggers.

Mr S. Evans¹, Dr M. Wege², Dr M. du Plessis^{1,3}, Prof. I. Ansorge¹, Dr A. Lowther⁴, Ass. Prof. N. de Bruyn².

¹Department of Oceanography, University of Cape Town, South Africa; ²Department of Zoology & Entomology, University of Pretoria, South Africa; ³Department of Marine Sciences, University of Gothenburg, Sweden; ⁴Norwegian Polar Institute, Norway.

This chapter should be cited as: Evans, S. (2021) 'Influence of upper ocean thermal structure on diving and foraging behaviour of subantarctic fur seals at Marion Island: A fine-scale study using on-board data loggers', *In Prep. Mar Ecol Prog Ser.*



A subantarctic fur seal pup waits for its mother's return from a foraging trip out at sea

Abstract

Observing the fine-scale (<1 m, <10 sec) foraging behaviour of fur seals in relation to their environment in the Southern Ocean was formerly difficult due to their geographic isolation and marine habitats. *In situ* data collected by 39 animal-borne telemetry devices fitted to adult female *A. tropicalis* from 2009-2015 at Marion Island were used to investigate the effect of upper ocean thermal structure on diving and foraging behaviour. Seasonal and diel trends of foraging effort were investigated and compared to upper ocean thermal structure. Dives were distinguished using the Clustering for Large Applications (CLARA) algorithm according to vertical movements made by seals. High effort dives differentiated from low effort dives, primarily based on bottom effort. High effort dives, associated with high vertical foraging effort, bottom effort, and dive efficiency, were more numerous when the seals were in well-mixed water columns. Generalised additive mixed-effects models showed that thermal water column structure plays a significant role in modulating dive types made by seals. The probability of high effort dives decreased with increasing stratification, while the relationship with the stability and mean temperature of the water column was complex, yet significant. Overall, seals are predicted to enhance vertical foraging effort and dive shallower in well-mixed, warmer water columns, with a strong association to diel and seasonal trends in mixing found. Diel phase and seasonal trends largely agree with the effect of upper ocean thermal water column structure on fine-scale diving behaviour. Summer diel trends in stratification and seal behaviours are probably linked by the diel vertical migration of prey. Seasonal, diel and dive-level effects of upper ocean thermal structure on vertical movements of seals may provide evidence for major strategies employed by seals to deal with changing environmental conditions across a multitude of spatio-temporal scales. However, seals do not appear to align their distribution of foraging depth with the MLD in either season. These results shed light on how SAFS at Marion Island allocate their time when foraging within the water column. By improving our understanding of what drives the foraging behaviour of fur seals, we can more accurately predict how regional and global change may affect these populations in the future, linking to more effective conservation and management.

Key words: Area-restricted search, *Arctocephalus tropicalis*, Cluster, dive, effort, forage, Marine top predators, Southern Ocean, Stability, Stratification, Variability, Vertical mixing.

Introduction

Background

Foraging success is a basic determinant of all life history traits and directly influences survival and reproductive success, with consequences for population growth (Stearns, 2000; Stevick *et al.*, 2002; Stephens and Krebs, 1986). Knowing how, when and where animals acquire resources can therefore help predict trends in animal population growth and persistence (Roncon *et al.*, 2018). Collecting direct observations of prey consumption by marine top predators remains difficult due to the challenges of exploring remote subsurface ocean habitats (Roncon *et al.*, 2018; Harcourt *et al.*, 2019). A substantial improvement in the way ecologists could collect data over the past few decades has changed the way we understand marine top predator movement behaviour (Hussey *et al.*, 2015), specifically in the harsh and remote Southern Ocean (Treasure *et al.*, 2017; Roncon *et al.*, 2018). Moreover, enhanced data accessibility, data storage, data management, and technology has driven a new era of marine mammal ecology (McIntyre, 2014). A major advantage of animal-borne devices is that they are capable of recording high spatial resolution (vertical ~1 m; horizontal <5 km), *in situ*, simultaneous behavioural and physical oceanographic metrics (Harcourt *et al.*, 2019), providing valuable information for the study of habitat use (McIntyre, 2014).

The observed slowing of marine mammal movements are thought to be indicative of increased foraging effort, commonly referred to as area-restricted search behaviour (ARS) (Carter *et al.*, 2016). The scale at which ARS occurs depends on environmental factors experienced by the forager, as well as the individual characteristics of the forager (Pinaud and Weimerskirch, 2005, 2007; Pirotta *et al.*, 2014). Because predictability of marine resources is dependent on the spatial-temporal scales considered (Weimerskirch, 2007), ARS of animals in the heterogeneous marine environment are evident over a multitude of scales (Barraquand and Benhamou, 2008). Using only horizontal location data to identify drivers of marine mammal distributions ignores a fundamental dimension used by air-breathing deep-diving animals (Photopoulou *et al.*, 2020). For a comprehensive investigation into the foraging ecology of diving predators in variable ocean conditions, studies are required to be based on both horizontal and vertical movements (Bailleul *et al.*, 2008; Bestley *et al.*, 2015).

Robust and holistic statistical techniques such as state space models (Jonsen *et al.*, 2013; Carter *et al.*, 2016) have been used to synthesise horizontal tracking metrics, into horizontal foraging effort, of marine mammals (Kuhn *et al.*, 2010; Dragon *et al.*, 2012; Tosh *et al.*, 2015; Kirkman *et al.*, 2016) and more specifically subantarctic fur seals (SAFS) (*Arctocephalus tropicalis*) at Marion Island (de Bruyn *et al.*, 2009, Wege *et al.*, 2019). Dragon *et al.*, 2012 has suggested that horizontal area-restricted search (hARS) of southern elephant seals is a good indicator of diving activity and foraging success. Although high horizontal residence times are likely indicative of important foraging areas over broad spatiotemporal scales (>100km), limitations to the accuracy of hARS indices in estimating foraging effort or success become apparent at smaller scales (Patterson *et al.*, 2016). In the presence of accompanying vertical, high resolution (<1 m, <10 sec) data, more sophisticated inference of foraging success can be made (Heerah *et al.*, 2014; Arthur *et al.*, 2016). Modern techniques have allowed for the inference of vertical foraging effort using vertical sinuosity ('wiggles') within each dive (Heerah *et al.*, 2014). This information may aid in determining potential drivers of foraging effort within a dive and potential threats to foraging in the future (Hussey *et al.*, 2015).

Individual seals dive within bouts (<12 hr intense diving activities) and foraging trips (searching for prey at sea) and alter their foraging behaviour over various spatial and temporal scales (Roncon *et al.*, 2018). There are several indices that can be derived to investigate diving and foraging behaviour of Southern Ocean diving predators (Roncon *et al.*, 2018), which include foraging effort, dive cost and dive optimality (efficiency). At small vertical (~1 m) and horizontal scales (<5 km), seal foraging effort provides a high resolution temporal-spatial distribution of energy expenditure without having to directly observe prey capture and consumption (Costa *et al.*, 2010; Heerah *et al.*, 2014; Arthur *et al.*, 2016). Foraging decisions of seals using environmental cues while diving are complex and are constrained by physiological limitations on diving depth and duration (Viviant *et al.*, 2016; Roncon *et al.*, 2018). Automated statistical methods have allowed for the classification of diving activity into behavioural groups or dive types. This has been a popular way to better understand the complex vertical movements of seals (Villegas-Amtmann *et al.*, 2013; Krause *et al.*, 2016), allowing for differentiation of the foraging strategies employed (Tinker *et al.*, 2007; Weise, Harvey and Costa, 2010) in response to environmental variability, as well as temporal and spatial variability in prey distributions (Lea *et al.*, 2002). Generalised additive mixed-effects models (GAMMs) offer an

opportunity to fit the complex, non-linear relationships that often occur between animals and their surrounding environment (Harrison *et al.*, 2018), and have been used extensively in the study of seal foraging ecology (Blanchet *et al.*, 2015; Cotté *et al.*, 2015; Hoskins, Costa and Arnould, 2015; Green *et al.*, 2020).

Aims and objectives

Investigating the drivers of foraging effort in marine systems is especially challenging, making the opportunity for such studies unique and rare (Arce *et al.*, 2019). There is a drive for more research to elucidate the role of physical oceanography in marine top predator behaviour (Carter *et al.*, 2016). Seals at Marion Island have been able to capture the ocean properties and behavioural parameters in otherwise inaccessible areas, thus assisting scientists in their efforts for physical oceanographic data collection and the assessment of seal foraging behaviour (Bester *et al.*, 2011; Chown and Froneman, 2008; Tosh *et al.*, 2015). Although studies at Marion Island have investigated basic diving metrics and horizontal searching behaviour of SAFS in relation to large-scale (>20 km) ocean features, no studies have considered incorporating contemporary on-board temperature records to investigate both vertical (diving) and horizontal foraging effort in relation to the upper ocean thermal structure at fine vertical (~1 m, <10 sec) and horizontal (1-10 km, <24 hr) scales. This chapter therefore aims to gain a comprehensive understanding of Marion SAFS foraging ecology in relation to the immediate ocean conditions experienced by each seal.

Specific objectives were to:

- Identify and describe the distinct types of dives made by SAFS representative of diving and foraging behaviour in three-dimensional space.
- Assess the influence of vertical water column mixing in the upper ocean on Marion SAFS diving behaviour over seasonal and diel time scales.
- Determine whether fine-scale diving and foraging behaviour is modulated by the upper ocean thermal structure.

I hypothesise that the fur seals at Marion Island make distinct types of dives, based on three-dimensional movements, in relation to upper ocean thermal structure. I further hypothesise that SAFS target stratified water columns, associated with high stability, and

concentrate foraging effort at the MLD. Lastly, I hypothesise that the patterns of upper ocean thermal structure explain the seasonal and diel trends in diving and foraging behaviour.

Materials and methods

Summary data in this study were reported as mean \pm standard deviation (SD), unless otherwise noted.

Ethics statement

All animal handling and experimentation were undertaken with approved ethics clearance from the Animal Use and Care Committee (AUCC) of the Faculty of Natural and Agricultural Sciences, University of Pretoria, South Africa, under AUCC 040827-023.

Study site, animal handling and instrumentation

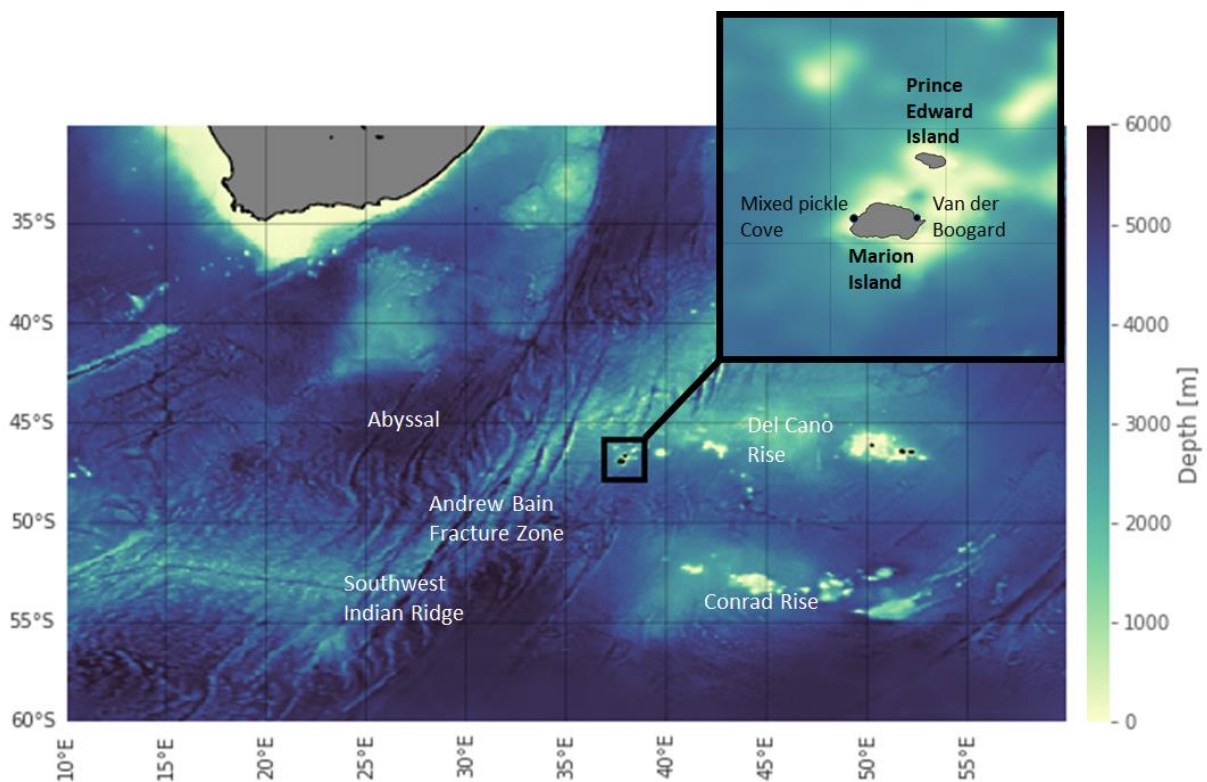


Figure 2.1: Bathymetry map (elevation in metres) obtained from the 'GEBCO_2020' global bathymetric gridded product released by the General Bathymetric Chart of the Oceans (GEBCO Compilation Group 2020) with a $1/240^\circ$ resolution. The location of the Prince Edward Archipelago's is shown in relation to South Africa and large topographic features (Fisher & Goodwillie, 1997). A zoomed-in map shows the two

deployment colonies on Marion Island, with Prince Edward Island approximately 20 km from Marion. The Van den Boogaard SAFS rookery is situated on the east side of the island, while the Mixed Pickle rookery is on the west.

Tags (Figure 2.2), used in this study for the purposes of tracking horizontal and vertical seal movements (Wildlife Computers, Redmond, Washington, USA; SirTrack, Seattle, Washington, USA) (Figure 2.3), were deployed at and recovered from 2009 to 2015 from two SAFS colonies; Van den Boogaard beach and Mixed Pickle Cove on Marion Island (46° 54' S, 37° 45' E) (**Error! Reference source not found.**). These tags also recorded concomitant depth and temperature data, forming part of the objectives of the Marion Island Marine Mammal Programme (MIMMP). In total 39 SAFS were fitted with devices. Only lactating females that were confidently seen suckling pups were individually caught in a hoop net (± 1 m diameter, ± 8 kg) and physically restrained, for a maximum of 30min. Devices were attached using double-component, quick-setting epoxy resin (Araldite AW2101, CIBA-GEIGY Ltd.) and stress were minimised to individuals following Field *et al.* (2012) and Horning *et al.* (2019). Wildlife Computers' SPLASH 10-351 tags (120g, 110 x 42 x 14 mm) are archival and Argos-linked satellite transmitting devices which record location and diving parameters simultaneously, while Wildlife Computers' MK-9 time-depth recorders (TDR) (30g, 67 x 17 x 17 mm) are archival loggers only, thus requiring concurrent deployment of Platform Transmitting Terminals (PTTs) to collect synchronous location information. TDRs were fastened with a hose-clamp to a nylon shade-netting strip in 2009 and 2010, and from 2011 was attached to the fur on the dorsal midline pelage of the female just posterior to the scapulae. Simultaneously, a Sirtrack Argos-linked satellite transmitter terminal tag (PTT) was attached alongside the TDR directly onto the fur of the animal. From 2011, TDRs were attached directly to the fur, instead of via a nylon shade-netting strip. Alternatively, from 2011, only a SPLASH tag was attached to the female using the same positioning protocol as the TDR. Upon retrieval, the device was carefully removed by cutting the guard hairs of the fur directly beneath the device.



Figure 2.2: A schematic of Wildlife Computers' SPLASH 10-351 tag (a) (Adapted from Wildlife Computers' product feature sheets) attached to a subantarctic fur seal (b) at Marion Island and a Wildlife Computers' TDR-MK9 (c) alongside a PTT tag (d). Pictures (b) and (c) were taken by Sean Evans, while (d) was taken

Chapter 2: Influence of upper ocean thermal structure on diving behaviour

by Chris Oosthuizen. A modified hoop net (± 1 m diameter, ± 8 kg) was used to catch seals for deployment. The devices were attached, using a double-component, quick-setting epoxy resin (Araldite AW2101, CIBA-GEIGY Ltd), through an opening of the net created by opening a dorsal aperture in the cone of the net while the seal was physically restrained.

Depth was sampled at one second intervals for MK9 and SPLASH tags while transmission frequencies for temperature readings varied due to trade-offs with tag battery life. SPLASH tags were set at one second (n=3), five second (n=18) and ten second (n=1) transmission frequencies using Wildlife Computers' MK10Host (Version: 1.26.3002), while MK-9 tags were set-up using Wildlife Computers' MK9Host (Version: 1.09.3000) at one second (n=10), two second (n=1) and five second (n=7) transmission frequencies. Both TDRs and SPLASH tags measure at a 0.5m depth (Accuracy: $\pm 1\%$ of reading) and 0.05 °C temperature (Accuracy: ± 0.1 °C) resolution. Seals carried devices for the duration of the battery life, 86 days on average (min = 22 days, max = 276 days, SD = 50 days). (see Supp.Table 1 for a summary of deployment details).

Wildlife Computers' HexDecode software (version 2.02.0030) was used to extract compressed hexadecimal files (".wch"), after which Wildlife Computers' Instrument Helper software was used for initial data visualisation and data exporting (<http://wildlifecomputers.com/support/downloads/>). Further processing and analyses of data were done using custom written software in R 4.0.3 (R Core Team, 2020) and Python 3.6.5 (Python Software Foundation, 2018). Diving records without supporting satellite tracking information were omitted from this study.

Tracking data and horizontal area-restricted search (hARS)

Interpolated tracking data from Wege *et al.*, 2019 were used to describe surface movements of seals in this study. Wege *et al.*, 2019 used Bayesian state space models (SSMs) in R (R Core Team, 2020) using the 'bsam' package (Jonsen *et al.*, 2013) to filter all tracking data containing inherent errors ranging from 0.5 to 10 km on average (Costa *et al.*, 2010). SSMs allow for inference of behavioural states, based on hARS modes along seal tracks, thereby providing information about whether a seal is 'foraging/resident' or 'travelling/transient'. In this study, SSM outputs included a continuous numeric variable (beta) ranging between one and two, which was rounded to the nearest integer and represented by a new binary variable 'hARS', where one = 'foraging', and two = 'transit'. When beta = 1.5, the corresponding hARS value was rounded up to two and labelled as 'transit'. Devices collected time in Greenwich Mean Time (GMT) which was converted to

local time based on the simultaneous geographic position of the seal (local solar time $\frac{1}{4}$ GMT + (degrees longitude)/15). Dives were grouped to the closest interpolated location in time along the seal track using dive start time (GMT) as reference. Behavioural modes inferred from SSM results were then appended to the dive record for later dive-level analyses (Arthur *et al.*, 2016). All dive analyses were thus based on filtered dive locations. Tracks were separated into individual foraging trips by considering females as 'at-sea' when tags measured a 'wet-period' for longer than six hours (Luque, Arnould and Guinet, 2008). This was done to exclude brief ocean visits for non-foraging related activities and contained only isolated short dives (<60 s), which occur mostly during daytime in SAFS (Georges *et al.*, 2000). For devices without wet-dry sensor information, trips were separated through visual inspection of seal locations in relation to Marion Island. The modelled accuracy of seal positions is such that estimated locations within about five km of the colony may still represent the animal residing on land (Patterson *et al.*, 2010). Furthermore, seals may behave differently during overnight foraging trips compared to multi-day foraging trips (Luque *et al.*, 2007). For results to be spatially robust, only trips in which the animals travelled more than five kilometres from the colony were initially considered in the analyses. However, to exclude any island-seal or inter-island-seal (Prince Edward and Marion Island) interactions and to differentiate discrete oceanic zone excursions, dives were excluded (0.48% of dives) if they occurred within overnight foraging trips and/or short trips (<1 day), where the total distance travelled was less than 40 km (chosen according to buffer used in Lombard *et al.*, 2007) from Marion Island. This placed more focus on open ocean/offshore seal movements in line with the objectives of this study.

Vertical movements

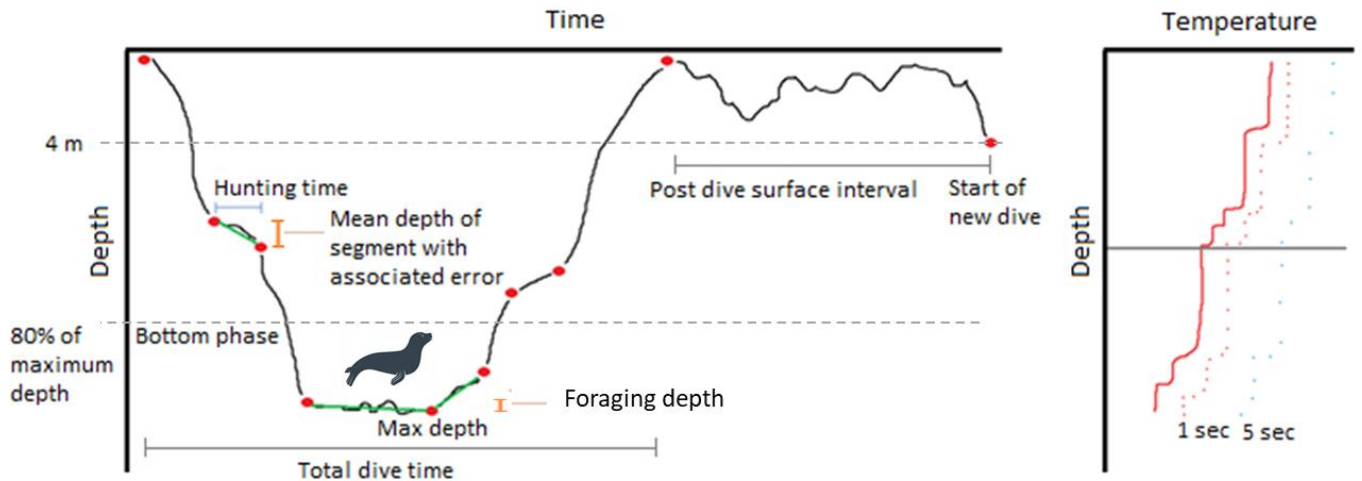


Figure 2.3: a) Schematic of a typical seal dive profile (black). The green segments within a dive are declared as 'foraging' segments according to the broken stick method (Heerah *et al.*, 2014), while the rest of the time the seal is predicted to be in 'transit' mode. Blue bars indicate the amount of time spent hunting within a foraging segment. The foraging depth is calculated as the vARS depth using the mean depth of the longest foraging segment within a given dive. The post dive surface interval (grey bar) is the amount of time it takes for the seal to transit from when it surfaces above four metres after a dive until it dives again below four metres. The bottom phase of the dive is defined as that below 80% of the maximum depth. b) An example of an interpolated (solid red), a one second sampling rate (dotted red) and a five second sampling rate (dotted blue) downcast temperature profile.

Fine-scale (~1 m, <10 sec) dive data were independently corrected for shifts in the pressure transducer accuracy of each seal-borne device using a customised zero-offset correction method (Luque and Ferguson, 2011) in R statistical computing software (R Core Team, 2020). A modal depth between five metres and 10 metres was considered, representative of the true surface, across a moving window of two hours based on the assumption that most of the time in this depth range would represent time on the surface. This depth was then subtracted from all depth values within the respective two-hour window to provide zero offset corrected depths (Arthur *et al.*, 2016). A dive threshold of four metres (Luque *et al.*, 2008; Womble *et al.*, 2013; Heerah *et al.*, 2014) for a given subsurface period exceeding 60 seconds was used to exclude dives that may be indistinguishable from surface noise remaining after adjustment of pressure transducer drifts, taking into account the accuracy of the pressure transducer (0.5 m). An initial threshold of 30 seconds (Womble *et al.*, 2013) was used to: (1) exclude prey handling behaviour, (2) remove travelling or other non-foraging activities, and (3) conform with methods in other studies for comparative reasons (Wege, 2017). However, to maximize computational efficiency, this threshold value was extended to 60 seconds (also used in

Heerah *et al.*, 2014 for Weddel seals), allowing for the effective use of a broken stick model (see below). For each dive, the maximum dive depth [m] and duration [sec] was calculated. The post dive surface interval [sec] of a dive was defined as the amount of time between the seal surfacing above four metres, following a dive, until diving below four metres again.

It is common for dive duration to proportionally increase with dive depth among fur seals (Croxall and Gentry, 1987). Seals mostly dive within their physiological limits; however, any oxygen reserves may allow for longer than usual pursuits in case the prey avoids capture (Georges *et al.*, 2000). This can be represented as a dive residual, estimated in this study using the Pearson residuals from a linear mixed-effect model (LMM) fitted via restricted maximum-likelihood estimation (REML) with individual seal fit as a random term, using the package 'lme4' (Bates *et al.*, 2015). The dive residual gives an indication of whether the duration of dives, for a given depth, were longer or shorter than expected (e.g. Bestley *et al.*, 2015).

From the remaining dive data ($n = 348\,760$ dives, 39 individual seals) a broken stick model (Heerah *et al.*, 2014) was used to reconstruct dives for an in-depth study of vertical movements within the water column. From each reconstructed dive profile, I calculated a set of candidate diving and foraging indices. To calculate the optimal number of broken stick points, a Gompertz model was fitted to the mean distance (mean error) between the original profile and the reconstructed profile using a sequence of broken stick points between six and 30 (Heerah *et al.*, 2014). The inflection point of this curve (example profile in Supp.Figure 1) was determined as the optimal number of broken stick points to describe the original profile. If the Gompertz model did not fit the curve for a given dive profile, a manual number of broken stick points were assigned to summarize the dive profile. For these dives, linearity of the relationship between the mean distance and the number of broken stick points increased (Heerah *et al.*, 2014). Six broken stick points, representing the median optimal number of broken stick points used when the model was found to fit the data, were chosen. Choosing more points would likely decrease residual error, yet increase complexity and computational time, while choosing less points could oversimplify the dive profile (Fedak, Lovell and Grant, 2001; Heerah *et al.*, 2015, 2019). Although the number of iterations in the broken stick model is critical to the quality of the abstracted dive (Photopoulou *et al.*, 2015), slight overestimation of feeding time that may arise (Heerah *et al.*, 2019) would be acceptable for the purposes of this study.

When foraging during a dive, seals tend to decrease their vertical speed and increase the sinuosity of their movements (Dragon *et al.*, 2012; Heerah *et al.*, 2019), referred to as vertical area-restricted search (vARS) (Dragon *et al.*, 2012). Segments produced by the broken stick method within dives were thus categorized as either ‘foraging’ or ‘transit’ based on the vertical sinuosity and vertical velocity between broken stick points using thresholds of 0.9 sinuosity (Heerah *et al.*, 2014) (example profile in Supp.Figure 2) and 0.4 m/s (Heerah *et al.*, 2015) respectively. Because some dives have multiple ‘foraging’ segments within a dive, the foraging depth per dive was determined as the mean depth of the longest (in time) ‘foraging’ segment within that dive (Photopoulou *et al.*, 2020). ‘Hunting’ and ‘foraging’ are used interchangeably in this dissertation. vARS is representative of ‘vertical foraging effort’ (Heerah *et al.*, 2014) and calculated as:

$$\text{vARS} = \text{total hunting time} / \text{total dive time}$$

where hunting time is the sum of durations of all ‘foraging’ segments within a dive and total dive time is the duration from when the seal descends below four metres to when it ascends above four metres (Arthur *et al.*, 2016). Furthermore, dives that had no vertical foraging effort segments present were referred to as ‘transit dives’ in this study. Similarly foraging indices can be derived from bottom effort and dive efficiency:

$$\text{Bottom effort} = \text{bottom time} / \text{total dive time}$$

assuming fur seals spend most of their time foraging in the bottom phase of dives (Dragon *et al.*, 2012), where bottom time is the amount of time [in sec] spent within the bottom phase of the dive. The bottom phase is the section of dive below 80% of the maximum dive depth calculated for each dive separately (Figure 2.3). *Dive efficiency* (Lee *et al.*, 2015; Viviant *et al.*, 2016) assumes anaerobic inefficiency (Ydenberg and Clark, 1989) and shows how much a seal distributes time to the bottom phase of a dive relative to recovery time required for that dive calculated as:

$$\text{Dive efficiency} = \text{bottom time} / (\text{post dive surface interval} + \text{total dive time})$$

Classifying dive types (Response variable)

Data were split into two subsets: ‘summer’ (15th October - 14th April) and ‘winter’ (15th April - 14th October) and were analysed separately. Similar to methods used in Dragon *et al.* (2012), dives were grouped into classes of “dive types” representing different foraging

strategies using a Clustering for Large Applications (CLARA) algorithm suggested by Rousseeuw and Kaufman (1990) for large data sets (more than several thousand observations) such as that used in this study. CLARA is an extension to k-medoids (PAM) methods, helping to reduce computing time and RAM storage problems using a sampling approach (Kodinariya and Makwana, 2013). K-medoids clustering is robust and preferred over k-means clustering for large datasets (Arora, Deepali and Varshney, 2016). In this study 50 samples were randomly drawn from the large dataset and the PAM clustering algorithm (Kaufman and Rousseeuw, 1987) applied to produce an optimal set of medoids. The algorithm then assigned all objects in the dataset to clusters, while repeating the sampling and clustering process, subsequently selecting the set of medoids with the minimal cost as the final clustering result used to alleviate sampling bias (Wei, Lee and Hsu, 2000).

The optimal number of clusters were determined and validated by means of a silhouette analysis, which measures how well an observation is clustered by estimating the mean distance between clusters for a varying number of homogeneous clusters. An "Euclidean" metric was used for calculating dissimilarities between observations, represented by the square root of the sum of squared distances between observations (Kaufman and Rousseeuw, 1987). The appropriate number of clusters is that which maximizes the average silhouette width over a range of possible numbers of clusters.

Prior to cluster analysis the following methods were used for dimension reduction (McDonald *et al.*, 2009) and for simpler interpretation of dive types while preserving variance (Zuur, Ieno and Elphick, 2010). A variance inflation factor (VIF) was calculated for each variable to combat multicollinearity (Zuur *et al.*, 2010). Using a VIF threshold of 10 (Quinn and Keough, 2002), dive duration was excluded from summer analyses, while all variables were included for winter analyses. A principal component analysis (PCA) was then used to exclude variables with a lower-than-expected average contribution to variance, as described in Husson, Lê and Pagès (2017).

Diving parameters of distinguished dive types were then represented in a table, where differences have been given by the confidence interval (CI) of a Welch Two Sample t-test. All correlations were made using Pearson correlation coefficients. All differences and correlations were considered significant at $p < 0.0001$.

Upper ocean thermal structure and vertical mixing (Explanatory variables)

Four variables were chosen to represent and describe upper water column thermal structure and vertical mixing experienced by the seal per dive:

- 1) Stratification [% stratified in groups of dives]
- 2) Stratification state [categorical state: mixed vs stratified]
- 3) Mean vertical stability [$1/s^2$]
- 4) Mean temperature of the water column [$^{\circ}C$]

It must be emphasised here that seal-borne loggers used in this study only record temperature and depth readings and do not measure salinity. Density in the ocean is a function of temperature, pressure (from depth) and salinity (IOC, SCOR and IAPSO, 2010). This means density values cannot be directly calculated and any derivations of density changes require a dominating contribution of temperature over salinity for best estimates of vertical stability (defined below). In this study I assume that temperature, instead of salinity, changes contribute the most to changes in density and that barrier layers (where vertical changes in salinity define the mixed layer while temperature remains mixed) are not present.

An Objective Analysis dataset with both salinity and temperature recordings within the Prince Edward Islands region was used to test and validate this assumption. The UK Met Office Hadley Centre obtains all types of available ocean data from profiling instruments, such as Argo floats, to generate global quality-controlled temperature and salinity profiles from the ocean surface to 1000 metres. Thermal biases are corrected for using methods in Gouretski and Reseghetti (2010) (<https://www.metoffice.gov.uk/hadobs/en4/download-en4-2-1.html>). Using this profile data, maps of monthly gridded data were obtained from an objective analysis with uncertainty estimates (Good, Martin and Rayner, 2013). Temperature-salinity-depth profiles are distributed on a horizontal spatial grid of 1° resolution with a vertical grid where depth resolution increases exponentially towards the surface, starting with large differences (50 metres) at 1000 metres depth and ending with small differences at the surface (one metre). Temperature-salinity-depth data were extracted for 2009-2015 to overlap with seal data.

To produce downcast seal-derived profiles, temperature readings continuously recorded throughout a single dive were reduced to measurements only taken during the descent

phase of the dive. The descent phase of a dive begins when the seal first moves below four metres and ends as the seal reaches its maximum depth of the dive for the first time. The mean descent and ascent rates of SAFS at Marion are similar (Wege *et al.*, 2016), thus making the choice of upcast or downcast profiles inconsequential. However, upcast profiles were removed to restrict approximations of upper ocean thermal structure to a single downcast-derived value per dive, instead of having both downcast- and upcast-derived approximations per dive. This allowed for comparison with per dive seal behavioural variables. Furthermore, as seals move horizontally when they dive, the downcast is closest in space to the location of the GPS coordinate associated with the dive, while the upcast may be several hundred metres away from the GPS coordinate. All seal-derived profiles and objective analysis profiles were vertically gridded to 1 m for comparative convenience and computational efficiency. From here on, the term 'dives' is interchangeable with 'profiles' in this study.

The mixed layer is the layer of water with homogenous density extending from the surface ocean downward. The mixed layer depth (MLD) is conventionally defined using a threshold value of temperature or density from a near-surface value at 10 m depth (temperature = 0.2 °C, density = 0.03 kg/m³) (de Boyer Montégut *et al.*, 2004; Huang, Lu and Zhou, 2018). By using a reference depth of 10 m any surface noise that may be created through diurnal cycle solar forcing within the boundary layer is excluded (McWilliams *et al.*, 2009). The thresholds used in this study were chosen after several temperature criteria were tested by comparing *in situ* seal-derived temperature profile estimates of MLD to objective analysis density and temperature estimates of MLD (See in Supp.Figure 4). Objective analysis MLDs were calculated according to de Boyer Montégut *et al.* (2004) thresholds using in-situ density [kg/m³] of seawater calculated from absolute salinity [g/kg], in-situ temperature [(ITS-90), °C] and sea pressure [(absolute pressure minus 10.1325 db), db] according to IOC *et al.* (2010). The temperature criteria that resulted in mean seasonal MLDs that were most closely correlated with MLDs from objective analysis, for the region, were chosen as the most reliable (see Supp.Figure 4 for objective analysis MLDs).

Lorbacher *et al.* (2006) also suggests the use of a gradient method. Therefore, I employ both methods by defining the MLD according to a hybrid method, where (1) the first vertical derivative of temperature with depth is greater than 0.1 °C, and (2) temperature first exceeds a threshold of 0.25 °C from a reference depth of 10 m. A temperature

threshold of 0.25 °C was chosen as it was closest to the recommended threshold of 0.20 °C with a 0.05 °C error limit to account for the 0.05 °C error in the device's temperature sensor. When a MLD was resolved in each *in situ* temperature profile according to these methods, i.e. the vertical temperature difference and gradient exceeds the given thresholds, the water column was considered 'stratified' and the depth of the mixed layer was stated. When temperature remained relatively constant with depth, within these thresholds, the water column was considered 'mixed' and no MLD was resolved or given.

Patches of enhanced sinuosity in the vertical movements of seals, i.e. when the seal is foraging, may have the potential to result in small-scale (<1 m, <10 sec) artificial mixing of water parcels, driving advection of thermodynamic properties such as temperature vertically in the water column. Due to the rapid response of tags to vertical gradients of temperature obtained as the seal is diving and the conservative/insensitive thresholds used for determining MLDs (discussed above), the influence of such artificial vertical mixing on distinguishing MLD presence was presumed to be negligible. I therefore assume that the tag response rate is sufficient for obtaining true vertical gradients of temperature to achieve my experimental objectives.

Motivation for identifying the MLD based solely on temperature was further validated by using the Objective Analysis product to investigate the relative contributions of vertical temperature and salinity gradients to vertical changes in density. The relative contribution of temperature and salinity variations to gradients of density were analysed using the stability ratio (Rudnick & Ferrari, 1999) given as:

$$R\rho = \alpha(\partial T/\partial z)/\beta(\partial S/\partial z)$$

The mean thermal expansion $\alpha = 1.3 \times 10^{-4} \text{ }^\circ\text{C}^{-1}$ and haline contraction ($\beta = 7.8 \times 10^{-4} \text{ kg.g}^{-1}$) coefficients for the region were calculated, together with *in situ* vertical temperature gradients (∂T) and salinity (∂S) gradients for each 1° grid cell. The stability ratio $R\rho = \pm 1$ would infer that changes in temperature and salinity provide equal changes to density, while deviations from ± 1 indicate that either salinity ($|R\rho| < 1$) or temperature ($|R\rho| > 1$) dominates changes in density.

Stratification is typically defined by the strength of the vertical density gradient. In this study, stratification is defined in two ways depending on the context. In the context of per dive analyses, the stratification state refers to the presence or absence of the MLD (stratified = MLD is present; mixed = MLD is absent). In the context of seasonal, hourly

or foraging trip scale analyses, the stratification is calculated as the percentage of seal-derived profiles that reflect the presence of a MLD over a given season, hour or foraging trip, considering that maximum dive depths of SAFS never exceed 211 m in this study (see chapter 2 results for details) and MLDs may exceed 211 m within the Southern Ocean region (de Boyer Montégut *et al.*, 2004; Carmack, 2007; Thomas *et al.*, 2008). Zero stratification indicates profiles that are insufficiently deep for MLD presence. In instances where a number of seal dives reach a similar depth, the profiles where MLD is absent will suggest that mixing is occurring, and the water is not stratified.

In support of stratification, another mixed layer property has been derived from seal-derived profiles. In this work, I use the term vertical stability to determine the strength of the vertical density gradient. This provides a metric to represent the stabilizing influence of buoyancy on the water column and is given by the Brunt-Väisälä coefficients (Pellichero *et al.*, 2017):

$$NT^2 = g\alpha\partial T/\partial z$$

$$NS^2 = -g\beta\partial S/\partial z$$

$$N^2 = NT^2 + NS^2$$

, where ∂T is the vertical change in conservative temperature and ∂S is the vertical change in absolute salinity with depth (IOC *et al.*, 2010). Alpha (α) and beta (β) values, as described previously, were averaged over the entire study region, while the gravitational acceleration of 9.8 m/s² was used. NT^2 was calculated for seal-derived profiles, while all Brunt-Väisälä coefficients were used with objective analysis data in the validation methods for assuming temperature dominance described above.

Stability was calculated for each depth and averaged vertically from below five metres, to exclude any surface noise, to the maximum depth of each profile. Vertical stability indicates the preconditioning of the mixed layer to mix deeper, where large stability indicates that more energy is required to mix the water column (Gill, 1982). Zero stability represents dives within a well-mixed water column to the maximum depth of the seal dive, however this does not necessarily indicate low stability of the full water column, but rather that the seal dives within the mixed part of the upper ocean.

Generalized Additive Mixed-Effects Model (GAMM) framework

Non-linear relationships often occur between mobile predators and their surrounding environment (Leathwick *et al.*, 2006). As simple linear models cannot holistically represent such relationships, I adopted a generalized additive model framework. These models follow an additive technique where the partial effect of each predictor variable is represented by a smooth function (smooths as plural), which can be linear or non-linear depending on the underlying trends in the data. These smooths are formed as a linear combination of basis functions.

The dive types identified through prior cluster analysis, summarized seal behaviours and were modelled as a binary response variable (high effort dives versus low effort dives) in GAMMs against explanatory variables namely: stratification state [mixed vs stratified], stability [$1/s^2$] and mean temperature [$^{\circ}C$], to investigate the influence of upper ocean thermal structure on seal diving behaviour. Stratification, as a categorical variable (mixed vs stratified), was treated as a linear term without smoothing (Buja, Hastie and Tibshirani, 2016; Wiley and Wiley, 2019) to test for differences between the effects of stability in stratified versus mixed water columns, as well as the effect of stratification itself.

There is extensive evidence for seasonal differences in intrinsic and extrinsic seal behaviours (Arthur *et al.*, 2016; Wege *et al.*, 2016, 2019) as well as known seasonal trends in Southern Ocean stratification and mixing (Dong *et al.*, 2008; Sallée *et al.*, 2010; du Plessis *et al.*, 2019) and separate models were therefore constructed for summer and winter. GAMMs were fitted in R statistical computing software (R Core Team 2020) using the function 'gam' (library: 'mgcv'; Wood, 2017) function, assuming a binomial error structure and logit link function. By including individual seals as a random effect due to variation among seals and foraging trips (Wege, 2017), the model expects different baseline levels of dive type. This controls for Type I error rate, tackles autocorrelation and increases detection power among individual variation (Schielzeth and Forstmeier, 2009).

Stability was log-transformed to achieve normality and stabilize the variances. Stability and mean temperature have different scales, and so to compare the relative strength of the effect among predictors, these predictors were normalised (mean set to zero and standard deviation of one) prior to model analysis. Furthermore, the variance inflation factor (VIF), which is a tool used to assess the severity of collinearity between predictor variables, was calculated and a threshold of 10 considered to fulfil minimal collinearity

between predictor variables. Collinearity among the predictors (i.e. stratification, stability, mean temperature) would cause problems in model interpretation, because they would explain some of the same variance in the response variable (i.e. dive type), with their effects unable to be estimated independently (Quinn and Keough, 2002; Harrison *et al.*, 2018).

I used the default penalized thin plate regression spline as a low-rank multi-dimensional isotropic smooth for the basis smoothing function (refer to Wood (2003) for details). Smoothing parameters were estimated using restricted maximum likelihood (REML), the typical smoothing parameter estimation for smooth components viewed as random effects (Wiley and Wiley, 2019), to prevent overfitting and correlated covariates. Internal smoothing also combats autoregressive processes in the data (Burns *et al.*, 2008) which may arise from increasing trends in maximum depth and dive duration observed as the seasons progress from summer to winter (Wege, 2017).

My model was specified as follows for each season:

Dive type ~ stratification (mixed versus stratified) + mean temperature + stability(by = stratification) + individual seal (random effect).

The basis dimensions (k) used for function approximation in model smooths must be chosen appropriately to avoid overfitting and reduce oversimplification. Smooths were first restricted to a maximum of $k = 5$ in line with methods of Green *et al.* (2020). Model convergence and basis dimensions were checked by comparing estimates of the residual variance, using the 'gam.check' function (library 'mgcv'; Wood, 2017). These estimates are based on differencing residuals that are near neighbours according to the covariates of the smooth (Wood, 2017). Given the penalization process (thin plate regression spline mentioned above), the exact choice of the number of base functions is not important, and can be seen as an upper limit to the flexibility of the term. The actual flexibility is determined via the penalization process (Wood, 2017). Secondly, concurvity, which measures how a smoothed variable can be approximated by another (i.e. variable dependence), was checked by using the 'estimate' scenario metric, the most reliable measure for concurvity, which returns a value between zero and one (0 = no concurvity, 1 = no identifiability between the variables). Concurvity may lead to noticeable errors (Buja *et al.*, 1989). There is no universal criteria for concurvity, yet 0.5 is used as the threshold above which noticeable errors become introduced according to He (2004).

Lastly, resultant models were checked whether they met the model assumptions using visual analysis of quantile-quantile (QQ) plots (deviance residuals vs theoretical quantiles), with a straight-line trend suggesting a correct model fit (Augustin, Sauleau and Wood, 2012).

Models were ranked using the Akaike's Information Criterion corrected for finite sample sizes (AICc) and the best model was selected based on smallest AICc value (Burnham and Anderson, 2004; Wagenmakers and Farrell, 2004). Model smooths were presented as plots on a probability scale and centred on the intercept to appropriately scale marginal effects from the log scale of model outputs for more intuitive interpretation. These plots show the prediction of the output, assuming other variables are at their average value. Because explanatory variables were scaled before model input, means of explanatory variables were represented on model output graphs as zero. Results were considered significant at $p \ll 0.001$.

Diurnal trends in stratification and foraging and seasonal differences between MLD and foraging depth

Considering the modulation of 'time of day' on diving behaviour and diving effort of SAFS previously found at Marion Island (Wege, 2013, 2017), I examined possible diel phase and hourly effects on vertical foraging effort and associations with diel variations in upper ocean stratification. Dives were grouped into diel phases based on local times of each dive versus local times of sunrise, sunset and the nautical twilight (when the geometric centre of the sun is 12° below the horizon), calculated using the National Oceanic Atmospheric Administration's (NOAA) solar calculator in the 'mapprools' package of R (Lewin-Koh and Bivand, 2016; R Core Team, 2020). The respective diel phases were 'day', 'dawn', 'dusk' and 'night'. Hourly stratification [%] was calculated as the percentage of dives where the maximum depth extends beyond the MLD within the respective hour.

Results

Seasonal summary statistics of seal foraging behaviour and upper ocean thermal structure

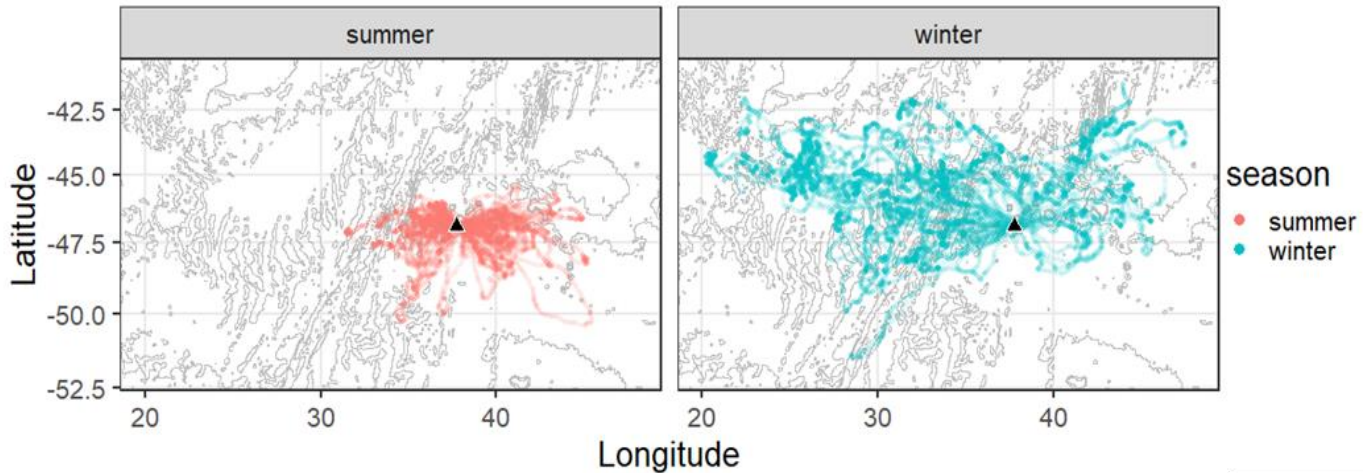


Figure 2.4: Seasonal differences (summer - red, winter - blue) in maternal fur seal movements from two subantarctic fur seal colonies at Marion Island (black triangle). Data are overlaid on a bathymetry map with contours at 1000, 2000, 3500 and 5000 m depth. Summer is defined as between 15 October and 15 April and winter as between 15 April and 15 October.

TDRs were retrieved successfully from 39 individuals (2009; 2011-2015). After removing surface dives that are shorter than 60 sec long and shallower than 4 m, 32.98 ± 2.74 % of total dives per seal were retained for analysis. In total, 346 760 dives were analysed with 23.67% during summer ($n = 82\ 090$, individuals = 20) and 76.33% during winter ($n = 264\ 670$, individuals = 19). More foraging trips were available for analysis in summer ($n = 97$) as opposed to winter ($n = 43$), despite a similar number of individuals (Table 2.1), while winter foraging trips were significantly longer (Mann-Whitney $W = 68$, $p < 0.0001$) and further ($W = 157$, $p < 0.0001$) from Marion Island than in summer (Figure 2.4, Table 2.1). Additionally, the number of dives per trip were higher ($W = 59$, $p < 0.0001$) in winter (Table 2.1). Winter foraging time ($W = 33$, $p < 0.0001$) and proportion of foraging time to trip time ($W = 477$, $p < 0.0001$) were higher per trip than in summer (Table 2.1). Seal maximum depth and time in vARS per dive was higher in winter than in summer (Table 2.1). The deepest dive was 211 m and 182 m in winter and summer, respectively. Stratification and stability showed summer enhancement, with particularly intense enhancement of stability in stratified water columns, while the average mean temperature experienced by seals was similar across seasons (Table 2.1). Overall, transit dives (those that do not include an vARS) made up 16.8% and 23.7% of summer and winter dives, respectively.

Table 2.1: Seasonal foraging trip- and dive-scale statistics of female subantarctic fur seal behaviour and upper ocean thermal structure from 2009-2015 deployments. Values are given as mean \pm SD. 'vARS' refers to vertical area-restricted Search - interchangeable with vertical foraging effort in this study.

	Summer	Winter
#Seals	20	19
#Foraging trips	97	43
#Dives	82 090	264 670
Stratification [%]	23.11	4.78
Per foraging trip		
#dives per trip	846 \pm 465	6155 \pm 4743
Distance travelled per trip [km]	503.6 \pm 287.3	2037.8 \pm 1694.1
Trip length [days]	8.0 \pm 3.4	36.9 \pm 22.7
Time in vARS [hrs]	5.9 \pm 3.57	63.1 \pm 41.3
Proportion of trip spent in vARS [%]	3.3 \pm 1.65	7.5 \pm 3.12
Per dive		
Maximum depth [m]	51.5 \pm 17,9	56.9 \pm 29,2
Time in vARS [sec]	24.9 \pm 22.2	36.9 \pm 34.1
Proportion of dive spent in vARS [%]	24.2 \pm 18.7	28.5 \pm 22.8
Stability [$1e^{-5}/s^2$]	0.45 \pm 0.84	0.03 \pm 0.31
Mean Temperature [$^{\circ}C$]	6.90 \pm 1.06	6.97 \pm 1.38

What kind of dives do subantarctic fur seals make?

Throughout summer and winter, vARS was independent of hARS (Pearson $r^2 = -0.01$) and post dive surface interval (pdsi) ($r^2 = -0.20$). The variances in principal component analyses for summer and winter were primarily explained by vertical foraging effort, bottom effort, and dive efficiency indices (Figure 2.5c,d), with a strong inverse relation to maximum dive depth according to opposing vectors (Figure 2.5a,b). Whereas, the contribution of hARS and pdsi to PCA variances were small, i.e. less than the expected average contribution to variance (Husson *et al.*, 2017), in both summer and winter (Figure

2.5c,d). Bottom effort contributes the most to variance in summer (~17%) and the second most in winter (~19%) for the first 2 PCA dimensions.

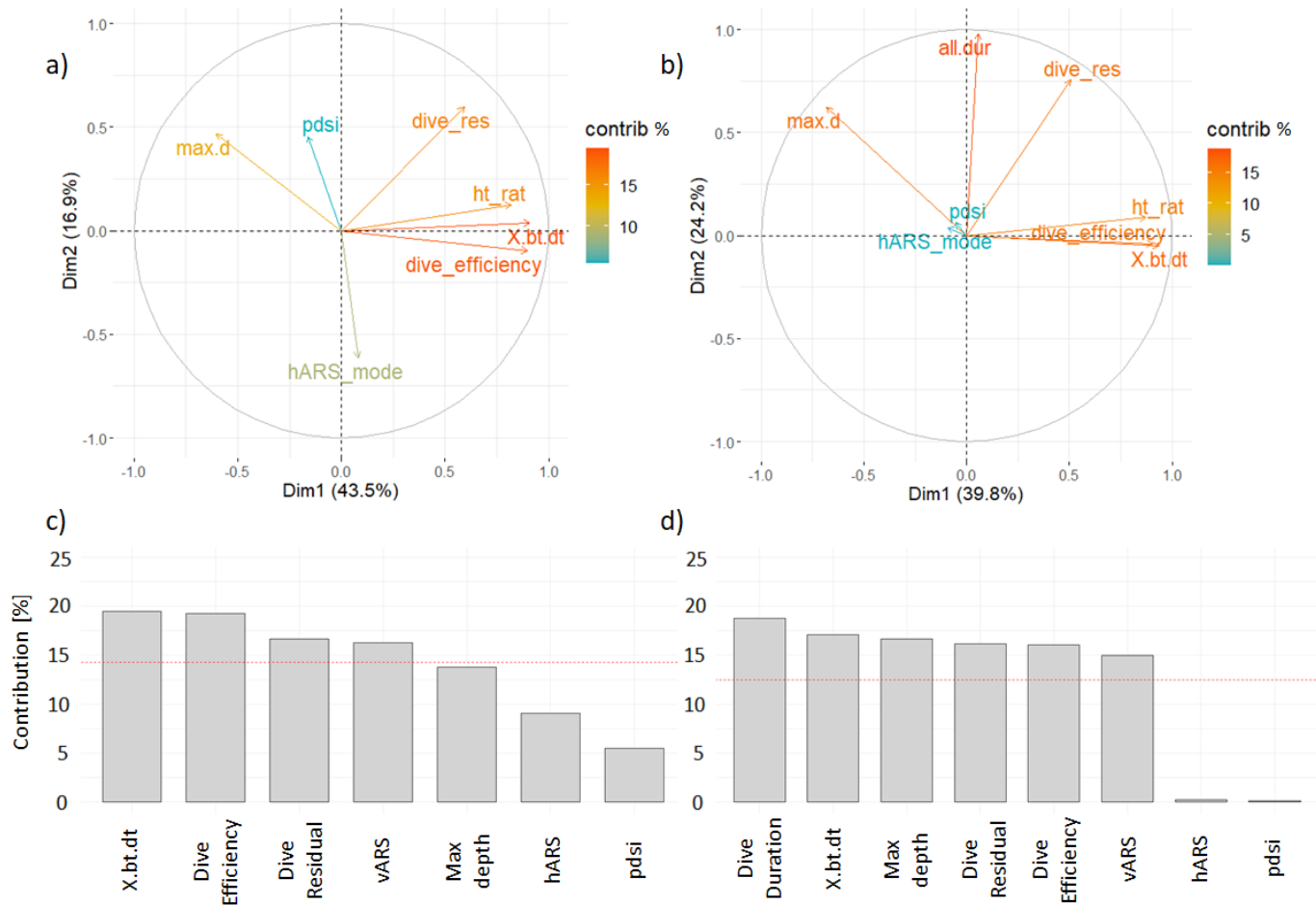


Figure 2.5: Principal component analyses showing the contribution (contrib) [%] of diving and foraging effort variables to the first two dimensions in summer (a,c) and winter (b,d). The red line in c) and d) indicates the expected average contribution to variance per season according to the methods in Husson et al. (2017). The bottom effort (X.bt.dt), dive efficiency, dive residual (dive_res), vertical area-restricted search (vARS interchangeable with ht_rat and vertical foraging effort), dive duration (all.dur), maximum depth (max.d), post dive surface interval (pdsi) and horizontal area-restricted search (hARS) are all analysed within the PCAs.

Increasing the number of groups (k) in cluster analysis caused a decreasing trend in average Silhouette widths in summer and winter (Figure 2.6), where maximum values (summer = 0.31, winter = 0.29) were associated with the use of two clusters (k = 2). This was therefore the appropriate number of clusters to use to describe the variance in the data, and consequently the main foraging strategies used within dives.

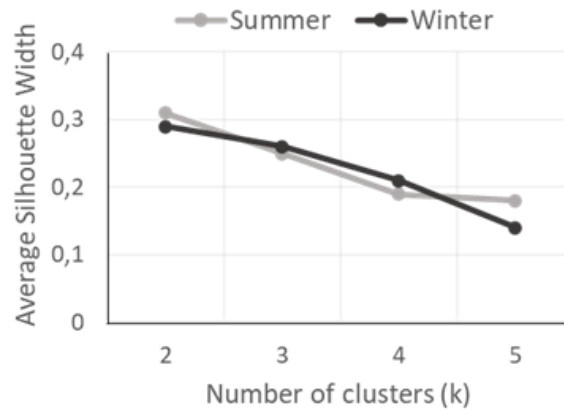


Figure 2.6: Silhouette plots for summer (grey) and winter (black), illustrating the decreasing trend in average silhouette width [unitless] with increasing number of clusters (k).

Figure 2.7 shows how the dive types clustered, with minimal overlap between clusters within each season. Dives in Divetype 2 were considered 'high effort' dives while dives in Divetype 1 were considered 'low effort' dives. Dive types in summer (low effort 1 = 34 704, high effort = 47 386) and winter (low effort = 131 342, High effort = 133 328) had consistently more high effort than low effort dives. Vertical foraging effort was positively correlated with dive efficiency (vARS:dive efficiency $r^2 = 0.61$), bottom effort (vARS:bottom effort $r^2 = 0.66$) and dive residuals (vARS:dive residual $r^2 = 0.46$).

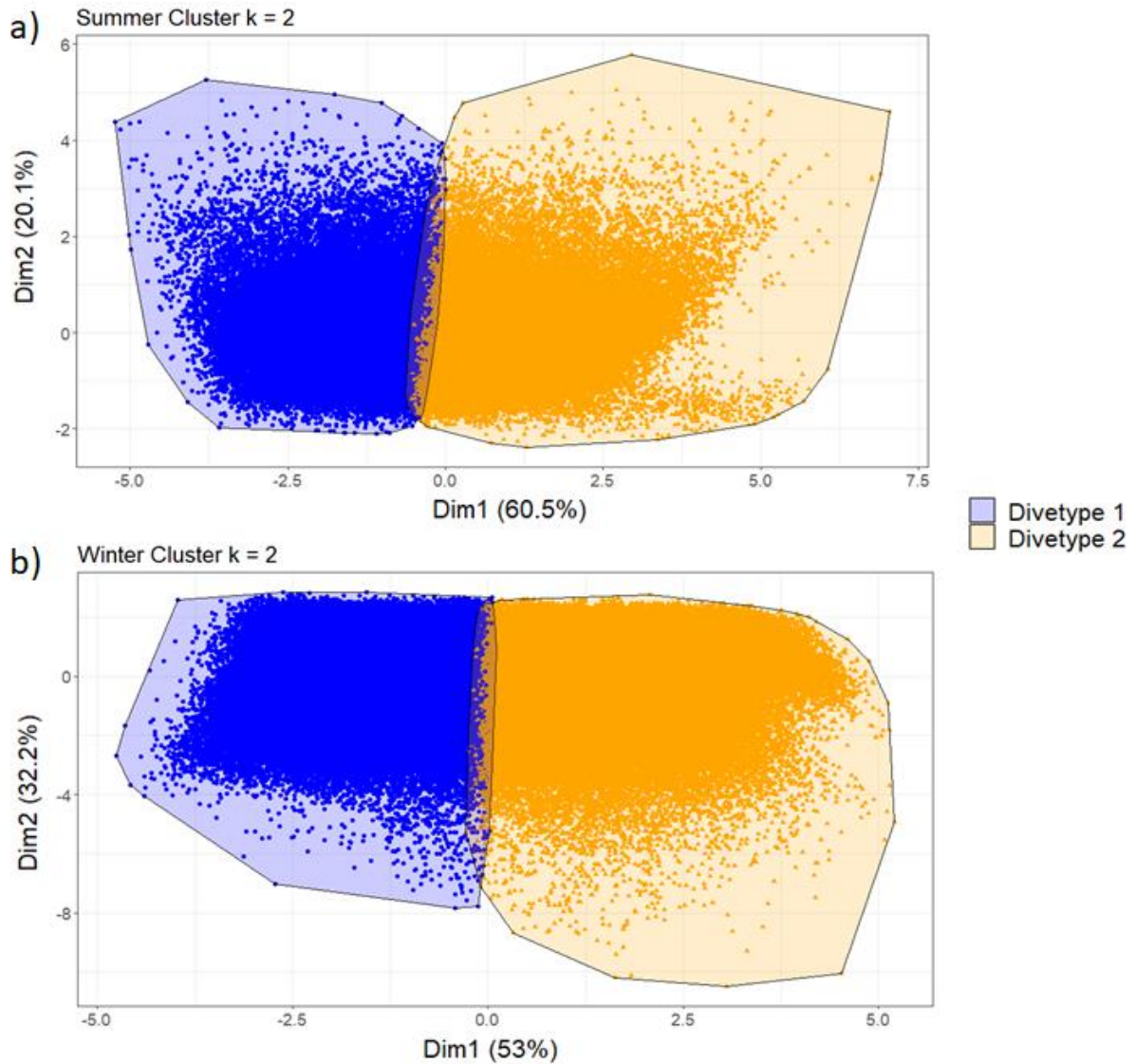


Figure 2.7: Cluster plots of a) summer (grey) and b) winter (black), where the number of clusters (k) were given as two. 'Dim1' and 'Dim2' are dimensions 1 and 2 that explain the magnitude of variance represented in round brackets. The two clusters are named 'Divetype 1' and 'Divetype 2' and represent 'low effort' and 'high effort' dives.

Associations between foraging behaviour and upper ocean thermal structure: Seasonal and diel trends

Only 9.12% of dives had stratified mixed layers and only 34.61% of these mixed layers were considered stable ($>1e^{-5} s^{-2}$). Vertical stability (Nt^2) and mean temperature were poorly correlated ($r^2 = 0.001$). Mean temperature showed little variation between seasonal water column stratification states, while stability is higher in stratified water columns relative to in mixed (Table 2.2). A lower proportion of high effort dives occurred in stratified water columns during both summer and winter than in mixed water columns (Table 2.2).

Maximum and foraging depths were positively correlated ($r^2 = 0.94$), and the mean distances between them were consistently <10 m between seasons and stratification states. In stratified water columns, maximum and foraging depths were considerably deeper than in mixed water columns in summer and winter (Table 2.2). Low seasonal variability was shown in mean distance from maximum depth to MLD, despite deeper and more variable winter MLDs than in summer (Table 2.2). MLD was positively correlated with seal maximum depth (Pearson $r^2 = 0.54$) and mean foraging depth (Pearson $r^2 = 0.49$). Average values of mean foraging depth distance to MLD were similar for winter and summer, with a larger variation in winter, when foraging depth, maximum depth and MLDs are deeper (Table 2.2). Bottom time and foraging time varied together ($r^2 = 0.80$). Vertical foraging effort were concentrated just below the MLD on average (Table 2.2).

Table 2.2: Seasonal mean (\pm SD) foraging and associated mixed layer properties between stratified and mixed water columns collected by seal-borne devices attached to subantarctic fur seals at Marion Island. Note, foraging (given by vertical area-restricted search) does not occur in all dives. Positive values of 'Difference between mean foraging depth and MLD' indicate deeper mean foraging depth than mixed layer depth (MLD). Maximum depth is always deeper than MLD and foraging depth.

Season:	Summer		Winter	
Water column stratification:	Mixed	Stratified	Mixed	Stratified
# Dives	63 119	18 971	252 024	12 646
% high effort dives	62.27	42.59	51.21	33.75
Stability [$1e^{-5}/s^2$]	0.09 ± 0.29	1.62 ± 0.98	0.00 ± 0.18	0.50 ± 1.05
Temp [$^{\circ}C$]	6.9 ± 1.1	7.0 ± 0.9	7.0 ± 1.4	6.9 ± 1.8
Foraging depth [m]	43.2 ± 16.3	50.6 ± 17.1	45.7 ± 25.6	58.2 ± 27.7
Difference between foraging and max depth	4.84 ± 5.81	6.24 ± 7.52	7.08 ± 9.25	8.48 ± 10.8
Mixed layer depth (MLD)	NA	40.8 ± 18.0	NA	51.2 ± 27.5
Difference between mean foraging depth and MLD [m]	NA	$+(10.1 \pm 17.2)$	NA	$+(7.6 \pm 29.1)$
Max distance below MLD [m]	NA	17.4 ± 16.9	NA	18.8 ± 28.1

Night dives makeup 87.51% (n = 303 468) of all dives, while only 1.70% (n = 5899), 0.787% (n = 2729), and 10% (n = 34 664) of dives are made during the day, dawn, and dusk, respectively. Median foraging time per night was 39 minutes and 15 minutes in winter and summer, respectively.

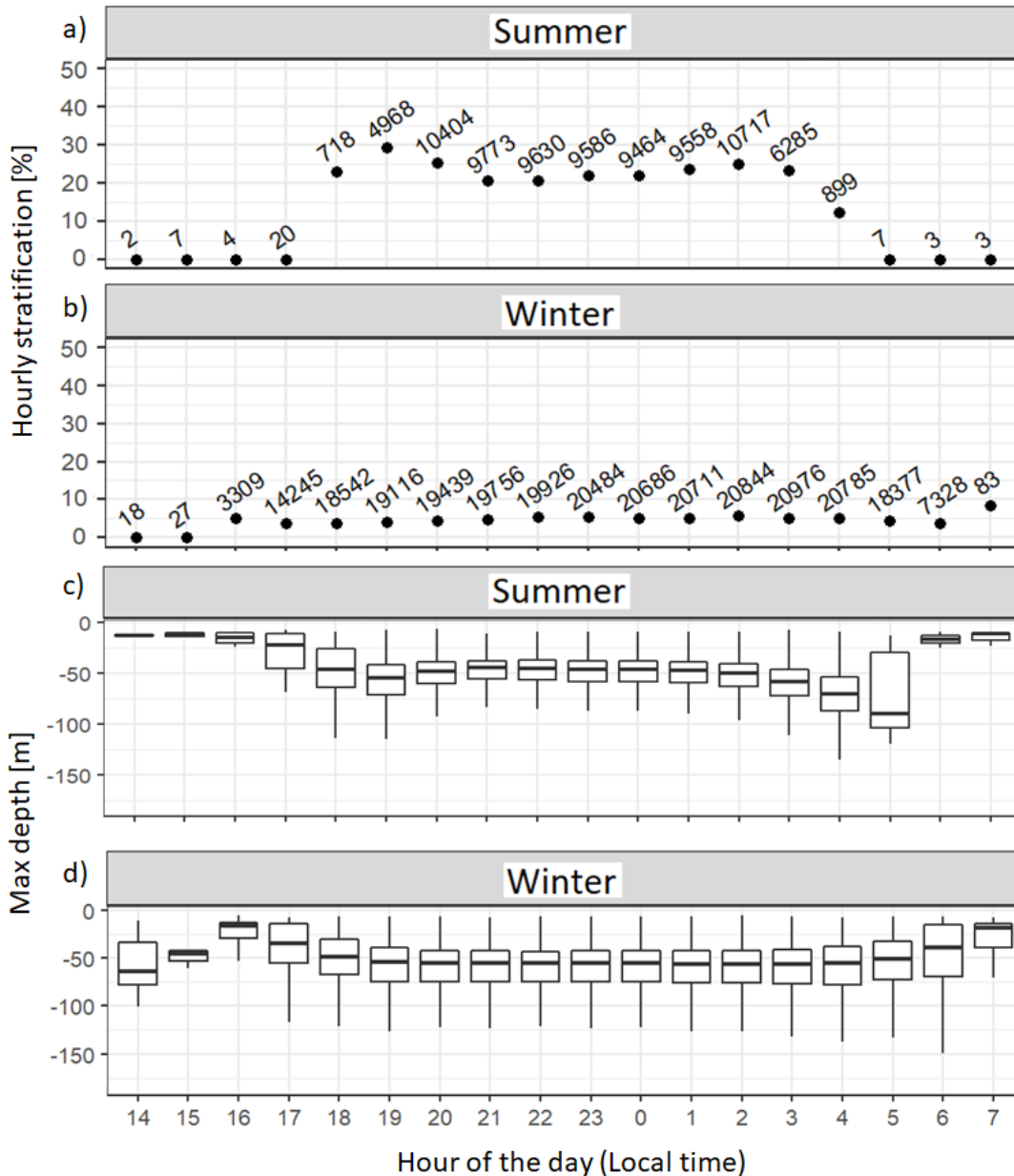


Figure 2.8: Percentage of stratified profiles per hour of the day from 14:00 to 07:00 in a) summer and b) winter, along with boxplots of maximum depth per hour of the day [m] in c) summer and d) winter. The corresponding sample number of dives used for each hour based on local time of dives is indicated above points in (a) and (b). In summer, seals follow diel vertical migration to optimize energy-efficiency in prey capture.

In summer, stratification [%] was positively associated with maximum depth [m] at hourly scales (Figure 2.8a,c). Peaks of stratification and maximum dive depths occurred

between 18:00 and 20:00, with maximum hourly stratification (29%) at 19:00 (Figure 2.8a,c). Maximum depth was shallower at night relative to crepuscular dives, independent of stratification state (stratified versus mixed) (Figure 2.8a,c). In stratified water columns, when night dives were shallower than crepuscular dives, night dives were associated with lower vertical foraging effort than crepuscular dives (Figure 2.9a,c). In well-mixed water columns, maximum depth was inversely associated with vertical foraging effort (Figure 2.9a,c). Transit dives made up 12.40%, 14.31%, 11.77% and 17.90% of dives during Dawn, Day, Dusk and Night, respectively.

In winter, hourly stratification remained below 10% with no observable hourly pattern (Figure 2.8b,d). Hourly and diel phase means of maximum depth both show increased night relative to crepuscular maximum depths (Figure 2.8, Figure 2.9). Diel means of maximum dive depth was negatively associated with mean vertical foraging effort, irrespective of stratification (Figure 2.9b,d). Transit dives made up 2.20%, 4.05%, 14.30% and 17.75% of dives during Dawn, Day, Dusk and Night, respectively.

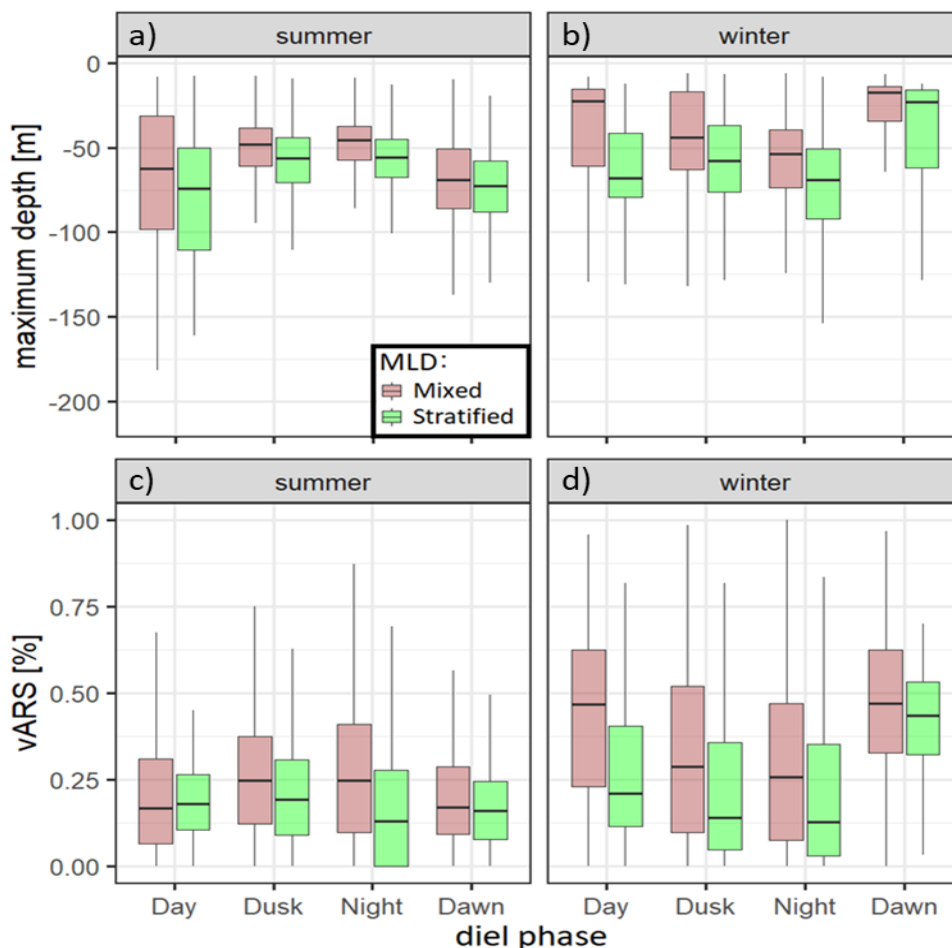


Figure 2.9: Diel patterns of vARS (vertical foraging effort) [%] (a,b) and maximum depth [m] (c,d) between stratified and mixed water masses in summer (a,c) and winter (b,d).

Response of diving and foraging behaviour to immediate oceanography

Table 2.3: Summary of generalised additive mixed-effects model (GAMM) comparisons: GAMMs of a) summer and b) winter dive types proportions. The chosen model is in bold. "mean_Temperature" = mean temperature of the water column per dive; "Stratification" = categorical variable representing a mixed or stratified water column; "Stability" = vertical stability averaged throughout a dive; "AICc" = Akaike's Information Criterion corrected for finite sample sizes; " Δ AICc" = difference in AICc from that of the best fitting model; "R-sq (adj)" = Adjusted R² value; "REML" = Restricted maximum likelihood; "k" = Number of base functions used in the model.

b) Summer: Divetype ~	R-sq (adj)	Deviance explained [%]	REML	k	AICc	Δ(AICc)
Stratification+s(mean_Temp)+s(log(Stability),by=Stratification)	0,0976	7,46	-51934	20	103626,7	-481,1
Stratification+s(mean_Temp)+s(log(Stability),by=Stratification)	0,0921	6,99	-52149	10	104107,8	0,0
s(mean_Temp)+s(log(Stability),by=Stratification)	0,092	6,98	-52154	10	104120,6	12,8
Stratification+s(log(Stability),by=Stratification)	0,0869	6,59	-52353	10	104541,7	433,9
s(log(Stability),by=Stratification)	0,0867	6,57	-52361	10	104560,3	452,5
Stratification+s(mean_Temp)+s(log(Stability),by=Stratification)	0,0717	5,42	-53018	5	105859,5	1751,7
Stratification+mean_Temp+log(Stability)	0,0604	4,56	-53438	10	106777,7	2669,9
Stratification+s(mean_Temp)	0,0584	4,34	-53574	10	107038,2	2930,4
Stratification	0,0525	3,89	-53803	10	107521,4	3413,6
s(mean_Temp)	0,0349	2,59	-54554	10	108998,1	4890,3
a) Winter: Divetype ~	R-sq (adj)	Deviance explained [%]	REML	k	AICc	Δ(AICc)
Stratification+s(mean_Temp)+s(log(Stability),by=Stratification)	0,172	13,4	-15910	20	317853,5	-2786,3
Stratification+s(mean_Temp)+s(log(Stability),by=Stratification)	0,164	12,6	-160440	10	320639,8	0,0
s(mean_Temp)+s(log(Stability),by=Stratification)	0,164	12,6	-160450	10	320648,7	8,9
Stratification+s(log(Stability),by=Stratification)	0,158	12,2	-161180	10	322157,3	1517,5
s(log(Stability),by=Stratification)	0,158	12,2	-161190	10	322173,6	1533,8
Stratification+s(mean_Temp)+s(log(Stability),by=Stratification)	0,1440	10,9	-163580	5	326975,5	6335,7
Stratification+s(mean_Temp)	0,135	10,2	-164910	10	329667,1	9027,3
s(mean_Temp)	0,133	9,97	-165260	10	330359,6	9719,8
Stratification+mean_Temp+log(Stability)	0,13	9,84	-165490	10	330848,9	10209,1
Stratification	0,129	9,76	-165620	10	331125,7	10485,9

When the number of base functions (k) was set to 20, model fit (Table 2.3) was overshadowed by difficulties in interpretability of model outputs. The second most parsimonious model was chosen in summer (n = 82 090, AICc = 104 107.8) and winter (n=264 670, AICc = 320 639.8) (Table 2.3Table 2.5). With dive type as the response variable, the model retained all predictor variables - water column stratification, stability and mean temperature (Table 2.3). VIF remained below the cut-off threshold (10), and concurrency estimates remained below the cut-off threshold (0.5) for all explanatory variables. Both summer (R² = 0.0921, Deviance explained = 6.99%, REML = -52 149) and winter (R² = 0.164, Deviance explained = 12.6%, REML = -160 440) models converged. Linearising the model in both summer and winter reduces model fit (Table 2.3).

QQ plots for each season show mostly straight-line trends of deviance residuals versus the quantiles of the estimated distribution (theoretical quantiles) (See in Supp.Figure 3). Model smooths estimate the probability of high effort dive occurrence relative to low effort dive occurrence of a typical seal, assuming all other variables are at average levels. Given a specific environmental state, the proportion of high effort dives and the proportion of low effort dives will add up to 1. For a response curve of a given fixed effect, a response of 1 indicated 100% probability of high effort dives, a response of 0 indicated 100% probability of low effort dives, and a response of 0.5 indicated a 50% chance of either high or low effort dives. Shaded regions of the model graphs (Figure 2.10,Figure 2.11) represent confidence intervals from the covariance matrix of the spline coefficients.

Table 2.4: Parametric coefficients and approximate significance of smooth terms from generalised additive mixed-effects models (GAMMs). Summer and winter results are presented for comparison. “edf” = Expected degrees of freedom; “Ref.df” = Reference degrees of freedom. Test statistics are given as ‘Z value’ and ‘Chi.sq’. ‘log_Nt’ = Vertical stability (Nt^2) on the log scale.

Parametric coefficients:	Estimate	Standard error	Z value	Pr(> z)
Summer: Intercept	0,288	0,103	2,81	0,005
Stratification	-0,216	0,056	-3,84	<0,001
Winter: Intercept	0,311	0,166	1,87	0,061
Stratification	-0,123	0,038	-3,25	<0,001
Approximate significance of smooth terms:	edf	Ref.df	Chi.sq	P-value
Summer: s(mean Temperature)	8,33	8,88	441	<0,001
s(log_Nt):Mixed	8,84	8,98	2432	<0,001
s(log_Nt):Stratified	8,44	8,89	344	<0,001
s(sealID)	18,82	19	2032	<0,001
Winter: s(mean Temperature)	8,79	8,99	1509	<0,001
s(log_Nt):Mixed	8,97	8,99	7431	<0,001
s(log_Nt):Stratified	8,56	8,94	760	<0,001
s(sealID)	17,97	18	26 826	<0,001

Stratification, stability, and mean temperature all elicit a significant non-linear response (effective degrees of freedom (edf) >1 , $p<0.001$) on the types of dives made by lactating female SAFS (Table 2.4). The probability of high effort dive occurrence significantly decreases with increasing stratification in summer (Z value = -3.84, Estimate = -0.216, $p<0.001$) and winter (Z value = -3.25, Estimate = -0.123, $p<0.001$) (Table 2.4). Mean temperature has a small overall positive effect on probability of high effort dive occurrence in summer ($\chi^2 = 441$, edf = 8.33, $p<0.001$) and winter ($\chi^2 = 1509$, edf = 8.79, $p<0.001$) (Table 2.4). A negative effect of mean temperature on dive response at temperatures <5 °C in both seasons were followed by a positive response until roughly the average mean temperature (~ 7 °C) (Figure 2.10c, Figure 2.11c). At mid-ranges, the mean temperature (8-10 °C) appears to have no influence on diving behaviour (Figure 2.10c, Figure 2.11c). Once mean temperature increases above extreme high mean temperatures (>10 °C), mean temperature is positively proportional to the probability of high effort dive occurrence (Figure 2.10c, Figure 2.11c). However, greatest uncertainty lies around extreme values of mean temperature across both seasons, with larger uncertainty in summer (Figure 2.10c, Figure 2.11c).

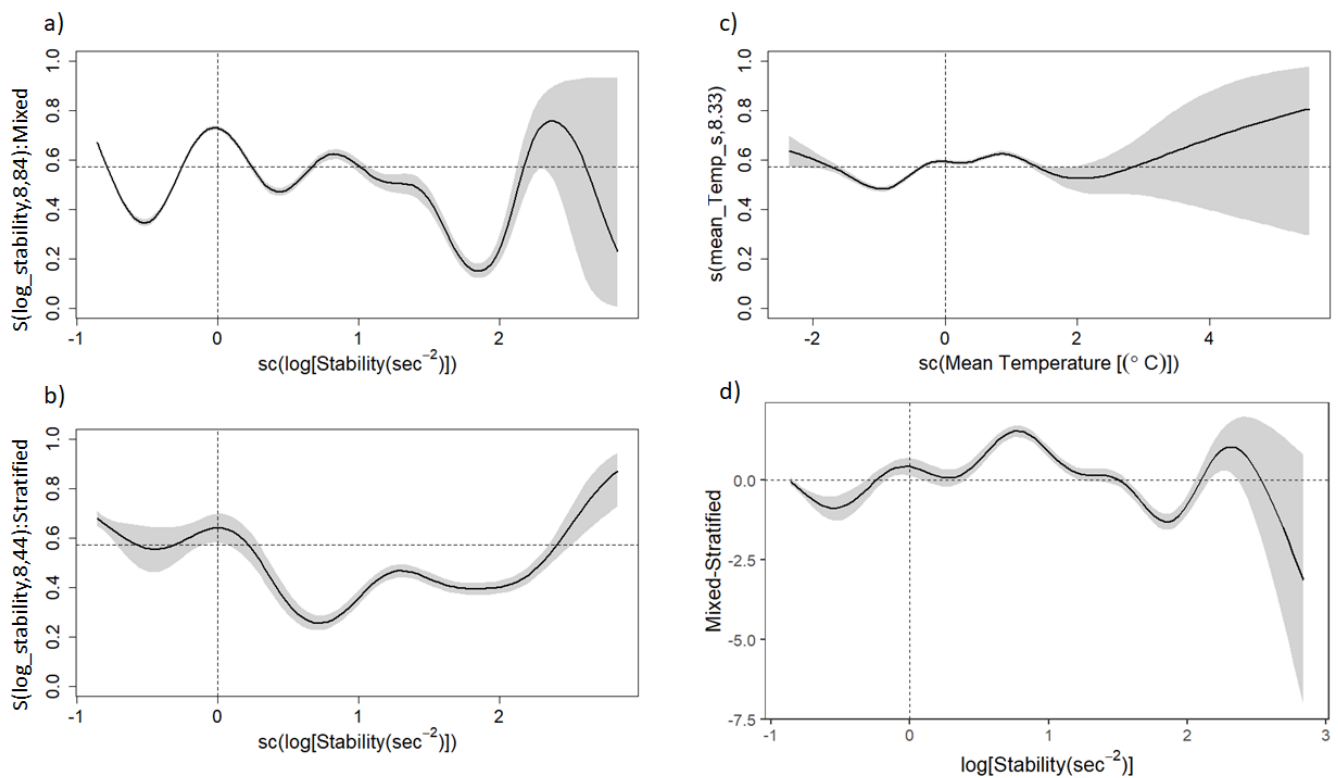


Figure 2.10: Summer model smooth estimates for the partial effects of stability in mixed (a) and stratified (b) water and mean temperature (c) on behavioural response. The y-axis is scaled by the smooth function of explanatory variables and the model intercept is indicated by a horizontal dotted line. All plots are converted to the probability scale for interpretation from the log scale of model outputs. The vertical dotted line represents the mean for each scaled variable. The difference between mixed and stratified effects of

stability are shown in (d). The horizontal dotted line signifies zero difference, while the vertical line indicates the centre of log-transformed and scaled stability. The grey bands represent 95% confidence intervals in all plots. The effective degrees of freedom are shown in brackets for each smooth function estimate.

The expected probability of high effort dive occurrence was high (>0.6) at summer mean stability ($0.45 \pm 0.84 \text{ e}^{-5} \text{ s}^{-2}$) (Figure 2.10a,b) and low (<0.4) at winter mean stability ($0.03 \pm 0.31 \text{ e}^{-5} \text{ s}^{-2}$) (Figure 2.11a,b). In well-mixed and unstable (stability $< 0.1 \text{ e}^{-5} \text{ s}^{-2}$) water columns, the seals tend to increase vertical foraging effort and dive shallower in summer and winter (Figure 2.10a, Figure 2.11a). High levels of stability ($>2 \text{ e}^{-5} \text{ s}^{-2}$) were associated with less confidence (Figure 2.10a,b, Figure 2.11a,b). In winter, the stability negatively affects the probability of occurrence of high effort dives below the mean stability level, yet positively affects it until stability values reach the model intercept (0.577) (Figure 2.11a,b). This is followed by a positive quadratic trend in stratified water and a sinuous trend in mixed water. Similar trends of stability effects with respect to stratification were observed in summer, however, the trend in summer was shifted towards lower stability values relative to the respective average (Figure 2.10a,b). Differences between effects of stability in mixed and stratified water columns illustrates a negative quadratic trend in both summer and winter, with both models peaking around one or two standard deviations above the respective mean stability values (Figure 2.10d, Figure 2.11d). This indicated stronger positive effects of stability in mixed water columns slightly above average stability values in high effort dive occurrence compared to in stratified water columns.

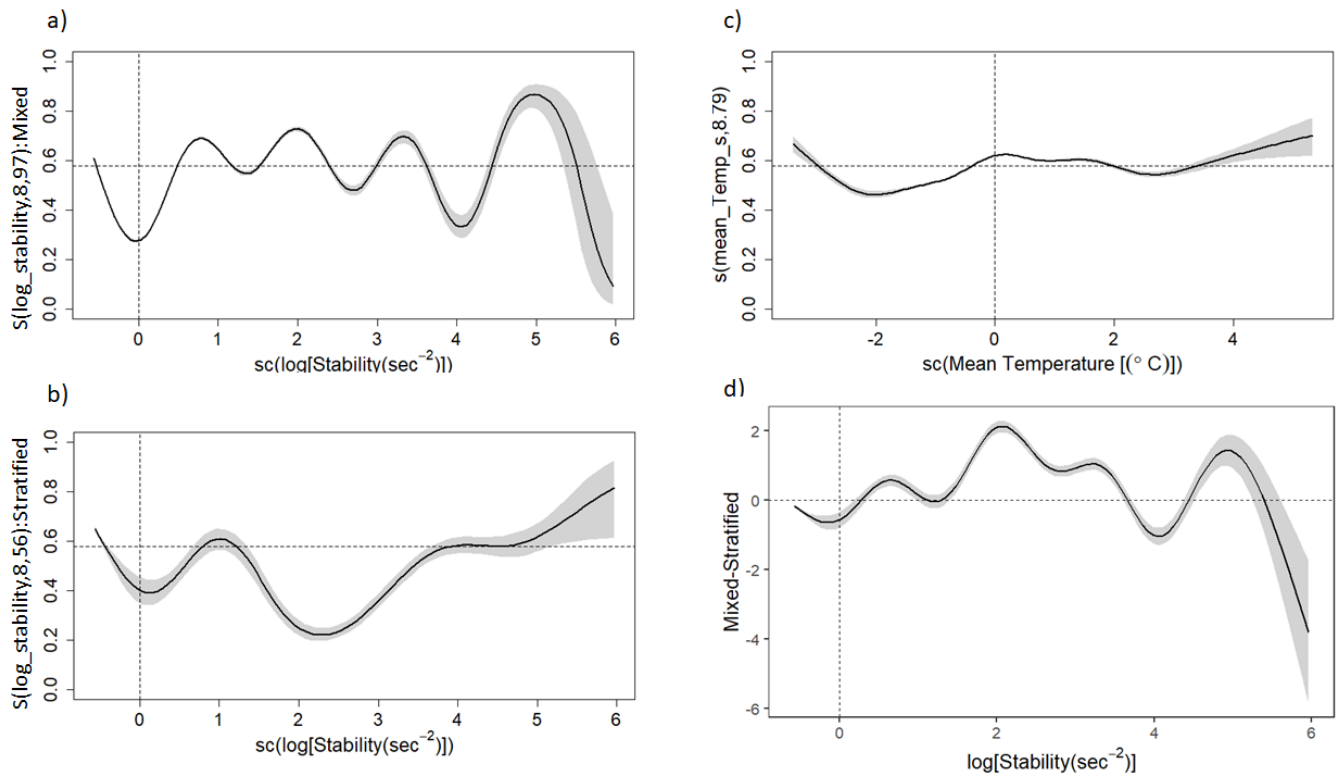


Figure 2.11: Winter model smooth estimates for the partial effects of stability [sec^{-2}] in a) mixed and b) stratified water and c) mean temperature [$^{\circ}\text{C}$] on dive type response. The y-axis is scaled by the smooth function of explanatory variables and the model intercept is indicated by a horizontal dotted line. All plots are converted to the probability scale for interpretation from the log scale of model outputs. The vertical dotted line represents the mean for each scaled variable. The difference between mixed and stratified effects of stability are shown in (d). The horizontal dotted line signifies zero difference, while the vertical line indicates the centre of log-transformed and scaled stability. The grey bands represent 95% confidence intervals in all plots. The effective degrees of freedom are shown in brackets for each smooth function estimate.

Discussion

This study investigated the effects of upper ocean thermal structure on the fine-scale diving and foraging behaviour of SAFS at Marion Island. To achieve this objective, the main types of dives made were distinguished and described according to the SAFS diving and foraging behaviours in three-dimensional space. Furthermore, the influence of vertical mixing on the seasonal and diel trends in diving behaviour was assessed. Specifically, the vertical distribution of foraging effort was analysed in relation to the MLD, providing an indication of whether MLDs are targeted by seals as foraging hot spots within the water column.

Types of dives made by SAFS

Firstly, no statistical agreement was found between horizontal and vertical area-restricted search values, contrasting the close agreements between vertical and horizontal efforts found for the sympatric population of Antarctic fur seals residing at Marion Island (Arthur *et al.*, 2016), as well as in southern elephant seals at the Kerguelen Islands (Dragon *et al.*, 2012). This suggested that foraging effort detected through surface tracking data may not always be an accurate predictor of vertical foraging effort. Based on PCA analysis, the percentage bottom time, dive efficiency, dive residual, vARS, dive duration and maximum depth were found to explain the majority of variance and were considered for selection for cluster analyses for both seasons, except for dive duration in summer. Consequently, hARS did not contribute statistically sufficiently to diving and foraging effort, thus further analysis was based not on three-dimensional habitat use but was rather restricted to the vertical use of the water column (vARS).

Table 2.5: Seasonal diving parameters associated with each dive type of female subantarctic fur seals from 2009-2015 deployments. 'vARS' refers to vertical area-restricted Search/vertical foraging effort. Values are given as mean \pm SD. Scaled and centred differences are illustrated by the confidence interval (CI) of a Welch Two Sample t-test. CI values are therefore unitless. All differences were significant at $p < 0.001$. Parameters are sorted from largest to smallest differences between dive types.

	Summer dives			Winter dives		
	Low effort	High effort	CI	Low effort	High effort	CI
Bottom effort [%]	39 \pm 12	63 \pm 9	-1.57; -1.55	33 \pm 12	66 \pm 0	-1.62; -1.61
vARS [%]	10 \pm 11	35 \pm 17	-1.31; -1.29	11 \pm 12	46 \pm 17	-1.54; -1.53
dive efficiency	0.21 \pm 0.09	0.42 \pm 0.10	-1.51; -1.49	0.21 \pm 0.09	0.47 \pm 0.12	-1.53; -1.52
dive residual	-10.53 \pm 16.56	7.47 \pm 19.83	-0.89; -0.86	-12.29 \pm 25.36	12.11 \pm 28.10	-0.84; -0.82
max depth [m]	62.70 \pm 18.47	43.31 \pm 12.11	1.07; 1.10	73.37 \pm 27.61	40.69 \pm 20.36	1.11; 1.13
dive duration [sec]	N/A	N/A	N/A	121.53 \pm 40.05	127.13 \pm 44.24	-0.14; -0.13

Clustering of dives simplifies large amounts of information about foraging and diving behaviour to gain a more holistic understanding of foraging behaviours and reduce model complexity for analyses of cues in the form of thermal water column structure that may be influencing decision making within a dive. High effort dives differentiated from low effort dives in both seasons (Table 2.5). Dives were similarly grouped in both winter and summer, irrespective of the seasonally modulated magnitudes of dive depth, duration and

effort previously observed at Marion Island (Wege, 2017). Bottom effort had the greatest normalized difference between high and low effort dives in both seasons relative to all other variables describing dive type (Table 2.5). Furthermore, PCA results (Figure 2.5c,d) show that bottom effort had the greatest overall contribution to explaining the variance in the data. This led to the distinction between the dive types of SAFS being based on effort and is therefore hereafter discussed accordingly.

As bottom effort and vertical foraging effort were positively correlated, this suggests that in high effort dives, seals spent more time in the bottom phase with increased sinuosity within the vertical plane. Due to this correlation and because average distances between maximum depth and foraging depth were small (<10 m), seals probably forage mostly within the bottom phase of the dive (Georges *et al.*, 2000; Hooker *et al.*, 2002; Weimerskirch *et al.*, 2007; Roncon *et al.*, 2018). However, while bottom effort is indicative of vertical foraging effort (Bailleul *et al.*, 2008), increasing bottom time does not necessarily relate to a high rate of prey encounters (Viviant *et al.*, 2016).

High effort dives were also represented by high dive efficiency and were longer than expected relative to their maximum depth, i.e. large positive dive residuals. Dive efficiency, vertical foraging effort and bottom effort were all negatively correlated with maximum depth (Figure 2.5a,b), i.e. the deeper the dive, the lower dive efficiency, vertical foraging effort and bottom effort. The negative correlation between diving efficiency and maximum depth was in line with studies on Antarctic fur seals (Viviant *et al.*, 2016) and Gentoo penguins (Lee *et al.*, 2015). Seals require less recovery when diving shallower, as is normally the case in marine mammals (Kooyman, Castellini and Davis, 1981). I propose that the two main dive types made by SAFS, (high effort and low effort) may represent the major strategies employed by seals to deal with changing environmental conditions at small temporal (<24 hr) and spatial scales (1-10 km). Considering that low vertical foraging effort corresponds with low dive efficiency, I additionally propose that anaerobic diving may be playing a role in benefitting seals when encountering mobile prey, with such behaviour having been in Western grebes shown to enable surplus exploitation before the prey escapes (Ydenberg and Clark, 1989).

Seasonal foraging trends in relation to seasonality of the upper ocean thermal structure

Diving and foraging effort is enhanced in winter relative to summer. Strong seasonality also exists in water stratification and stability, with higher stratification and stability in summer, akin to other studies within the Southern Ocean (Dong *et al.*, 2008; Sallée *et al.*, 2010; du Plessis *et al.*, 2019), whilst mean water column temperature did not change between seasons. Weak seasonality in mean temperatures could be a result of the compensating effect of some seals travelling further north in winter towards warmer waters, when sea surface temperatures are expected to decrease around the islands (Chown and Froneman, 2008). Overall, water stratification, where lactating females had lower vertical foraging effort, was relatively low (summer = 23.11%; winter = 4.78%) compared to in studies of northern fur seals (autumn = 31.9%; Kuhn, 2011). In well-mixed water columns, which accounts for the majority of those experienced by seals, MLD absence suggests that seals don't appear to align their vertical foraging effort in relation to the MLD. Although SAFS reach the MLD more frequently during summer, seals rarely dive deeper than the MLD irrespective of season.

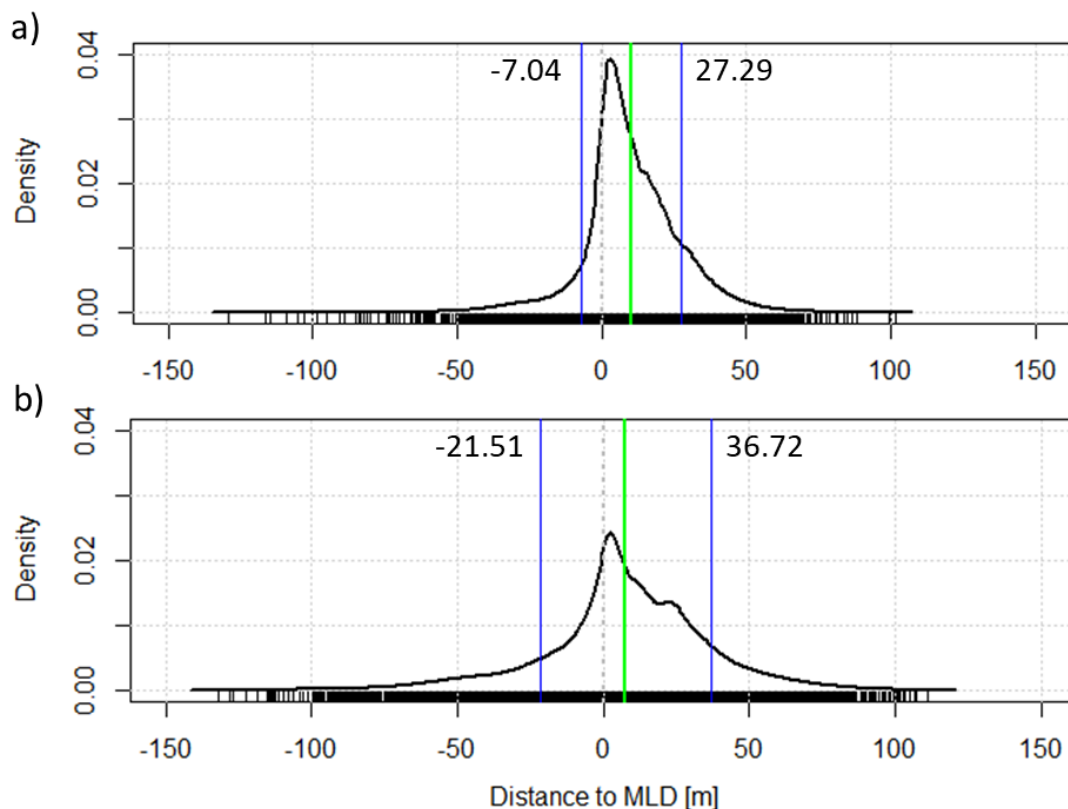


Figure 2.12: Density plots of mean foraging depth minus mixed layer depth (MLD) [m] for summer (a) and winter (b) dives. Positive values illustrate dives with deeper foraging depth than MLD. Only dives where the maximum depth extends beyond the mixed layer (i.e. stratified water column) are represented. Blue lines associated with annotated numbers indicate 1 standard deviation from the mean difference (green). The

mean differences were 10.1 and 7.6 m for summer and winter, respectively. The grey dotted line is a reference to zero difference between mean foraging depth and MLD.

SAFS dives in stratified water columns were deeper on average, akin to northern fur seal dives (Kuhn, 2011). Furthermore, the mean proximity of the maximum dive depth below the MLD of ~20 m was similar to that found in studies of Northern fur seals (Kuhn, 2011), with low seasonal variability, despite deeper winter MLDs. This is explained by the strong association found between maximum dive depth and MLDs. Foraging depths also had a strong association with MLDs. Seals tended to focus foraging effort about 10 m below the MLD on average, with weak seasonality, despite larger intra-seasonal variation in winter than in summer (Figure 2.12). Since, the mean time in vARS per dive was higher in winter than in summer, I propose that deeper winter maximum dive depths may be driven by increased vertical searching behaviour, resulting in a greater range of foraging depths, which is probably influenced by the presumably scarce prey of the Southern Ocean (Moore and Abbott, 2000), the unpredictability of prey, and out of reach MLDs experienced in winter.

Shallow mixed layers, which are typically more common in summer in the Southern Ocean (de Boyer Montégut *et al.*, 2004; du Plessis *et al.*, 2019), are known to enhance primary productivity (Moore *et al.*, 2000) by allowing for photosynthesis through the trapping of nutrients and phytoplankton in the euphotic (light-lit) zone. Trophic cascades occur from phytoplankton to zooplankton at the MLD (Pakhomov *et al.*, 1994; Froneman *et al.*, 1999; Lea and Dubroca, 2003), with an associated vertical distribution of pelagic myctophid fish (Pakhomov and McQuaid, 1996; Bakun, 2007; Koubbi *et al.*, 2011), which dominates the dietary composition of SAFS (Klages & Bester 1998; Reisinger *et al.*, 2018). As such, I propose that in stratified water, shallower diving and more concentrated foraging effort just below (~10 m) the MLD in summer is driven by the available biological productivity associated with a shallower summer MLD.

The seasonal differences in diel trends of seal diving and foraging behaviour in relation to water stratification (Figure 2.8, Figure 2.9), provides an indication that small temporal scale (<24 hr) modifications are made by seals. Winter hourly stratification was negligible (<10%) throughout the diurnal cycle, whereas summer intensification of stratification was observed in the late afternoon (18:00-20:00) and remained high until early morning (~03:00) (Figure 2.8). On average, SAFS dive deeper and spend less vertical foraging effort in stratified water columns per diel phase (Figure 2.9), likely following deep and

profitable prey patches associated with the MLD (Green *et al.*, 2020). I propose that these low effort-deep dives may in fact suggest higher foraging success in productive, deep waters. As such, seals may be compensating for high vertical foraging effort by reducing depth, in an attempt to balance the energy demands of both foraging and diving in relation to the energy gain(s) through food consumption (Pyke, 1984). However, no energetic analytics or direct foraging success measurements were produced in this study. Future investigation into foraging success and/or energetic analyses is suggested to provide further insight into the possible driving forces of these behavioural observations at fine scales.

Diel foraging trends in relation to patterns of the upper ocean thermal structure

In both mixed and stratified water columns, summer dives were shallower at night relative to deeper crepuscular dives, a typical trend in SAFS (Figure 2.9) (Goldsworthy, Hindell and Crowley, 1997; Georges, Tremblay and Guinet, 2000; Luque, Arnould and Guinet, 2008; Wege, 2013). Certain myctophid fish species rise towards the surface at night (Bost *et al.*, 2002) forming patchy prey distributions for higher trophic levels (Perissinotto *et al.*, 2000). Seals can therefore exploit these nycthemeral vertically migrating prey without needing to dive deeper (Croxall *et al.*, 1985; Klages and Bester, 1998; Georges *et al.*, 2000; Lea *et al.*, 2002). Although vertical foraging effort and maximum depth were negatively associated within their respective diel phases, this association does not always hold true along the diel cycle (Figure 2.9). Stratification state was shown to influence the relationship between maximum depth and vertical foraging effort over diel cycles. For example, in summer stratified water columns observed in this study (23.11% of summer dives), decreased vertical foraging effort at night relative to crepuscular dives followed a decreasing trend in maximum depth (Figure 2.9). I propose that this anomalous positive summer association, may be indicative of highly productive patches of prey entering shallow waters at night, associated with a shallow MLD (Perissinotto *et al.*, 2000), in turn requiring less vertical foraging effort associated with shallower dives (Ydenberg and Clark, 1989). This contrasts with diel patterns of summer dives in mixed water columns, where seals are proposed to be spending more time searching for food in shallow water at night, when the MLD is supposedly out of reach. These diel variations of the MLD can potentially be caused by strong winds acting to mix the upper ocean and deepen the MLD, while during quiescent wind periods, the MLD is then able to restratify (shallow) again (du Plessis *et al.*, 2019).

Findings of this study, as well as Wege (2013), show that in winter, when the MLD is deeper, seals do not appear to follow diel vertical migrations of prey. As maximum seal dive depths are physiologically constrained (Viviant *et al.*, 2016), MLDs may be too deep for seals to focus their foraging effort on myctophids whose vertical distributions are associated with the MLD. Alternatively, winter diel variability of maximum dive depths, with deeper dives at night than crepuscular dives, may be a result of seals switching prey sources, possibly favouring cephalopods over myctophid fish, as suggested by Wege (2013). However, the intrinsic or environmental cues that drive possible prey switching is yet to be studied.

From these results it is evident that although stratification [%] was generally low for most of the study period, stratification state [mixed vs stratified] may influence foraging and diving behaviour differently at small (<24 hr) temporal scales. However, because these results could be an artefact of coincidental associations, and to prevent false inferences of causation, further investigation of upper ocean thermal structure influences on diving and foraging behaviour were made using GAMMs.

Effect of upper ocean thermal structure on fine-scale diving and foraging behaviour

Dive type was modelled as a probability between seals either making high or low effort dives in relation to environmental fixed effects. Stratification state, stability and mean temperature all significantly ($p < 0.001$) and non-linearly modulated the types of dives made by SAFS (Table 2.4). The probability of high effort dive occurrence was negatively influenced by stratification state, across seasons, with a higher proportion of high effort dives in well-mixed water columns.

Although significant, the relationship between water stability and dive type was complex, with no observable overarching trend (Figure 2.10, Figure 2.11). High effort dives are predicted to occur more often than low effort dives in summer, when the seal experiences average summer stability within the region (Figure 2.10), while in winter, low effort dives were expected to dominate during periods of average winter stability. Variation in the effects of stability may be related to the spatio-temporal variation of seals to experience coherent oceanographic features, such as submesoscale fronts which are capable of locally enhancing stability and stratification (Lévy *et al.*, 2012).

Mean temperature of the water column had a small, yet significant, non-linear positive effect on the probability of high effort dive occurrence (Table 2.4). Therefore, higher mean temperature (>7 °C) is predicted to increase the amount of vertical foraging effort. Minimum and maximum values of temperature in summer and winter were in line with findings from Toolsee *et al.*, (2021) (2 °C in winter and 8 °C in summer). However, potentially greater temperature ranges, e.g. predicted to be experienced due to increasing temperatures with climate change within the Southern Ocean (Constable *et al.*, 2014) and PEI region (Ansorge *et al.*, 2014), could have far reaching impacts on fur seal foraging behaviour, particularly with respect to requirements for increased vertical foraging effort.

Seasonal increases in sea surface temperatures tend to be delayed by about two months (~February) following maximum incoming solar radiation (~December) (Toolsee *et al.*, 2021). This increase in surface temperatures falls in line with the temporal range of summer seal foraging trips (15th Oct - 14th April). Increases in sea surface temperatures were assumed to reflect in the subsurface mean temperatures of seal-derived profiles, meaning that, with the positive effect of mean temperature on high effort dive occurrence, summer seals tend to increase effort and dive shallower as summer progresses, as reflected in the model results.

In this study, I assumed that the differences in sampling rate between devices used did not influence model outcomes. Future studies should investigate the influence of sampling rate when modelling behavioural responses to environmental conditions. Nevertheless, all model assumptions were met according to model convergence, concavity and optimal number of base functions. The smaller sample size in summer relative to winter was reflected in larger summer uncertainty around model estimates (Figure 2.10, Figure 2.11). Both summer and winter models were found to converge as well as fit similar trends, despite few anomalous areas of decreased confidence, typically at extreme values of explanatory variables. VIF and concavity analysis indicated that there were no major sources of collinearity in covariates prior to model input. Model checks suggested that model re-fitting was necessary by doubling the number of basis dimensions (k) until the optimal number of functions were determined. Although a higher number of base functions resulted in a higher model fit (Table 2.3), functional smooths were restricted in the final model to a maximum of $k = 10$ (the function default in R), for improved computational efficiency and interpretability (Wood, 2017). The models improved (AICs decreased) with non-linear terms, implying that the effects of stability and

mean temperature were best approximated by using non-linear relations to the response variable. However, overall, seals showed no clear choice of distinct habitat areas based on upper ocean thermal structure.

Conclusions

A pressing concern surrounding the collecting of large amounts of data is the need for effective and efficient methods to simplify and extract important information from a haze of large data. Although cluster analysis has been used extensively for dive classification in seal ecology studies (Lea *et al.*, 2002; Lidgard *et al.*, 2003; Boyd, Bowen and Iverson, 2010; Krause *et al.*, 2016), no such analyses had been made on the diving behaviour of SAFS at Marion Island. Consequently, large amounts of seal-derived data were clustered according to diving and foraging metrics to distinguish distinct types of dives made by SAFS at Marion Island, providing valuable information about their diving behaviour. High effort dives, associated with shallow maximum dive depth, vertical foraging effort, bottom effort, and dive efficiency, differentiated from low effort dives. The probability of high effort dives significantly decreased with increasing water column stratification, while the relationship with the stability and mean temperature of the water column was complex, yet significant. Overall, seals appear to intensify vertical foraging effort in well-mixed, warmer (>7 °C) water columns. Seals show a strong association in diving behaviour to the diel and seasonal trends in vertical mixing. Stratification state was shown to influence the relationship between maximum depth and vertical foraging effort over diel cycles. The seasonal, diel and dive-level effects of upper ocean thermal structure on foraging and diving behaviour of SAFS may provide evidence for major strategies employed by seals to deal with changing environmental conditions across a multitude of temporal scales.

When MLDs were within the depth limits of seals (imposed by physiological limitations), seals concentrated vertical foraging effort just below the MLD in both seasons. For the remainder of the dives in either season i.e. those in well-mixed water columns, which accounted for the majority, the MLD absence suggests that seals don't appear to align their vertical foraging effort in relation to the MLD. Although SAFS reach the MLD more frequently during summer, they rarely dive below the mixed layer irrespective of season. Although effects of upper ocean thermal structure to foraging and diving behaviours were significant, overall, seals showed no clear choice of distinct habitat areas based on upper

ocean thermal structure. Nevertheless, these results shed light on how seals allocate their time when foraging out at sea in relation to upper ocean thermal structure.

Findings from this study offer greater understanding of the fine-scale influences of the immediate physical environment experienced by SAFS on their diving and foraging behaviour. Consequently, disentangling potential threats to the foraging ecology of these seals in the future, such as climate change (Hussey *et al.*, 2015), linking to more effective conservation and management (Taylor *et al.*, 2011; Arthur *et al.*, 2017).

Chapter 3: Small-scale topographic influences on seasonal submesoscale processes and restratification at the Prince Edward Islands and links to fur seal foraging effort: An upstream versus downstream comparison

Mr. S. Evans¹, Dr M. du Plessis^{1,2}, Dr M. Wege³, Prof. I. Ansorge¹, Dr A. Lowther⁴, Ass. Prof. N. de Bruyn³.

¹Department of Oceanography, University of Cape Town, South Africa ; ²Department of Marine Sciences, University of Gothenburg, Sweden; ³Department of Zoology & Entomology, University of Pretoria, South Africa; ⁴Norwegian Polar Institute, Norway.

This chapter should be cited as: Evans, S. (2021) 'Small-scale topographic influences on seasonal submesoscale processes and restratification at the Prince Edward Islands and links to fur seal foraging effort: An upstream versus downstream comparison', *In Prep. Mar Ecol Prog Ser.*



An adult male subantarctic fur seal protects his territory. A southern elephant seal yearling in the background.

Abstract

Historically, a lack of observations in the relatively inaccessible Southern Ocean has led to poor quantification of submesoscale (hours to days, 1-10 km) upper ocean physical processes. Additionally, fine-scale (<24 hr, ~1 m) ecological studies of animal movements in this isolated region are scarce. Recent advancements in technology have allowed for the development of animal-borne devices that can be deployed on seals to fill these gaps in scale. Temperature-depth sensors were deployed on 39 diving subantarctic fur seals (SAFS), allowing the opportunity to explore the oceanographic setting of the Prince Edward Islands, the seasonality of this oceanography, and the seasonal impacts of small island topography on downstream flows, with the use of concomitant satellite remote sensing ocean products. Furthermore, I aimed to link the diving and foraging behaviour of SAFS to upstream and downstream topographic influences on ocean mixing. Submesoscale transport fronts and mesoscale (100-200 km) activity were seasonally co-located and locally enhanced around the islands in summer due to the northward shift of the ACC fronts associated with the summer intensification of the ACC and interactions with large bathymetry. Elsewhere, ocean mixing was enhanced in winter by enhanced winter atmospheric forcing of zonal wind stress. This seasonal contrast is a result of surface warming through positive heat fluxes resulting in increasing mean mixed layer temperature, leading to summer restratification and shallow mixed layers. Upstream submesoscale surface mixing deepens the upstream mixed layer. This study provides evidence for topographic stirring and dissipation of these ocean fronts and eddies upstream of PEI, which I propose ultimately enhance downstream restratification in summer, when the MLD is shallow, setting up a heterogeneous downstream landscape of phytoplankton blooms, which is expected to feed higher trophic levels. Contrary to what was predicted, levels of foraging effort, expressed as horizontal and vertical area-restricted search, did not change in response to downstream topographically forced upper ocean mixing and thermal structure. This study emphasizes how concurrent measurements of oceanographic and behavioural data collected from diving samplers can be used to study the downstream effects on both physical oceanography and foraging ecology surrounding small islands.

Key words: Animal-borne loggers, Eddy kinetic energy, Foraging ecology, Mesoscale stirring, Restratification, Seasonal, Southern Ocean, Submesoscale filaments, Topographic effects.

Introduction

Study area: Prince Edward Islands (PEI) within the Southern Ocean

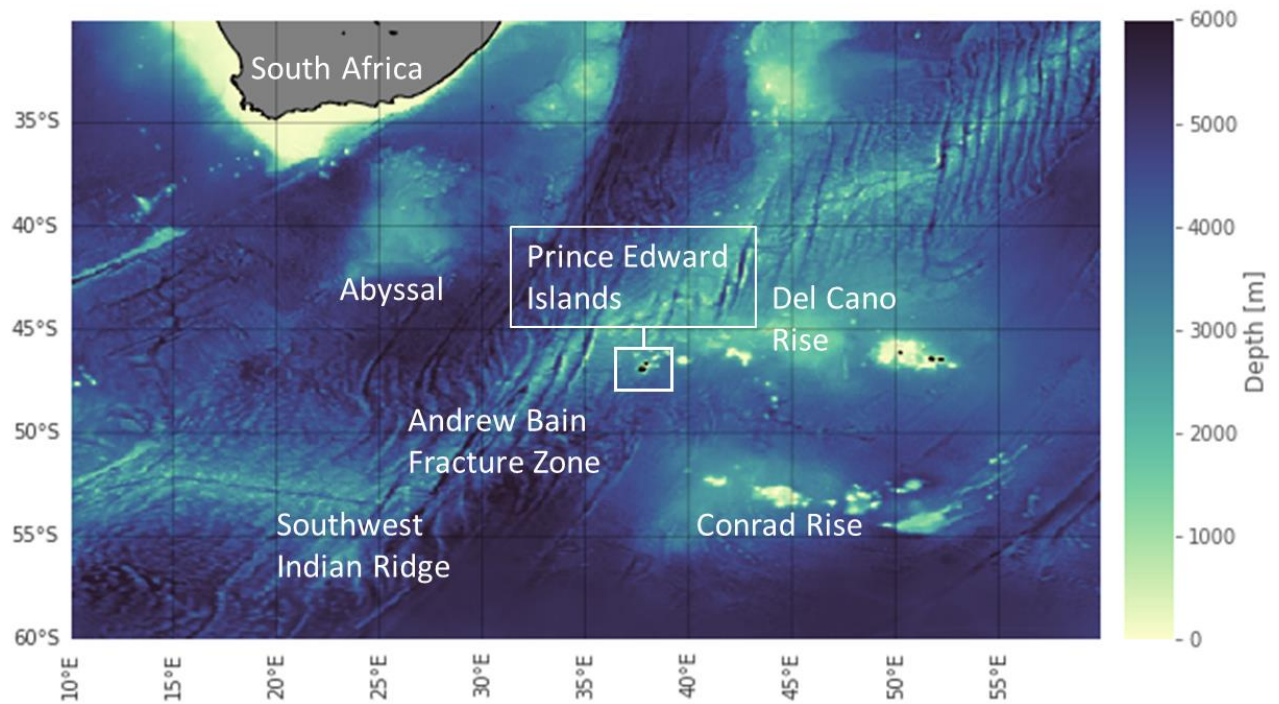


Figure 3.1: Bathymetry map (elevation in metres) obtained from the ‘GEBCO_2020’ global bathymetric gridded product released by the General Bathymetric Chart of the Oceans (GEBCO Compilation Group 2020) with a $1/240^\circ$ resolution. The location of the Prince Edward Islands is shown in relation to South Africa and large topographic features.

The Prince Edward Islands ($46^\circ 54' S$, $37^\circ 45' E$) (PEI) (Marion Island and Prince Edward Island) (Figure 3.1) are of particular importance to the Southern Ocean due to their pristine state (Ansorge and Lutjeharms, 2007), sensitivity to climate-scale perturbations (Ansorge *et al.*, 2014) and profitable surrounding ocean dynamics (Smith, 2008; Smith and Froneman, 2008). Moreover, the surrounding waters are important for marine top predator foraging (Reisinger *et al.*, 2018). The islands lie in the path of the Antarctic Circumpolar Current (ACC) (Lutjeharms and Valentine, 1984; Lutjeharms *et al.*, 1985; Rintoul *et al.*, 2001b) and its associated oceanic surface fronts (Orsi *et al.*, 1995; Ansorge *et al.*, 1999; Ansorge and Lutjeharms, 2000; Toolsee *et al.*, 2021). The ACC fronts contain multiple frontal filaments and jets (Sokolov and Rintoul, 2007), which are characterised by strong horizontal temperature, salinity, and density gradients (Bost *et al.*, 2009). These fronts are predictable and may act as cues for the decision of marine diving predators to enhance area-restricted search (Bost *et al.*, 2009), where predators slow their movements to optimize the time spent in productive prey patches (Carter *et al.*, 2016).

Mesoscale activity and biological impact

Southern Ocean circulation and variability is complex and spans a wide range of horizontal scales (Chapman *et al.*, 2020; Siegelman *et al.*, 2020). Strong surface currents typically occur at mesoscales (Klein and Lapeyre, 2009), with horizontal length scales of 100-200 km and timescales of days to weeks, and are steered by the balance between Coriolis and pressure gradient forces.

Mesoscale eddy generation and trajectories are influenced by changes in bathymetry, velocity fields and positions of the ACC fronts (Lamont and van den Berg, 2020). The sub-Antarctic Front and Polar Front are associated with the genesis of mesoscale eddies (Ansorge and Lutjeharms, 2000). Within the ACC, the Southwest Indian Ridge is a well-known area of localised eddy generation (Ansorge and Lutjeharms, 2007) (**Error! Reference source not found.**) and there is some evidence for these eddies to be advected towards the PEI (Durgadoo, Ansorge and Lutjeharms, 2010; 2014; Lamont and van den Berg, 2020) via the mean currents of the ACC (Cushman-Roisin, 1990). However, very few of these eddies have been observed to reach the PEI region and are instead trapped within the polar frontal zone (Ansorge and Lutjeharms, 2000; Lamont and van den Berg, 2020) with relatively small (<150 km) eddy propagation distances from their source. Instead, the mesoscale ocean circulation surrounding the PEI is dominated by eddies formed locally (Lamont and van den Berg, 2020), but at lower magnitudes than at the Southwest Indian Ridge (Lamont and van den Berg, 2020).

Eddy kinetic energy (EKE) can be used in characterizing mesoscale activity in the ocean. EKE surrounding the PEI, including the 'horse-shoe hotspot' typically observed upstream (Ansorge and Lutjeharms, 2003, 2005), shows strong seasonality with higher EKE in winter than in summer (Asdar, 2018). Over longer timescales (1993-2017), EKE has decreased (Asdar, 2018). At the PEI, Asdar (2018) has shown that mesoscale features passing the islands influence the depth of the mixed layer. Furthermore, foraging seals from sub-Antarctic islands appear to target these exceptionally productive mesoscale eddies (Biuw *et al.*, 2007; Bost *et al.*, 2009; Tosh *et al.*, 2012, 2015; Cotté *et al.*, 2015; Arthur *et al.*, 2016).

The role of submesoscales in marine ecology

Although the ocean kinetic energy is dominated by mesoscale EKE, energy cascades can be directed towards finer scales (e.g. submesoscales) (Ferrari and Wunsch, 2009). Submesoscale processes are therefore vital for the transfer of energy from mesoscale to smaller scales (Thomas *et al.*, 2008). Submesoscale turbulence is three-dimensional and classified by a forward cascade of energy through advection and diffusion allowing viscous dissipation (Mensa *et al.*, 2013). In the upper ocean, submesoscale turbulence is stronger in winter than in summer (Callies *et al.*, 2015; Buckingham *et al.*, 2016). Enhanced submesoscale features in winter, which are set by buoyancy losses and wind stresses, have been found to sustain winter mesoscale eddy structures and EKE (Sasaki *et al.*, 2014).

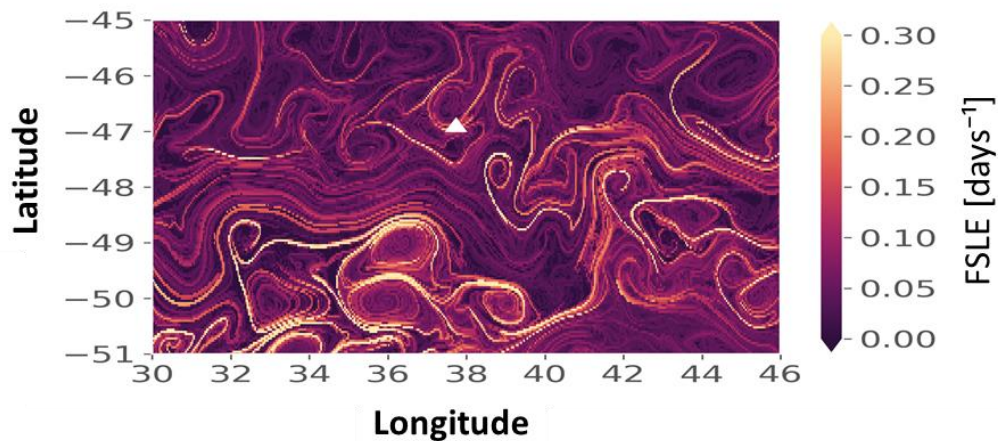


Figure 3.2: A snapshot (1st June 2012) of a mesoscale stirring field (represented by Finite-Size Lyapunov Exponents [days⁻¹]) surrounding the Prince Edward Islands (white triangle). This depicts the variability in ocean flows surrounding the Prince Edward Islands.

Submesoscale filaments are generated by chaotic, mesoscale stirring of flows. A snapshot of the mesoscale stirring field surrounding the Prince Edward Islands is shown in Figure 3.2. These transport and mixing structures form within the upper water column (<500 m) and are constrained to small spatial (1-10 km) and temporal (hours to days) scales (Boccaletti *et al.*, 2007; Fox-Kemper *et al.*, 2008). They are referred to as near inertial frequencies because submesoscale flows depart from the balance between Coriolis and pressure gradient forces through inertial and centrifugal force dominance, and are represented by Richardson and Rossby numbers approaching $O(1)$ (Boccaletti *et al.*, 2007; Thomas *et al.*, 2008; Siegelman *et al.*, 2020).

Mesoscale and submesoscale variability can directly impact vertical mixing (Klein and Lapeyre, 2009). The MLD over the global ocean shallows in summer (de Boyer Montégut *et al.*, 2004). In the Southern Ocean, stratification gradually increases from winter to summer due to a seasonal warming of the mixed layer (du Plessis *et al.*, 2019). Here, submesoscale ocean variability is associated with mesoscale activity (Lapeyre, Klein and Hua, 2006; Brannigan *et al.*, 2017; Lodise *et al.*, 2020) and submesoscales processes play a vital role in modulating upper ocean vertical fluxes of heat, biogeochemical tracers and momentum (Thomas, Tandon and Mahadevan, 2008).

The Southern Ocean is low in nutrients with ephemeral spring phytoplankton blooms contributing substantially to Southern Ocean primary productivity (Smetacek and Nicol, 2005). This heterogeneous landscape is largely driven by physical ocean variability and access of primary producers to sunlight (Swart *et al.*, 2015). Restratification can occur within the upper ocean through the absorption of solar radiation and through the slumping of horizontal buoyancy gradients within the mixed layer (du Plessis *et al.*, 2019). Mixed layer restratification is an important influence on local ecology (Pakhomov and Chown, 2003). At submesoscale fronts, vertical mixing is inhibited through restratification and phytoplankters are constrained to the euphotic zone (Levy *et al.*, 2012), where growth is enhanced relative to outside of frontal areas when phytoplankton growth is limited by light (Swart, Thomalla and Monteiro, 2015). As phytoplankton are light limited in large parts of the Southern Ocean, enhanced primary productivity is associated with submesoscale filaments (Levy *et al.*, 2012). Such phytoplankton blooms can feed higher trophic levels with trophic cascades that may influence marine top predator prey availability (Lea and Dubroca, 2003; Koubbi *et al.*, 2011; Bestley *et al.*, 2020). Recent studies have found that penguin (Lowther *et al.*, 2014; Whitehead *et al.*, 2016) and seal (Lowther *et al.*, 2014; Siegelman *et al.*, 2019) foraging behaviour in the Southern Ocean is associated with submesoscale filaments.

Topographic influences on downstream ocean variability and impacts on marine ecology

Throughout the Southern Ocean, the interaction of the ACC with large-scale (>200 km) topography drives upwelling of nutrients into the euphotic zone (Sokolov and Rintoul, 2007), which are then advected downstream through the preferential formation and north-eastward propagation of cyclonic and anticyclonic eddies (Ansorge and Lutjeharms,

2003, 2005; Durgadoo *et al.*, 2010, 2011; Chelton, Schlax and Samelson, 2011; Lamont and van den Berg, 2020), thus contributing to both the flow balance of the ACC and most of the persistent downstream blooms observed (Sokolov and Rintoul, 2007). The interaction of the ACC with small-scale (<100 km radius) topography, such as seamounts, has been shown to shallow the MLD. Here moderate blooms are generated but are able to sustain productive prey patches for marine diving predators (Sergi *et al.*, 2020).

Rough and small-scale topography also catalyses dissipation of geostrophic flows that are forced by wind and heat fluxes, sustaining turbulent mixing in the ocean interior (Nikurashin, Vallis and Adcroft, 2013; Yang *et al.*, 2019). Specifically, geostrophic (mesoscale) eddies can split or merge as they interact with surrounding topography (Chelton *et al.*, 2011). Eddy kinetic energy would be enhanced in the case of absent small-scale, O(1-100 km), topography in the Southern Ocean (Zhang and Nikurashin, 2020). Small-scale bottom topography facilitates transient mesoscale flow dissipation through the generation of strong topographic form stress (Yang *et al.*, 2019; Zhang and Nikurashin, 2020). The generation of submesoscale motions in the lee of small islands also acts to transfer mesoscale eddy energy down to small dissipation scales (Yang *et al.*, 2019). Small island bathymetry and small-scale bottom topography are therefore suggested to play a significant role in the dynamical momentum balance of the ACC (Yang *et al.*, 2019; Zhang and Nikurashin, 2020) and play an important role in setting the vertical structure of the flow and the equilibration and position of flow meanders (Yang *et al.*, 2019).

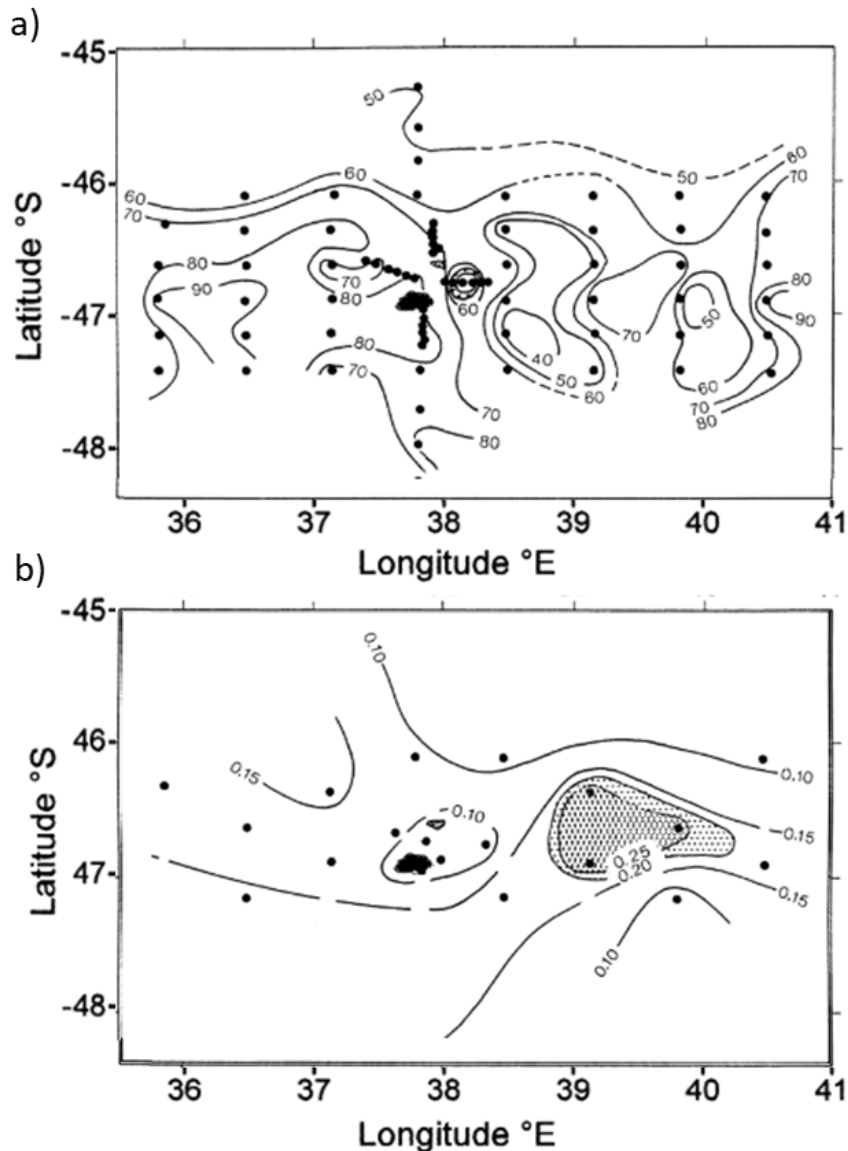


Figure 3.3: Observations at Marion Island (black) of a) the mixed layer depth [m] and b) zooplankton biomass [ml DV m⁻³] in the upper 100-300 m layer. These figures were adapted from Perissinotto *et al.* (2000) and the data were collected by ship measurements (black dots) between 7 and 19 April 1989. These figures illustrate the upstream and downstream variability of the region, and downstream effects on biological productivity.

The interaction of the ACC with the PEI bathymetry produces an island mass effect (Boden, 1988; Treasure *et al.*, 2015), a downstream periodic enhancement of phytoplankton and zooplankton biomass (Figure 3.3b), that is found throughout the Southern Ocean where the ACC interacts with small islands (Perissinotto *et al.*, 2000; Sergi *et al.*, 2020). The combination of advection and freshwater run-off, which increases vertical stability and nutrient input from island breeders, is suggested to enhance downstream primary productivity (Perissinotto *et al.*, 1990), which has been shown to be associated with downstream vortices (Allanson *et al.*, 1985). This downstream vortex

field, resembling a Von Karman street, is driven by the topographic impacts on the flow of the ACC, resulting in enhanced leeward turbulence and shoaling of the MLD (Sallée *et al.*, 2010). Submesoscale motions will likely be active in regions of large vorticity (Hagen *et al.*, 2001). Topographic disturbance of geostrophic currents increases downstream vorticity (Srinivasan *et al.*, 2019), thus creating ideal conditions for strong downstream submesoscale flows at the PEI (Perissinotto *et al.*, 2000). Furthermore, a large-scale (~150 km) downstream wake feature (Ansorge & Lutjeharms 2002) has been associated with enhanced stability and shallowing of the mixed layer (Perissinotto *et al.*, 2000) (Figure 3.3a).

The wake in the lee of the island is observed and predicted to drive interactions between the island and associated eddies of the fronts, causing mesoscale mixing of eddies across the PFZ towards the islands (Ansorge and Lutjeharms, 2002). A downstream zone of enhanced meridional exchange of physical and chemical properties, affecting zooplankton species community (Ansorge *et al.*, 1999) is also reflected in the patchy nature of chlorophyll distribution in the vicinity of the islands (Froneman *et al.*, 1999). Zooplankton density and vertical distribution modulates myctophid fish movements (Duhamel, Koubbi and Ravier, 2000). Myctophid fish dominate the mesopelagic species of the oceanic zone (Koubbi *et al.*, 2011), and make up most of the SAFS diet (Klages & Bester 1998; Reisinger *et al.*, 2018), linking zooplankton and seals within the Southern Ocean, and contributing to the control of energy cascades between trophic levels (Koubbi *et al.*, 2011). Southern elephant seals, for example, have been found to use downstream phytoplankton plumes (O'Toole *et al.*, 2017) as foraging hotspots.

Interactions between the atmosphere and the ocean influences the distribution of the ACC fronts (Turner *et al.*, 2014), and therefore the interaction between these fronts and island bathymetry, potentially increasing the distance that predators must travel to find their prey (Bost *et al.*, 2015; Chown and Froneman, 2008). This would have negative consequences, specifically for the ecology of central place foraging marine top predators, where changes in foraging trip duration may influence the survival of their young (Tosh *et al.*, 2015; Massardier-Galatà *et al.*, 2017; Carpenter-Kling *et al.*, 2019). Therefore, improving our understanding of the impacts of topographic effects on foraging ecology of marine top predators could improve the way we predict the effects of climate change on predator population growth (Pakhomov and Froneman, 1999).

Subantarctic fur seals (SAFS) and using seals as ocean samplers

Historically, a lack of observations in the relatively inaccessible Southern Ocean (Treasure *et al.*, 2017) has led to poor quantification of marine mammal foraging behaviour (Fedak, 2004; McIntyre, 2014) and the physical upper ocean processes that may influence them (Roncon *et al.*, 2018; Chapman *et al.*, 2020). This is especially true at small temporal (<24 hr) and spatial scales (1-10 km). With recent advances in animal-borne telemetry, marine mammals can act as autonomous ocean samplers (Harcourt *et al.*, 2019), collecting detailed and important behavioural and oceanographic information as they move through three-dimensional space (Hussey *et al.*, 2015), increasing global coverage for improved monitoring of the world's oceans (Harcourt *et al.*, 2019).

Subantarctic fur seals (SAFS) (*Arctocephalus tropicalis*) are mobile marine diving predators inhabiting the PEI. With the introduction of animal-borne sensors, a continuous data record of environmental and biological metrics has been established by the Marion Island Marine Mammal Programme for purposes of foraging ecology studies (Bester *et al.*, 2011), and for the purpose of ocean observation (Treasure *et al.*, 2017).

Upwelling of nutrients is localized where ocean fronts and bathymetry interact throughout the Southern Ocean (Chapman *et al.*, 2020). Large lateral-scale (>100 km) bathymetric features, sea surface temperature fronts and mesoscale eddies appear to be important foraging areas for Marion SAFS (de Bruyn *et al.*, 2009; Taylor *et al.*, 2011). However, using Boosted Regression Tree species distribution models, Wege *et al.*, 2019 suggests that, at the >100 km horizontal scale, latitude, longitude, and current speeds are the major influences on horizontal area-restricted search of Marion SAFS, while other environmental variables, such as bathymetry, sea surface temperature and sea surface height are not as important in predicting their horizontal movements. No studies at Marion Island have focussed on both vertical (diving) and horizontal foraging behaviour at fine vertical (~1 m, <10 sec) and horizontal (1-10 km, <24 hr) scales.

The simultaneous *in situ* sampling of both environmental and behavioural parameters has improved our understanding of how these animals use their habitat (Bost *et al.*, 2009; Tosh *et al.*, 2012; 2015) and provides valuable hydrographic data for physical oceanographers (Roquet *et al.*, 2013; Treasure *et al.*, 2017). In this study, seal-derived data will be used to investigate the ocean variability surrounding the Prince Edward

Islands, in addition, the topographic influences on local ocean variability and impacts of ocean variability on fur seal foraging behaviour.

Aims and objectives

Previous studies have shown strong seasonality in ocean horizontal circulation and vertical mixing at the submesoscale (Sasaki *et al.*, 2014; Callies *et al.*, 2015; Buckingham *et al.*, 2016; Viglione *et al.*, 2018; du Plessis *et al.*, 2019; Biddle and Swart, 2020) and particularly around topographical features (Rosso *et al.*, 2015). In the present study, I intend to provide evidence for such seasonality in the PEI region and link horizontal and vertical ocean dynamics across multiple scales, using both satellite and *in situ* data. In particular, I aim to investigate the influence of small-scale topography on the meso- to submesoscale ocean variability both up- and downstream of the Prince Edward Island region and relate that variability to impacts on fine vertical (~1 m, <10 sec) and horizontal (1-10 km, <24 hr) scale foraging efforts of SAFS over seasonal scales.

As SAFS dive both up- and downstream of the Prince Edward Islands throughout both seasons (Wege *et al.*, 2016), the foraging trips of seals used in this study have statistically sufficient west-east spatial coverage (Figure 3.4) throughout both seasons to provide an appropriate case study for up versus downstream comparisons in high resolution oceanography and foraging behaviour.

My main objectives are to:

- Describe the topographic influence of the small-scale topography of the PEIs on mesoscale (100-200 km, days to weeks) and submesoscale (1-10 km, hours to days) ocean variability and upper ocean thermal structure (~1 m), and the seasonality of these effects.
- Assess seasonal differences between upstream versus downstream fine vertical (~1 m) and horizontal (1-10 km, <24 hr) scale foraging effort of SAFS in relation to possible topographic effects on ocean flows and variability.

In chapter two, thermal structure of the upper ocean significantly affected seal diving and foraging behaviour at fine scales (per dive). In chapter three I hypothesise, based on the findings of chapter two and of previous research, that seal-borne loggers will show clear evidence for topographically enhanced submesoscale variability downstream of Marion

throughout the year, with cascading effects on seal foraging behaviour. In particular, seals are expected to consistently increase vertical and horizontal foraging effort and decrease maximum dive depth in relation to enhanced variability and restratification.

Methods

Summary data in this study were reported as mean \pm SE, unless otherwise noted. Standard error ($SE = \text{standard deviation} / \sqrt{\text{sample size}}$) is a measure of uncertainty associated with the mean. To address the main questions in this study the following methodology was carried out.

Study site, animal handling, instrumentation, and behavioural indexes

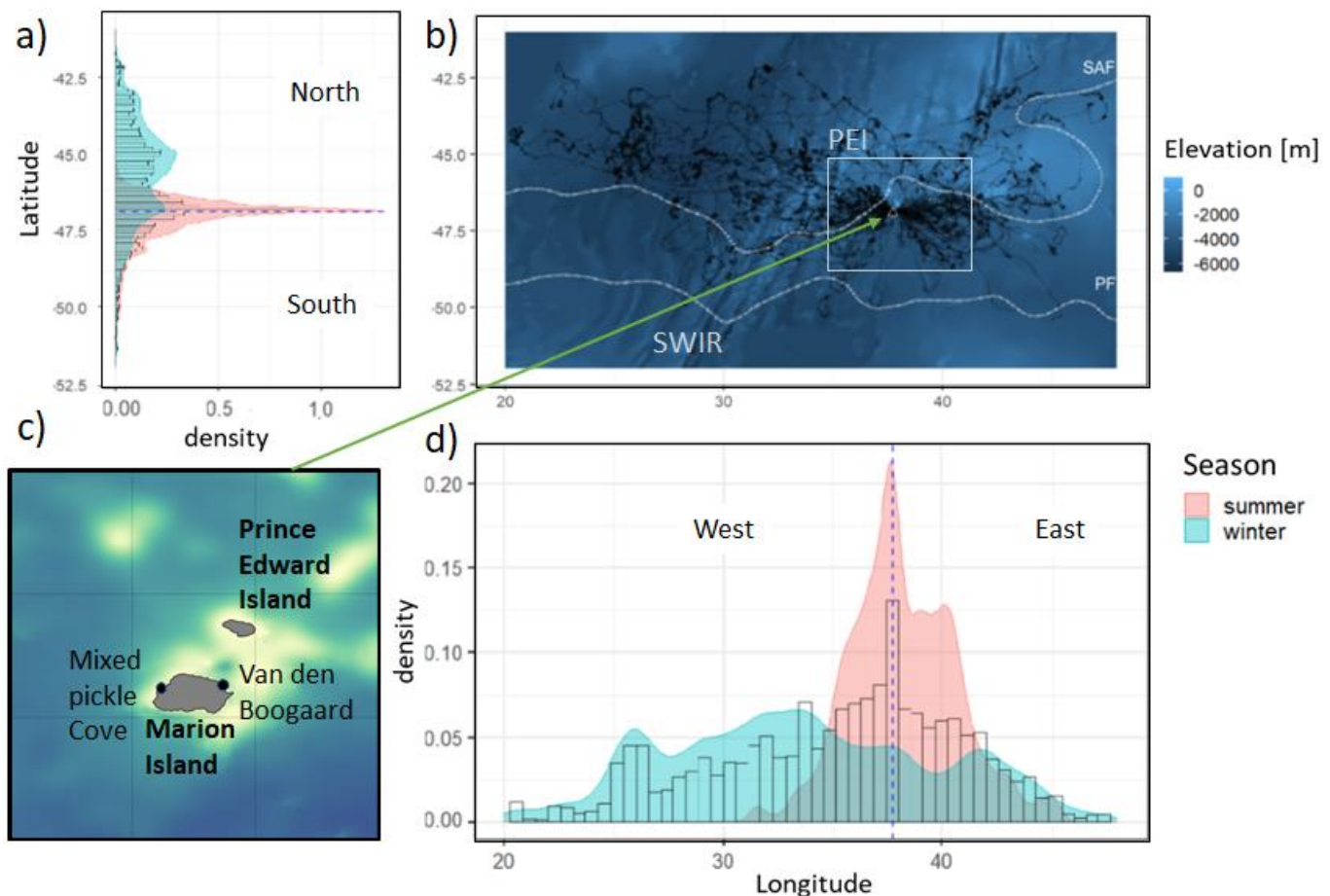


Figure 3.4: b) Distribution of 39 lactating subantarctic fur seals from Marion Island from 2009-2015 during summer and winter. Seal distributions (in black) are overlaid on a bathymetry map (elevation in metres) (GEBCO 1/240° resolution grid). The mean (from 1993-2012) position of the sub-Antarctic Front (SAF) and the Polar Front (PF) are shown as white dotted lines, obtained from Park and Durand (2019), as well as the position of the Southwest Indian Ridge (SWIR) and Prince Edward Islands (PEI) region. c) A zoomed-in

map of the Prince Edward Archipelago. The two deployment colonies are Van den Boogaard beach and Mixed Pickle Cove. Seasonal a) latitudinal and d) longitudinal distributions of seal foraging trips, with blue dotted lines indicating the coordinates of the Prince Edward Archipelago. The area to the west of the islands is characterised in this chapter as 'upstream' and the area to the east as 'downstream'.

The study site, animal handling procedures and raw tracking data for this chapter were the same as in chapter 2, however in this chapter I distinguished the area to the west of the islands as 'upstream' and the area to the east of the islands as 'downstream' and made comparisons between upstream and downstream ocean circulation and seal foraging effort. Similar to in chapter 2, the two seasons defined and discussed in chapter 3 were characterized by two periods: 'summer' (15th Oct - 14th April) and 'winter' (15th April - 14th Oct). Profile temporal distributions are shown below (Figure 3.5).

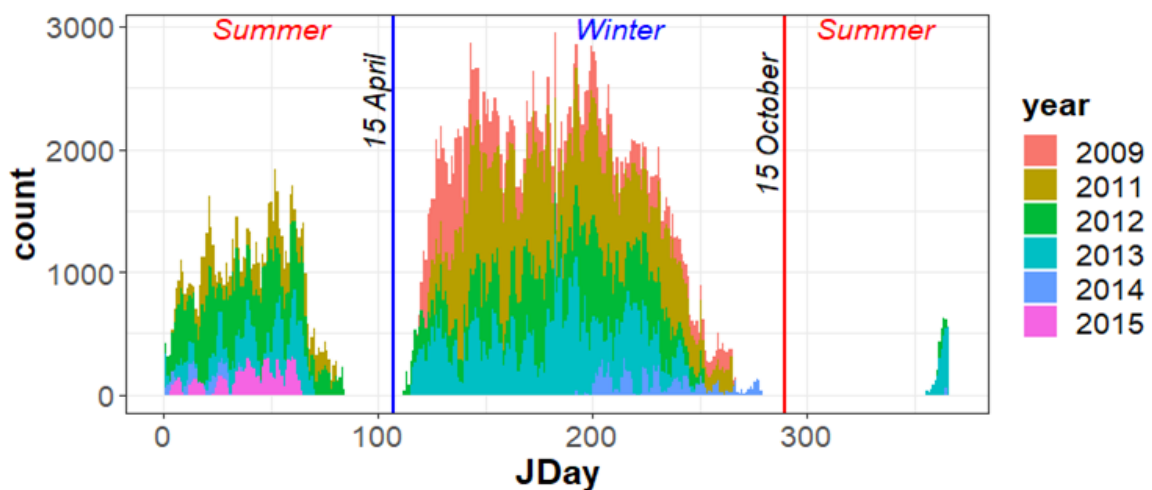


Figure 3.5: Seasonal distribution of temperature profiles collected by the 39 animal-borne loggers on 39 different diving seals from winter 2009 to the first summer months of 2015. The blue vertical line represents the first Julian day ('JDay') of the 'winter' period (15th April), while the red vertical line represents the first day of the 'summer' period (15th October), as defined in this dissertation.

For each dive, the maximum dive depth was calculated. Furthermore, the horizontal and vertical foraging effort variables used in this chapter were derived from the horizontal and vertical area restricted search methods in chapter 2.

In situ upper ocean thermal structure: mixed layer depth (MLD), stratification, stability and horizontal buoyancy gradients (b_x)

As derived in Chapter 2, the mixed layer depth (MLD), stratification and stability of the upper ocean were calculated. Submesoscale flows manifest in the form of horizontal buoyancy gradients if these gradients are computed over the relevant distance (1-10 km) and time (1-24 hr) scales that are associated with submesoscale ocean processes (Lévy

et al., 2012). Using seals to derive submesoscale gradients has been a recent focus of research (e.g. Siegelman *et al.*, 2019; Biddle and Swart, 2020). Similar to these studies, I show that the horizontal distance travelled between trip locations were less than 10 km over 64.41% and 56.59% of the upstream and downstream profiles, respectively. Furthermore, 100% of location estimates within a foraging trip were within 24 hours of each other, with ~75% of locations within 3 hours of each other. Horizontal buoyancy gradients were computed using the along-track locations of each foraging trip separately, as foraging trips vary in spacing and timing of initiation and termination of each trip. In using the along-track gradient of temperature to determine horizontal gradients, I assumed that submesoscale fronts were quasi-stationary when the seal crosses them. Temperature was gridded onto a uniform 5 km horizontal grid for each depth from surface (0 m) to 200 m, as approximately 5 km was the mean difference between location estimates (see Supp. Figure 5). This is likely to only show the lower bound of horizontal gradients of the region as Swart *et al.* (2020) show a logarithmic increase in the strength of submesoscale fronts as the sampling resolution is increased from 10 km to 0.1 km. Nevertheless, the objective here is to provide a relative contrast of horizontal buoyancy gradients upstream and downstream of the PEI and so the likely underestimation of the magnitude of submesoscale fronts is not important to the results of this work. The calculation of seal-derived b_x was then as follows:

$$b_x = g\alpha \partial T / \partial x$$

, where g is the gravitational acceleration, α is the mean thermal expansion coefficient for the region, ∂T [°C] is the horizontal change in interpolated mean *in situ* temperature of all profiles within 1.25 hr of a nearest location estimate, and ∂x is the along-track gridded distance between *in situ* profiles (5 km). The mean thermal coefficient was computed over all seasons for the entire seal foraging region using the objective analysis product according to IOC *et al.* (2010). Gradients were averaged over a constant depth range from 10 to 20 m below the surface and were not averaged over the entire mixed layer as in du Plessis *et al.* (2019). This is because seal-derived profiles did not always encompass the entire mixed layer (MLDs were not always reached by diving seals). However, by definition, the MLD is homogenous in temperature and salinity and thus the 10 to 20 m range should be representative of the entire mixed layer.

Furthermore, like with other autonomous sampling platforms, seals may underestimate the true gradients of fronts. For example, gliders show on average, a 64% underestimation of the true frontal strength (du Plessis *et al.*, 2019). This is because the use of b_x to infer submesoscale fronts depends on the orientation of seal movements to the orientation of frontal structures, i.e. If a seal moves along a front, the front will not be evident in the b_x . It is unclear as to whether seal data can provide a comprehensive display of frontal features in the PEI region using b_x alone, considering no study has been made into the accuracy of seal-derived b_x . However, this was our best estimate available at the time of the study and still provided valuable insight into the variability of upper ocean instabilities surrounding the islands.

Satellite remote sensing of flow variability

Although high vertical resolution (<10 m) data can be collected by *in situ* observations for investigating upper ocean variability, remotely sensed altimetry is an effective way of observing larger scale (>10 km) horizontal ocean variability (Lamont *et al.*, 2019). With the use of satellite and *in situ* data, I formulated a multi-scale understanding of the oceanography of the PEI region.

The maximum zonal and meridional extent of foraging trips made by seals at Marion Island determines the maximum spatial extent of available profiles for comparison with satellite data. As seals forage further away from the PEI in winter (Figure 3.4), available profiles (42-52 °S; 20-50 °E) overlap with areas outside and inside of the PEI region (44.6–48.6 °S; 35–41 °E) defined in Lamont *et al.* (2020). In summer, available profiles (45-49 °S; 32-45 °E) were mostly only sampled by seals within the PEI region. Lamont *et al.* (2020) also defines an area discussed in this study called the Southwest Indian Ridge region (48.6–52.6 °S; 27–33 °E), centred around the Andrew Bain Fracture Zone (50°S; 30°E). These regions were defined, illustrated, and discussed within this study for spatially robust comparisons between *in situ* and satellite data.

Daily maps of delayed-time surface geostrophic velocities were obtained for the analysis of geostrophic surface currents and mesoscale variability surrounding the PEI. Data were downloaded from the Copernicus Marine Environment Monitoring Service global ocean merged and gridded level 4 reanalysis product (<https://www.copernicus.eu>) processed by the Data Unification and Altimeter Combination System (version 2018), a multi-mission

altimeter data processing system. Optimal interpolation of along-track multi-satellite altimeter observations from all altimeter missions produces gridded absolute dynamic topography, which is used to derive geostrophic velocities. These data are 0.25 degree spatial and daily temporal resolution, where positive zonal values indicate west to east flow, while positive meridional values indicate south to north flow, and vice versa for negative values.

Within my study area, the long-term mean Eddy Kinetic Energy (EKE) of the flow was used as a common Eulerian tool, i.e. fixed measurements in a flow field over time, to study the mesoscale variability of geostrophic flows (Waugh, Abraham and Bowen, 2006). The mean zonal (\bar{u}) and mean meridional (\bar{v}) components of geostrophic velocities (from above) from 1993-2012 were subtracted from absolute zonal (u) and meridional (v) component values of geostrophic velocity, that had been calculated from absolute dynamic topography (Wang *et al.*, 2017), to derive deviations from the mean ($u' = u - \bar{u}$; $v' = v - \bar{v}$). EKE was then calculated as:

$$EKE = 0.5 (u'^2 + v'^2)$$

As well as quantifying dynamics of mesoscale flows, I decided to relate these flow dynamics to the stirring at smaller scales. Therefore, maps of backward-in-time, Finite-Size Lyapunov Exponents (FSLE) (daily & 0.04° resolution) provided by AVISO (www.aviso.altimetry.fr) were used as a Lagrangian diagnostic, i.e. computed along particle trajectories, to quantify stirring in the surface velocity field. Specifically, FSLE measures the exponential rate (λ) of separation of initially neighbouring particles within a flow regime during a time advection (τ) by altimeter-detected mesoscale velocities (geostrophic current velocities above) calculated every 4 days since 1994/04/01 and updated every year until 2018.

FSLE ridges (outflowing manifolds) approximate hyperbolic Lagrangian Coherent structures (Karrasch and Haller, 2013) that are time-independent. These ridges exhibit areas of high stretching produced by chaotic stirring with directions parallel to flow divergence, while areas away from FSLE ridges represent areas that are more inert (d'Ovidio *et al.*, 2009). FSLE is calculated as: $\lambda = \tau^{-1} \cdot \log(\delta f / \delta 0)$, where initial separation $\delta 0$ was set at 0.02° (~2.2 km) and maximum separation δf was set at 0.6° (~66 km), which is smaller than altimetry-detected eddy radii (Cotté *et al.*, 2011). The time taken for the particles to reach a maximum separation (τ), i.e. maximum integration

window, was given as 200 days. Seasonal means of FSLE allow classification of areas according to their mixing activity (d'Ovidio *et al.*, 2004).

FSLE were obtained most importantly to underline submesoscale filaments which play a significant role in vertical mixing in the upper ocean (Lapeyre and Klein, 2006). FSLEs that overlap in space and time with a single seal's tracks were subsequently compared to $|b_x|$, calculated using data from the same seal, to provide a representation of the general relationship between submesoscale filaments and horizontal buoyancy gradients for summer 2012. A moving average with a window width of 5 km was applied to both FSLE and $|b_x|$ to remove any intermittency and allow for clear comparisons between the two variables.

Data was supplied by Park and Durand (2019) for the mean position of the ACC fronts shown in maps of this study were constructed from mean dynamic topography (1/8°-resolution) (Park *et al.*, 2019) of Centre National d'Etudes Spatiales-Collect Localisation Satellites 2018 (CNES-CLS18) for the 1993-2012 reference period (Mulet *et al.*, 2021).

In the following results section, 'West' represents the upstream region and 'East' represents the downstream region, i.e. 'West' and 'East' are interchangeable with upstream and downstream, respectively.

Results

Time-depth recorders were retrieved successfully from 39 individuals (2009; 2011-2015). After removing surface dives that are shorter than 60 sec long and shallower than 4 m, 32.98 ± 2.74 % of total dives per seal were retained for analysis. In total, 346 760 dives were analysed. Profiles collected between 15 October and 15 April were considered 'summer' profiles ($n = 82\ 090$ (23.67%), individuals = 20), while 'winter' profiles spanned 15 April to 15 October ($n = 264\ 670$ (76.33%), individuals = 19). The deepest profile (i.e. maximum dive depth) was 211 m and 182 m in winter and summer, respectively.

Contribution of temperature and salinity to density gradients

Contributions of vertical temperature variations to density gradients dominate north of 55°S (Figure 3.6a). South of this latitude, salinity changes dominate vertical gradients in density (Figure 3.6b). Furthermore, seasonal variability exists, where upstream of PEI,

salinity has a larger role in the vertical density gradients during winter than summer (Figure 3.6b). The PEI are situated in a transition zone between alpha and beta oceans to the north and south, respectively. In summer, when stratification is high, the mean value of $|Rp|$ is mostly above 1 for the region encompassing available profiles (Figure 3.6c), indicating the tendency for vertical gradients in temperature to impact stratification over salinity gradients in the region of the islands. However, mean $|Rp|$ values less than 1 (salinity dominated regime) appear in winter when the surface ocean undergoes atmospheric cooling (April-September), indicating larger salinity contribution to density changes in the vertical (Figure 3.6d).

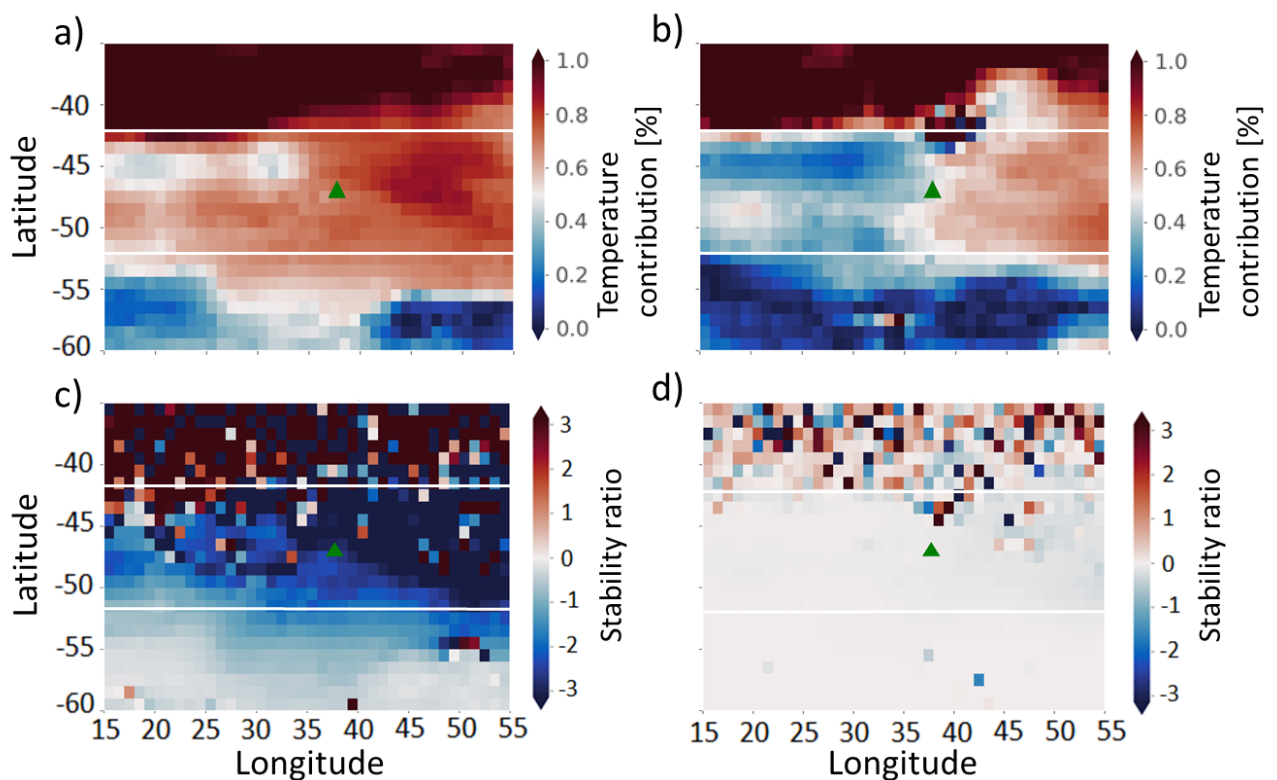


Figure 3.6: Mean contribution of variations in heat (Temperature contribution [%]) to stratification over a constant depth range of 15 m, directly below the mixed layer base for summer (a) and winter (b). Mean stability ratio (R) is also plotted for summer (c) and winter (d) where values of $|Rp| > 1$ indicate that heat contributes to stratification and values where $|Rp| < 1$ indicates that salt contributes to stratification. Horizontal white lines represent the meridional extent of subantarctic fur seals (and thus available profiles) during this study, while the green triangles indicate the position of the Prince Edward Islands.

Time-mean and time-varying local ocean circulation, stirring and mixing

Mean amplitude and direction of geostrophic velocities (Figure 3.7) highlights a relatively homogeneous eastward zonal component representing the ACC. Immediately southwest of PEI, a standing ACC jet is seen with values greater than 0.35 m/s extending from 51°S

to the PEI (Figure 3.7). This jet provides an immediate contrast to the flow dynamics up and downstream of the Island. Meanwhile, meridional geostrophic velocities are spatially varied with no dominant mean southward or northward flow throughout the study area (Figure 3.7). Despite the large spatial variation of mean geostrophic flows, seasonal differences appear to be small and cancel each other out over the large-scale (Figure 3.7a-d). However, in the location of the PEI, the seasonal difference of mean zonal geostrophic velocity indicates a northward summer shift in the ACC jet that lies directly southwest of the islands, resulting in enhanced velocities of around 0.35 m/s during summer (Figure 3.7e), with a westward summer shift in mean meridional velocities observed (Figure 3.7f). Throughout the year, a less strong (>0.1 m/s) eastward jet far (~ 400 km) downstream of the islands is directly followed by equatorward flow at around 48° E (east of the PEI), westward flow and then sharp eastward flow again to the north in an area characterized as the deflection or meandering of the sub-Antarctic Front (Koubbi *et al.*, 2016). These flows are typically greater than 0.1 m/s and less than 0.3 m/s throughout the deflection region yet flows associated with this feature become less intense (~ 0.05 m/s) in summer.

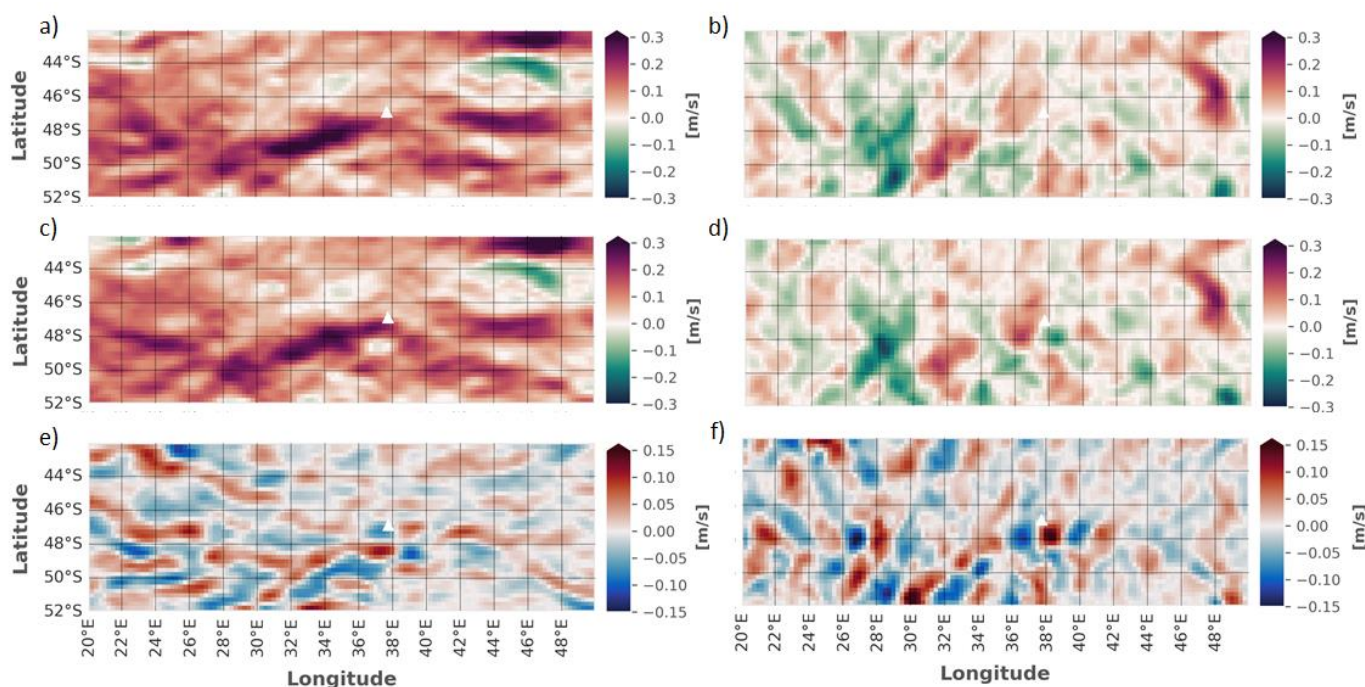


Figure 3.7: Time-mean winter (a,b) and summer (c,d) daily absolute surface geostrophic velocities from 2009-2015 at a 0.25° resolution. The zonal (a,c) and meridional (b,d) components are depicted with seasonal anomalies (winter-summer values) (e,f), with negative values representing higher mean summer velocities than winter. Positive zonal and meridional values indicate west to east and south to north flow, respectively. The position of the Prince Edward Islands is indicated by a small white triangle.

From 2009 to 2015, the mean EKE over the South West Indian Ridge (south-west upstream) and Subtropical Convergence Zone (north-west upstream) is visibly high ($>0.05 \text{ m}^2/\text{s}^2$), relative to the surrounding waters in both winter (Figure 3.8a) and summer (Figure 3.8b). Mean EKE is considerably lower ($<0.03 \text{ m}^2/\text{s}^2$) downstream and to the north of the islands (Figure 3.8). High ($>0.05 \text{ m}^2/\text{s}^2$) EKE values manifest in zones of large mean zonal geostrophic velocities ($>|0.2| \text{ m/s}$) such as the ACC jets. As the strong ACC jet moves slightly north in the summer and south in the winter, intense mesoscale variability shifts with it and is evident in marginally higher ($\sim 0.01 \text{ m}^2/\text{s}^2$) EKE during the summer than in winter within the PEI region (Figure 3.8c). Over most of the study region however, the EKE is higher ($\sim 0.01 \text{ m}^2/\text{s}^2$) in winter than in summer (Figure 3.8c).

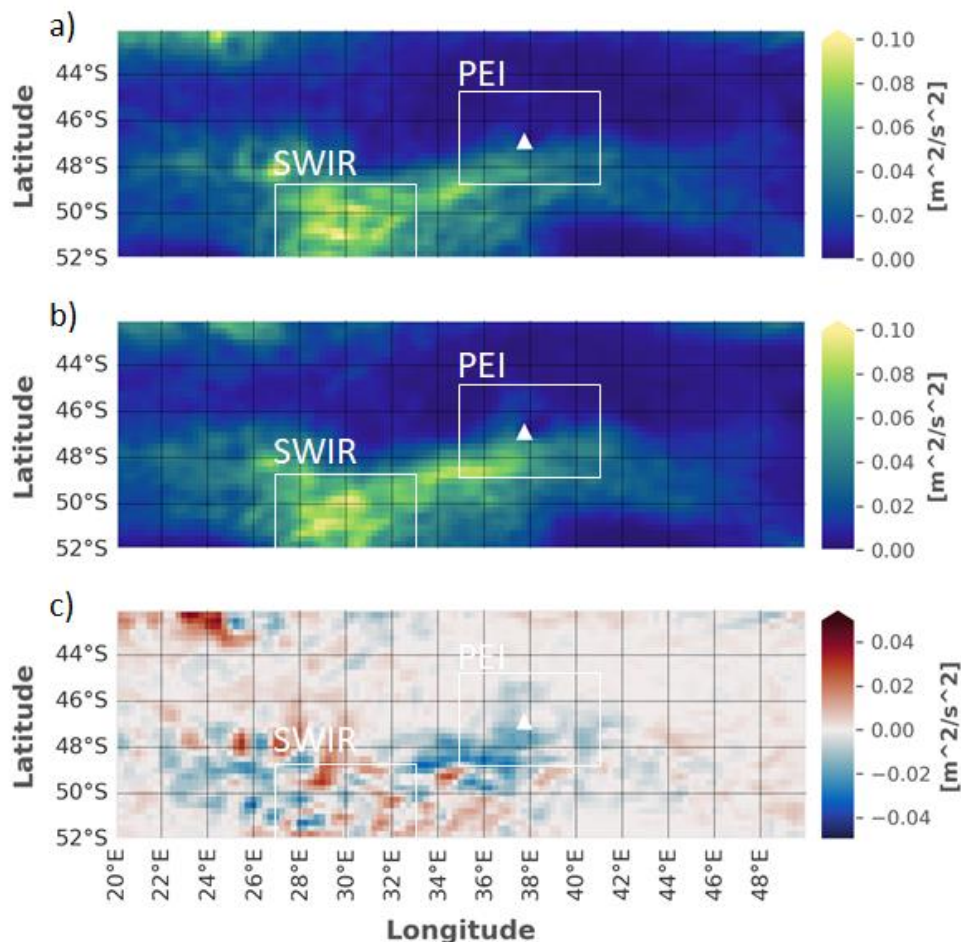


Figure 3.8: Seasonal climatology of winter (a) and summer (b) surface eddy kinetic energy (EKE) (m^2/s^2) from 2009-2015 at a 0.25° resolution, calculated using geostrophic velocity anomalies within the spatial extent of seal foraging trips. c) The seasonal anomaly (winter-summer values) of EKE is also presented. Negative values represent higher mean summer EKE than mean winter EKE. The Southwest Indian Ridge region (SWIR) ($48.6\text{--}52.6^\circ\text{S}$; $27\text{--}33^\circ\text{E}$) and Prince Edward Islands (PEI) (white triangle - $44.6\text{--}48.6^\circ\text{S}$; $35\text{--}41^\circ\text{E}$) are indicated.

EKE propagates eastward through time, from the SWIR towards the PEIs. There is a strong contrast of EKE up and downstream of PEI, where EKE is consistently dissipated

directly downstream of the PEI (Figure 3.9), especially evident in summer. Intense EKE shown in Figure 3.8 overlaps with the Southwest Indian Ridge region, where eddies are produced and propagated (Figure 3.9a) north eastward (Lamont *et al.*, 2020). There does not appear to be any interannual variation of EKE within the PEI region ($0.004 \pm 0.005 \text{ m}^2/\text{s}^2$) (Figure 3.9b). Rather, EKE variability is characterised by noticeably intense ($>0.5 \text{ m}^2/\text{s}^2$) and extended (>2 months) events, with high EKE observed in the summer of 2013 and 2015 (Figure 3.9b). The observed downstream decay of EKE shows interannual variation, within the PEI region, with higher standard deviation in summer interannual differences between upstream and downstream EKE ($0.007 \text{ m}^2/\text{s}^2$) than in winter ($0.003 \text{ m}^2/\text{s}^2$). This indicates that upstream enhancement of eddy activity in summer is more noticeably reduced downstream relative to winter, when eddy activity within the PEI region is lower either side of the islands.

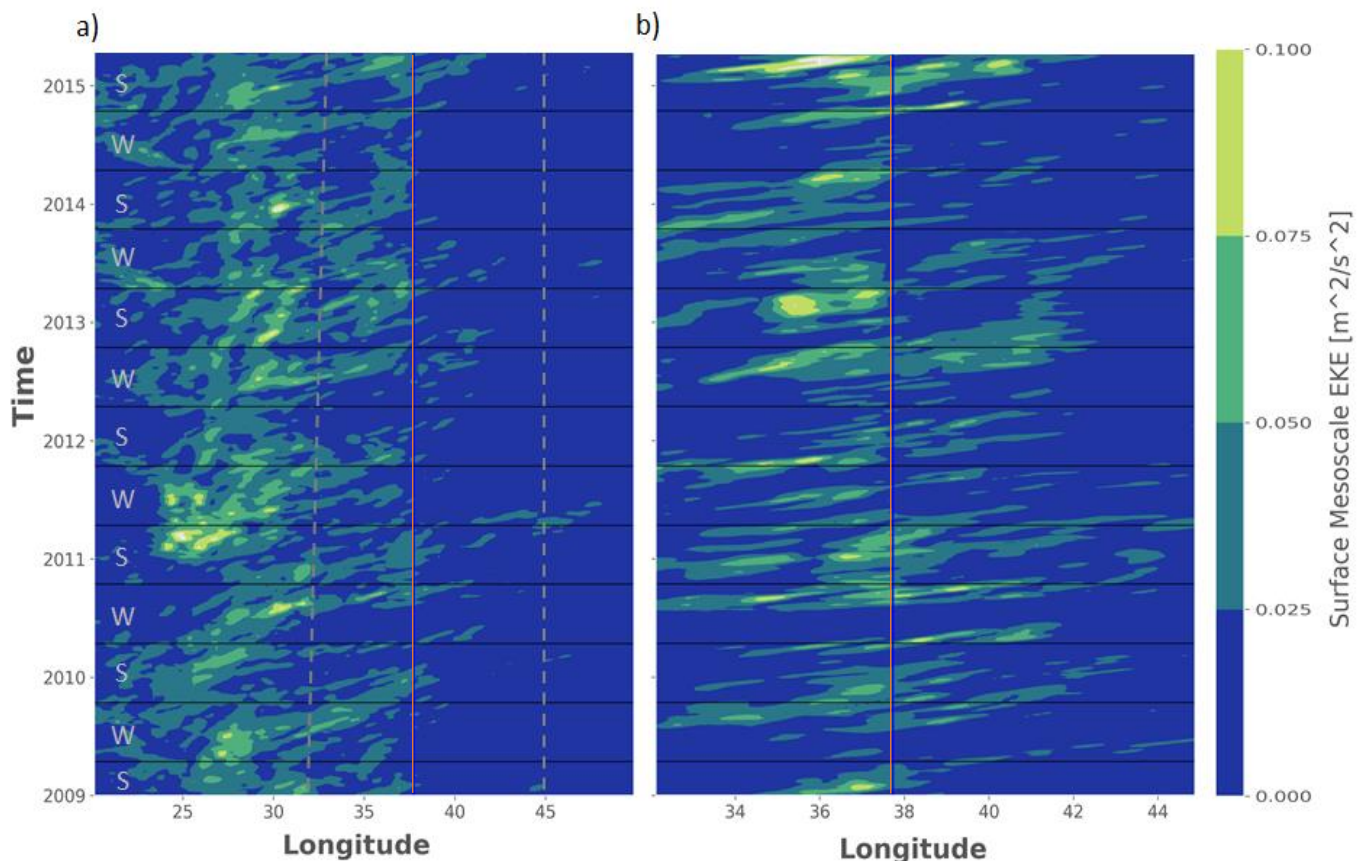


Figure 3.9: Hovmöller plots of daily surface eddy kinetic energy (EKE)[m²/s²] from 2009-2015 calculated as the a) mean EKE within the maximum extent of seal foraging trips, i.e. available profiles (42-52 °S; 20-50 °E), which overlap with the Southwest Indian Ridge region (48.6–52.6 °S; 27–33 °E) and PEI region (44.6–48.6 °S; 35–41 °E) defined by Lamont *et al.* (2020), and the b) mean EKE within the maximum extent of seal foraging trips in summer (45-49 °S; 32-45 °E), which overlaps only with the PEI region only. The longitudinal position of Marion Island is indicated by the blue vertical line in each plot, while vertical grey lines in (a) represent the longitudinal range in (b).

Maps of FSLE (Figure 3.10) represent submesoscale mixing and transport properties of surface mesoscale currents (d'Ovidio *et al.*, 2004). Regions of large mixing activity such as the Southwest Indian Ridge and PEI regions (and in between) overlap with areas of intense EKE (Figure 3.8). Large time-mean FSLEs ($>0.15 \text{ days}^{-1}$) show that submesoscale flows are ubiquitous south of Marion, synonymous with proposed eddy trajectories (Lamont *et al.*, 2020) generated and propagated along the ACC. Large FSLEs ($>0.15 \text{ days}^{-1}$) are also associated with the Subtropical Convergence Zone.

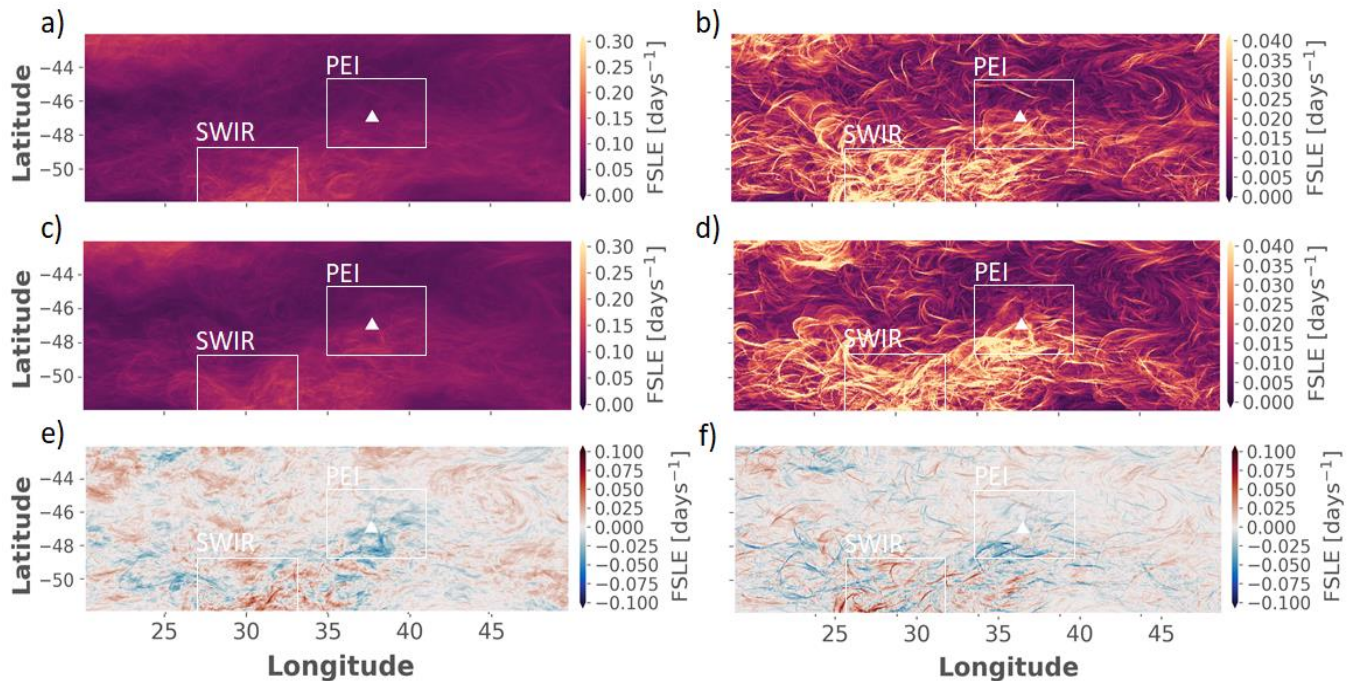


Figure 3.10: Time-mean (a,c) and standard deviation (b,d) of winter (a,b) and summer (c,d) Finite-Size Lyapunov Exponents (FSLE)[days⁻¹]. The seasonal anomaly (winter-summer values) of time-mean (e) and standard deviation (f) of FSLE, where negative values indicate higher values in summer than in winter, are shown. Triangles represent the position of the Prince Edward Islands (PEI). Boxes represent the Prince Edward Island and Southwest Indian Ridge (SWIR) regions. Geographical areas of different levels of mixing activity and variation in mixing activity can be observed.

Prominent submesoscale fronts are advected towards the PEI region indicating non-uniform local stirring linked to mean flows. These fronts appear to be enhanced near the islands spreading downstream, often for distances exceeding 1000 km, following the deflection of an ACC jet at around 45°E (Figure 3.10), where the sub-Antarctic front is known to meander (Koubbi *et al.*, 2016). Large values of mean FSLE ($>0.1 \text{ days}^{-1}$) and standard deviations (0.03 days^{-1}) are co-located, indicating high mesoscale variability linked to FSLE rather than standing frontal meanders. The large ($>0.03 \text{ days}^{-1}$) daily variation in submesoscale features (Figure 3.10b,d) illustrates oceanic variability at daily scales. North of the PEI, mean FSLE values appear relatively low ($<0.1 \text{ days}^{-1}$) on average, with low ($<0.03 \text{ days}^{-1}$) variability, suggesting less of an influence of

submesoscale fronts on the flow dynamics of this area. Seasonality of FSLE shows that summer submesoscale flows are intensified (Figure 3.10e) and become increasingly variable (Figure 3.10f) within the islands' region. This is especially evident to the south and downstream of the islands, as illustrated by negative ($\sim 0.05 \text{ days}^{-1}$) seasonal anomalies (winter - summer). However, throughout the study region, winter submesoscale flows are greater ($\sim 0.05 \text{ days}^{-1}$) in winter than in summer. Markedly enhanced mesoscale activity (Figure 3.8c) seen to the far North West of the islands ($< 44^\circ\text{S}$) is associated with the influence of the Subtropical Convergence (Ansorge and Lutjeharms, 2003) and is co-located with intense submesoscale transport fronts (Figure 3.10).

Submesoscale variability determined from seal-track data

Along-track absolute horizontal buoyancy gradients ($|b_x|$) were calculated using all available tracks measured by the seal-borne devices. The distribution of $|b_x|$ shows that the upper limits ($> 1e^{-7} \text{ 1/s}^2$) in winter are greater than in summer (Figure 3.11a), displaying strong seasonality in the region. In both seasons, the upper limits of $|b_x|$ are lower downstream than upstream, yet the winter contrast (Figure 3.11b) is more pronounced than in summer (Figure 3.11c). In winter, seals travel much further from the islands (Wege, 2013). Therefore, upstream $|b_x|$ includes that which occurs far outside of the PEI region where (sub-)mesoscale variability is intensified (e.g. the Southwest Indian Ridge region or Subtropical Convergence Zone) (Figure 3.8, Figure 3.10). In contrast, summer $|b_x|$ were calculated based on relatively uniformly distributed seal tracks found consistently within or near the PEI region (Figure 3.4), owing to shorter summer trips.

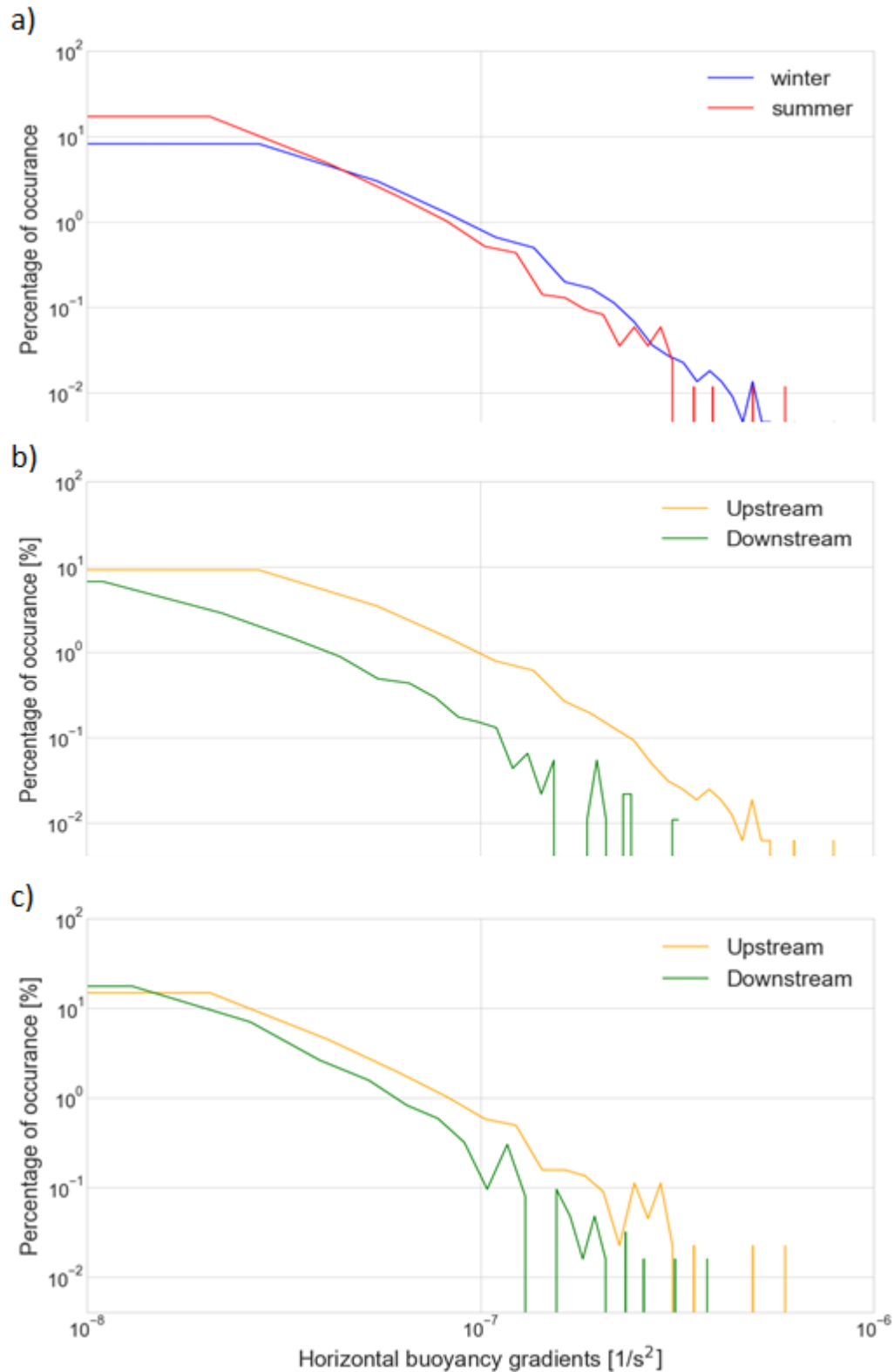


Figure 3.11: a) Seasonal distribution of absolute horizontal buoyancy gradients ($|b_x|$) are presented along with b) winter and c) summer comparisons between upstream (orange) and downstream (green) $|b_x|$ distributions averaged from 10-20 metres depth.

Multi-year (2009-2015) seal deployments over both summer and winter months show a distinct seasonal evolution of stratification surrounding the PEI (Figure 3.19), with lower

overall stratification in winter (4.78%) than in summer (23.11%). Downstream, the stratification is higher in summer (39.64%) than in winter (7.25%). However, this was reversed upstream where stratification was lower in summer (0.83%) than in winter (4.11%). The difference between upstream and downstream stratification per season shows an observably greater difference in summer (38.81%) than in winter (3.14%), with downstream stratification being consistently higher than upstream. To investigate whether the seasonal signal of enhanced downstream stratification may have underlying spring/autumn influences, summer was further split into ‘Early’ (before Jan 15th) and ‘Late’ (after Jan 15th) summer. However, there were no subseasonal patterns of stratification observed.

Case study (summer 2012): Topographic influences on downstream upper ocean physics

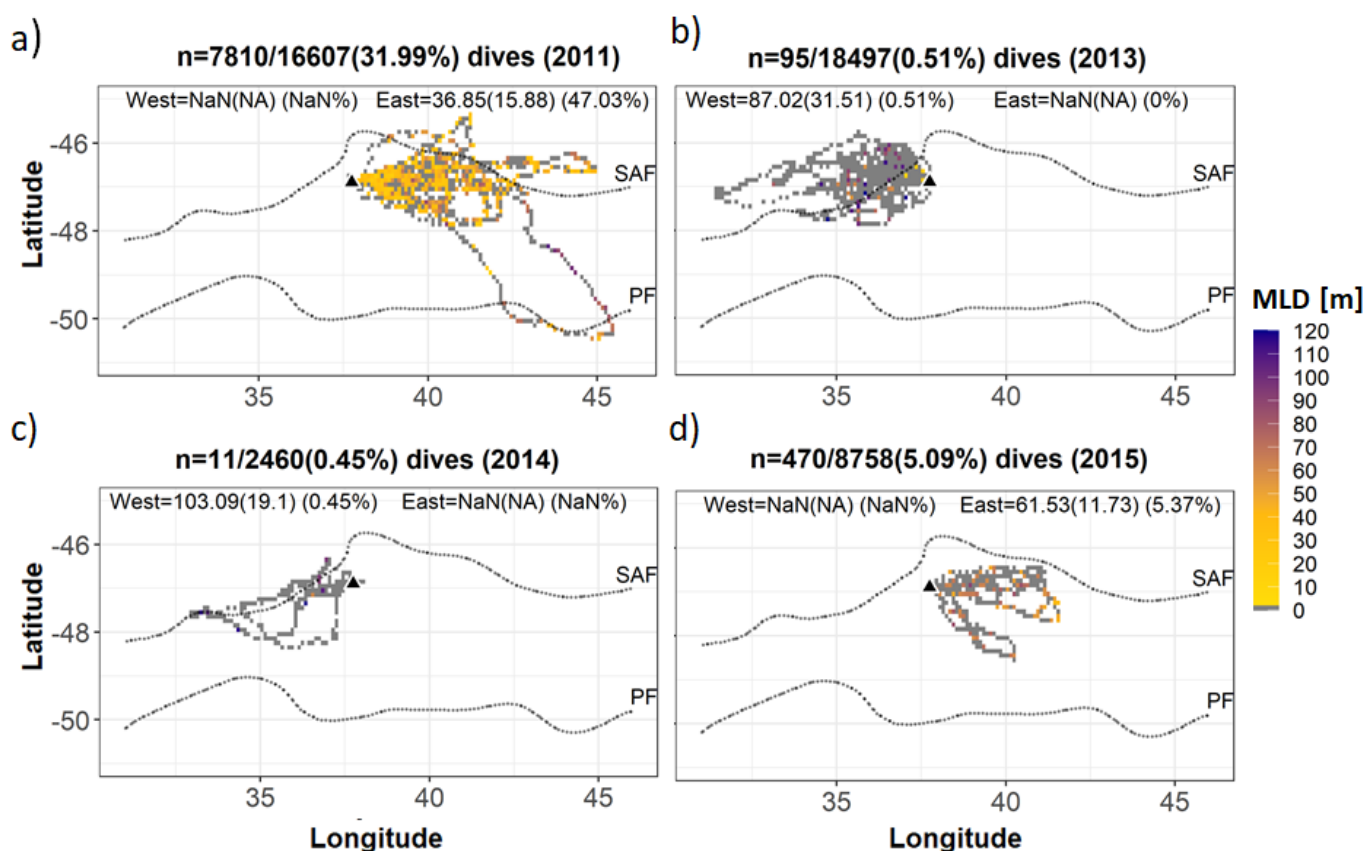


Figure 3.12: Spatial distribution of summer mixed layer depth (MLD) (here labelled as ‘T dep’) for summers of 2011 (a), 2013 (b), 2014 (c) and 2015 (d). Data are gridded at a 0.1° spatial resolution. Grey cells indicate profiles that are insufficiently deep for MLD presence; here the mixed layer is deeper than the maximum depth of the gridded mean profile. The mean (from 1993-2012) position of the sub-Antarctic Front (SAF) and the Polar Front (PF) are shown as black dotted lines, obtained from Park and Durand (2019). Zero (grey cells) ‘T dep’ represents dives within well-mixed water masses where profiles are insufficiently deep for MLD presence.

Summer mixed layer depths were deeper upstream than downstream of the islands, irrespective of the year (Figure 3.12). A case study was developed to further investigate how small-scale topography of the PEI influences downstream upper ocean thermal structure in summer. All seal profiles from 2012 were chosen for analysis as i) it had the most available profiles on either side of the islands, and ii) to eliminate any inter-annual variability in stratification that may prevent temporal bias, i.e. changes in climatology due to annual anomalies, which can arise through interannual influences on environmental structure such as the Southern Annular Mode (Screen *et al.*, 2009) and/or El Nino (Arthur *et al.*, 2018).

Figure 3.13 illustrates deep (90.8 ± 30.7 m) upstream and shallow (41.5 ± 16.4 m) downstream mixed layers corresponding with mean temperature and vertical stability profiles. Over similar depth ranges (~0-150 m), upstream and downstream mean temperatures remain relatively uniform and decrease sharply with depth, respectively (Figure 3.13b,c). Also, the contrast in the temperature profiles seems to show that above (below) 75 m, the water is warmer (cooler) downstream, illustrating the separation between the two systems. These mean temperatures are associated with low (<1 °C) variability throughout the water column, with lower confidence in observations beyond 100 m after which counts drop below 1 % of occurrence (Figure 3.13f,g). Contrasts of the mean vertical stability profile show stronger stratification downstream at all depths, while the peak in vertical stability is deeper than mean MLDs by about 30 m (Figure 3.13d,e). The mean downstream vertical stability profile shows higher variability than upstream. The maximum dive depths are similar for upstream and downstream profiles, thus showing minimal bias in the depth of profiles analysed, with 100% of profiles shallower than 200 m.

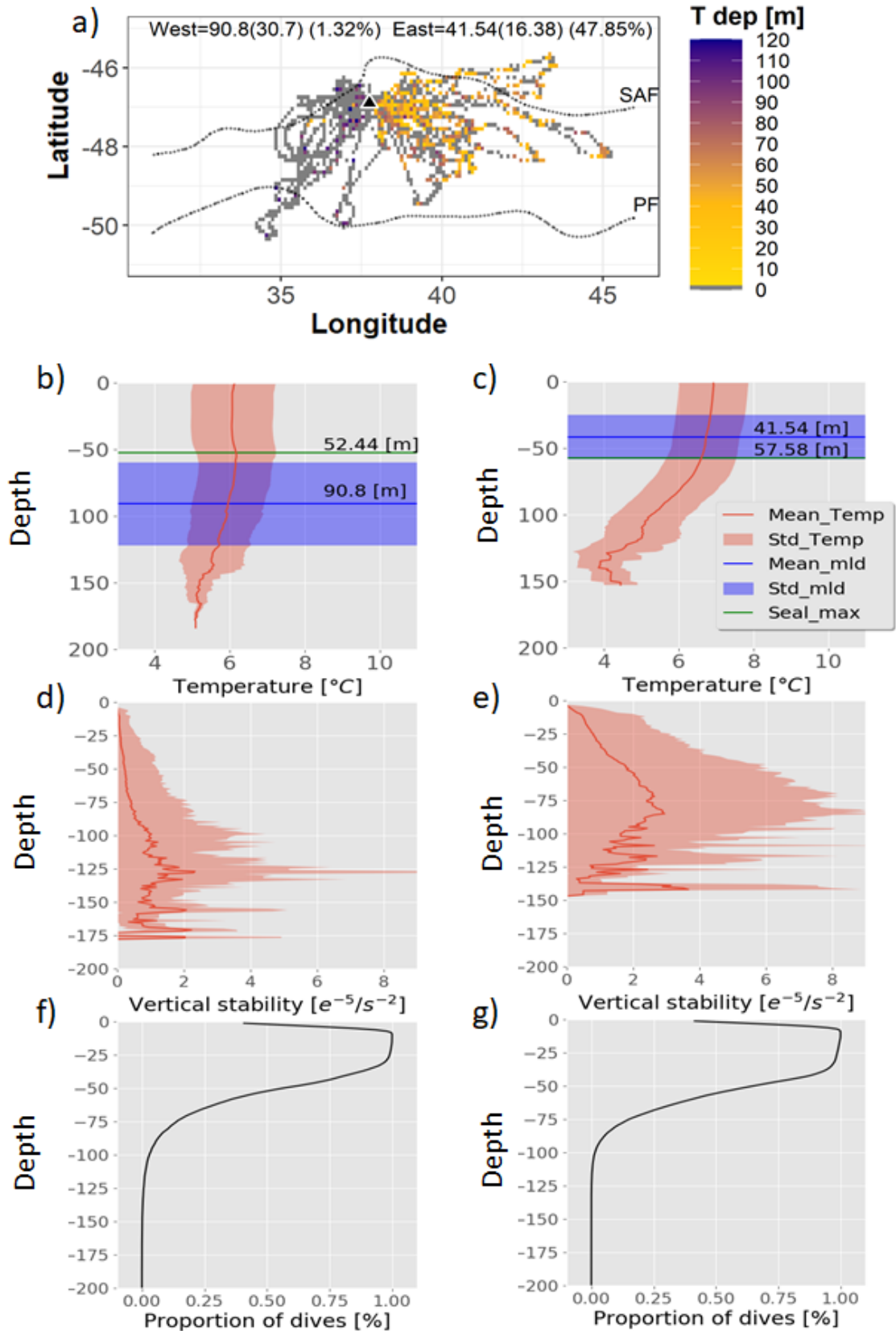


Figure 3.13: Mean gridded (0.1°) mixed layer depth (MLD) for summer of 2012 are presented in (a). Grey cells indicate profiles that are insufficiently deep for MLD presence i.e. well-mixed. Mean temperature [$^\circ\text{C}$] (red line) profiles with standard deviation (red shading) from upstream ($n=14170$ dives) (b) and downstream ($n=21396$ dives) (c) dives are shown with mean (blue line) and standard deviation (blue shading) of the MLD. The mean maximum seal-derived profile depth upstream and downstream is shown by a green line.

Chapter 3: Downstream influences on submesoscales and foraging behaviour

Vertical stability (N^2 [$1e^{-5}/s^2$]) changes with depth (mean \pm SD) upstream (d) and downstream (e) of the Prince Edward Islands are shown in red. Correspondingly, (f) and (g) illustrate the percentage of seal occurrence per depth bin (1 m). The mean (from 1993-2012) position of the sub-Antarctic Front (SAF) and the Polar Front (PF) are shown as black dotted lines, obtained from Park and Durand (2019).

Upper limits of *in situ* absolute horizontal buoyancy gradients ($|b_x|$), representative of submesoscale filaments, were slightly greater upstream of the islands than downstream (Figure 3.14). In contrast, satellite remotely sensed FSLE, representative of stirring at submesoscale, greatly enhances (>0.1 days $^{-1}$) following a downstream eastward propagation. Water parcels are squeezed and stretched as they meet the sloping topography of the PEI. This eastward evolution of FSLE (Figure 3.15b) appears to correspond with the evolution of intense EKE (Figure 3.15a), although enhanced FSLE continues further downstream ($>42^\circ$ E) through time, despite dissipation of EKE after 42° E.

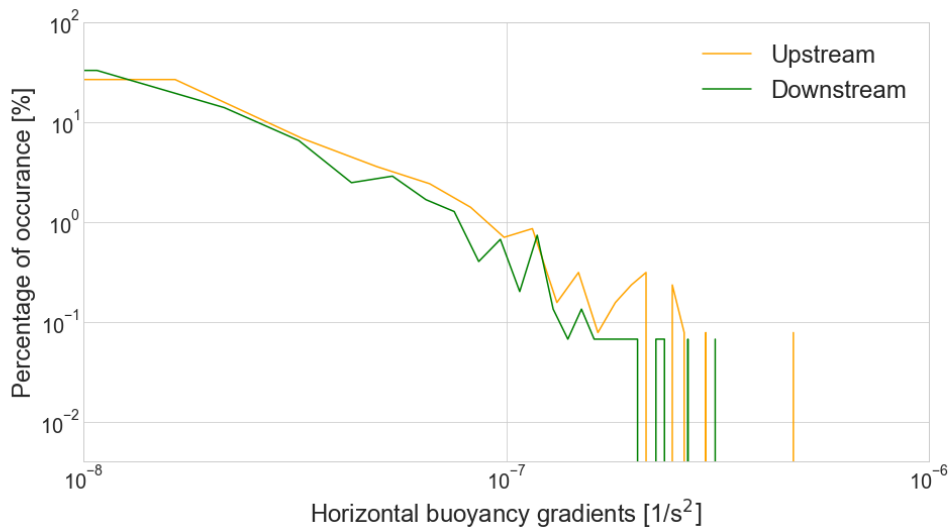


Figure 3.14: Distributions of absolute horizontal buoyancy gradients ($|b_x|$) were compared between upstream (orange) and downstream (green), averaged from 10-20 metres depth.

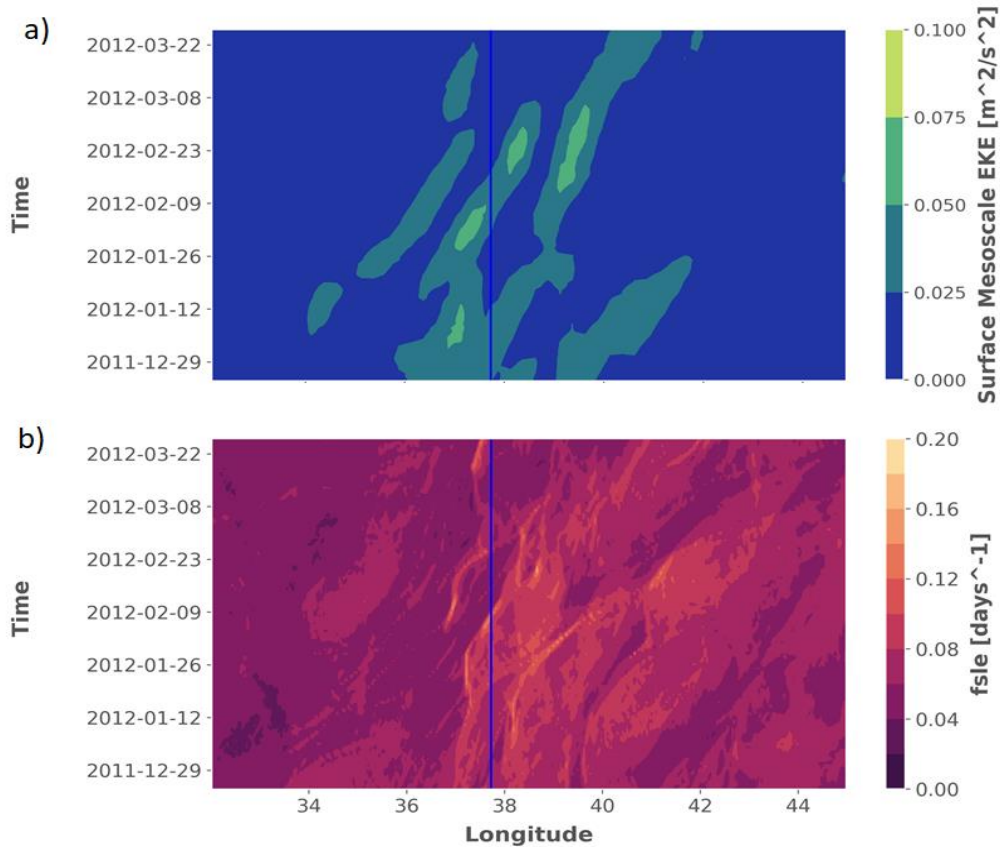


Figure 3.15: Time evolution of mesoscale activity and stirring, upstream (west of 37° 45' E) and downstream (east of 37° 45' E) of the Prince Edward Islands. Hovmöller plot of daily surface mesoscale Eddy Kinetic Energy (EKE) [m²/s²] (a) and daily Finite-Size Lyapunov Exponents (FSLE) [day⁻¹] (b) averaged over the latitudinal extent of summer seal foraging trips (-49° to -45° latitude). The blue line represents the longitude of Marion Island (37° 45' E).

Comparisons between seasonal upstream and downstream vertical structure and seal behaviour

Seasonal climatology maps of seal behaviours and upper ocean thermal structure were plotted at a common spatial resolution (0.1 degree) or visual comparison of upstream and downstream foraging behaviour in relation to upstream and downstream thermal structure (Figure 3.16, Figure 3.17). This was achieved by re-projecting profiles into raster grids in R (R Core Team, 2020) over a coordinate range of 40°S-52°S, 20°E-50°E, therefore encompassing winter and summer sampled foraging trips from 2009-2015. Spatial ranges of available profiles in winter (>2500 km) far exceed those covered in summer (<1200 km) (Figure 3.4). Summer and winter climatology maps (Figure 3.16, Figure 3.17) show that seals do not drastically change vARS, hARS, or maximum depth at the sub-Antarctic front, nor the Polar front, despite mean upstream and downstream variation in frontal distributions.

Summer maximum depths of seals diving upstream (52.65 ± 19.52 m) and downstream (50.65 ± 16.56 m) of the islands were relatively similar, considering maximum depths reached greater than 150 m. Furthermore, no mentionable downstream change in vertical or horizontal area-restricted search was apparent (Figure 3.16). Despite strong downstream enhancement of stratification and stability across a large zonal scale of $O(>500$ km), mean temperature remained relatively constant along latitudes (Figure 3.16). Mean temperature does, however, illustrate the typically dominant meridional increasing temperature trend towards the equator (Figure 3.16), albeit this does not appear to impact seal diving behaviour.

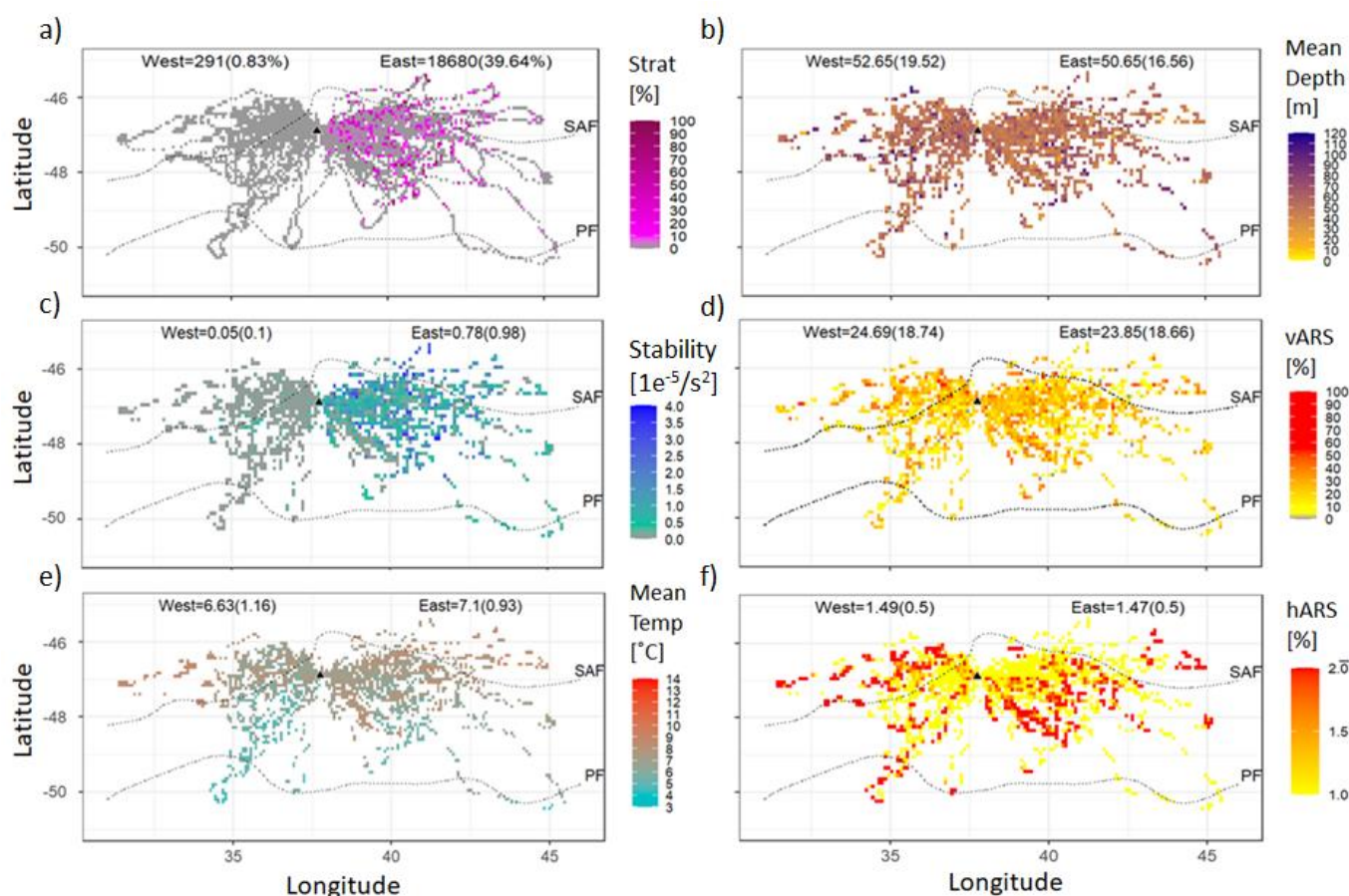


Figure 3.16: Graphs of summer gridded (0.1°) mean estimates presented for the period 2009-2015. Stratification [%] (a), stability [$1e^{-5}/s^2$] (c), and mean temperature (e) are the environmental variables used for comparison with spatial distribution of foraging effort in summer. Foraging effort is represented by mean (of maximums) depth [m] (b), vertical area-restricted search (vARS) [%] (d), and horizontal area-restricted search (hARS) [%] (f). Zero (grey cells) stratification and stability represents dives within well-mixed water masses where temperature ceases to change with depth within a given profile and does not necessarily indicate low stratification and stability, respectively. The position of Marion Island is represented by the black triangle, while the mean (from 1993-2012) position of the sub-Antarctic Front (SAF) and the Polar Front (PF) are shown as black dotted lines, obtained from Park and Durand (2019). The top text in each graph illustrates the mean (\pm SD) for each variable to the 'East' (i.e. Upstream) and the 'West' (i.e. Downstream) of the islands.

In winter, seals dived deeper upstream (59.53 ± 29.62 m) than downstream (47.17 ± 25.43 m) on average, while downstream mean vARS (37.37 ± 20.4 %) exceeded that of upstream mean vARS (26.17 ± 22.88 %). Maximum dive depths either side of the islands had higher variability in winter (~ 27 m) than in summer (~ 17 m). In the horizontal plane, mean and standard deviations of winter hARS were equivalent ($\sim 1.57 \pm 0.5$) upstream and downstream of the islands (Figure 3.17), similar to summer means (1.47 ± 0.5) (Figure 3.16). No zonal differences in mean temperatures were observed, while meridional gradients are shown to follow the meandering of ocean fronts, with cooler waters extending from south west to north east (Figure 3.17). An area north west of the islands (~ 25 - 27 °E, 43 - 46 °S) shows deeper maximum depths associated with warmer temperatures, low vertical and high horizontal foraging effort. No corresponding changes in stratification, stability or mean temperatures are observed in this area.

In both seasons and independent of spatially varying environmental parameters, vARS is consistently lower when seals dive deeper (summer $r^2 = 0.42$, winter $r^2 = 0.54$), while vARS and hARS are not well correlated (summer $r^2 = 0.06$, winter $r^2 = -0.05$) throughout the region.

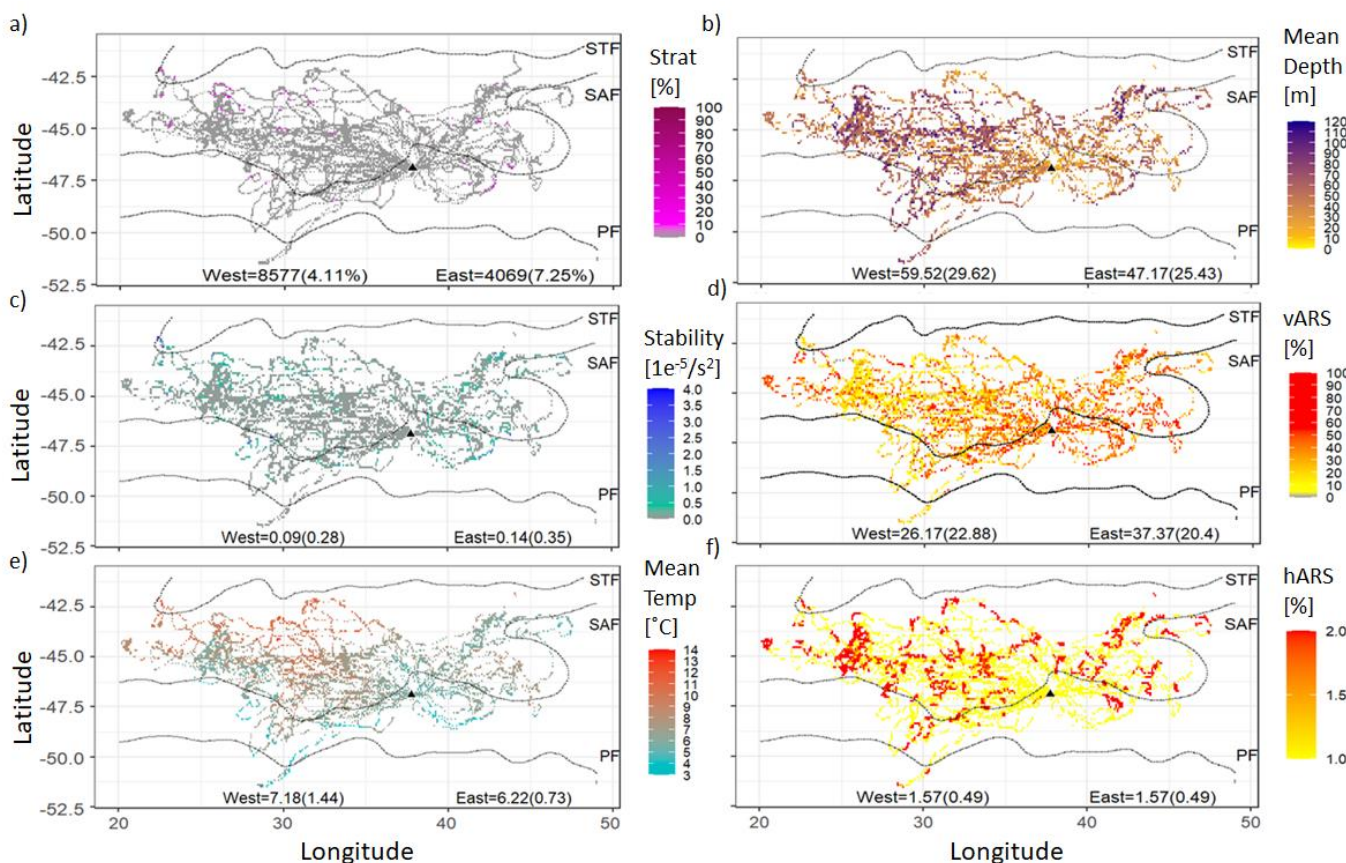


Figure 3.17: Graphs of winter gridded (0.1°) mean estimates presented for the period 2009-2015. Stratification [%] (a), stability [$10^{-5}/s^2$] (c), and mean temperature (e) are the environmental variables used for comparison with spatial distribution of foraging effort in winter. Foraging effort is represented by mean (of maximums) depth [m] (b), vertical area-restricted search (vARS) [%] (d), and horizontal area-restricted search (hARS) [%] (f). The position of Marion Island is represented by the black triangle, while the mean (from 1993-2012) position of the Subtropical Front (STF), sub-Antarctic Front (SAF) and the Polar Front (PF) are shown as white dotted lines, obtained from Park and Durand (2019). The bottom text in each graph illustrates the mean (\pm SD) for each variable to the 'East' (i.e. Upstream) and the 'West' (i.e. Downstream) of the islands.

Foraging depth was resolved for 82.85% of dives. Of these dives, MLDs were resolved 9.12% of the time. In summer, more time was spent foraging below the MLD downstream of the islands, while upstream of the islands, more time was spent foraging above the MLD (Table 3.1). In winter, more time was spent foraging below the MLD upstream, while the seals appeared to forage at the MLD downstream (Table 3.1). High variability in the relative vertical distribution of foraging to MLD (>15 m) was associated with both seasons and regions (Table 3.1).

Table 3.1: Seasonal upstream and downstream differences in diving behaviour relative to thermal water column structure. Positive values of 'distance to MLD [m]' indicate deeper foraging depth than mixed layer depth (MLD), while negative values indicate the opposite. Values are given as mean \pm SD.

	summer	summer	winter	winter
	Upstream	Downstream	Upstream	Downstream
#dives, Stratification [%]	34 962, 0.83%	47 128, 39.64%	208 525, 4.11%	56 145, 7.25%
MLD [m]	90.0 \pm 30.7	40.1 \pm 16.6	52.14 \pm 28.3	49.1 \pm 25.5
Max depth [m]	52.7 \pm 19.5	50.7 \pm 16.6	59.5 \pm 29.6	47.2 \pm 25.4
Mean foraging depth [m]	46.3 \pm 18.4	43.7 \pm 15.2	47.9 \pm 26.4	40.8 \pm 23.1
Distance to MLD [m]	-(18.9 \pm 32.8)	+(10.7 \pm 16.3)	+(12.3 \pm 25.1)	+(0.2 \pm 33.2)

Discussion

In the present study, investigation was made into the seasonality in ocean horizontal circulation and vertical mixing in the PEI region and surrounding Southern Ocean by linking these ocean dynamics across multiple scales, using both satellite and *in situ* data. Furthermore, I aimed to provide evidence for the topographic influence of these small islands to act as barriers to ocean flows, whilst investigating their effects on vertical stratification. Lastly, if the above seasonal and topographic influences on oceanography were evident, I was to investigate the impacts of these oceanographic changes on subantarctic fur seal fine-scale diving and foraging behaviour at large temporal (seasonal) and spatial (>500 km) scales.

Geostrophic and inertial ocean circulation surrounding the Prince Edward Islands

Steady (across seasons), homogeneous zonal (eastward) flow was shown by high values (>0.35 m/s) of zonal geostrophic velocities (Figure 3.7), representative of the ACC

(Hofmann, 1985; Perissinotto *et al.*, 2000; Lamont and van den Berg, 2020; Toolsee *et al.*, 2021), which was found to dominate over smaller and more variable meridional flows typical of the PEI region (Harris and Stavropoulos, 1978; Ansorge and Lutjeharms, 2007). The ACC is steered by large-scale (>200 km) bottom topography, much like in the neighbouring Kerguelen Plateau region (Rosso *et al.*, 2015) and forced equatorward as it flows over the Southwest Indian Ridge (Pollard and Read, 2001; Park *et al.*, 2019), where intense long-term (2009-2015) EKE was observed. This intensification of EKE is centred around the Andrew Bain Fracture Zone (ABFZ) at 50°S; 30°E (Figure 3.8), a well-known region of localised eddy generation along the Southwest Indian Ridge (Ansorge and Lutjeharms, 2003, 2005; Durgadoo *et al.*, 2010, 2011; Lamont and van den Berg, 2020).

As flows cross over shallow bathymetry, such as ridges, the depth mean flow is 'squeezed'. To conserve potential vorticity, relative vorticity must change (Hogg, 1973; Moore *et al.*, 1999), resulting in meandering downstream flows and the generation of mesoscale eddies (Ansorge and Lutjeharms, 2005; Chelton *et al.*, 2007). Although more eddies are generated in the Southwest Indian Ridge region (Asdar, 2018), and only few eddies tend to have long enough lifespans to reach the PEI region through ACC advection (Ansorge and Lutjeharms, 2003, 2007; Lamont and van den Berg, 2020), substantial levels of EKE (>0.05 m²/s²) was observed within the PEI region (Figure 3.8). Results of this study corroborate those of Lamont *et al.* (2020) with a presiding eastward mesoscale eddy pathway and intense upstream eddy activity found in the PEI region (Figure 3.9). This eddy advection is driven by the prominent zonal (eastward) component of mean background geostrophic currents of the ACC (Cushman-Roisin, 1990; Lamont and van den Berg, 2020), akin to the net eastward propagation of eddies observed in other regions influenced by the ACC (Chelton *et al.*, 2011; Klocker and Marshall, 2014). This eastward propagation (eddy drift) may also be related to eddy interactions and Rossby wave activity (Asdar, 2018), where the positions of various branches of the sub-Antarctic Front and the Antarctic Polar Front (Figure 3.18) (Lamont and van den Berg, 2020; Toolsee *et al.*, 2021) may be affected by the interactions between them (Ansorge and Lutjeharms, 2002).

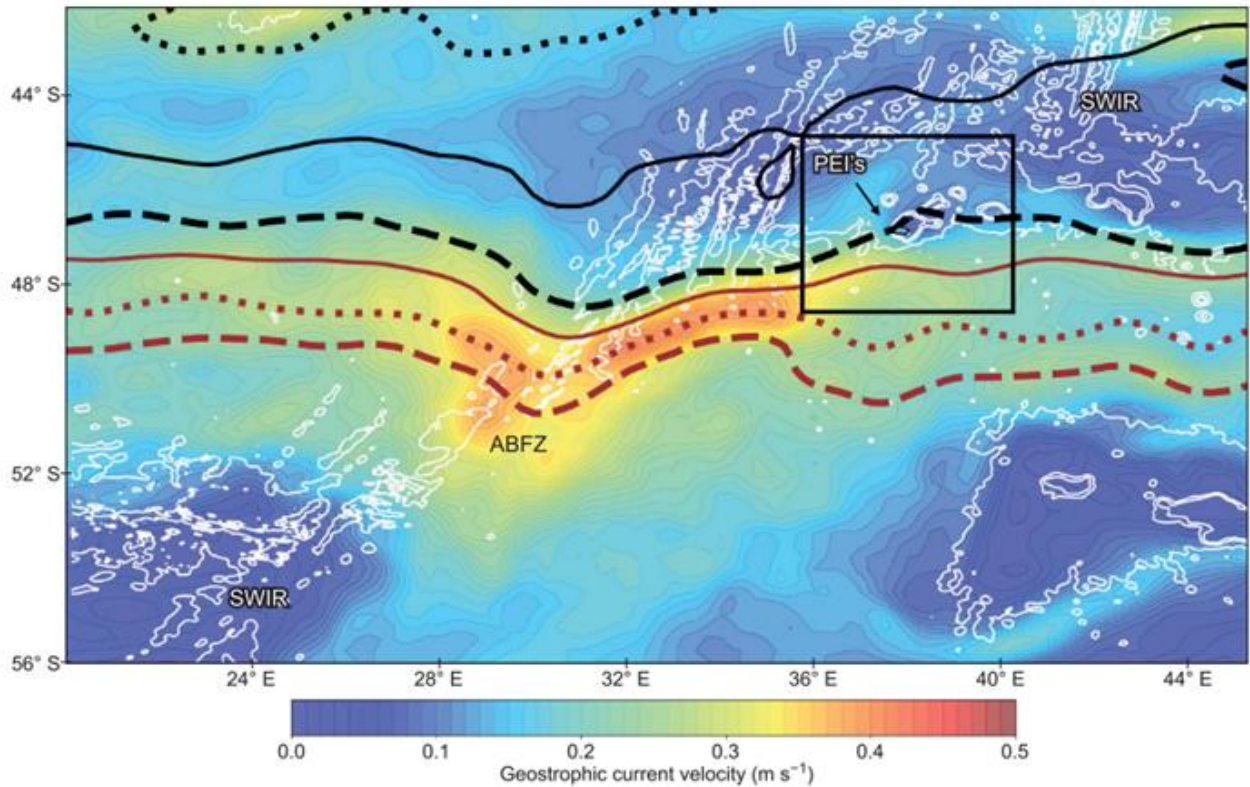


Figure 3.18: Geostrophic current velocities [$m \cdot s^{-1}$] from 1993 to 2016, and branches of the Antarctic Circumpolar Current fronts in relation to the Prince Edward Islands (PEI), with overlaid bathymetry, indicated in white (-3000 m, -2000 m, -1000 m). The Prince Edward Island region is indicated by a black square. This image is sourced from Toolsee *et al.* (2021), who states 'The northern (N-SAF), middle (M-SAF), and southern (S-SAF) branches of the sub-Antarctic Front are represented by the dotted/solid/dashed black lines, respectively. The northern (N-APF), middle (M-APF), and southern (S-APF) branches of the Antarctic Polar Front are represented by the solid/dotted/dashed red lines, respectively.'. ABFZ=Andrew Bain Fracture Zone, SWIR = Southwest Indian Ridge.

Seasonality of (sub-)mesoscale flows and mixing within the upper ocean

Outside of the PEI region, ocean variability is enhanced in winter relative to summer (Figure 3.8c), whereas within the PEI region summer ocean variability is enhanced (Figure 3.8c). Despite the transient mesoscale eddies continually traversing the islands throughout the year (Figure 3.9; Chown and Froneman, 2008), with little inter-annual variation, there is strong seasonality of EKE around the islands, which contrasts the strong seasonality of EKE observed outside of the PEI region (Figure 3.8c). Directly south of the islands, but still within the PEI region, a zone of stronger background zonal flow and high EKE relative to the north, in line with findings from Toolsee *et al.* (2021), was co-located with large seasonal means of submesoscale activity (Figure 3.10). This zone of high EKE shifts northward (towards the islands) in summer, seasonally enhancing (sub-)mesoscale activity within the PEI region, along with concurrent northward shifts in strong

(>0.35 m/s) easterly current velocities (Figure 3.7). The position and seasonal shifting of this zone is most likely related to the position and seasonality of the ACC jet (Toolsee *et al.*, 2021) and its associated fronts, which occur within the vicinity of the islands (Ansonge *et al.*, 1999; Ansonge and Lutjeharms, 2000). For example, the southern branch of the sub-Antarctic front, whose climatological position tends to remain near the islands (Ansonge & Lutjeharms, 2000; Chown and Froneman, 2008), was found to shift slightly north of the islands during summer (Toolsee *et al.*, 2021). This seasonal meridional shift has previously been linked to the intensity of the ACC when it encounters the Andrew Bain Fracture Zone (Craneguy and Park, 1999).

Although mesoscale eddies account for most of the kinetic energy in the open ocean (Xu, Shang and Huang, 2014), eddies consist of smaller scale (submesoscale) filaments or fronts (instabilities) that can carry and spread a significant amount of kinetic energy (Ferrari and Wunsch, 2009). Large values of both *in situ* $|b_x|$ ($>1e-7 \text{ s}^{-2}$) and remotely sensed FSLE ($>0.2 \text{ days}^{-1}$) observations showed strong evidence for active mixed layer instabilities and ubiquitous submesoscale flows adjacent to and extending either side of the PEI (Figure 3.10, Figure 3.11). *In situ* $|b_x|$, collected along seal tracks restricted to the PEI region in summer and including the area outside of the region in winter, illustrated that intense winter instabilities were less pronounced in summer throughout the study area (Figure 3.11), despite higher summer submesoscale activity observed within the PEI region. This suggests that the winter enhancement of instabilities dominates the seasonality of the study area over the local impacts of seasonally shifting fronts. Although this winter enhancement of submesoscales contrasted findings from *in situ* Southern Ocean data (du Plessis *et al.*, 2019), it was replicated in findings from the North Pacific (Sasaki *et al.*, 2014), North Atlantic (Mensa *et al.*, 2013; Callies *et al.*, 2015) and global (Uchida, Abernathy and Smith, 2017; Su *et al.*, 2018) numerical simulation studies. This seasonality is believed to be driven by the seasonality of the MLD (Mensa *et al.*, 2013), which controls the available potential energy for instabilities (Callies *et al.*, 2015). As suggested by Uchida *et al.* (2017), I suggest that the observed instabilities may be responsible for the seasonality of EKE outside of the PEI region.

I therefore propose that the disparity in seasonality in ocean variability of the PEI region in comparison to the surrounding waters is due to the spatial variation in relative dominance of driving forces, such as the seasonality of MLDs and ACC fronts, demonstrating the dynamical nature of the area in terms of flow variability and the

influence on island dynamics. By comparing maps of EKE and FSLE, it was further evident that submesoscale transport fronts (underlined by FSLE) and mesoscale activity (represented by EKE) are seasonally co-located. This is likely a result of energy transfers that link meso- and submesoscale variability in the open ocean (Capet *et al.*, 2008b; Ferrari and Wunsch, 2009; Klein and Lapeyre, 2009; Brannigan *et al.*, 2017; Lodise *et al.*, 2020; Siegelman *et al.*, 2020). In particular, these submesoscale filaments are thought to provide a pathway for downscale transfers of available potential energy from mesoscale eddies to finer scales (Thomas *et al.*, 2008) in the form of EKE. Energy cascades are applied through intense frontogenesis and frontal-instability events in the upper ocean (Capet *et al.*, 2008b; Klein and Lapeyre, 2009) by ageostrophic baroclinic instabilities (Boccaletti *et al.*, 2007). These instabilities can occur within the mixed layer and are therefore referred to as mixed layer instabilities (Boccaletti *et al.*, 2007). Importantly, these submesoscale instabilities can control vertical fluxes of heat, carbon and momentum between the atmosphere and the ocean interior (Thomas *et al.*, 2008; Sallée *et al.*, 2021), as well as support upwelling of nutrients into and trapping phytoplankton within the sunlit (euphotic) zone for phytoplankton production. Therefore, the strong instabilities co-located with eastward propagating mesoscale eddies past the islands may indicate a pathway of localized areas of phytoplankton blooms (Mahadevan, 2016), which could provide food for higher trophic levels such as SAFS.

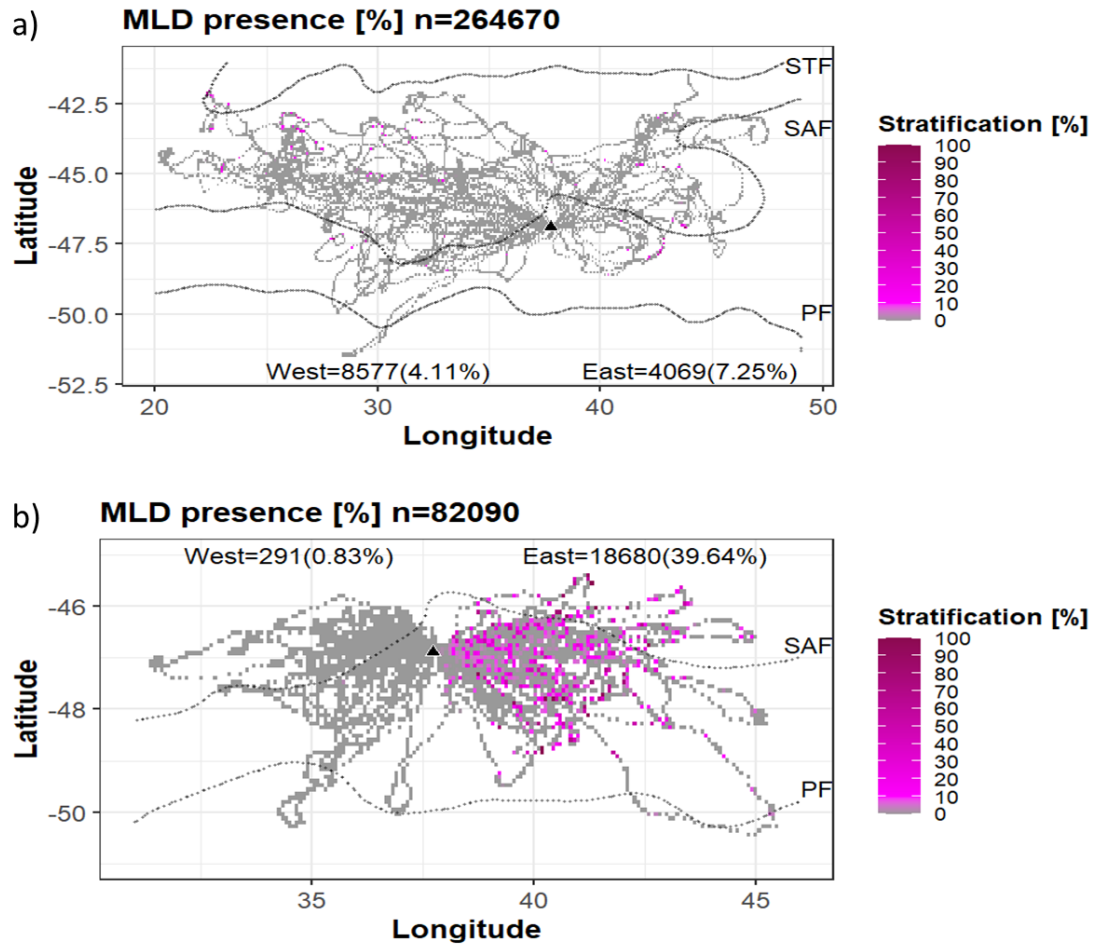


Figure 3.19: Winter (a) and summer (b) stratification. Grid cells represent the proportion of presence vs absence of a mixed layer depths in the profiles for that location. A total of 264670 and 82090 profiles were sampled in winter and summer, respectively. Total number of west (upstream) and east (downstream) profiles representing stratified water masses (proportion of stratified profiles relative to the number of profiles available to the west and east separately) indicated by text. Zero stratification indicates profiles that are insufficiently deep for MLD presence. The mean (from 1993-2012) position of the sub-Antarctic Front (SAF) and the Polar Front (PF) are shown as white dotted lines, obtained from Park and Durand (2019).

Considering the widely observed seasonality of ocean mesoscale flows discussed above, it is not surprising that submesoscale fronts too show seasonality. Submesoscale filaments play a critical role, through ageostrophic secondary circulation, in vertical mixing within the upper water column (Boccaletti *et al.*, 2007). As found within other areas of the Southern Ocean (Dong *et al.*, 2008; Sallée *et al.*, 2010; du Plessis *et al.*, 2019), the seal-derived profiles show a strong seasonal cycle of stratification, stability and MLDs in the upper ocean. Vertical mixing is enhanced during winter where stratification is observably low surrounding the PEI region (Figure 3.19) and MLDs are deep. In summer, shoaling of the mixed layer was observed, which was complemented by enhanced stratification and stability relative to winter. These *in situ* findings were further supported by similar findings using an objective analysis product (see Supp. Figure 4). Similarly, downstream

seasonality in thermoclines were found ~30 yrs prior (Allanson *et al.*, 1985), with shallow (~90 m) thermoclines in summer relative to winter (~200 m). This seasonal contrast is a result of surface warming through positive heat fluxes resulting in increasing mean mixed layer temperature, leading to restratification (Pellichero *et al.*, 2017). du Plessis *et al.* (2019) used glider data in the sub-Antarctic Zone to show that this restratification can be delayed by up to two months (~December) once surface heat flux becomes positive (~October). Therefore, with the earliest available summer seal foraging trip occurring in December, it is assumed that the observed seal-derived results are representative of progressive summer restratification. The observed seasonality of ocean surface flows mentioned above is therefore thought to induce a strong seasonal cycle of upper ocean structure (Boccaletti *et al.*, 2007; Siegelman *et al.*, 2020).

Gradients of both salinity and temperature are ocean stratifying properties that contribute to changes in density (Carmack, 2007). The relative dominance of heat and salt on stratification classifies alpha and beta oceans, respectively (Stewart and Haine, 2016). At large scales (1° resolution) and with the addition of salinity recordings, Objective Analysis data showed that the PEI region and surrounding waters can largely be classified as an alpha ocean (Figure 3.6), much like the rest of the midlatitudes (Stewart & Haine, 2016) and ice-free Southern Ocean (Pellichero, J. B. Sallée, *et al.*, 2017). In this study, I therefore assumed changes in temperature to set stratification within the mixed layer, a valuable assumption to allow assessment of stratification and stability within mixed layers using temperature only data acquired from the SAFS. However, this assumption may undergo some level of scrutiny as seasonal variation in compensation was evident to a small degree (Figure 3.6).

Rintoul and Trull (2001) showed that the relative contribution of temperature and salinity to changes in buoyancy in the upper ocean changes from temperature dominance to salinity dominance across the sub-Antarctic Zone from north to south. Similarly, the PEI region may be a transition zone between alpha and beta oceans where stratification is seasonally set by changes in temperature or salinity (Stewart & Haine, 2016). This seasonality of compensation observed is most likely a response to seasonality in vertical mixing and heat distribution in the upper ocean (Rudnick and Martin, 2002; du Plessis *et al.*, 2019). Specifically, the stability ratio (the ratio of the heat-to-salt contributions to the stratification (IOC *et al.*, 2010) was used to identify the role of temperature and salinity to the vertical stability. In summer, vertical density gradients are dominated by temperature

variations ($|R_p| > 1$), providing further evidence of temperature dominance. Relative to summer, overall winter stability ratios were low ($|R_p| < 1$) (Figure 3.6) and often peaked at $|R_p| = 0$ either side of the islands when the surface ocean undergoes atmospheric cooling, suggesting that vertical changes in salinity may be playing more of a role in ocean stratification in the waters surrounding the islands than previously assumed in this study. However, salinity intrusions are typically found further south of the Polar Front, where salinity effects are expected to dominate over temperature effects on density gradients (Rintoul and Trull, 2001; Pellichero *et al.*, 2017; Swart *et al.*, 2020).

It has recently been suggested, by numerical modelling, that deep MLDs, large buoyancy gradients and along-front wind stress enhance submesoscale activity in the Southern Ocean in winter (Su *et al.*, 2018). *In situ* results from the present study show that mixed layers deepen, and buoyancy gradients are enhanced in winter, in line with the findings above. Considering that the seasonality of submesoscale processes found within this study, linked to greater (mesoscale) scales of variability, is evident in other areas of the ocean such as the North Atlantic (Callies *et al.*, 2015) and Antarctic Marginal Ice Zone (Biddle and Swart, 2020), a widely agreed-upon global seasonality in submesoscale activity seems likely, despite local influences on mixing.

Topographic influences on downstream local variability in the upper ocean

The flow regime downstream of the PEI is complex and dynamic (Ansorge & Lutjeharms, 2002). The PEI are known to act as barriers to laminar geostrophic flows (Toolsee *et al.*, 2021), causing flow meanders (Perissinotto *et al.*, 2000) that drive interactions between the ACC fronts and their associated eddies (Ansorge & Lutjeharms, 2002, 2007). Little is known about whether/how the sloping topography of the PEI could/may modulate downstream submesoscale processes such as filamentary structure generation and vertical mixing within the upper water column. In this study, the topography of the PEI, i.e. island bathymetry, was crudely referred to as small-scale slanting of bathymetry contours.

As with other small-scale topographic features (Yang *et al.*, 2019; Zhang and Nikurashin, 2020), I propose that the PEI are capable of producing a small downstream wake, associated with the weakening of downstream climatologies of geostrophic velocities, and the dissipation of upstream transient eddies through topographic form stress. This

generated enhanced variability in downstream submesoscale turbulence and vertical mixing, thereby shoaling, restabilizing and stratifying the mixed layer downstream. Although MLDs were sufficiently shallow in summer for seal-derived data to illustrate the topographic effects on vertical mixing, winter effects on deep MLDs could not be directly observed, due to physiological limitations on the maximum depth of each dive reached by individual seals. However, due to the previously discussed links between horizontal ocean variability at (sub-)mesoscales and vertical mixing, and the reduction of downstream ocean variability observed in winter, I assume that topographic effects are also realised in winter.

In this study, island sloping topography was crudely labelled as 'small-scale' based on similarities with the terminology used in other studies (Yang *et al.*, 2019; Zhang and Nikurashin, 2020) and in comparison, to larger bathymetric features. Initial findings provided evidence for a small-scale topographic influence of the PEI across multiple scales of flow. Opposite to intense upstream mesoscale activity, downstream mean EKE was considerably low (Figure 3.9) in both summer and winter. Identical patterns were found in submesoscale flows, where seasonal means of $|b_x|$ indicated strong upstream transport fronts (calculated on length scales of 1-100 km) as opposed to less pronounced downstream fronts (Figure 3.11). This could be explained by observed downstream restratification (Figure 3.19) due to the weaker mesoscale turbulence associated with the lower EKE (Figure 3.10), thus generating insufficient available potential energy for the development of horizontal buoyancy gradients and submesoscale fronts (Thomas *et al.*, 2008; Mensa *et al.*, 2013). Contrastingly, large-scale topography such as the Shackleton Fracture Zone (Viglione *et al.*, 2018), the Kerguelen Plateau (Rosso *et al.*, 2015) and the Southwest Indian Ridge (Ansorge & Lutjeharms, 2005), also within the ACC of the Southern Ocean, have shown to enhance downstream (sub-)mesoscale activity.

To date no studies have considered the observed downstream reduction in the climatologies of multi-scale flows within the PEI region. This suggests that the nature of topographic modulation could be dependent on the size of the topographic features causing these effects. Further studies are required to investigate the importance of topographic scale with respect to topographic influence on flows surrounding the PEIs. Further analysis, using a case study of the summer of 2012, showed how small-scale topography, exerted by the PEI, can in fact enhance downstream submesoscale processes (Figure 3.15b) through the dissipation of EKE (Figure 3.15a). This prevents an

unconstrained build-up of downstream EKE, potentially contributing to the maintenance of energy balance within the Southern Ocean (Lazar, Zhang and Thompson, 2018).

Mesoscale eddies are known to be a source of energy dissipation into smaller scales (Ferrari and Wunsch, 2009; Callies *et al.*, 2015; Wunsch, 2016). Mesoscale eddies entering the PEI region, and their associated relative vorticity, may be irreversibly stretched into filaments that are advected far eastward by the background flow of the ACC. Eastward drift of mesoscale eddies is hampered as eddies interact with the PEI topography, with little interannual and seasonal variation found (Figure 3.9). Long-term (8-year means) eddy dissipation has previously been estimated downstream of the islands using idealised regional simulations (Asdar, 2018). Despite weaker horizontal buoyancy gradients measured downstream relative to upstream in 2012 (Figure 3.14), FSLE showed intense downstream mesoscale stirring associated with the dissipation of EKE (Figure 3.15) and intensification of submesoscale motions, akin to results of high resolution (1 km x 1 km) idealized simulations of flow over sloping topography (Lazar *et al.*, 2018). The observed patchiness in downstream MLDs (Figure 3.13) further suggests enhanced submesoscale variability (Boccaletti, Ferrari and Fox-Kemper, 2007; Mensa *et al.*, 2013).

Seal foraging trips (7 in total) from a single seal (Seal ID = 21) over the summer of 2012 were used as an along-track example of *in situ* $|b_x|$ alongside co-located in time and space with satellite remotely sensed FSLE. Observable downstream peaks in FSLE (Figure 3.20) illustrate the stretching of flows around the Prince Edward Archipelago, often for distances exceeding 200 km. Along-track horizontal buoyancy gradients are variable at submesoscales and occasionally exceed 10^{-7} s^{-2} . Irrespective of whether seals travelled across (Figure 3.20d) or along (Figure 3.20e) fronts, it was observed that high values of FSLE and b_x were frequently co-located in time and space (Figure 3.20a). This suggests higher submesoscale activity downstream, agreeing with Siegelman *et al.* (2020), and supporting evidence for locally active submesoscale fronts directly downstream of the islands in summer. The lower downstream horizontal buoyancy gradients observed from the 2012 seal profiles (Figure 3.14) could likely be a consequence of topographic stirring and cascade of energy of persistent fronts to length scales smaller than those observed by the seals (i.e. <5 km).

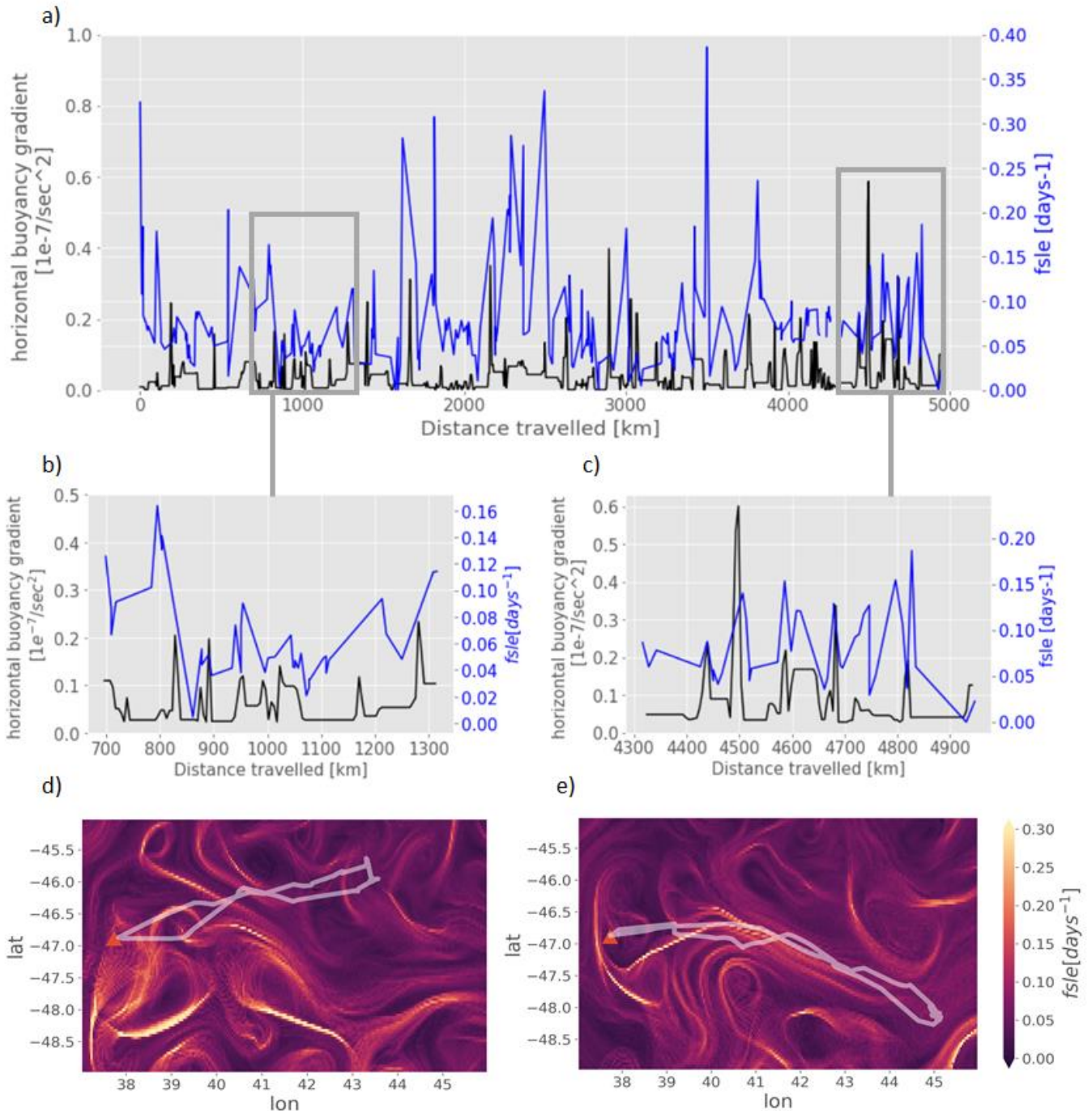


Figure 3.20: Case study showing a single subantarctic fur seal's (seal ID = 21) foraging track data in the summer of 2012. Mean along-track absolute horizontal buoyancy gradients ($|b_x|$) [$10^{-7}/s^2$], calculated between 10 and 15 m depth from seal-derived profiles, and corresponding (in space and time) surface Finite-Size Lyapunov Exponents (FSLE) [$days^{-1}$] are depicted in (a). Plots are zoomed into the 3rd (b,d) and 7th (c,e) foraging trips. Maps of cross-frontal (d) and along-frontal (e) trajectories of seal tracks are overlaid on FSLE averaged over the time extent of each respective foraging trip (typically ~ 8 days in summer).

Overall, this study proposes that strong upper ocean (10-15 m depth) horizontal buoyancy gradients of order 1-100 km upstream of the island drives the development of downstream surface fronts at submesoscales, $O(1-10$ km). Values of b_x were comparable with open

ocean studies (Thompson *et al.*, 2016; du Plessis *et al.*, 2019), yet not with regions preconditioned for stronger mesoscale eddy fields (Viglione *et al.*, 2018) and large-scale topographical influence (Rosso *et al.*, 2015), where b_x values were found to be an order of magnitude stronger. It is suggested that stronger gradients would likely result if sampling had been at a higher (<5 km) resolution (Swart *et al.*, 2020).

The co-located summer peaks in downstream b_x and FSLE may also result from the stagnation or slowing of eastward propagation through topographic stirring (Durgadoo *et al.*, 2008), likely allowing for a locally shallower pool where summer atmospheric surface heating can warm the entire mixed layer (du Plessis *et al.*, 2019). In this instance, warming mixed layer temperatures would lead to the shoaling of the MLD (du Plessis *et al.*, 2019), which was observed downstream. In contrast, upstream flows would be too large and vigorous for surface heating to influence mixed layer properties.

Another theory suggests that downstream shoaling of the thermocline (Perissinotto *et al.*, 2000) is elicited by freshwater input from island run-off. However, this study was constrained to local (100-200 km from the PEI) effects and has not accounted for further downstream (~1000 km). In a relatively beta ocean, such as the PEI in winter, topographic trapping of circulations entering the PEI region may allow for build-up of freshwater run-off with the potential to locally intrude and elevate sea water freshness and buoyancy (stability) (Perissinotto *et al.*, 2000) and shoal the mixed layer through compensation of density gradients in the vertical, with consequences for transient phytoplankton blooms and higher trophic levels that may rely on them (Pakhomov and Chown, 2003; Bestley *et al.*, 2020). However, I suggest here that considering the lack of evidence for winter shoaling, I believe that freshwater effects probably do not play a compounding role further downstream (~1000 km).

Lastly, the shallower bathymetry to the east of the PEI (Fisher and Goodwillie, 1997) may also play a role in downstream shoaling of the MLD through flow disturbance, enriching phytoplankton growth near the surface (Perissinotto and McQuaid, 1992; Read, Pollard and Allen, 2007) and potentially providing suitable prey fields for subantarctic fur seals (de Bruyn *et al.*, 2009). As discussed in the seasonality section above, overall restratification occurs in the PEI region in summer by atmospheric surface heating (Swart *et al.*, 2015). As seasonal restratification only occurs downstream (Figure 3.19), I propose that seasonal surface heating cannot be the only influence on restratification in the region, otherwise upstream water would also have been equally stratified.

Seasonal restratification is likely arrested in this upstream region by the strong laminar geostrophic flow of the ACC jet and intense (sub-)mesoscale energy associated with its fronts (du Plessis *et al.*, 2019), thereby sustaining well-mixed and deep mixed layers throughout the year. Furthermore, consistently deep upstream MLDs (as is observed in this study) could provide potential energy available for mixed layer instabilities to sustain submesoscale fronts throughout the year (Thomas *et al.*, 2008; Mensa *et al.*, 2013). However, as the topography of the islands acts on eastward propagating mesoscale eddies, the associated submesoscale density gradients, dominated by temperature gradients and manifested as $|b_x|$, dissipate downstream. As the submesoscale flows become baroclinically unstable, they slump from horizontal to vertical within the mixed layer, thereby redistributing buoyancy (Boccaletti *et al.*, 2007; Fox-Kemper *et al.*, 2008; Siegelman *et al.*, 2020). This downstream slumping can generate the 'patchy' horizontal distribution of stratification observed in my results (Hosegood, Gregg and Alford, 2006; Swart *et al.*, 2015).

Particularly, in the summer of 2012, the mean upstream temperature and stability profiles showed a well-mixed and unstable water column compared to a stratified and stable downstream water column, with little (<1 °C) variations around mean temperature values with depth (Figure 3.13). Upstream MLDs are deep, likely due to enhanced upstream mesoscale turbulence, while strong downstream stability is associated with weaker flow which allows for restratification and mixed layer warming. The higher variability around downstream vertical stability profiles relative to upstream profiles is likely due to the higher number of downstream profiles that are averaged over in this study. This downstream restratification, restabilization and shoaling of the MLD provides evidence for indirect topographic inhibition of vertical downstream mixing (Mensa *et al.*, 2013). The kinetic energy generated in these shallow downstream mixed layers may be transferred to smaller than submesoscales in the horizontal plane, which can easily escape the influence of rotation (McWilliams *et al.*, 2009), preventing the instability from energizing submesoscales further (Capet *et al.*, 2008a).

Although the abrupt zonal change from well-mixed to stratified water is only observed in summer, this is not to say that winter topographic influences are discounted, but instead that upstream-downstream summer mixed layer contrast is probably enhanced by the northward shift of energetic flows into the PEI region, and magnified by warming of the mixed layer through summer surface heating by the atmosphere.

Does seasonally- and topographically influenced oceanography surrounding the PEI impact seasonal seal foraging effort?

The PEI region is important for marine top predator foraging (Reisinger *et al.*, 2018). Submesoscale filaments, such as those discussed earlier and found to be enhanced in the summer upstream region, have been shown to enhance foraging ecology of diving marine predators throughout the Southern Ocean (Lowther *et al.*, 2014; Whitehead *et al.*, 2016; Siegelman *et al.*, 2019). Furthermore, topographic influences on the flow regime surrounding the islands have previously been shown to enhance downstream primary productivity (Perissinotto *et al.*, 1990), with potential cascading impacts on higher trophic levels. Further analysis of topographic influences was therefore extended to ecological investigations in this study, to align with overarching aims and objectives of the dissertation.

Possible associations between topographic disturbance of flows and seasonal climatologies of the spatial distribution of marine top predator vertical or horizontal foraging behaviours were studied. Based on conclusions from Chapter 2 of this dissertation, mean temperature, stratification, and stability all play a significant, yet complex role in foraging and diving behaviour. Therefore, I predicted that topographic disturbance of flows would drive differences between downstream and upstream foraging behaviours at seasonal scales, with decreases in downstream foraging effort aligning with the observed restratification. Despite significant fine-scale (per dive) effects of upper ocean thermal structure on diving and foraging behaviour, and although strong seasonality was found in both foraging effort and the effects of small-scale topography on PEI oceanography in chapter 3, climatologies of upstream versus downstream foraging effort showed no association with downstream restratification. Specifically, in summer, when the topographic effect of the PEI on stratification and stability was evident, mean downstream seal foraging effort and dive depth showed no corresponding zonal disparity (Figure 3.16). Summer downstream horizontal stirring and vertical mixing therefore had no large-scale effect on fine-scale foraging ecology.

A well-established seasonal signal in female SAFS foraging and diving behaviour at individual foraging trip and dive scales (chapter 2 of this dissertation; Wege, 2017) is suggested to be driven by seasonal changes in pup demands, food availability, and

pregnancy (Wege, 2013, 2016). Although these possibly undeterred, inherent drivers are thought to dominate seasonality in foraging, it remains unclear as to whether seals are seasonally impacted by environmental drivers across all foraging scales. I suggest that investigating patterns of foraging behaviour depends on the scales assessed, replicating suggestions by other studies on marine mammals (Pinaud and Weimerskirch, 2005; Bailleul *et al.*, 2008; Cotté *et al.*, 2011).

Limitations of the study

As most (>90%) subantarctic fur seal dives occur at night, only nocturnal ocean processes were observed and a diurnal study may show different outcomes. Within the first 500 metres of the water column described by the objective analysis product, the MLD was observed for 98.30% and 93.65% of the time in summer and winter, respectively. For the remainder of the time the mixed layer may extend past 500 metres. MLDs were only observed in 23.11% (summer) and 4.78% (winter) of the seal dives and as such, the seals were not diving deep enough to capture the MLD. However, the MLD is sensitive to the criteria used in this study, and using other criteria is likely to lead to different results. Furthermore, the use of salinity in determining the MLD will improve the estimation of the MLD. Comparing the seal-derived MLDs to the objective analysis product is a useful way to validate the use of temperature to determine the MLD, however, a lack of available data in the region to ingest into the objective analysis product may lead to interpolation errors and therefore different conditions than what the seals would experience at any given time.

Observed vertical mixing may be an artefact of variation in device set up, where higher sampling frequencies e.g. 1 sec, that can capture higher resolution profiles resulted in higher stability and stratification downstream in summer (see in Supp.Figure 6). However, after controlling for sampling rate by selecting a single interval class (5 sec) where seals spanned multiple years (2011, 2012, 2013) and seasons (summer and winter), stability trends remained constant (see in Supp.Figure 7), suggesting that sampling rate does not impact vertical mixing shown in my results. I therefore attribute the higher stratification and stability produced by sampling intervals of 1 sec to the coincidence that devices with 1sec are mostly attached to seals that dive downstream in summer months where stratification and stability is higher.

In this study, we expected the upper limit of winter $|b_x|$ to be greater than in summer according to past papers of horizontal buoyancy gradients in the Southern Ocean (e.g. Callies *et al.*, 2015; Lazar, Zhang and Thompson, 2018), however the opposite was the case. This unexpected 'reverse' seasonality of $|b_x|$ is probably due to the seasonal differences in spatial distribution and extent of foraging trips, with seals foraging further away from the islands in winter relative to summer. Winter tracks therefore include areas outside of the PEI region that are not necessarily representative of the flow regime entering the region that is under investigation for topographic responses. Seal orientation with respect to the fronts determines efficacy of seal-derived data to resolve large horizontal buoyancy gradients representative of frontal features. Although little is known about SAFS movements in relation to submesoscale fronts in the PEI region, I assumed that seal-derived $|b_x|$ provide a statistical representation of the submesoscale landscape due to the sufficiently large sample size of observation. It is plausible to consider that an under-estimation of true $|b_x|$ from the seal profiles is consistent with that of glider-derived $|b_x|$, i.e. ~64% (du Plessis *et al.*, 2019), as in both measurement techniques, the horizontal buoyancy gradients were calculated using along-track distances with varying distances. Another important consideration when using seal-derived profile data to estimate horizontal gradients around the PEI is that profiles are generally further apart downstream than upstream, which may reduce the strength of downstream $|b_x|$ in a region where small-scale fronts are ubiquitous (Figure 3.10). Swart *et al.* (2020) show an exponential increase in horizontal buoyancy gradients when the sampling resolution increases from 10 to 1 km. As the seals provide a resolution of surface locations separated by 5 km, the data shown here may have been more representative of submesoscale to mesoscale instabilities instead of purely submesoscale instabilities alone. However, a case study of $|b_x|$ in relation to submesoscale transport structures (represented by FSLE) showed that despite the potential for induced errors, horizontal buoyancy gradients do well in representing submesoscale instabilities. Nevertheless, horizontal buoyancy gradients need to be filtered in future studies according to those that are calculated using distances less than 5 km (to account for uncertainty in location estimates) for greater confidence in submesoscale (1-10 km) estimates. This was not done in this study due to time constraints and will be considered for future work.

Conclusions

In this study, I provide the first high resolution *in situ* measurements from shallow diving animals for seasonal upstream versus downstream comparisons of (sub-)mesoscale processes within the ACC of the Southern Ocean and impacts on region-wide (>500 km) subantarctic fur seal foraging. This study provides evidence for topographic stirring and dissipation of mesoscale (10-100 km, days to weeks) flows upstream of PEI, which I propose ultimately enhance downstream restratification, with larger effects observed in summer months when the MLD is shallow. Additionally, and contrary to what was expected, these topographic influences on ocean flows and variability show no link, whether direct or indirect, to SAFS fine-scale foraging behaviour upstream and downstream of the island.

These results provide valuable insight into topographically driven three-dimensional mixing and impacts on SAFS foraging behaviour at the PEI. Despite past investigations into the surrounding PEI physical and biological oceanography, to my knowledge, this study pioneers the investigation of the topographic effect of the PEI on multiple scales of ocean flows and mixing. Seal-derived data were generally within the submesoscale range $O(1-100\text{km})$, meaning the feasibility of seal data to resolve submesoscale flows was adequate (e.g. Siegelman *et al.*, 2019; Biddle and Swart, 2020). Additionally, this is the first study to investigate the seasonal impacts of local topographically forced ocean variability on seasonal upstream and downstream means of SAFS diving and foraging effort.

Submesoscale activity is a key component of the Earth's climate because it is responsible for vertical heat fluxes between the air-sea boundary and ocean pycnocline with far reaching consequences for ocean ventilation (Su *et al.*, 2018). The zonal disparity in submesoscale activity, found in this study to ultimately be a result of topographic disturbance, may have large impacts on the transport of heat through the mixed layer and should be considered in climate model analysis. This is vital considering firstly the contrasting findings related to submesoscales and topographic disturbance, and secondly that a recent study has found that submesoscale fronts largely transport heat from water below the surface mixed layer upward to the ocean surface, with the potential to alter oceanic heat uptake, especially in the eddy-rich ACC (Siegelman *et al.*, 2020).

Chapter 4: General conclusion



A subantarctic fur seal pup swims in a shallow rockpool.

Synthesis

In summary, telemetry was successfully used at Marion Island to investigate the influence of small-scale topography on ocean variability and vertical mixing and further to formulate an improved understanding of SAFS foraging and diving behaviour in relation to environmental structure and variability in the Southern Ocean.

Foraging and dive strategies

Habitat use of individual central place foragers differs according to the spatial scales considered (Pinaud and Weimerskirch, 2005). In this study, I identified patterns of habitat use across multiple scales of foraging behaviour at Marion Island. I found scale-dependent adjustments of foraging behaviour in relation to upper ocean thermal structure. At the dive scale, the data collected by lactating SAFS revealed significant links between upper ocean thermal structure and fine-scale vertical foraging effort, meaning seals spent more time in mixed, warmer (>7 °C) water columns. This appeared to manifest through to diel and seasonal trends in foraging. Despite upstream versus downstream seasonal differences in upper ocean thermal structure, which was found to be driven by small-scale topographic effects on (sub-)mesoscale ocean variability, and contrary to predictions, no

corresponding differences in seasonally driven horizontal or vertical (diving) foraging behaviours were found. This suggested that there is no link between seal foraging and diving behaviour and submesoscale variability up- and downstream of the island. Again, showing that bottom-up processes are not always the main driver of foraging decisions as previously suggested by Wege et al. (2019)

For a more comprehensive investigation into the response of seal foraging to upper ocean thermal structure, further studies need to be developed to not only fill the gaps in scale (Pirodda *et al.*, 2014) e.g., investigate the direct influence of submesoscales on SAFS foraging, but also to compare influences across all possible scales to investigate possible hierarchical responses (Fauchald, Erikstad and Skarsfjord, 2000; Fritz, Said and Weimerskirch, 2003). This is vital for understanding seal movements and how the present climate change crisis may affect future SAFS population trends.

What can animal-borne data loggers inform about the Prince Edward Islands surrounding physical oceanographic landscape?

The small-scale (1-10 km, hours to days) oceanography surrounding the Prince Edward Islands (PEI), an immensely important biological hotspot (Pakhomov and Chown, 2003), is poorly understood. Observational gaps across multiple spatial and temporal scales are prevalent because of the inaccessibility and large costs involved in sampling such a region. This study attempted to fill the knowledge gaps, with specific reference to submesoscale oceanographic variable structure and vertical mixing. This study used a combination of satellite and *in situ* observations in the Antarctic Circumpolar Current (ACC) to investigate seasonal physical oceanographic trends and diagnose and describe the topographic stirring effects of small islands on ocean flows and variability.

To conclude, seasonal climatologies revealed strong seasonality in upstream and downstream flows across multiple scales of flow (meso- to submesoscales) and vertical mixing within the PEI region. The disparity in seasonality in ocean variability of the PEI region in comparison to the surrounding waters is due to the spatial variation in relative dominance of driving forces, such as the seasonality of mixed layer depths (MLDs) and ACC fronts, demonstrating the dynamical nature of the area in terms of flow variability and the influence on island dynamics.

However, deep mixed layers and strong mesoscale and submesoscale horizontal mixing upstream of the islands is consistent throughout the year. As mesoscale eddies, associated with strong submesoscale flows, enter the PEI region in summer, a mesoscale strain exponentially increases buoyancy gradients until they reach the islands, after which downstream restratification takes place through atmospheric surface heating and warming of the mixed layer. This results in a shallow summer downstream mixed layer depth, setting up the potential energy for deep winter mixing.

Importance and future work

Oceanography and climate models

Although providing valuable high resolution upstream and downstream comparisons, seal-derived profiles were restricted in the maximum depth reached by the animal, and stratification definitions rely on a sufficient vertical range being sampled (at least to maximum MLDs previously observed for the given region). Summer stratification comparisons were assumed reliable as seals dive to similar depths downstream and upstream of the island in summer. However, seals dive considerably deeper upstream than downstream in winter. Therefore, assimilating winter observations using deeper (>200 m) profiles, such as those collected by Argo floats, are required in future studies to assess the winter influence of the PEI on restratifying downstream mixed layers, considering seal-derived profiles may not be sufficiently deep (<200 m) to observe any influences on winter mixing, where winter mixed layers can reach ~200 m (Mensa *et al.*, 2013).

Intensity of Eddy Kinetic Energy (EKE) has increased in the past decade by increases in wind stress over the Southern Ocean, with implications for overturning circulation, carbon cycling, and climate (Hogg *et al.*, 2014; Rosso *et al.*, 2015). Considering that EKE is linked to submesoscale variability, which connects the atmosphere and ocean interior (Su *et al.*, 2018), the effect of small-scale topography on EKE needs to be parameterised in future climate models. This study helps to link patterns of EKE to topographic stirring, thus contributing to the efforts in improving parameterizations.

Ubiquitous submesoscale instabilities, shown in Chapter 3 to be seasonally and topographically enhanced in the PEI region, influence mixed layer dynamics, which moderates ocean-atmosphere exchanges in the Southern Ocean, the largest natural sink

for anthropogenic heat and carbon. These findings may help improve climate model parameterizations and the quality of projections provided by ocean climate models (Treasure *et al.*, 2017) that may not have resolved such underlying influences (Griffies *et al.*, 2009).

The seasonal contrast in mixed layer depths, found using seal-derived data in this study, has given an indication of summer restratification. However, future studies should use the data retrieved by SAFS at Marion Island to investigate the timing and potential drivers of this restratification process. Improving our understanding of this process over local and fine scales could lead to improved parameterization of climate models.

Climate change, conservation and management

Climate change can drive changes in the physical ocean, with potential negative impacts on prey distributions and thus fur seal foraging behaviour (Hofmeyr 2015; Kovacs *et al.*, 2012; Learmonth *et al.*, 2006; McDonald *et al.*, 2012). The PEI are extremely sensitive to climatological environmental perturbations, such as climatological increases in sea surface temperature (Ansorge *et al.*, 2014), making them an ideal study area for understanding and monitoring the potential impacts of climate change (Constable *et al.*, 2014). In this study, it is suggested that the PEI region is a transition zone between alpha and beta oceans. The shift in temperature contributions to density changes here may be most sensitive to changes in climate relative to polar or tropical regions, with important implications for future predictions of Southern Ocean climate (Timmermans & Jayne 2016).

Since the 1970's, although regionally dependent, mixed layers have been deepening by 5 to 10 metres per decade and the strength of the vertical density contrast across the base of the mixed layer has increased by ~9 % per decade (10^{-6} - 10^{-5} per second² per decade) (Sallee *et al.*, 2021). SAFS vertical foraging movements don't appear to align closely with the MLD, found in this study, therefore I propose that these decadal changes may not impact the foraging efforts of seals at Marion Island. However, the MLD is not resolved in this study if seals dive just above it. The sensor information is limited to the immediate surroundings experienced by individual seals, and the spatial variation of measurements depends entirely on that of the seal's movements. To improve identification of environmental thresholds or gradients that dictate the limits of SAFS

foraging movements, one must place its behaviour in a broader context (Lowther *et al.*, 2015). Therefore, future studies are required to assimilate alternative sources of high resolution *in situ* environmental data, such as that collected by Argo floats or other diving animals in the vicinity of the SAFS being studied, that can be used to resolve the MLD independent of seal diving depth, as the vertical foraging efforts may align more with the MLD than suggested in this study.

Although there is strong variability associated with the meridional positioning of the ACC fronts over small (days to weeks) time scales (Hunt *et al.*, 2001), an *in situ* climatological rise in sea surface temperatures in the Southern Ocean (Gille, 2002), and specifically at the PEIs (Melice *et al.*, 2003), of >1 °C since the 1950s and the expected southward shift of the ACC fronts of between 50 km and 70 km (Ansorge *et al.*, 2014; Turner 2014), along with the possibility of enhanced EKE within the PEI region (Lamont *et al.*, 2019; Meredith & Hogg, 2006; Fyfe & Saenko 2006; Hogg 2015), and increased downstream variability via increased current speeds (Lamont *et al.*, 2019), is predicted to have negative consequences for higher trophic levels (Hunt *et al.*, 2001). These changes are all predicted to be modulated by climate model predictions of an underlying long-term increase in zonal wind stress driving the ACC (Fyfe & Saenko, 2005,2006; Hogg 2016). Some studies have already described the direct consequences of these shifting fronts on marine predator foraging behaviour and demography within the Southern Ocean (Bost 2015; Massardier-Galata 2017). This is especially important considering that marine top predators are in decline (Taylor *et al.*, 2011). Therefore, it is vital to better understand marine predator foraging ecology for improved management and policy (Taylor *et al.*, 2011). This paper provides insight into the fine-scale foraging ecology of SAFS at Marion Island and sets the base for discussions on the potential impact of climate-related change on SAFS foraging behaviours.

The foraging range of diving marine species of the Southern Ocean, such as central-place foraging King penguins (Peron *et al.*, 2012), have been predicted to shift poleward with warming temperatures projected by climate models of the International Panel on Climate Change. Although the future of downstream ocean variability may be susceptible to climate change, diving and foraging behaviour of female SAFS was found in this study not to be linked to topographically forced mixing and variability upstream and downstream of the islands. Instead, they show opportunistic foraging behaviour by increasing foraging

effort according to the thermal structure of the immediate surroundings. I therefore predict that climate change, through these channels, may not have a dramatic effect on the future foraging effort required by SAFS at Marion to sustain their pups and themselves, unless other indirect consequences of climate change occur.

As winds supply energy for vertical mixing (Wunsch, 2016), changing wind patterns that drive the ACC as a result of climate change (Hogg, 2015) may have consequences for the PEI summer downstream restratification, however, as shown in chapter 3 of this thesis, this would not impact downstream fine-scale foraging behaviour of SAFS. These winds can, however, act to generate or destroy baroclinic instabilities that are associated with submesoscale filaments (du Plessis *et al.*, 2019), which have been shown to drive foraging of marine animals (Lowther *et al.*, 2014; Siegelman *et al.*, 2019; Whitehead *et al.*, 2016). With potential consequences for breeding success and population trends, future studies should shift focus to the direct relationship between fine-scale foraging behaviour of SAFS and submesoscale filaments of the Southern Ocean.

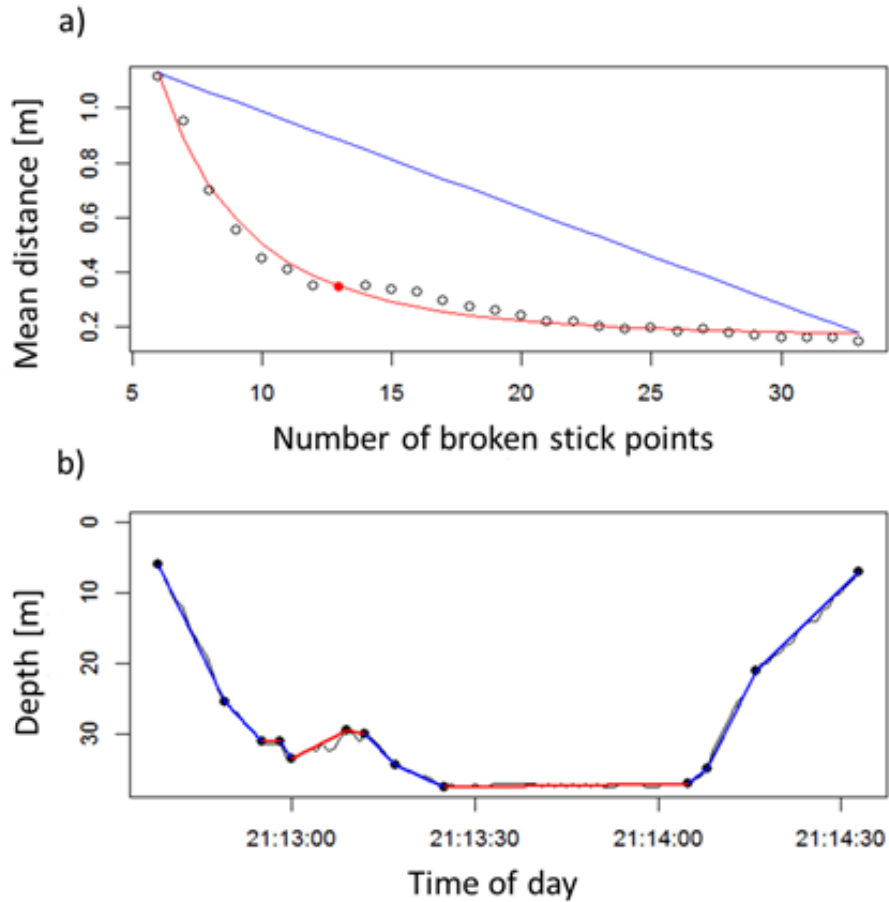
This study contributes to the efforts of the special Marine Protected Area of the Prince Edward Islands and the ongoing global initiatives towards protecting our deep oceans. This special Marine Protected Area is part of a comprehensive conservation management regime for the marine ecosystem of the islands and their oceanic surrounds (Lombard *et al.*, 2017). SAFS tend to remain within the Exclusive Economic Zone of the PEI and mostly feed within the extent of the Marine Protected Area, making them and their prey relatively well protected (Kirkman *et al.*, 2016). However, increased understanding of SAFS foraging ecology is required for dynamic management efforts suitable for shifting habitats (Arthur *et al.*, 2017; Kirkman *et al.*, 2016). This is critical to inform future conservation management incorporating the potential effects of short (i.e. El Niño Southern Oscillation and Southern Annular Mode) and long-term oceanographic changes (i.e. climate change) on the foraging success of this species.

Lastly, this study contributes to the sustainable development goals of the United Nations General Assembly. In particular, it contributes to one of the major targets of the 14th goal by increasing scientific knowledge of life below water.

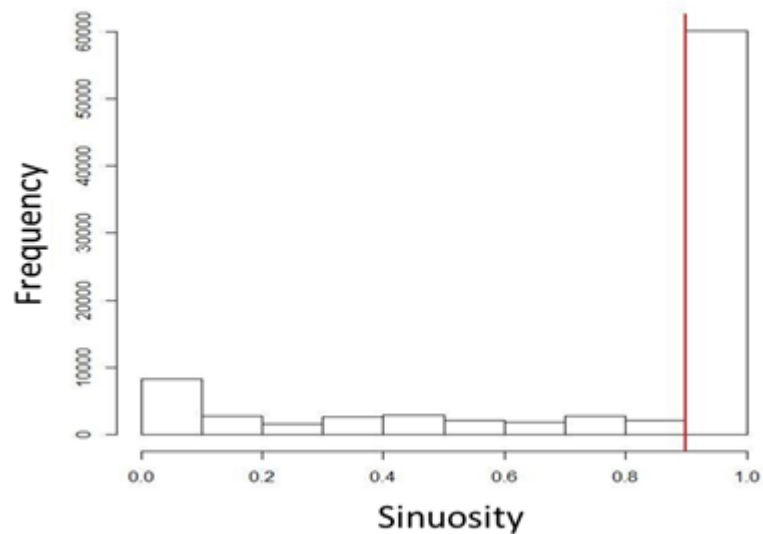
Supplementary Material

Supp. Table 1: Deployments on Subantarctic fur seals at Marion Island from 2009-2015. Deployments were 89 days long on average (min = 22 days, max = 276 days). 'ID' is the unique number given to each seal in the study. Seal 5 was deployed on twice. Major seal colonies on Marion Island have an associated site code (MM067=Van den Boogaard, MM042=Mixed Pickle). In summer, individual seals either travelled west (upstream) or east (downstream) ('WE') of Marion Island. N/A values indicate foraging trips that cover both upstream and downstream regions. Sampling rates for depth (Dive interval) and external temperature (Ext Temp) are given in units of seconds.

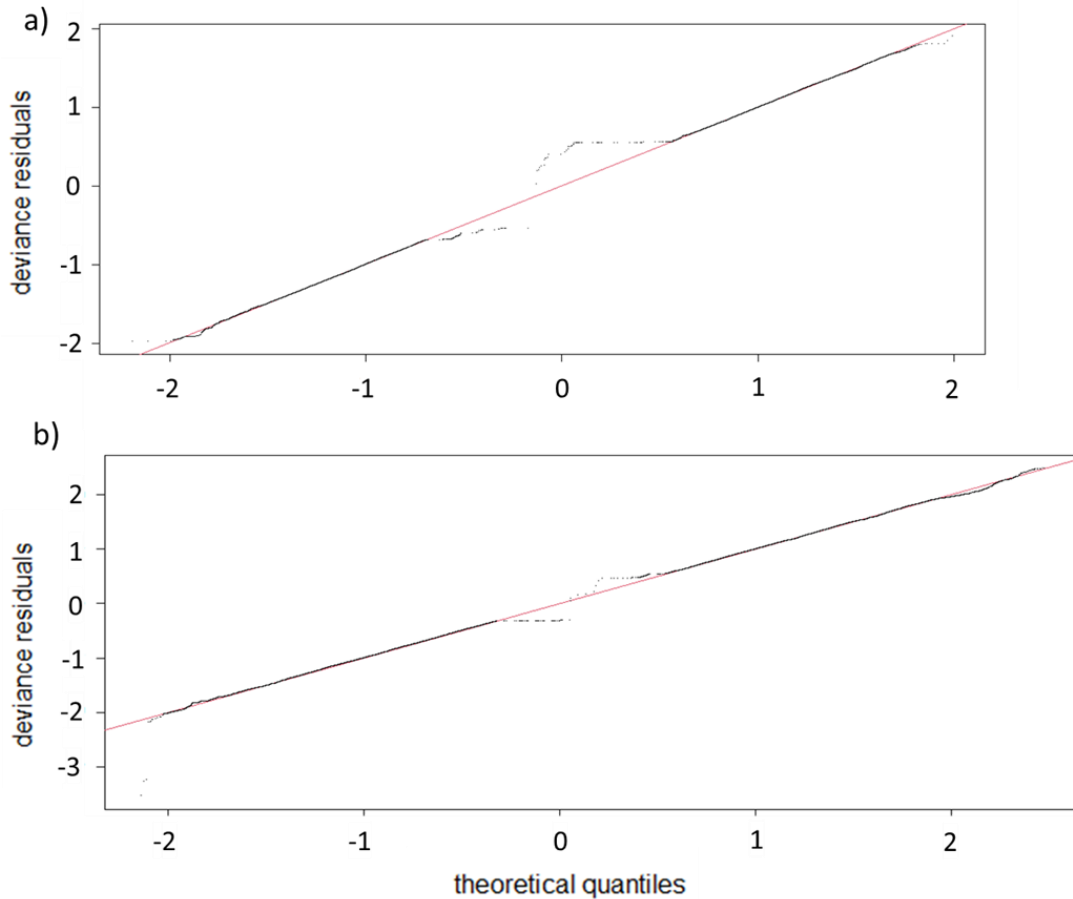
ID	Year	season	Site	WE	Animal Tag	DeviceID	TDR/Splash tag	Ass. device ID	Dive inter. [sec]	Ext. Temp. [sec]	Depl. date	Retr. date	Depl. length
1	2009	Winter	MM067	N/A	GW522	0890438	TDR+PTT	907591	1	1	39927	39955	28
2	2009	Winter	MM067	N/A	GW495	0890425	TDR+PTT	90760	1	1	39927	39974	47
4	2009	Winter	MM067	N/A	FB515	0890439	TDR+PTT	90762	1	1	39931	39974	43
5	2009	Winter	MM067	N/A	FB513	0890440	TDR+PTT	907631	1	1	39931	39959	28
5	2009	Winter	MM067	N/A	FB513	0990062	TDR+PTT	907631	1	1	39959	40085	126
13	2011	Summer	MM067	East	A142	0990474	TDR+PTT	97803	1	1	40546	40621	75
14	2011	Summer	MM067	East	GW503	0990471	TDR+PTT	97804	1	1	40545	40616	71
15	2011	Summer	MM067	East	A188	0990473	TDR+PTT	978051	1	1	40545	40621	76
16	2011	Summer	MM067	East	LB504	0900476	TDR+PTT	978061	1	1	40546	40611	65
17	2011	Winter	MM067	N/A	A160	0990468	TDR+PTT	65641	1	5	40668	40745	77
18	2011	Winter	MM067	N/A	LB491	0990440	TDR+PTT	935321	1	5	40662	40786	124
19	2011	Winter	MM067	N/A	OO440	0990470	TDR+PTT	978082	1	5	40662	40797	135
20	2012	Summer	MM067	East	LB504	0990428	TDR+PTT	935301	1	5	40901	40985	84
21	2012	Summer	MM067	East	GW503	0990469	TDR+PTT	93531	1	5	40904	40994	90
22	2012	Summer	MM067	East	LB563	0990464	TDR+PTT	907633	1	5	40909	40977	68
23	2012	Summer	MM067	East	A200	0990435	TDR+PTT	978072	1	5	40901	40977	76
24	2012	Winter	MM067	N/A	A146	44744	SPLASH	447441	1	5	41058	41117	59
25	2012	Winter	MM067	N/A	A396 (LB508)	0990476	TDR+PTT	978052	1	1	41034	41147	113
31	2013	Winter	MM067	N/A	A602	0990464	TDR+PTT	907634	1	2	41409	41639	230
47	2011	Winter	MM042	N/A	A303	10L0204	SPLASH	386121	1	5	40675	40817	142
49	2011	Winter	MM042	N/A	A302	10L0209	SPLASH	386151	1	5	40675	40740	65
50	2011	Winter	MM042	N/A	A310	10L0210	SPLASH	386161	1	5	40676	40801	125
51	2011	Winter	MM042	N/A	A306	10L0221	SPLASH	386171	1	5	40675	40749	74
52	2012	Summer	MM042	West	A330	11L0011	SPLASH	397401	1	5	41271	41346	75
53	2012	Summer	MM042	West	A333	11L0012	SPLASH	397551	1	5	41271	41341	70
57	2012	Summer	MM042	West	A331	11L0010	SPLASH	397371	1	5	41271	41314	43
58	2012	Summer	MM042	West	A442	11L0010	SPLASH	397372	1	5	40954	40976	22
62	2012	Winter	MM042	N/A	A321	11L0081	SPLASH	1173711	1	5	41020	41296	276
63	2013	Summer	MM042	West	A484	11L0079	SPLASH	1173691	1	5	41263	41342	79
64	2013	Summer	MM042	West	A482	10L0057	SPLASH	447302	1	5	41262	41341	79
65	2013	Summer	MM042	West	A481	10L0074	SPLASH	447462	1	5	41262	41346	84
66	2013	Summer	MM042	West	A483	11L0074	SPLASH	1173651	1	5	41263	41298	35
67	2013	Summer	MM042	West	A205	11L0074	SPLASH	1173652	1	5	41302	41342	40
68	2013	Winter	MM042	N/A	A125	10L0209	SPLASH	386152	1	5	41389	41521	132
69	2013	Winter	MM042	N/A	A446	10L0210	SPLASH	386162	1	5	41389	41507	118
70	2013	Winter	MM042	N/A	A482	10L0221	SPLASH	386172	1	5	41389	41476	87
109	2014	Winter	MM067	N/A	A605	11L0074	SPLASH	1173653	1	1	41804	41919	115
110	2015	Summer	MM067	East	A874 (A134)	10L0079	SPLASH	447673	1	1	42035	42068	33
112	2015	Summer	MM067	East	A611	11L0081	SPLASH	1173712	1	1	42006	42069	63
113	2014	Summer	MM042	West	A311	11L0012	SPLASH	397552	1	10	41629	41703	74



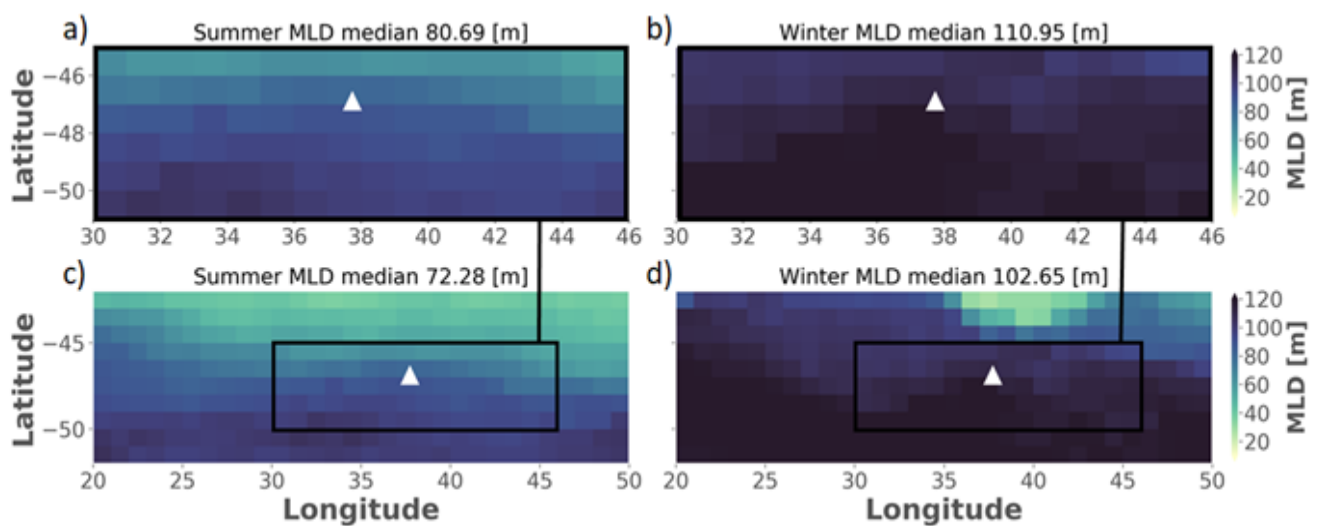
Supp. Figure 1: Broken stick model example dive by a seal at night. a) Gompertz model curve (red line) for the determination of the inflection point (red dot), describing the optimal number of broken stick points to adequately describe segments of 'wiggleness' (Heerah et al., 2014). b) Original (black line) and reconstructed dive profiles with red ('hunting') and blue ('transit') segments.



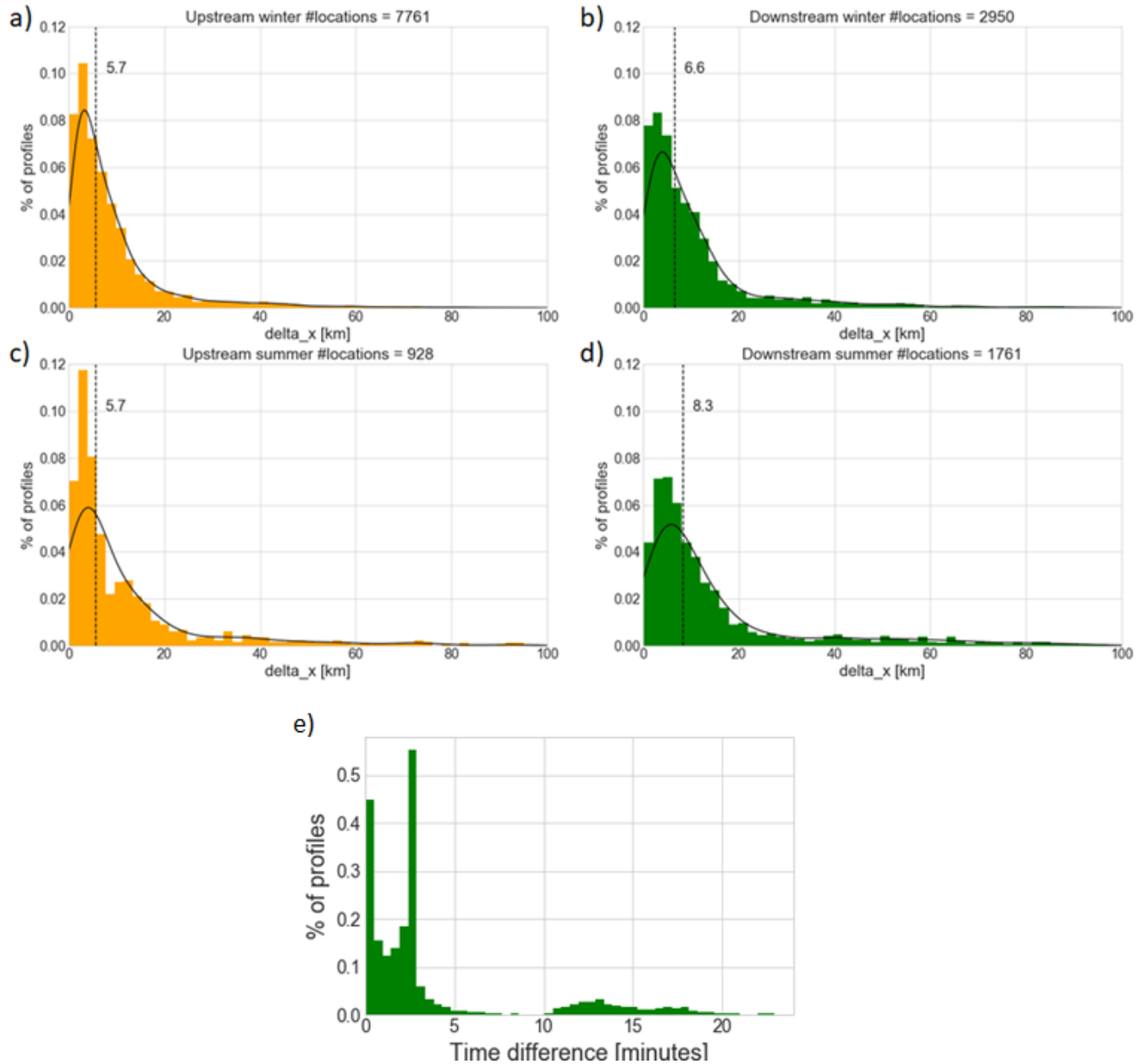
Supp. Figure 2: Determining the sinuosity threshold (0.9) for the broken stick model.



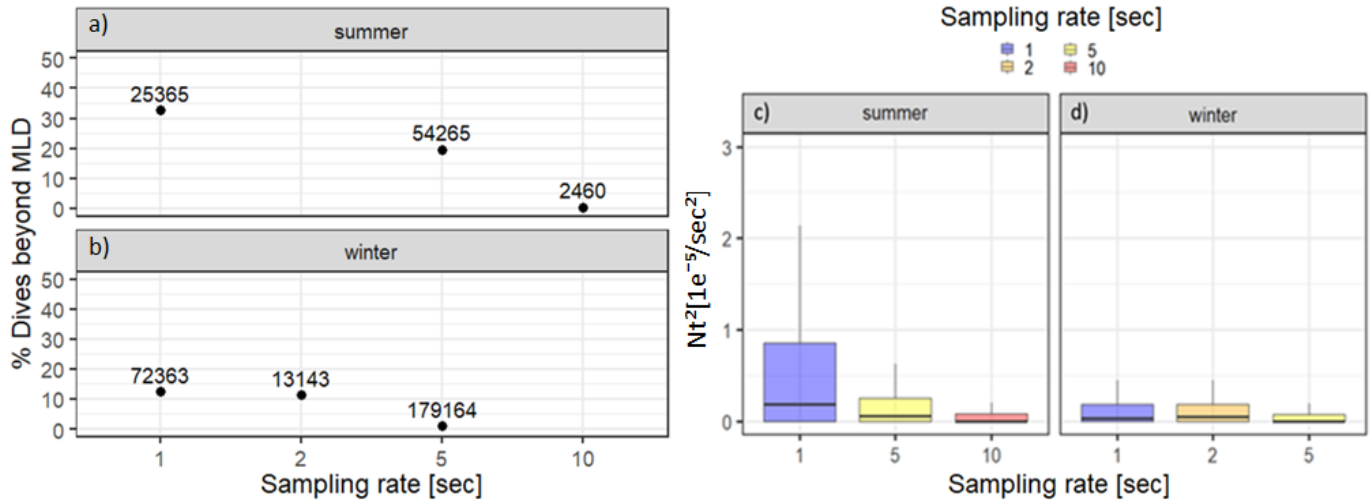
Supp. Figure 3: Quantile-quantile plots of deviance residuals against theoretical quantiles for a) summer and b) winter generalised additive mixed-effects models (GAMMs). Both models show a straight-line trend.



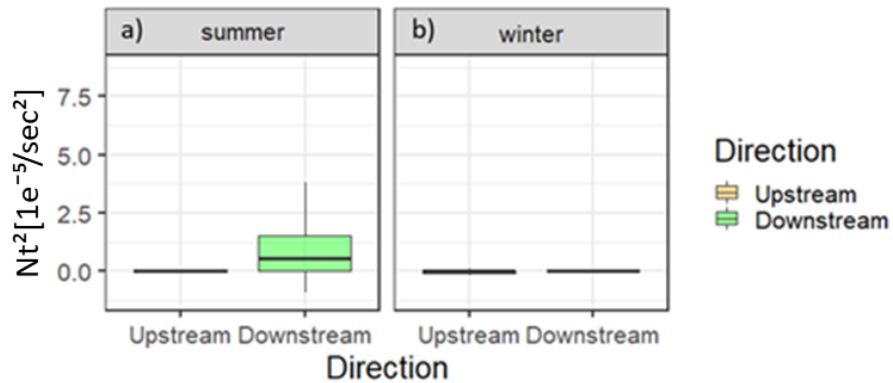
Supp. Figure 4: Climatology of mixed layer depths (MLD) for summer (a,c) and winter (b,d) observations within the first 500 metres of the upper water column derived from objective analysis data. Means are presented for the spatial extent of seal foraging trips in summer (a,b) and winter (c,d), where foraging trips are further from the island in winter than summer.



Supp. Figure 5: Histograms showing distributions of distances (Δx) [km] between mean temperature profiles per foraging trip in winter (a,b) and summer (c,d) downstream (green) and upstream (orange) of Marion Island for the calculation of horizontal buoyancy fluxes. The estimated time difference between profiles is shown in e). The dashed lines represent the 50th percentile of the data.



Supp. Figure 6: The percentage of dives beyond the mixed layer in summer (a) and winter (b) grouped by sampling rate [sec]. The number of dives extending below the mixed layer are annotated beside each point on the graph (a,b). Vertical stability (Nt^2) [$10^{-5}/\text{sec}^2$] was calculated from records deployed at various sampling rates for summer (c) and winter (d). Note that summer devices were set at 1, 5 and 10 seconds, while winter devices were set at 1, 2 and 5 seconds.



Supp. Figure 7: Vertical stability (Nt^2) ($10^{-4}/\text{s}^2$) downstream vs upstream of Marion Island calculated from 2012 summer and winter devices that were set up to sample temperature at 5 sec intervals only. The number of summer dives to the upstream.

REFERENCES

- Allanson, B. R., Boden, B., Parker, L. and Rae, C. D. (1985) 'A contribution to the oceanology of the Prince Edward Islands.', *Antarctic nutrient cycles and food webs*, pp. 38–45. doi: 10.1007/978-3-642-82275-9_6.
- Ansorge, I. J., Durgadoo, J. V and Treasure, A. M. (2014) 'Sentinels to climate change. The need for monitoring at South Africa's Subantarctic laboratory', *South African Journal of Science*, 110(1/2), pp. 1–4. doi: 10.1590/sajs.2014/a0044.
- Ansorge, I. J., Froneman, P. W., Pakhomov, E. A., Lutjeharms, J. R. E., Perissinotto, R. and van Ballegooyen, R. C. (1999) 'Physical-biological coupling in the waters surrounding the Prince Edward Islands (Southern Ocean)', *Polar Biology*, 21(3), pp. 135–145. doi: 10.1007/s003000050344.
- Ansorge, I. J. and Lutjeharms, J. R. E. (2000) 'Twenty-five years of physical oceanographic research at the Prince Edward Islands', *South African Journal of Science*, p. 557.
- Ansorge, I. J. and Lutjeharms, J. R. E. (2002) 'The hydrography and dynamics of the ocean environment of the Prince Edward Islands (Southern Ocean)', in *Journal of Marine Systems*, pp. 107–127. doi: 10.1016/S0924-7963(02)00198-7.
- Ansorge, I. J. and Lutjeharms, J. R. E. (2003) 'Eddies originating at the South-West Indian Ridge', *Journal of Marine Systems*, 39(1–2), pp. 1–18. doi: 10.1016/S0924-7963(02)00243-9.
- Ansorge, I. J. and Lutjeharms, J. R. E. (2005) 'Direct observations of eddy turbulence at a ridge in the Southern Ocean', *Geophysical Research Letters*, 32(14), pp. 1–4. doi: 10.1029/2005GL022588.
- Ansorge, I. and Lutjeharms, J. (2007) 'The influence of the Antarctic Circumpolar Current on the oceanographic setting of a sub-Antarctic island', *Papers and Proceedings of the Royal Society of Tasmania*, 141(1), pp. 59–66. doi: 10.26749/rstpp.141.1.59.
- Arce, F., Bestley, S., Hindell, M. A., McMahon, C. R. and Wotherspoon, S. (2019) 'A quantitative, hierarchical approach for detecting drift dives and tracking buoyancy changes in southern elephant seals', *Scientific Reports*, 9(1), pp. 1–13. doi: 10.1038/s41598-019-44970-1.
- Arnould, J. P. Y., Boyd, I. L. and Speakman, J. R. (1996) 'The relationship between foraging behaviour and energy expenditure in Antarctic fur seals', *Journal of Zoology*, 239(4), pp. 769–782. doi: 10.1111/j.1469-7998.1996.tb05477.x.
- Arora, P., Deepali and Varshney, S. (2016) 'Analysis of K-Means and K-Medoids Algorithm for Big Data', *Physics Procedia*, 78(December 2015), pp. 507–512. doi: 10.1016/j.procs.2016.02.095.
- Arthur, B., Hindell, M., Bester, M., De Bruyn, P. J. N., Trathan, P., Goebel, M. and Lea, M.-A. (2017) 'Winter habitat predictions of a key Southern Ocean predator, the Antarctic fur seal (*Arctocephalus gazella*)', *Deep Sea Research Part II: Topical Studies in Oceanography*, 140, pp. 171–181. doi: 10.1016/j.dsr2.2016.10.009.

- Arthur, B., Hindell, M., Bester, M. N., Oosthuizen, W. C., Wege, M. and Lea, M. (2016) 'South for the winter? Within-dive foraging effort reveals the trade-offs between divergent foraging strategies in a free-ranging predator', pp. 1623–1637. doi: 10.1111/1365-2435.12636.
- Asdar, S. (2018) 'Climate Change Impact on Ecosystems of Prince Edward Islands: Role of Oceanic Mesoscale Processes', *PhD Thesis*, University of Cape Town (June 2018).
- Augustin, N. H., Sauleau, E. A. and Wood, S. N. (2012) 'On quantile quantile plots for generalized linear models', *Computational Statistics and Data Analysis*, 56(8), pp. 2404–2409. doi: 10.1016/j.csda.2012.01.026.
- Bailleul, F., Cotté, C. and Guinet, C. (2010) 'Mesoscale eddies as foraging area of a deep-diving predator, the southern elephant seal', *Marine Ecology Progress Series*, 408, pp. 251–264. doi: 10.3354/meps08560.
- Bailleul, F., Pinaud, D., Hindell, M., Charrassin, J. and Guinet, C. (2008) 'Assessment of scale-dependent foraging behaviour in southern elephant seals incorporating the vertical dimension: a development of the First Passage Time method', *Journal of Animal Ecology*, 77(5), pp. 948–957. doi: 10.1111/j.1365-2656.2008.01407.x.
- Bakun, A. (2007) 'Frentes y remolinos como estructuras clave en el habitat de las larvas de peces marinos: oportunidad, respuesta adaptativa y ventaja competitiva', *Scientia Marina*, 70(S2), pp. 105–122. Available at: <http://scientiamarina.revistas.csic.es/index.php/scientiamarina/article/view/171>.
- Barraquand, F. and Benhamou, S. (2008) 'Animal movements in heterogeneous landscapes: Identifying profitable places and homogeneous movement bouts', *Ecology*, 89(12), pp. 3336–3348. doi: 10.1890/08-0162.1.
- Bates, D., Mächler, M., Bolker, B. M. and Walker, S. C. (2015) 'Fitting linear mixed-effects models using lme4', *Journal of Statistical Software*, 67(1). doi: 10.18637/jss.v067.i01.
- Beauplet, G., Dubroca, L., Guinet, C., Cherel, Y., Dabin, W., Gagne, C. and Hindell, M. (2004) 'Foraging ecology of subantarctic fur seals *Arctocephalus tropicalis* breeding on Amsterdam Island: seasonal changes in relation to maternal characteristics and pup growth', 273, pp. 211–225.
- Benoit-Bird, K. J., Battaile, B. C., Nordstrom, C. A. and Trites, A. W. (2013) 'Foraging behavior of northern fur seals closely matches the hierarchical patch scales of prey', *Marine Ecology Progress Series*. 479(April), pp. 283–302. doi: 10.3354/meps10209.
- Benoit-Bird, K. J., Moline, M. A. and Southall, B. L. (2017) 'Prey in oceanic sound scattering layers organize to get a little help from their friends', *Limnology and Oceanography*, 62(6), pp. 2788–2798. doi: 10.1002/lno.10606.
- Bester, M.N. (1981) 'Seasonal changes in the population composition of the fur seal *Arctocephalus tropicalis* at Gough Island', *South African Journal of Wildlife Research-24-month delayed open access*, 11(2), pp.49-55.

- Bester, M. N. (1995) 'Reproduction in the Female Subantarctic Fur Seal, *Arctocephalus Tropicalis*', *Marine Mammal Science*, 11(3), pp. 362–375. doi: 10.1111/j.1748-7692.1995.tb00291.x.
- Bester, M. N., de Bruyn, P. J. N., Oosthuizen, W. C., Tosh, C. A., McIntyre, T., Reisinger, R. R., Postma, M., van der Merwe, D. S. and Wege, M. (2011) 'The Marine Mammal Programme at the Prince Edward Islands: 38 years of research', *African Journal of Marine Science*, 33(3), pp. 511–521. doi: 10.2989/1814232X.2011.637356.
- Bestley, S. *et al.* (2020) 'Marine Ecosystem Assessment for the Southern Ocean: Birds and Marine Mammals in a Changing Climate', *Frontiers in Ecology and Evolution*, 8(November). doi: 10.3389/fevo.2020.566936.
- Bestley, S., Jonsen, I. D., Hindell, M. A., Harcourt, R. G. and Gales, N. J. (2015) 'Taking animal tracking to new depths: Synthesizing horizontal - vertical movement relationships for four marine predators', *Ecology*, 96(2), pp. 417–427. doi: 10.1890/14-0469.1.
- Biddle, L. C. and Swart, S. (2020) 'The Observed Seasonal Cycle of Submesoscale Processes in the Antarctic Marginal Ice Zone', *Journal of Geophysical Research: Oceans*, 125(6). doi: 10.1029/2019JC015587.
- Billany, W., Swart, S., Hermes, J. and Reason, C. J. C. (2010) 'Variability of the Southern Ocean fronts at the Greenwich Meridian', *Journal of Marine Systems*, 82(4), pp. 304–310. doi: 10.1016/j.jmarsys.2010.06.005.
- Biuw, M. *et al.* (2007) 'Variations in behavior and condition of a Southern Ocean top predator in relation to in situ oceanographic conditions', 104(34), pp. 13705–13710.
- Blanchet, M. A., Lydersen, C., Ims, R. A. and Kovacs, K. M. (2015) 'Seasonal, oceanographic and atmospheric drivers of diving behaviour in a temperate seal species living in the high arctic', *PLoS ONE*, 10(7), pp. 1–28. doi: 10.1371/journal.pone.0132686.
- Boccaletti, G., Ferrari, R. and Fox-Kemper, B. (2007) 'Mixed layer instabilities and restratification', *Journal of Physical Oceanography*, 37(9), pp. 2228–2250. doi: 10.1175/JPO3101.1.
- Boden, B. P. (1988) 'Observations of the island mass effect in the Prince Edward archipelago', *Polar Biology*, 9(1), pp. 61–68. doi: 10.1007/BF00441765.
- Bost, C. A., Cotté, C., Bailleul, F., Cherel, Y., Charrassin, J. B., Guinet, C., Ainley, D. G. and Weimerskirch, H. (2009) 'The importance of oceanographic fronts to marine birds and mammals of the southern oceans', *Journal of Marine Systems*, 78(3), pp. 363–376. doi: 10.1016/j.jmarsys.2008.11.022.
- Bost, C. A., Cotté, C., Terray, P., Barbraud, C., Bon, C., Delord, K., Gimenez, O., Handrich, Y., Naito, Y., Guinet, C. and Weimerskirch, H. (2015) 'Large-scale climatic anomalies affect marine predator foraging behaviour and demography', *Nature Communications*, 6. doi: 10.1038/ncomms9220.
- Bost, C., Zorn, T., Le Maho, Y. and Duhamel, G. (2002) 'Feeding of diving predators and diel vertical migration of prey: King penguin diet versus trawl sampling at Kerguelen Islands', *Marine Ecology*

- Progress Series*, 227, pp. 51–61. doi: 10.3354/meps227051.
- Boyd, I. L. and Arnborn, T. (1991) 'Diving behaviour in relation to water temperature in the southern elephant seal: foraging implications', *Polar Biology*, 11(4), pp. 259–266. doi: 10.1007/BF00238460.
- Boyd, I. L., Bowen, W. D. and Iverson, S. J. (2010) *Marine mammal ecology and conservation : a handbook of techniques*
- de Boyer Montégut, C., Madec, G., Fischer, A. S., Lazar, A. and Iudicone, D. (2004) 'Mixed layer depth over the global ocean: An examination of profile data and a profile-based climatology', *Journal of Geophysical Research C: Oceans*, 109(12), pp. 1–20. doi: 10.1029/2004JC002378.
- Brannigan, L., Marshall, D. P., Garabato, A. C. N., Nurser, A. J. G. and Kaiser, J. (2017) 'Submesoscale instabilities in mesoscale eddies', *Journal of Physical Oceanography*, 47(12), pp. 3061–3085. doi: 10.1175/JPO-D-16-0178.1.
- De Bruyn, P. J. N., Tosh, C. A., Oosthuizen, W. C., Bester, M. N. and Arnould, J. P. Y. (2009) 'Bathymetry and frontal system interactions influence seasonal foraging movements of lactating subantarctic fur seals from Marion Island', *Marine Ecology Progress Series*, 394, pp. 263–276. doi: 10.3354/meps08292.
- Buckingham, C. E., Naveira Garabato, A. C., Thompson, A. F., Brannigan, L., Lazar, A., Marshall, D. P., George Nurser, A. J., Damerell, G., Heywood, K. J. and Belcher, S. E. (2016) 'Seasonality of submesoscale flows in the ocean surface boundary layer', *Geophysical Research Letters*, 43(5), pp. 2118–2126. doi: 10.1002/2016GL068009.
- Buja, B. Y. A., Hastie, T. and Tibshirani, R. (1989) 'Linear Smoothers and Additive Models', *The Annals of Statistics*, 17(2), pp. 453–510.
- Burnham, K. P. and Anderson, D. R. (2004) 'Multimodel Inference', *Sociological Methods & Research*, 33(2), pp. 261–304. doi: 10.1177/0049124104268644.
- Burns, J. M., Hindell, M. A., Bradshaw, C. J. A. and Costa, D. P. (2008) 'Fine-scale habitat selection of crabeater seals as determined by diving behavior', *Deep-Sea Research Part II: Topical Studies in Oceanography*, 55(3–4), pp. 500–514. doi: 10.1016/j.dsr2.2007.11.012.
- Callies, J., Ferrari, R., Klymak, J. M. and Gula, J. (2015) 'Seasonality in submesoscale turbulence', *Nature Communications*, 6, pp. 1–8. doi: 10.1038/ncomms7862.
- Capet, X., McWilliams, J. C., Molemaker, M. J. and Shchepetkin, A. F. (2008a) 'Mesoscale to submesoscale transition in the California Current system. Part II: Frontal processes', *Journal of Physical Oceanography*, 38(1), pp. 44–64. doi: 10.1175/2007JPO3672.1.
- Capet, X., McWilliams, J. C., Molemaker, M. J. and Shchepetkin, A. F. (2008b) 'Mesoscale to submesoscale transition in the California current system. Part III: Energy balance and flux', *Journal of Physical Oceanography*, 38(10), pp. 2256–2269. doi: 10.1175/2008JPO3810.1.
- Carmack, E. C. (2007) 'The alpha/beta ocean distinction: A perspective on freshwater fluxes, convection,

- nutrients and productivity in high-latitude seas', *Deep-Sea Research Part II: Topical Studies in Oceanography*, 54(23–26), pp. 2578–2598. doi: 10.1016/j.dsr2.2007.08.018.
- Carpenter-Kling, T., Handley, J. M., Connan, M., Crawford, R. J. M., Makhado, A. B., Dyer, B. M., Froneman, W., Lamont, T., Wolfaardt, A. C., Landman, M., Sigqala, M. and Pistorius, P. A. (2019) 'Gentoo penguins as sentinels of climate change at the sub-Antarctic Prince Edward Archipelago, Southern Ocean', *Ecological Indicators*, 101(August 2018), pp. 163–172. doi: 10.1016/j.ecolind.2019.01.008.
- Cartamil, D., Wegner, N. C., Aalbers, S., Sepulveda, C. A., Baquero, A. and Graham, J. B. (2010) 'Diel movement patterns and habitat preferences of the common thresher shark (*Alopias vulpinus*) in the Southern California Bight', *Marine and Freshwater Research*, 61(5), pp. 596–604. doi: 10.1071/MF09153.
- Carter, M. I. D., Bennett, K. A., Embling, C. B., Hosegood, P. J. and Russell, D. J. F. (2016) 'Navigating uncertain waters: A critical review of inferring foraging behaviour from location and dive data in pinnipeds', *Movement Ecology*, 4(1), pp. 1–20. doi: 10.1186/s40462-016-0090-9.
- Chapman, C. C., Lea, M., Meyer, A., Sallée, J. and Hindell, M. (2020) 'Defining Southern Ocean fronts and their influence on biological and physical processes in a changing climate', *Nature Climate Change*, 10(3), pp. 209–219. doi: 10.1038/s41558-020-0705-4.
- Charrassin, J. B. and Bost, C. A. (2001) 'Utilisation of the oceanic habitat by king penguins over the annual cycle', *Marine Ecology Progress Series*, 221, pp. 285–297. doi: 10.3354/meps221285.
- Chelton, D. B., Schlax, M. G. and Samelson, R. M. (2011) 'Global observations of nonlinear mesoscale eddies', *Progress in Oceanography*, 91(2), pp. 167–216. doi: 10.1016/j.pocean.2011.01.002.
- Chelton, D. B., Schlax, M. G., Samelson, R. M. and de Szoeke, R. A. (2007) 'Global observations of large oceanic eddies', *Geophysical Research Letters*, 34(15), pp. 1–5. doi: 10.1029/2007GL030812.
- Chown, S. and Froneman, P.W. (2008) The Prince Edward Islands: land-sea interactions in a changing ecosystem. *African Sun Media*. pg.121-164
- Constable, A. J., Melbourne-thomas, J., Corney, S. P., Arrigo, K. R., Barbraud, C., Barnes, D. K. A., Takahashi, K. T., Trathan, P. N. and Welsford, D. C. (2014) 'Climate change and Southern Ocean ecosystems I : how changes in physical habitats directly affect marine biota', pp. 3004–3025. doi: 10.1111/gcb.12623.
- Costa, D. P., Robinson, P. W., Arnould, J. P. Y., Harrison, A. L., Simmons, S. E., Hassrick, J. L., Hoskins, A. J., Kirkman, S. P., Oosthuizen, H., Villegas-Amtmann, S. and Crocker, D. E. (2010) 'Accuracy of ARGOS locations of pinnipeds at-sea estimated using fastloc GPS', *PLoS ONE*, 5(1). doi: 10.1371/journal.pone.0008677.
- Cotté, C., D'Ovidio, F., Chaigneau, A., Lévy, M., Taupier-Letage, I., Mate, B. and Guinet, C. (2011) 'Scale-dependent interactions of Mediterranean whales with marine dynamics', *Limnology and Oceanography*, 56(1), pp. 219–232. doi: 10.4319/lo.2011.56.1.0219.

- Cotté, C., D'Ovidio, F., Dragon, A. C., Guinet, C. and Lévy, M. (2015) 'Flexible preference of southern elephant seals for distinct mesoscale features within the Antarctic Circumpolar Current', *Progress in Oceanography*, 131, pp. 46–58. doi: 10.1016/j.pocean.2014.11.011.
- Craneguy, P. and Park, Y.H. (1999) 'Topographic control of the Antarctic Circumpolar Current in the south Indian Ocean', *Comptes Rendus de l'Academie des Sciences Series IIA Earth and Planetary Science*, 9(328), pp.583-589.
- Croxall, J. P., Everson, I., Kooyman, G. L., Ricketts, C. and Davis, R. W. (1985) 'Fur Seal Diving Behaviour in Relation to Vertical Distribution of Krill', *The Journal of Animal Ecology*, 54(1), p. 1. doi: 10.2307/4616.
- Croxall, J. P. and Gentry, R. L. (1987) 'Status, biology and ecology of fur seals', *Proc. of an Int. Symp. & Workshop, Cambridge, England, 23-27 April 1984*, (April 1984), pp. 212 pp.; bibliogr.
- Cushman-Roisin, B. (1990) 'Modeling of oceanic vortices', *Eos, Transactions American Geophysical Union*, 71(36), p. 1065. doi: 10.1029/EO071i036p01065.
- d'Ovidio, F., Isern-Fontanet, J., López, C., Hernández-García, E. and García-Ladona, E. (2009) 'Comparison between Eulerian diagnostics and finite-size Lyapunov exponents computed from altimetry in the Algerian basin', *Deep-Sea Research Part I: Oceanographic Research Papers*, 56(1), pp. 15–31. doi: 10.1016/j.dsr.2008.07.014.
- D'Ovidio, F., De Monte, S., Alvain, S., Dandonneau, Y. and Lévy, M. (2010) 'Fluid dynamical niches of phytoplankton types', *Proceedings of the National Academy of Sciences of the United States of America*, 107(43), pp. 18366–18370. doi: 10.1073/pnas.1004620107.
- Dong, S., Sprintall, J., Gille, S. T. and Talley, L. (2008) 'Southern ocean mixed-layer depth from Argo float profiles', *Journal of Geophysical Research: Oceans*, 113(6), pp. 1–12. doi: 10.1029/2006JC004051.
- Dragon, A. C., Bar-Hen, A., Monestiez, P. and Guinet, C. (2012) 'Horizontal and vertical movements as predictors of foraging success in a marine predator', *Marine Ecology Progress Series*, 447, pp. 243–257. doi: 10.3354/meps09498.
- Duhamel, G., Koubbi, P. and Ravier, C. (2000) 'Day and night mesopelagic fish assemblages off the Kerguelen Islands (Southern Ocean)', *Polar Biology*, 23(2), pp. 106–112. doi: 10.1007/s003000050015.
- Durgadoo, J. V., Ansorge, I. J., De Cuevas, B. A., Lutjeharms, J. R. E. and Coward, A. C. (2011) 'Decay of eddies at the South-West Indian Ridge', *South African Journal of Science*, 107(11–12), pp. 1–10. doi: 10.4102/sajs.v107i11/12.673.
- Durgadoo, J. V., Ansorge, I. J. and Lutjeharms, J. R. E. (2010) 'Oceanographic observations of eddies impacting the Prince Edward Islands, South Africa', *Antarctic Science*, 22(3), pp. 211–219. doi: 10.1017/S0954102010000088.
- Durgadoo, J. V., Lutjeharms, J. R. E., Biastoch, A. and Ansorge, I. J. (2008) 'The Conrad Rise as an

- obstruction to the Antarctic Circumpolar Current', *Geophysical Research Letters*, 35(20), pp. 1–6. doi: 10.1029/2008GL035382.
- Fauchald, P., Erikstad, K. E. and Skarsfjord, H. (2000) 'Scale-dependent predator-prey interactions: The hierarchical spatial distribution of seabirds and prey', *Ecology*, 81(3), pp. 773–783. doi: 10.1890/0012-9658(2000)081[0773:SDPPIT]2.0.CO;2.
- Fedak, M. (2004) 'Marine animals as platforms for oceanographic sampling: a "win/win" situation for biology and operational oceanography', *Memoirs of National Institute of Polar Research. Special issue*, 58, pp. 133–147.
- Fedak, M. A., Lovell, P. and Grant, S. M. (2001) 'Two approaches to compressing and interpreting time-depth information as collected by time-depth recorders and satellite-linked data recorders', *Marine Mammal Science*, 17(1), pp. 94–110. doi: 10.1111/j.1748-7692.2001.tb00982.x.
- Ferrari, R. and Wunsch, C. (2009) 'Ocean circulation kinetic energy: Reservoirs, sources, and sinks', *Annual Review of Fluid Mechanics*, 41, pp. 253–282. doi: 10.1146/annurev.fluid.40.111406.102139.
- Field, I. C., Harcourt, R. G., Boehme, L., De Bruyn, P. J. N., Charrassin, J. B., McMahon, C. R., Bester, M. N., Fedak, M. A. and Hindell, M. A. (2012) 'Refining instrument attachment on phocid seals', *Marine Mammal Science*, 28(3), pp. 1–9. doi: 10.1111/j.1748-7692.2011.00519.x.
- Fisher, R. L. and Goodwillie, A. M. (1997) 'The physiography of the Southwest Indian Ridge', *Marine Geophysical Research*, 19(6), pp. 451–455. doi: 10.1023/A:1004365019534.
- Fox-Kemper, B., Ferrari, R. and Hallberg, R. (2008) 'Parameterization of mixed layer eddies. Part I: Theory and diagnosis', *Journal of Physical Oceanography*, 38(6), pp. 1145–1165. doi: 10.1175/2007JPO3792.1.
- Fritz, H., Said, S. and Weimerskirch, H. (2003) 'Scale-dependent hierarchical adjustments of movement patterns in a long-range foraging seabird', *Proceedings of the Royal Society B: Biological Sciences*, 270(1520), pp. 1143–1148. doi: 10.1098/rspb.2003.2350.
- Froneman, P. W., Anson, I. J., Pakhomov, E. A. and Lutjeharms, J. R. E. (1999) 'Plankton community structure in the physical environment surrounding the Prince Edward Islands (Southern Ocean)', *Polar Biology*, 22(3), pp. 145–155. doi: 10.1007/s003000050404.
- Fyfe, J. C. and Saenko, O. A. (2006) 'Simulated changes in the extratropical Southern Hemisphere winds and currents', *Geophysical Research Letters*, 33(6), pp. 1–4. doi: 10.1029/2005GL025332.
- GEBCO Compilation Group (2020) GEBCO 2020 Grid. <https://doi.org/10.5285/a29c5465-b138-234d-e053-6c86abc040b9>
- Georges, A. J., Bonadonna, F., Guinet, C., Georges, J., Bonadonna, F. and Guinet, C. (2018) 'Subantarctic fur seals in relation to sea-surface Foraging habitat and temperatures at Amsterdam Island', 196, pp. 291–304.
- Georges, J. Y. and Guinet, C. (2000) 'Maternal care in the subantarctic fur seals on Amsterdam Island',

- Ecology*, 81(2), pp. 295–308. doi: 10.1890/0012-9658(2000)081[0295:MCITSF]2.0.CO;2.
- Georges, J. Y., Tremblay, Y. and Guinet, C. (2000) 'Seasonal diving behaviour in lactating subantarctic fur seals on Amsterdam Island', *Polar Biology*, 23(1), pp. 59–69. doi: 10.1007/s003000050008.
- Gill, A.E. (1982) Atmosphere-ocean dynamics. *Int. Geophys. Ser.*, 30, p.662p.
- Godø, O. R., Samuelsen, A., Macaulay, G. J., Patel, R., Hjøllø, S. S., Horne, J., Kaartvedt, S. and Johannessen, J. A. (2012) 'Mesoscale eddies are oases for higher trophic marine life', *PLoS ONE*, 7(1), pp. 1–10. doi: 10.1371/journal.pone.0030161.
- Goldsworthy, S.D., Hindell, M.A. and Crowley, H.M. (1997) 'Diet and diving behaviour of sympatric fur seals *Arctocephalus gazella* and *A. tropicalis* at Macquarie Island', *Marine mammal research in the Southern Hemisphere*, 1(1), pp. 151-163.
- Good, S. A., Martin, M. J. and Rayner, N. A. (2013) 'EN4: Quality controlled ocean temperature and salinity profiles and monthly objective analyses with uncertainty estimates', *Journal of Geophysical Research: Oceans*, 118(12), pp. 6704–6716. doi: 10.1002/2013JC009067.
- Gouretski, V. and Reseghetti, F. (2010) 'On depth and temperature biases in bathythermograph data: Development of a new correction scheme based on analysis of a global ocean database', *Deep-Sea Research Part I: Oceanographic Research Papers*, 57(6), pp. 812–833. doi: 10.1016/j.dsr.2010.03.011.
- Grant, S., Constable, A., Raymond, B. and Doust, S. (2006) 'Bioregionalisation of the Southern Ocean: report of experts workshop', *Hobart, September*.
- Green, D. B., Bestley, S., Trebilco, R., Corney, S. P., Lehodey, P., McMahon, C. R., Guinet, C. and Hindell, M. A. (2020) 'Modelled mid-trophic pelagic prey fields improve understanding of marine predator foraging behaviour', *Ecography*, 43(7), pp. 1014–1026. doi: 10.1111/ecog.04939.
- Griffies, S., Adcroft, A., Hewitt, H. T. and Chassignet, E. P. (2009) 'Problems and prospects in large-scale ocean circulation models Climate Modeling View project Oceanography and Machine Learning View project', *Researchgate.Net*, (January). Available at: <https://www.researchgate.net/publication/228634132>.
- Hagen, E., Feistel, R., Agenbag, J. J. and Ohde, T. (2001) 'Seasonal and interannual changes in Intense Benguela Upwelling (1982 – 1999)', 24(6).
- Hannah, D. M., Brown, L. E. E. E. and Milner, A. M. (2007) 'CASE STUDIES AND REVIEWS Integrating climate – hydrology – ecology for alpine river systems', *Aquatic Conservation: Marine and Freshwater Ecosystems*, 656(October 2006), pp. 636–656. doi: 10.1002/aqc.
- Harcourt, R. *et al.* (2019) 'Animal-borne telemetry: An integral component of the ocean observing toolkit', *Frontiers in Marine Science*, 6(JUN). doi: 10.3389/fmars.2019.00326.
- Harris, T. F. W. and Stavropoulos, C. C. (1978) 'Satellite-Tracked Drifters between Africa and Antarctica', *Bulletin of the American Meteorological Society*, 59(1), pp. 51–59. doi: 10.1175/1520-0477-59.1.51.

- Harrison, X. A., Donaldson, L., Correa-Cano, M. E., Evans, J., Fisher, D. N., Goodwin, C. E. D., Robinson, B. S., Hodgson, D. J. and Inger, R. (2018) 'A brief introduction to mixed effects modelling and multi-model inference in ecology', *PeerJ*, 2018(5), pp. 1–32. doi: 10.7717/peerj.4794.
- Heerah, K., Cox, S. L., Blevin, P., Guinet, C. and Charrassin, J. B. (2019) 'Validation of dive foraging indices using archived and transmitted acceleration data: The case of the weddell seal', *Frontiers in Ecology and Evolution*, 7(FEB), pp. 1–15. doi: 10.3389/fevo.2019.00030.
- Heerah, K., Hindell, M., Guinet, C. and Charrassin, J. B. (2014) 'A new method to quantify within dive foraging behaviour in marine predators', *PLoS ONE*. Edited by A. Fahlman, 9(6), p. e99329. doi: 10.1371/journal.pone.0099329.
- Heerah, K., Hindell, M., Guinet, C. and Charrassin, J. B. (2015) 'From high - resolution to low - resolution dive datasets : a new index to quantify the foraging effort of marine predators', *Animal Biotelemetry*, pp. 1–12. doi: 10.1186/s40317-015-0074-3.
- Hindell, M. *et al.* (2008) 'Southern Ocean frontal structure and sea-ice formation rates revealed by elephant seals'
- Hofmann, E. E. (1985) 'The Large-Scale Horizontal Structure of the Antarctic Circumpolar Drifters ϕ s', 90, pp. 7087–7097.
- Hofmeyr, G. J. G. (2015) 'Arctocephalus tropicalis', *The IUCN Red List of Threatened Species 2015*, 8235. doi: 10.2305/IUCN.UK.2015-4.RLTS.T2062A45224547.en.
- Hofmeyr, G.G. and Bester, M.N. (2018) Subantarctic Fur Seal: *Arctocephalus tropicalis*. In Encyclopedia of Marine Mammals (pp. 957-960). *Academic Press*. <https://doi.org/10.1016/B978-0-12-804327-1.00252-1>
- Hofmeyr, G. J. G., Bester, M. N., Makhado, A. B. and Pistorius, P. A. (2006) 'Population changes in Subantarctic and Antarctic fur seals at Marion Island', *African Journal of Wildlife Research*, 36(1), pp. 55–68.
- Hofmeyr, G. J. G., Bester, M. N., Pistorius, P. A., Mulaudzi, T. W., De Bruyn, P. J. N., Ramunasi, J. A., Tshithabane, H. N., McIntyre, T. and Radzilani, P. M. (2007) 'Median pupping date, pup mortality and sex ratio of fur seals at Marion Island', *African Journal of Wildlife Research*, 37(1), pp. 1–8. doi: 10.3957/0379-4369-37.1.1.
- Hofmeyr, G.J.G., de Bruyn, P.J.N., Wege, M., Bester, M.N. (2016) A conservation assessment of *Arctocephalus tropicalis*. In *Child MF, Roxburgh L, Do Linh San E, Raimondo D, Davies-Mostert HT, editors. The Red List of Mammals of South Africa, Swaziland and Lesotho. South African National Biodiversity Institute and Endangered Wildlife Trust, South Africa.*
- Hogg, N.G. (1973) 'On the stratified Taylor column', *Journal of Fluid Mechanics*, 58(3), pp.517-537.
- Hogg, A. M., Meredith, M. P., Chambers, D. P., Abrahamsen, E. P., Hughes, C. W. and Morrison, A. K. (2014) 'Recent trends in the Southern Ocean eddy field', *Journal of Geophysical Research*:

- Oceans, (120), pp. 257–267. doi: 10.1002/2014JC010470.Received.
- Hooker, S. K., Boyd, I. L., Jessopp, M., Cox, O., Blackwell, J., Boveng, P. L. and Bengtson, J. L. (2002) 'Monitoring the prey-field of marine predators: Combining digital imaging with datalogging tags', *Marine Mammal Science*, 18(3), pp. 680–697. doi: 10.1111/j.1748-7692.2002.tb01066.x.
- Horning, M. *et al.* (2019) 'Best practice recommendations for the use of external telemetry devices on pinnipeds', *Animal Biotelemetry*. doi: 10.1186/s40317-019-0182-6.
- Hosegood, P., Gregg, M. C. and Alford, M. H. (2006) 'Sub-mesoscale lateral density structure in the oceanic surface mixed layer', *Geophysical Research Letters*, 33(22), pp. 1–6. doi: 10.1029/2006GL026797.
- Hoskins, A. J., Costa, D. P. and Arnould, J. P. Y. (2015) 'Utilisation of intensive foraging zones by female Australian fur seals', *PLoS ONE*, 10(2), pp. 1–19. doi: 10.1371/journal.pone.0117997.
- Huang, P. Q., Lu, Y. Z. and Zhou, S. Q. (2018) 'An objective method for determining ocean mixed layer depth with applications to WOCE data', *Journal of Atmospheric and Oceanic Technology*, 35(3), pp. 441–458. doi: 10.1175/JTECH-D-17-0104.1.
- Hunt, B. P. V. and Hosie, G. W. (2005) 'Zonal structure of zooplankton communities in the Southern Ocean South of Australia: Results from a 2150 km continuous plankton recorder transect', *Deep-Sea Research Part I: Oceanographic Research Papers*, 52(7), pp. 1241–1271. doi: 10.1016/j.dsr.2004.11.019.
- Hunt, B. P. V., Pakhomov, E. A. and McQuaid, C. D. (2001) 'Short-term variation and long-term changes in the oceanographic environment and zooplankton community in the vicinity of a sub-Antarctic archipelago', *Marine Biology*, 138(2), pp. 369–381. doi: 10.1007/s002270000467.
- Hussey, N. E., Kessel, S. T., Aarestrup, K., Cooke, S. J., Cowley, P. D., Fisk, A. T., Harcourt, R. G., Holland, K. N., Iverson, S. J., Kocik, J. F., Flemming, J. E. M. and Whoriskey, F. G. (2015) 'Aquatic animal telemetry: A panoramic window into the underwater world', *Science*, 348(6240), p. 1255642. doi: 10.1126/science.1255642.
- Husson, F., Lê, S. and Pagès, J. (2017) 'Exploratory multivariate analysis by example using R', *CRC press*.
- IOC, SCOR and IAPSO (2010) 'The international thermodynamic equation of seawater – 2010: Calculation and use of thermodynamic properties', *Intergovernmental Oceanographic Commission, Manuals and Guides No. 56*, (June), p. 196.
- Jonsen, I. D., Basson, M., Bestley, S., Bravington, M. V., Patterson, T. A., Pedersen, M. W., Thomson, R., Thygesen, U. H. and Wotherspoon, S. J. (2013) 'State-space models for bio-loggers: A methodological road map', *Deep-Sea Research Part II: Topical Studies in Oceanography*, 88–89(January), pp. 34–46. doi: 10.1016/j.dsr2.2012.07.008.
- Kara, A. B., Rochford, P. A. and Hurlburt, H. E. (2000) 'An optimal definition for ocean mixed layer depth', *Journal of Geophysical Research: Oceans*, 105(C7), pp. 16803–16821. doi:

10.1029/2000jc900072.

- Karrasch, D. and Haller, G. (2013) 'Do finite-size Lyapunov exponents detect coherent structures?', *Chaos*, 23(4), pp. 1–22. doi: 10.1063/1.4837075.
- Kaufman, L. and Rousseeuw, P. E. (1987) 'Clustering by means of Medoids', *Statistical Data Analysis Based on the L1 Norm and Related Methods*, pp. 405–416.
- Kerley, G.I. (1985) 'Pup growth in the fur seals *Arctocephalus tropicalis* and *A. gazella* on Marion Island', *Journal of Zoology*, 205(3), pp.315-324.
- Kirkman, S. P., Costa, D. P., Harrison, A. L., Kotze, P. G. H., Oosthuizen, W. H., Weise, M., Botha, J. A. and Arnould, J. P. Y. (2019) 'Dive behaviour and foraging effort of female Cape fur seals *Arctocephalus pusillus pusillus*', *Royal Society Open Science*, 6(10). doi: 10.1098/rsos.191369.
- Kirkman, S. P., Yemane, D. G., Lamont, T., Meyer, M. A. and Pistorius, P. A. (2016) 'Foraging behavior of subantarctic fur seals supports efficiency of a marine reserve's design', *PLoS ONE*, 11(5), pp. 1–19. doi: 10.1371/journal.pone.0152370.
- Kirkman, S. R., Bester, M. N., Hofmeyr, G. J. G., Pistorius, R. A. and Makhado, A. B. (2002) 'Pup growth and maternal attendance patterns in Subantarctic fur seals', 37(April).
- Klages, N. T. W. and Bester, M. N. (1998) 'Fish prey of fur seals *Arctocephalus* spp. at subantarctic Marion Island', *Marine Biology*, 131(3), pp. 559–566. doi: 10.1007/s002270050348.
- Klein, P. and Lapeyre, G. (2009) 'The oceanic vertical pump induced by mesoscale and submesoscale turbulence', *Annual Review of Marine Science*, 1, pp. 351–375. doi: 10.1146/annurev.marine.010908.163704.
- Klocker, A. and Marshall, D. P. (2014) 'Advection of baroclinic eddies by depth mean flow', *Geophysical Research Letters*, 41(10), pp. 3517–3521. doi: 10.1002/2014GL060001.
- Knox, G.A. (2007) *Biology of the Southern Ocean*. Taylor & Francis Group, Florida.
- Kodinariya, T. M. and Makwana, P. R. (2013) 'Review on determining number of Cluster in K-Means Clustering', *International Journal of Advance Research in Computer Science and Management Studies*, 1(6), pp. 2321–7782.
- Kooyman, G. L. (2004) 'Genesis and evolution of bio-logging devices : 1963 – 2002', pp. 15–22.
- Kooyman, G. L., Castellini, M. A. and Davis, R. W. (1981) 'Physiology of diving in marine mammals.', *Annual review of physiology*, 43(June), pp. 343–356. doi: 10.1146/annurev.ph.43.030181.002015.
- Koubbi, P., Mignard, C., Causse, R., Da Silva, O., Baudena, A., Bost, C., Cotté, C., D'Ovidio, F., Della Penna, A., Delord, K., Fabri-Ruiz, S., Ferrieux, M., Guinet, C., Lo Monaco, C., Saucède, T. and Weimerskirch, H. (2016) *Ecoregionalisation of the Kerguelen and Crozet islands oceanic zone. Part II: The Crozet oceanic zone.*, *CCAMLR Report*. doi: 10.13140/RG.2.2.30699.95528.
- Koubbi, P., Moteki, M., Duhamel, G., Goarant, A., Hulley, P. A., O'Driscoll, R., Ishimaru, T., Pruvost, P., Tavernier, E. and Hosie, G. (2011) 'Ecoregionalization of myctophid fish in the Indian sector of the

- Southern Ocean: Results from generalized dissimilarity models', *Deep-Sea Research Part II: Topical Studies in Oceanography*, 58(1–2), pp. 170–180. doi: 10.1016/j.dsr2.2010.09.007.
- Krause, D. J., Goebel, M. E., Marshall, G. J. and Abernathy, K. (2016) 'Summer diving and haul-out behavior of leopard seals (*Hydrurga leptonyx*) near mesopredator breeding colonies at Livingston Island, Antarctic Peninsula', *Marine Mammal Science*, 32(3), pp. 839–867. doi: 10.1111/mms.12309.
- Kuhn, C. E. (2011) 'The influence of subsurface thermal structure on the diving behavior of northern fur seals (*Callorhinus ursinus*) during the breeding season', *Marine Biology*, 158(3), pp. 649–663. doi: 10.1007/s00227-010-1589-z.
- Kuhn, C. E., Tremblay, Y., Ream, R. R. and Gelatt, T. S. (2010) 'Coupling GPS tracking with dive behavior to examine the relationship between foraging strategy and fine-scale movements of northern fur seals', *Endangered Species Research*, 12(2), pp. 125–139. doi: 10.3354/esr00297.
- Lamont, T. and van den Berg, M. A. (2020) 'Mesoscale eddies influencing the sub-Antarctic Prince Edward Islands Archipelago: Origin, pathways, and characteristics', *Continental Shelf Research*, 210(January), p. 104257. doi: 10.1016/j.csr.2020.104257.
- Lamont, T., van den Berg, M. A., Tutt, G. C. O. and Ansorge, I. J. (2019) 'Impact of deep-ocean eddies and fronts on the shelf seas of a sub-Antarctic Archipelago: The Prince Edward Islands', *Continental Shelf Research*, 177(March), pp. 1–14. doi: 10.1016/j.csr.2019.03.001.
- Lapeyre, G. and Klein, P. (2006) 'Impact of the small-scale elongated filaments on the oceanic vertical pump', *Journal of Marine Research*, 64(6), pp. 835–851. doi: 10.1357/002224006779698369.
- Lapeyre, G., Klein, P. and Hua, B. L. (2006) 'Oceanic restratification forced by surface frontogenesis', *Journal of Physical Oceanography*, 36(8), pp. 1577–1590. doi: 10.1175/JPO2923.1.
- Lazar, A., Zhang, Q. and Thompson, A. F. (2018) 'Submesoscale turbulence over a topographic slope', *Fluids*, 3(2). doi: 10.3390/fluids3020032.
- Lea, M.-A., Hindell, M., Guinet, C. and Goldsworthy, S. (2002) 'Variability in the diving activity of Antarctic fur seals, *Arctocephalus gazella*, at Iles Kerguelen', *Polar Biology*, 25(4), pp. 269–279. doi: 10.1007/s00300-001-0339-6.
- Lea, M. A. and Dubroca, L. (2003) 'Fine-scale linkages between the diving behaviour of antarctic fur seals and oceanographic features in the southern Indian ocean', *ICES Journal of Marine Science*, 60(5), pp. 990–1002. doi: 10.1016/S1054-3139(03)00101-2.
- Leathwick, J. R., Elith, J. and Hastie, T. (2006) 'Comparative performance of generalized additive models and multivariate adaptive regression splines for statistical modelling of species distributions', *Ecological Modelling*, 199(2), pp. 188–196. doi: 10.1016/j.ecolmodel.2006.05.022.
- Lee, W. Y., Kokubun, N., Jung, J. W., Chung, H. and Kim, J. H. (2015) 'Diel diving behavior of breeding gentoo penguins on King George Island in Antarctica', *Animal Cells and Systems*, 19(4), pp. 274–281. doi: 10.1080/19768354.2015.1074107.

- Lévy, M., Ferrari, R., Franks, P. J. S., Martin, A. P. and Rivière, P. (2012) 'Bringing physics to life at the submesoscale', *Geophysical Research Letters*, 39(14), pp. 1–13. doi: 10.1029/2012GL052756.
- Lewin-Koh, N.j. and Bivand, R. (2008) *Maptools: tools for reading and handling spatial objects. R package version 0.7-12*
- Lidgard, D. C., Boness, D. J., Bowen, W. D. and McMillan, J. I. (2003) 'Diving behaviour during the breeding season in the terrestrially breeding male grey seal: implications for alternative mating tactics', *Canadian Journal of Zoology*, 81(6), pp. 1025–1033. doi: 10.1139/z03-085.
- Lodise, J., Özgökmen, T., Gonçalves, R. C., Iskandarani, M., Lund, B., Horstmann, J., Poulain, P. M., Klymak, J., Ryan, E. H. and Guigand, C. (2020) 'Investigating the formation of submesoscale structures along mesoscale fronts and estimating kinematic quantities using lagrangian drifters', *Fluids*, 5(3), pp. 1–38. doi: 10.3390/fluids5030159.
- Lombard, A. T., Reyers, B., Schonegevel, L. Y., Cooper, J. and Nel, D. C. (2007) 'Conserving pattern and process in the Southern Ocean : designing a Marine Protected Area for the Prince Edward Islands', 19(1), pp. 39–54. doi: 10.1017/S0954102007000077.
- Lorbacher, K., Dommenget, D., Niiler, P. P. and Köhl, A. (2006) 'Ocean mixed layer depth: A subsurface proxy of ocean-atmosphere variability', *Journal of Geophysical Research: Oceans*, 111(7), pp. 1–22. doi: 10.1029/2003JC002157.
- Lowther, A. D., Lydersen, C., Biuw, M., De Bruyn, P. J. N., Hofmeyr, G. J. G. and Kovacs, K. M. (2014) 'Post-breeding at-sea movements of three central-place foragers in relation to submesoscale fronts in the Southern Ocean around Bouvetøya', *Antarctic Science*, 26(5), pp. 533–544. doi: 10.1017/S0954102014000170.
- Lowther, A. D., Lydersen, C. and Kovacs, K. M. (2015) 'A sum greater than its parts: Merging multi-predator tracking studies to increase ecological understanding', *Ecosphere*, 6(12), pp. 1–13. doi: 10.1890/ES15-00293.1.
- Lukas, R. and Lindstrom, E. (1991) 'The mixed layer of the western equatorial Pacific Ocean', *Journal of Geophysical Research*, 96(S01), p. 3343. doi: 10.1029/90jc01951.
- Luque, P. and Ferguson, S. H. (2011) 'Satellite tracking of a killer whale (*Orcinus orca*) in the eastern Canadian Arctic documents ice avoidance and rapid , long-distance movement into the North Atlantic', pp. 1091–1096. doi: 10.1007/s00300-010-0958-x.
- Luque, S., Arnould, J. and Guinet, C. (2008) 'Temporal structure of diving behaviour in sympatric Antarctic and subantarctic fur seals', *Marine Ecology Progress Series*, 372, pp. 277–287. doi: 10.3354/meps07689.
- Luque, S. P., Arnould, J. P. Y., Miller, E. H., Cherel, Y. and Guinet, C. (2007) 'Foraging behaviour of sympatric Antarctic and subantarctic fur seals: Does their contrasting duration of lactation make a difference?', *Marine Biology*, 152(1), pp. 213–224. doi: 10.1007/s00227-007-0677-1.
- Lutjeharms, J.R.E. and Valentine, H.R. (1984) 'Southern Ocean thermal fronts south of Africa', *Deep Sea*

- Research Part A. Oceanographic Research Papers*, 31(12), pp.1461-1475.
- Lutjeharms, J.R.E., Walters, N.M. and Allanson, B.R. (1985) 'Oceanic frontal systems and biological enhancement', *Antarctic nutrient cycles and food webs*
- Maes, C. and Kane, T. O. (2014) 'stratification in the Tropics', pp. 1706–1722. doi: 10.1002/2013JC009366. Received.
- Mahadevan, A. (2016) 'The Impact of Submesoscale Physics on Primary Productivity of Plankton', *Annual Review of Marine Science*, 8, pp. 161–184. doi: 10.1146/annurev-marine-010814-015912.
- Makhado, A. B., Bester, M. N., Somhlaba, S. and Crawford, R. J. M. (2013) 'The diet of the subantarctic fur seal *Arctocephalus tropicalis* at Marion Island', *Polar Biology*, 36(11), pp. 1609–1617. doi: 10.1007/s00300-013-1380-y.
- Massardier-Galatà, L., Morinay, J., Bailleul, F., Wajnberg, E., Guinet, C. and Coquillard, P. (2017) 'Breeding success of a marine central place forager in the context of climate change: A modeling approach', *PLoS ONE*, 12(3), pp. 1–24. doi: 10.1371/journal.pone.0173797.
- McDonald, B. I., Goebel, M. E., Crocker, D. E., Tremblay, Y. and Costa, D. P. (2009) 'Effects of maternal traits and individual behavior on the foraging strategies and provisioning rates of an income breeder, the Antarctic fur seal', *Marine Ecology Progress Series*, 394, pp. 277–288. doi: 10.3354/meps08308.
- McIntyre, T. (2014) 'Trends in tagging of marine mammals: a review of marine mammal biologging studies', *African Journal of Marine Science*, 36(4), pp. 409–422. doi: 10.2989/1814232X.2014.976655.
- McIntyre, T., Bornemann, H., Plötz, J., Tosh, C. A. and Bester, M. N. (2011) 'Water column use and forage strategies of female southern elephant seals from Marion Island', *Marine Biology*, 158(9), pp. 2125–2139. doi: 10.1007/s00227-011-1719-2.
- Mcquaid, C. D. and Froneman, P. W. (2004) 'The Southern Ocean Group at Rhodes University : seventeen years of biological oceanography in the Southern Ocean reviewed', (December), pp. 571–577.
- McWilliams, J. C., Huckle, E. and Shchepetkin, A. F. (2009) 'Buoyancy effects in a stratified Ekman layer', *Journal of Physical Oceanography*, 39(10), pp. 2581–2599. doi: 10.1175/2009JPO4130.1.
- Mélice, J. L., Lutjeharms, J. R. E., Rouault, M. and Ansorge, I. J. (2003) 'Sea-surface temperatures at the sub-Antarctic islands Marion and Gough during the past 50 years', *South African Journal of Science*, 99(7–8), pp. 363–366.
- Mensa, J. A., Garraffo, Z., Griffa, A., Özgökmen, T. M., Haza, A. and Veneziani, M. (2013) 'Seasonality of the submesoscale dynamics in the Gulf Stream region', *Ocean Dynamics*, 63(8), pp. 923–941. doi: 10.1007/s10236-013-0633-1.
- Moore, J. K. and Abbott, M. R. (2000) 'Phytoplankton chlorophyll distributions and primary production in the Southern Ocean', *Journal of Geophysical Research: Oceans*, 105(C12), pp. 28709–28722.

doi: 10.1029/1999jc000043.

- Moore, J. K., Abbott, M. R. and Richman, J. G. (1999) 'Location and dynamics of the Antarctic Polar Front from satellite sea surface temperature data', *Journal of Geophysical Research: Oceans*, 104(C2), pp. 3059–3073. doi: 10.1029/1998jc900032.
- Mulet, S., Rio, M.-H., Etienne, H., Artana, C., Cancet, M., Dibarboure, G., Feng, H., Husson, R., Picot, N., Provost, C. and Strub, P. T. (2021) 'The new CNES-CLS18 Global Mean Dynamic Topography', *Ocean Science Discussions*, (January), pp. 1–31. doi: 10.5194/os-2020-117.
- Nel, D. C., Lutjeharms, J. R. E., Pakhomov, E. A., Ansorge, I. J., Ryan, P. G. and Klages, N. T. W. (2001) 'Exploitation of mesoscale oceanographic features by grey-headed albatross *Thalassarche chrysostoma* in the southern Indian Ocean', 217, pp. 15–26.
- Nikurashin, M., Vallis, G. K. and Adcroft, A. (2013) 'Routes to energy dissipation for geostrophic flows in the Southern Ocean', *Nature Geoscience*, 6(1), pp. 48–51. doi: 10.1038/ngeo1657.
- Nordstrom, C. A., Battaile, B. C., Cotté, C. and Trites, A. W. (2012) 'Foraging habitats of lactating northern fur seals are structured by thermocline depths and submesoscale fronts in the eastern Bering Sea', *Deep Sea Research Part II: Topical Studies in Oceanography*, 88–89, pp. 78–96. doi: 10.1016/j.dsr2.2012.07.010.
- O'Toole, M., Guinet, C., Lea, M. A. and Hindell, M. A. (2017) 'Marine predators and phytoplankton: How elephant seals use the recurrent Kerguelen plume', *Marine Ecology Progress Series*, 581, pp. 215–227. doi: 10.3354/meps12312.
- Orsi, A. H., Whitworth, T. and Nowlin, W. D. (1995) 'On the meridional extent and fronts of the Antarctic Circumpolar Current', *Deep-Sea Research Part I*, 42(5), pp. 641–673. doi: 10.1016/0967-0637(95)00021-W.
- Pakhomov, E. . and Froneman, P. . (1999) 'The Prince Edward Islands pelagic ecosystem, south Indian Ocean: a review of achievements, 1976–1990', *Journal of Marine Systems*, 18(4), pp. 355–367. doi: 10.1016/S0924-7963(97)00112-7.
- Pakhomov, E. A. and Chown, S. L. (2003) 'The Prince Edward Islands: Southern Ocean Oasis†', *Ocean Yearbook Online*, 17(1), pp. 348–379. doi: 10.1163/221160003X00140.
- Pakhomov, E. A., Froneman, P. W., Ansorge, I. J. and Lutjeharms, J. R. E. (2000) 'Temporal variability in the physico-biological environment of the Prince Edward Islands (Southern Ocean)', *Journal of Marine Systems*, 26(1), pp. 75–95. doi: 10.1016/S0924-7963(00)00041-5.
- Pakhomov, E. A. and McQuaid, C. D. (1996) 'Distribution of surface zooplankton and seabirds across the Southern Ocean', *Polar Biology*, 16(4), pp. 271–286. doi: 10.1007/s003000050054.
- Pakhomov, E. A., Perissinotto, R. and McQuaid, C. D. (1994) 'Comparative structure of the macrozooplankton micronekton communities of the subtropical and Antarctic polar fronts', *Marine Ecology Progress Series*, 111(1–2), pp. 155–170. doi: 10.3354/meps111155.
- Park, Y. H., Park, T., Kim, T. W., Lee, S. H., Hong, C. S., Lee, J. H., Rio, M. H., Pujol, M. I., Ballarotta, M.,

- Durand, I. and Provost, C. (2019) 'Observations of the Antarctic Circumpolar Current Over the Udintsev Fracture Zone, the Narrowest Choke Point in the Southern Ocean', *Journal of Geophysical Research: Oceans*, 124(7), pp. 4511–4528. doi: 10.1029/2019JC015024.
- Patterson, T. A., McConnell, B. J., Fedak, M. A., Bravington, M. V. and Hindell, M. A. (2010) 'Using GPS data to evaluate the accuracy of state–space methods for correction of Argos satellite telemetry error', *Ecology*, 91(1), pp. 273–285. doi: 10.1890/08-1480.1.
- Patterson, T. A., Sharples, R. J., Raymond, B., Welsford, D. C., Andrews-Goff, V., Lea, M. A., Goldsworthy, S. D., Gales, N. J. and Hindell, M. (2016) 'Foraging distribution overlap and marine reserve usage amongst sub-Antarctic predators inferred from a multi-species satellite tagging experiment', *Ecological Indicators*, 70, pp. 531–544. doi: 10.1016/j.ecolind.2016.05.049.
- Pelland, N. A., Sterling, J. T., Lea, M. A., Bond, N. A., Ream, R. R., Lee, C. M. and Eriksen, C. C. (2014) 'Fortuitous encounters between Seagliders and adult female northern fur seals (*Callorhinus ursinus*) off the Washington (USA) coast: Upper ocean variability and links to top predator behavior', *PLoS ONE*, 9(8). doi: 10.1371/journal.pone.0101268.
- Pellichero, V., Sallée, J.-B., Schmidtko, S., Roquet, F. and Charrassin, J.-B. (2017) 'The ocean mixed layer under Southern Ocean sea-ice: Seasonal cycle and forcing', *Journal of Geophysical Research: Oceans*, 122(2), pp. 1608–1633. doi: 10.1002/2016JC011970.
- Perissinotto, R., Duncombe Rae, C., Boden, B. and Allanson, B. (1990) 'Vertical stability as a controlling factor of the marine phytoplankton production at the Prince Edward Archipelago (Southern Ocean)', *Marine Ecology Progress Series*, 60, pp. 205–209. doi: 10.3354/meps060205.
- Perissinotto, R., Laubscher, R. K. and McQuaid, C. D. (1992) 'Marine productivity enhancement around Bouvet and the South Sandwich Islands (Southern Ocean)', *Marine Ecology Progress Series*, 88(1), pp. 41–53. doi: 10.3354/meps088041.
- Perissinotto, R., Lutjeharms, J. R. E. and Van Ballegooyen, R. C. (2000) 'Biological-physical interactions and pelagic productivity at the Prince Edward Islands, Southern Ocean', *Journal of Marine Systems*, 24(3–4), pp. 327–341. doi: 10.1016/S0924-7963(99)00093-7.
- Perissinotto, R. and McQuaid, C. D. (1992) 'Land-based predator impact on vertically migrating zooplankton and micronekton advected to a Southern Ocean archipelago', *Marine Ecology Progress Series*, 80(1), pp. 15–27. doi: 10.3354/meps080015.
- Phillips, E. M. and Harvey, J. T. (2009) 'A captive feeding study with the Pacific harbor seal (*Phoca vitulina richardii*): Implications for scat analysis', *Marine Mammal Science*, 25(2), pp. 373–391. doi: 10.1111/j.1748-7692.2008.00265.x.
- Photopoulou, T., Heerah, K., Pohle, J. and Boehme, L. (2020) 'Sex-specific variation in the use of vertical habitat by a resident Antarctic top predator', *Proceedings of the Royal Society B: Biological Sciences*, 287(1937), p. 20201447. doi: 10.1098/rspb.2020.1447.
- Photopoulou, T., Lovell, P., Fedak, M. A., Thomas, L. and Matthiopoulos, J. (2015) 'Efficient abstracting of dive profiles using a broken-stick model', *Methods in Ecology and Evolution*, 6(3), pp. 278–288.

doi: 10.1111/2041-210X.12328.

- Pinaud, D. (2008) 'Quantifying search effort of moving animals at several spatial scales using first-passage time analysis: Effect of the structure of environment and tracking systems', *Journal of Applied Ecology*, 45(1), pp. 91–99. doi: 10.1111/j.1365-2664.2007.01370.x.
- Pinaud, D. and Weimerskirch, H. (2005) 'Scale-dependent habitat use in a long-ranging central place predator', *Journal of Animal Ecology*, 74(5), pp. 852–863. doi: 10.1111/j.1365-2656.2005.00984.x.
- Pinaud, D. and Weimerskirch, H. (2007) 'At-sea distribution and scale-dependent foraging behaviour of petrels and albatrosses: A comparative study', *Journal of Animal Ecology*, 76(1), pp. 9–19. doi: 10.1111/j.1365-2656.2006.01186.x.
- Pirotta, E., Thompson, P. M., Miller, P. I., Brookes, K. L., Cheney, B., Barton, T. R., Graham, I. M. and Lusseau, D. (2014) 'Scale-dependent foraging ecology of a marine top predator modelled using passive acoustic data', *Functional Ecology*, 28(1), pp. 206–217. doi: 10.1111/1365-2435.12146.
- du Plessis, M., Swart, S., Ansorge, I. J., Mahadevan, A. and Thompson, A. F. (2019) 'Southern Ocean seasonal restratification delayed by submesoscale wind-front interactions', *Journal of Physical Oceanography*, 49(4), pp. 1035–1053. doi: 10.1175/JPO-D-18-0136.1.
- Pollard, R. T. and Read, J. F. (2001) 'Circulation pathways and transports of the Southern Ocean in the vicinity of the Southwest Indian Ridge', *Journal of Geophysical Research: Oceans*, 106(C2), pp. 2881–2898. doi: 10.1029/2000jc900090.
- Pyke, G. H. (1984) 'Optimal Foraging Theory: A Critical Review', *Annual Review of Ecology and Systematics*, 15(1), pp. 523–575. doi: 10.1146/annurev.es.15.110184.002515.
- Queiroz, N., Humphries, N. E., Noble, L. R., Santos, A. M. and Sims, D. W. (2010) 'Short-term movements and diving behaviour of satellite-tracked blue sharks *Prionace glauca* in the northeastern Atlantic Ocean', *Marine Ecology Progress Series*, 406(August), pp. 265–279. doi: 10.3354/meps08500.
- Quinn, G. P. and Keough, M. J. (2002) 'Introduction', in *Experimental Design and Data Analysis for Biologists*. Cambridge University Press, pp. 1–13. doi: 10.1017/CBO9780511806384.002.
- R Core Team (2020) *A Language and Environment for Statistical Computing*, R Foundation for Statistical Computing, Vienna, Austria. Available at: <http://www.r-project.org>.
- Read, J. F. Å., Pollard, R. T. and Allen, J. T. (2007) 'Sub-mesoscale structure and the development of an eddy in the Subantarctic Front north of the Crozet Islands', 54, pp. 1930–1948. doi: 10.1016/j.dsr2.2007.06.013.
- Reisinger, R. R. *et al.* (2018) 'Habitat modelling of tracking data from multiple marine predators identifies important areas in the Southern Indian Ocean', *Diversity and Distributions*, 24(4), pp. 535–550. doi: 10.1111/ddi.12702.
- Rintoul, R. and Trull, W. (2001) 'Water mass properties along a north-south hydrographic', *Journal of*

- Geophysical Research*, 106(C12), pp. 31447–31462.
- Rintoul, S., Hughes, C. and Olbers, D. (2001) *The Antarctic Circumpolar Current System, Ocean Circulation and Climate*. Available at:
<http://www.agu.org/pubs/crossref/2011/2011GL046898.shtml%5Cnpapers2://publication/doi/10.1029/2011GL046898>.
- Roncon, G., Bestley, S., McMahon, C. R., Wienecke, B. and Hindell, M. A. (2018) 'View from below: Inferring behavior and physiology of Southern Ocean marine predators from dive telemetry', *Frontiers in Marine Science*, 5(DEC), pp. 1–23. doi: 10.3389/fmars.2018.00464.
- Roquet, F. *et al.* (2013) 'Estimates of the Southern Ocean general circulation improved by animal-borne instruments', *Geophysical Research Letters*, 40(23), pp. 6176–6180. doi: 10.1002/2013GL058304.
- Rosso, I., Hogg, A. M. C., Kiss, A. E. and Gayen, B. (2015) 'Topographic influence on submesoscale dynamics in the Southern Ocean', *Geophysical Research Letters*, 42(4), pp. 1139–1147. doi: 10.1002/2014GL062720.
- Rudnick, D. L. and Martin, J. P. (2002) 'On the horizontal density ratio in the upper ocean', *Dynamics of Atmospheres and Oceans*, 36(1–3), pp. 3–21. doi: 10.1016/S0377-0265(02)00022-2.
- Sallée, J. B., Pellichero, V., Akhoudas, C., Pauthenet, E., Vignes, L., Schmidtko, S., Garabato, A. N., Sutherland, P. and Kuusela, M. (2021) 'Summertime increases in upper-ocean stratification and mixed-layer depth', *Nature*, 591(7851), pp. 592–598. doi: 10.1038/s41586-021-03303-x.
- Sallée, J. B., Speer, K., Rintoul, S. and Wijffels, S. (2010) 'Southern ocean thermocline ventilation', *Journal of Physical Oceanography*, 40(3), pp. 509–529. doi: 10.1175/2009JPO4291.1.
- Sasaki, H., Klein, P., Qiu, B. and Sasai, Y. (2014) 'Impact of oceanic-scale interactions on the seasonal modulation of ocean dynamics by the atmosphere', *Nature Communications*, 5. doi: 10.1038/ncomms6636.
- Scales, K. L., Miller, P. I., Hawkes, L. A., Ingram, S. N., Sims, D. W. and Votier, S. C. (2014) 'On the front line: Frontal zones as priority at-sea conservation areas for mobile marine vertebrates', *Journal of Applied Ecology*, 51(6), pp. 1575–1583. doi: 10.1111/1365-2664.12330.
- Schielzeth, H. and Forstmeier, W. (2009) 'Conclusions beyond support: Overconfident estimates in mixed models', *Behavioral Ecology*, 20(2), pp. 416–420. doi: 10.1093/beheco/arn145.
- Sergi, S., Baudena, A., Cotté, C., Ardyna, M., Blain, S. and d'Ovidio, F. (2020) 'Interaction of the Antarctic Circumpolar Current With Seamounts Fuels Moderate Blooms but Vast Foraging Grounds for Multiple Marine Predators', *Frontiers in Marine Science*, 7(June). doi: 10.3389/fmars.2020.00416.
- Siegelman, L., Klein, P., Rivière, P., Thompson, A. F., Torres, H. S., Flexas, M. and Menemenlis, D. (2020) 'Enhanced upward heat transport at deep submesoscale ocean fronts', *Nature Geoscience*, 13(1), pp. 50–55. doi: 10.1038/s41561-019-0489-1.
- Siegelman, L., O'Toole, M., Flexas, M., Rivière, P. and Klein, P. (2019) 'Submesoscale ocean fronts act as biological hotspot for southern elephant seal', *Scientific Reports*, 9(1), pp. 1–13. doi:

- 10.1038/s41598-019-42117-w.
- Smetacek, V. and Nicol, S. (2005) 'Polar ocean ecosystems in a changing world', 437(September). doi: 10.1038/nature04161.
- Smith, V. and Froneman, P. W. (2008) 'Nutrient dynamics in the vicinity of the Prince Edward Islands', *The Prince Edward Islands: Land-Sea Interactions in a Changing Ecosystem.*, pp. 165–179. doi: 10.18820/9781928357063/07.
- Smith, V. R. (2002) 'Climate change in the sub-antarctic: an illustration from marion island', 1968, pp. 345–357.
- Smith, V. R. (2008) 'Energy flow and nutrient cycling in the Marion Island terrestrial ecosystem: 30 years on', *Polar Record*, 44(3), pp. 211–226. doi: 10.1017/S0032247407007218.
- Sokolov, S. and Rintoul, S. R. (2007) 'On the relationship between fronts of the Antarctic Circumpolar Current and surface chlorophyll concentrations in the Southern Ocean', *Journal of Geophysical Research: Oceans*, 112(7), pp. 1–17. doi: 10.1029/2006JC004072.
- Stearns, S. C. (2000) 'Life history evolution: successes, limitations, and prospects', *Naturwissenschaften*, 87(11), pp. 476–486. doi: 10.1007/s001140050763.
- Stewart, K. D. and Haine, T. W. N. (2016) 'Thermobaricity in the transition zones between alpha and beta oceans', *Journal of Physical Oceanography*, 46(6), pp. 1805–1821. doi: 10.1175/JPO-D-16-0017.1.
- Su, Z., Wang, J., Klein, P., Thompson, A. F. and Menemenlis, D. (2018) 'Ocean submesoscales as a key component of the global heat budget', *Nature Communications*, 9(1), pp. 1–8. doi: 10.1038/s41467-018-02983-w.
- Swart, S., du Plessis, M. D., Thompson, A. F., Biddle, L. C., Giddy, I., Linders, T., Mohrmann, M. and Nicholson, S. A. (2020) 'Submesoscale Fronts in the Antarctic Marginal Ice Zone and Their Response to Wind Forcing', *Geophysical Research Letters*, 47(6), pp. 1–10. doi: 10.1029/2019GL086649.
- Swart, S., Thomalla, S. J. and Monteiro, P. M. S. (2015) 'The seasonal cycle of mixed layer dynamics and phytoplankton biomass in the Sub-Antarctic Zone: A high-resolution glider experiment', *Journal of Marine Systems*, 147, pp. 103–115. doi: 10.1016/j.jmarsys.2014.06.002.
- Takahashi, A., Matsumoto, K., Hunt, G. L., Shultz, M. T., Kitaysky, A. S., Sato, K., Iida, K. and Watanuki, Y. (2008) 'Thick-billed murres use different diving behaviors in mixed and stratified waters', *Deep-Sea Research Part II: Topical Studies in Oceanography*, 55(16–17), pp. 1837–1845. doi: 10.1016/j.dsr2.2008.04.005.
- Taylor, F. E., Ryan, P. G., Makhado, A. B., Bruyn, P. J. N. De and Weimerskirch, H. (2011) 'The seasonal distribution and habitat use of marine top predators in the southern Indian Ocean', in *Habitat of Marine Top Predators. Southern Indian Ocean Regional Workshop to Facilitate the Description of Ecologically or Biologically Significant Marine Areas (EBSAs)*, p. 30.

- Thomas, L. N., Tandon, A. and Mahadevan, A. (2008) 'Submesoscale processes and dynamics', *Geophysical Monograph Series*, 177, pp. 17–38. doi: 10.1029/177GM04.
- Thompson, A. F., Lazar, A., Buckingham, C., Garabato, A. C. N., Damerell, G. M. and Heywood, K. J. (2016) 'Open-ocean submesoscale motions: A full seasonal cycle of mixed layer instabilities from gliders', *Journal of Physical Oceanography*, pp. 1285–1307. doi: 10.1175/JPO-D-15-0170.1.
- Thompson, D., Moss, S. E. W. and Lovell, P. (2003) 'Foraging behaviour of South American fur seals *Arctocephalus australis*: extracting fine scale foraging behaviour from satellite tracks', 260, pp. 285–296.
- Tinker, M. T., Costa, D. P., Estes, J. A. and Wieringa, N. (2007) 'Individual dietary specialization and dive behaviour in the California sea otter: Using archival time-depth data to detect alternative foraging strategies', *Deep-Sea Research Part II: Topical Studies in Oceanography*, 54(3–4), pp. 330–342. doi: 10.1016/j.dsr2.2006.11.012.
- Toolsee, T., Lamont, T., Rouault, M. and Ansorge, I. (2021) 'Characterising the seasonal cycle of wind forcing, surface circulation and temperature around the sub-Antarctic Prince Edward Islands', *African Journal of Marine Science*, 43(1), pp. 61–76. doi: 10.2989/1814232X.2021.1873858.
- Tosh, C. A., de Bruyn, P. J. N., Steyn, J., Bornemann, H., van den Hoff, J., Stewart, B. S., Plötz, J. and Bester, M. N. (2015) 'The importance of seasonal sea surface height anomalies for foraging juvenile southern elephant seals', *Marine Biology*, 162(10), pp. 2131–2140. doi: 10.1007/s00227-015-2743-4.
- Tosh, C. A., Steyn, J., Bornemann, H., Hoff, J. Van Den, Stewart, B. S., Plötz, J. and Bester, M. N. (2012) 'Marine habitats of juvenile southern elephant seals from Marion Island', 17, pp. 71–79. doi: 10.3354/ab00463.
- Treasure, A. *et al.* (2017) 'Marine Mammals Exploring the Oceans Pole to Pole: A Review of the MEOP Consortium', *Oceanography*, 30(2), pp. 132–138. doi: 10.5670/oceanog.2017.234.
- Treasure, A. M., Ruzicka, J. J., Moloney, C. L., Gurney, L. J. and Ansorge, I. J. (2015) 'Land–sea interactions and consequences for sub-antarctic marine food webs', *Ecosystems*, 18(5), pp. 752–768. doi: 10.1007/s10021-015-9860-2.
- Turner, J. *et al.* (2014) 'Antarctic climate change and the environment: An update', *Polar Record*, 50(3), pp. 237–259. doi: 10.1017/S0032247413000296.
- Uchida, T., Abernathey, R. and Smith, S. (2017) 'Seasonality of eddy kinetic energy in an eddy permitting global climate model', *Ocean Modelling*, 118, pp. 41–58. doi: 10.1016/j.ocemod.2017.08.006.
- Venables, H. J., Pollard, R. T. and Popova, E. E. (2007) 'Physical conditions controlling the development of a regular phytoplankton bloom north of the Crozet Plateau, Southern Ocean', *Deep-Sea Research Part II: Topical Studies in Oceanography*, 54(18–20), pp. 1949–1965. doi: 10.1016/j.dsr2.2007.06.014.
- Viglione, G. A., Thompson, A. F., Flexas, M. M., Sprintall, J. and Swart, S. (2018) 'Abrupt Transitions in

- Submesoscale Structure in Southern Drake Passage: Glider Observations and Model Results', *Journal of Physical Oceanography*, 48(9), pp. 2011–2027. doi: 10.1175/JPO-D-17-0192.1.
- Villegas-Amtmann, S., Jeglinski, J. W. E., Costa, D. P., Robinson, P. W. and Trillmich, F. (2013) 'Individual Foraging Strategies Reveal Niche Overlap between Endangered Galapagos Pinnipeds', *PLoS ONE*, 8(8). doi: 10.1371/journal.pone.0070748.
- Viviant, M., Jeanniard-du-Dot, T., Monestiez, P., Authier, M. and Guinet, C. (2016) 'Bottom time does not always predict prey encounter rate in Antarctic fur seals', *Functional Ecology*. Edited by D. Costa, 30(11), pp. 1834–1844. doi: 10.1111/1365-2435.12675.
- Wagenmakers, E. J. and Farrell, S. (2004) 'AIC model selection using Akaike weights', *Psychonomic Bulletin and Review*, 11(1), pp. 192–196. doi: 10.3758/BF03206482.
- Wallace, B. P., Zolkewitz, M. and James, M. C. (2015) 'Fine-scale foraging ecology of leatherback turtles', *Frontiers in Ecology and Evolution*, 3(FEB), pp. 1–15. doi: 10.3389/fevo.2015.00015.
- Wang, M., Du, Y., Qiu, B., Cheng, X., Luo, Y., Chen, X. and Feng, M. (2017) 'Mechanism of seasonal eddy kinetic energy variability in the eastern equatorial Pacific Ocean', *Journal of Geophysical Research: Oceans*, 122(4), pp. 3240–3252. doi: 10.1002/2017JC012711.
- Waugh, D. W., Abraham, E. R. and Bowen, M. M. (2006) 'Spatial variations of stirring in the surface ocean: A case study of the Tasman sea', *Journal of Physical Oceanography*, 36(3), pp. 526–542. doi: 10.1175/JPO2865.1.
- Wege, M. (2013) *Maternal foraging behaviour of Subantarctic fur seals from Marion Island*, MSc. Thesis
- Wege, M. (2017) *Population trend and foraging ecology of Antarctic and Subantarctic fur seals at Marion Island*. University of Pretoria
- Wege, M., De Bruyn, P. J. N., Hindell, M. A., Lea, M. A. and Bester, M. N. (2019) 'Preferred, small-scale foraging areas of two Southern Ocean fur seal species are not determined by habitat characteristics', *BMC Ecology*, 19(1), pp. 1–14. doi: 10.1186/s12898-019-0252-x.
- Wege, M., Nevoux, M., De Bruyn, P. J. N. and Bester, M. N. (2014) 'Multi-state mark-recapture models as a novel approach to estimate factors affecting attendance patterns of lactating subantarctic fur seals from Marion Island', *Antarctic Science*, 30(6). doi: 10.1017/S0954102014000716.
- Wege, M., Tosh, C. A., De Bruyn, P. J. N. and Bester, M. N. (2016) 'Cross-seasonal foraging site fidelity of subantarctic fur seals: Implications for marine conservation areas', *Marine Ecology Progress Series*, 554, pp. 225–239. doi: 10.3354/meps11798.
- Wei, C. P., Lee, Y. H. and Hsu, C. M. (2000) 'Empirical comparison of fast clustering algorithms for large data sets', in *Proceedings of the Annual Hawaii International Conference on System Sciences*, pp. 1–10.
- Weimerskirch, H. (2007) 'Are seabirds foraging for unpredictable resources?', *Deep-Sea Research Part II: Topical Studies in Oceanography*, 54(3–4), pp. 211–223. doi: 10.1016/j.dsr2.2006.11.013.

- Weimerskirch, H., Pinaud, D., Pawlowski, F. and Bost, C. A. (2007) 'Does prey capture induce area-restricted search? A fine-scale study using GPS in a marine predator, the wandering albatross', *American Naturalist*, 170(5), pp. 734–743. doi: 10.1086/522059.
- Weise, M. J., Harvey, J. T. and Costa, D. P. (2010) 'The role of body size in individual-based foraging strategies of a top marine predator', *Ecology*, 91(4), pp. 1004–1015. doi: 10.1890/08-1554.1.
- Whitehead, T. O., Kato, A., Ropert-Coudert, Y. and Ryan, P. G. (2016) 'Habitat use and diving behaviour of macaroni Eudyptes chrysolophus and eastern rockhopper E. chrysocome filholi penguins during the critical pre-moult period', *Marine Biology*, 163(1), pp. 1–20. doi: 10.1007/s00227-015-2794-6.
- Womble, J. N., Horning, M., Lea, M. A. and Rehberg, M. J. (2013) 'Diving into the analysis of time-depth recorder and behavioural data records: A workshop summary', *Deep-Sea Research Part II: Topical Studies in Oceanography*, 88–89, pp. 61–64. doi: 10.1016/j.dsr2.2012.07.017.
- Wood, S. N. (2003) 'Thin plate regression splines', *Journal of the Royal Statistical Society. Series B: Statistical Methodology*, 65(1), pp. 95–114. doi: 10.1111/1467-9868.00374.
- Wunsch, C. (2016) 'Ocean Mixing : Oxford Encyclopedia .', *Oxford Encyclopedia*
- Xu, C., Shang, X. D. and Huang, R. X. (2014) 'Horizontal eddy energy flux in the world oceans diagnosed from altimetry data', *Scientific Reports*, 4, pp. 1–7. doi: 10.1038/srep05316.
- Yang, Q., Nikurashin, M., Sasaki, H., Sun, H. and Tian, J. (2019) 'Dissipation of mesoscale eddies and its contribution to mixing in the northern South China Sea', *Scientific Reports*, 9(1), pp. 1–9. doi: 10.1038/s41598-018-36610-x.
- Ydenberg, R. C. and Clark, C. W. (1989) 'Aerobiosis and anaerobiosis during diving by western grebes: An optimal foraging approach', *Journal of Theoretical Biology*, 139(4), pp. 437–447. doi: 10.1016/S0022-5193(89)80064-5.
- Zhang, X. and Nikurashin, M. (2020) 'Small-Scale Topographic Form Stress and Local Dynamics of the Southern Ocean', *Journal of Geophysical Research: Oceans*, 125(8), pp. 1–18. doi: 10.1029/2019JC015420.
- Zuur, A. F., Ieno, E. N. and Elphick, C. S. (2010) 'A protocol for data exploration to avoid common statistical problems', *Methods in Ecology and Evolution*, 1(1), pp. 3–14. doi: 10.1111/j.2041-210X.2009.00001.x.